538512

AIRBORNE GEOSCIENCE

Atmosphere • Land • Ocean

Fourth Airborne Geoscience Workshop

The Embassy Suites Hotel
La Jolla, California

January 29 – February 1, 1991

(NASA-TM-104983) FOURTH AIRBORNE GEOSCIENCE WORKSHOP (NASA) 278 p CSCL 08B
N91-25445
--THRU--
N91-25493
Unclas
G3/42 0020113

An Interagency and Interdisciplinary Forum on the Scientific Results and Future Needs of Airborne Research

Hosted by:

NASA

Fourth Airborne Geoscience Workshop

The Embassy Suites Hotel
La Jolla, California

January 29 – February 1, 1991

An Interagency and Interdisciplinary Forum on the Scientific Results and Future Needs of Airborne Research

Hosted by:
NASA

Fourth Airborne Geoscience Workshop

Hosted by

National Aeronautics and Space Administration

with

National Oceanic and Atmospheric Administration (NOAA)
National Science Foundation (NSF) with NCAR
U.S. Geological Survey (USGS)
Office of Naval Research
Air Force Geophysics Laboratory

Steering Committee

J. Huning, NASA
Chairman

A. Barnes, AFGL
L. Bronstein, CCRS
T. Gerish, NOAA
A. Jochum, DLR
W. Johnson, NCAR
R. Leifer, DOE
P. Mascart, Météo France
I. McPherson, NRC of Canada
S. Melfi, NASA
R. Navarro, NASA
B. Nolan, SMSRC
E. Peterson, NASA
R. Speer, NOAA
G. Tesi, NSF
G. Vane, JPL
A. Weinstein, USN

Foreword

The Airborne Geoscience Workshops are sponsored by the Interagency Steering Group on Airborne Geoscience, a panel composed of prominent domestic and international facility managers and scientists representing agencies that operate aircraft as instrument platforms for acquiring scientific data. The participating entities and their representatives are listed on the preceding page.

These Workshops provide an excellent forum to obtain the latest information on experiment results, flight opportunities, instrumentation, and future plans in airborne geoscience. In generating comprehensive agendas, planners make every effort to organize themes, speaker selection, and panel membership to yield a format covering contemporary airborne geoscience issues and concerns. To this end, the Fourth Airborne Geoscience Workshop focuses on how the airborne community can assist in achieving the goals of the Global Change Research Program. Only through concentrated remote sensing programs can an accurate global perspective of planet Earth be derived. Limited resources further underscore the need for coordination amongst all governmental agencies involved in the Earth sciences. The primary goal of the 1991 Workshop is to describe and discuss the many activities that employ airborne platforms and sensors, hopefully leading to fruitful agency and international collaboration.

The 1989 Workshop introduced a format that successfully promoted participant interaction. Poster sessions were added to the agenda, and panel sessions were structured to allow additional time for questions and discussion. This format was enthusiastically accepted. The Fourth Airborne Geoscience Workshop has been structured similarly; however, the poster sessions have been expanded greatly, with the number of presenters virtually doubling. Present-day issues, concerns, needs, and opportunities spanning all disciplines will be examined in detail to further understanding of airborne participation in global change research.

James R. Huning
Chairman, Interagency Steering Committee

Table of Contents

Interagency Airborne
Geoscience Steering Group

FOURTH AIRBORNE GEOSCIENCE WORKSHOP
PRELIMINARY AGENDA

December 20, 1990

The Global Change Research Program has been developed to provide the focus for activities of each of the governmental agencies involved in the Earth Sciences. The primary goal of this workshop is to describe and discuss the many agency activities using airborne platforms and sensors.

Tuesday, January 29, 1991

7:00 - 8:30 am	**Registration**	
9:00 - 12:00 noon	**Morning Session**	
	Welcome, Workshop Chairman	Huning
	Keynote Theme - Global Change Perspectives	
	Keynote Speakers	
	NASA	Keller
	NSF	Shedlovsky
	NOAA	Hooke
	ONR	Weinstein
12:00 noon	**Lunch**	
1:30 - 3:30 pm	**Afternoon Session**	
	Poster Previews	
	Session Leader	Melfi
5:30 - 7:30 pm	**Poster Session and Mixer,** Faculty Club, UCSD	

Chairman Dr. James R. Huning
Code SE
NASA HQ, Washington, DC 20546 (202) 453-1728

Exec. Sec. Bernard Nolan
Earth Science Support Office
Suite 440, 600 Maryland Avenue, S.W.
Washington, D.C. 20024 (202) 479-0360/(703)780-1938

Participants
National Aeronautics and Space Administration (NASA)
National Oceanic and Atmospheric Administration (NOAA)
National Science Foundaton (NSF)
National Center for Atmospheric Research (NCAR)
U.S. Geological Survey (USGS)
U.S.A.F./Air Force Geophysics Laboratory
U.S.N./Office of Naval Research
U.S. Department of Energy (DoE)
With agencies of Canada, France and Germany

FOURTH AIRBORNE GEOSCIENCE WORKSHOP
PRELIMINARY AGENDA

December 20, 1990

Wednesday, January 30, 1991

8:30 - 12:00 noon	**Morning Session**	
	Agency Activities in Airborne Geoscience Panel Session and Discussion	
	Session Leader	Watson
	NASA	Watson
	NOAA	To Be Announced
	NCAR	Serafin
	DoD	Weinstein
	DOE	Leifer
	Canada	MacPherson
	Europe	Jochum
	Panel Discussion	
12:00 noon - 2:00 pm	**Luncheon with Paul MacCready** "Unusual Vehicles for Fun, Profit and Science"	
2:00 - 5:45 pm	**Afternoon Session**	
	Platforms and Instrument Developments Panel Session and Discussion	
	Session Leader	Johnson
	Mid-Sized Jet	Johnson/R. Smith
	Very High Altitude, Unmanned	Tuck
	Airships	Blanc
	Ultralights	McCreight

FOURTH AIRBORNE GEOSCIENCE WORKSHOP
PRELIMINARY AGENDA

December 20, 1990

Wednesday, January 30, 1991 (Continued)

2:00 - 5:45 pm	**Afternoon Session (Continued)**	
	Airborne Oceanography	Bane
	Airborne Turbulent Flux Measurements	Lenschow
	Airborne LIDAR Research	Melfi
	SAR Measurements	van Zyl
	Airborne Doppler Radar - Deriving Wind Fields	Jorgensen
	Laser Measurements - Atmospheric Chemistry	Webster
	Cloud Physics	Cooper
	Airborne Hyperspectral Imaging	Goetz
	Airborne Passive Microwave Measurements	Swift
	Airborne Data Collection	Goldstein
	Discussion	
Evening	Free	

Thursday, January 31, 1991

8:30 - 12:00 noon	**Morning Session**	
	Selected Field Projects Panel Session and Discussion	
	Session Leader	Weinstein
	TOGA-COARE	Kuettner
	Airborne Arctic Ozone Expedition	Margitan
	ASTEX	Albrecht
	High Resolution Remote Sensing	Herr
	Terrestrial Ecosystems/MACs	Wickland
	GEWEX	D. Vane
	GTE	McNeal
	STORMS	Dirks
	Panel Discussion	

FOURTH AIRBORNE GEOSCIENCE WORKSHOP
PRELIMINARY AGENDA

December 20, 1990

Thursday, January 31, 1991 (Continued)

12:00 noon	**Lunch**	
2:00 - 3:30 pm	**Afternoon Session**	
	Poster Previews	
	Session Leader	Gerish
5:30 - 7:30 pm	**Poster Session and Mixer,** Faculty Club, UCSD	

Friday, February 1, 1991

8:30 - 11:00 am	**Morning Session**	
	Facility Managers' - Users' Forum Overview of Facilities and Discussion	
	Session Leader	G. Vane
	Panelists' Overviews of facilities used in support of interagency/international geoscience programs	
	NCAR	Radke
	NASA	W. Hall Navarro
	NOAA	Moran
	Canada	Bronstein
	DLR	Jochum
	France	Chalon
	DOE	Leifer
	Universities	P. Smith
	Discussion	
11:00 am	**Summary Impressions of Workshop**	Lawless
12:00 noon	**Adjourn**	

Scientific Poster Presentations
and Informal Reception
January 29 and January 31, 1991
University of California, San Diego Campus
Faculty Club

PROGRAM*

Tuesday, January 29 **5:30 - 7:30 pm**

1 & 2 **Koozer, Mark A.**, NASA/Ames Research Center
Ames Research Center C-130

3 **Arnone, Robert A.** and Paul E. LaViolette, NASA/Stennis Space Center
Aircraft Laser Derived Chlorophyll Distribution Across the Iceland-Faeroe Front

4 **Bellmore, Michael A.**, Dan J. Rusk, R. Lynn Rose, and D. Ray Booker, Aeromet, Inc.
An Aircraft-Deployed Rawinsonde for Use in Remote or Hazardous Areas

5 **Bowen, Stuart W.**, San Jose State University; K. Roland Chan, and T. Paul Bui, NASA/Ames Research Center
Calibration of the ER-2 Meteorological Measurement System

6 **Brock, Charles A.**, Lawrence F. Radke, Peter V. Hobbs, University of Washington; and Bruce M. Morley, SRI International
Airborne Lidar Studies of Arctic Hazes

7 **Browell, Edward V.**, NASA/Langley Research Center; Marta A. Fenn, and Susan A. Kooi, ST Systems Corporation
Airborne Lidar Measurements of Ozone During the 1989 Airborne Arctic Stratospheric Expedition

8 **Chan, K. Roland**, Leonhard Pfister, T. Paul Bui, NASA/Ames Research Center; Stuart W. Bowen, and Jonathan Dean-Day, San Jose State University
Applications of the ER-2 Meteorological Measurement System

9 **Deck, Bruce**, Martin Wahlen, Wadsworth Center for Laboratories and Research; Harley Weyer, NASA/Johnson Space Center; Peter Kubik, Pankaj Sharma, and Harry Gove, Nuclear Structure Research Laboratory
^{36}Cl in the Stratosphere

---

*Numbers refer to poster position at Faculty Club. Detailed poster layout will be provided at registration. Please check in with Dawn Cardascia.

Tuesday, January 29 **5:30 - 7:30 pm**

10 **Evans, Diane L.**, Jet Propulsion Laboratory and Raymond E. Arvidson, Washington University
The Geologic Remote Sensing Field Experiment (GRSFE): The First Geology Multisensor Airborne Campaign

11 **Friehe, Carl A.** and Djamal Khelif, University of California, Irvine
Fast-Response Aircraft Temperature Sensors

12 **Gasiewski, Albin J.**, D.M. Jackson, Georgia Institute of Technology; R.F. Adler, L.R. Dod, and J.C. Shiue, NASA/Goddard Space Flight Center
The Millimeter-Wave Imaging Radiometer (MIR)

13 **Griffis, Andrew J.**, Calvin T. Swift, University of Massachusetts; and David LeVine, Goddard Space Flight Center
An Electrically Scanned Thinned Array Radiometer for Earth Remote Sensing

14 **Hacker, Jorg M.**, Flinders University
A Small, Lightweight Integrated Flight Data System (IADS) For Flight Testing

15 **Hammer, Philip D.**, Francisco P.J. Valero, David L. Peterson, NASA/Ames Research Center; and William Hayden Smight, Washington University
Remote Sensing of Earth's Atmosphere and Surface using a Digital Array Scanned Interferometer-A New Type of Imaging Spectrometer

16 **Higdon, Noah S.** and Edward V. Browell, NASA/Langley Research Center
Airborne Water Vapor DIAL System and Measurements of Water Vapor and Aerosol Profiles

17 **Hoff, Axel M.**, Aerodata FlugmeBtechnik GmbH; W. Muller, Niedersachsisches Landesamt f. Immissionsschutz; and J. Werhahn, Fraunhofer-Inst. f. Atmospharische Umweltforschung
An Airborne Measurement System for Mass Fluxes of Air Pollutants

18 **Holmes, LaMont** and Jim Hochstetler, Pacific Missile Test Center
Airborne Stabilized Optical Systems

19 **Ismail, Syed** and Edward V. Browell, NASA/Langley Research Center
Lidar Measurements of Polar Stratospheric Clouds during the 1989 Airborne Arctic Stratospheric Expedition

Tuesday, January 29 **5:30 - 7:30 pm**

20 **Johnson, Lee F.**, TGS Technology, Inc.; and David L. Peterson, NASA/Ames Research Center
Hyperspectral Data Analysis for Estimation of Foliar Biochemical Content Along the Oregon Transect

21 **Kover, Allan N.**, James W. Schoonmaker, Jr., and Clark H. Cramer, U.S. Geological Survey
The USGS Side-Looking Airborne Radar (SLAR) Program: An Update-SLAR Data on CD-ROM

22 **Langford, John S.**, Aurora Flight Sciences Corporation; and James G. Anderson, Harvard University
The PERSEUS Unmanned Scientific Research Aircraft

23 **Leifer, Robert**, Ronald H. Knuth, and Lawrence E. Hinchliffe, U.S. Department of Energy
Tethered Aerostat Sampling Over Grand Bahama Island

24 **MacPherson, J. Ian**, National Research Council (Canada)
Recent Developments in Airborne Flux Measurement

25 **Mason, Allen S.**, David L. Finnegan, Gregory K. Bayhurst, Robert Raymond, Jr., Roland C. Hagan, Gary Luedemann, and Kenneth H. Wohletz, Los Alamos National Laboratory
MISERS GOLD Dust Collection and Cloud Characterization

26 **Menzies, Robert T.**, David M. Tratt, Alan M. Brothers, Stephen H. Dermenjian, and Carlos Esproles, Jet Propulsion Laboratory
Aerosol and Cloud Backscatter Measurements in the Thermal Infrared using an Airborne Backscatter Lidar

27 **Pelletier-Travis, Ramona**, NASA/Stennis Space Center
Airborne Ground Penetrating Radar (GPR) for Peat Analyses in the Canadian Northern Wetlands Study

28 **Rogers, David P.**, Scripps Institution of Oceanography; Douglas W. Johnson, Royal Aerospace Establishment (England); and Carl A. Friehe, University of California, Irvine
The Structure of a Stable Internal Boundary Layer over the Coastal Ocean

29 **Rusk, Dan J.**, Ray Harris-Hobbs, and Mark Bradford, Aeromet, Inc.
Observations of High Altitude Tropical (HAT) Cirrus and Their Implications

Tuesday, January 29 **5:30 - 7:30 pm**

30 **Scofield, Christine P.** and Chien Nguyen, NASA/Ames Research Center
C-130 Data Distribution System (CADDS)

31 **Shemdin, Omar H.** and Dayalan Kasilingham, Ocean Research and Engineering
SAR Imaging of Slicks in SAXON:CLT

32 **Smith, Paul L.** and Andrew G. Detwiler, South Dakota School of Mines and Technology
Measurements of Electric Field using the Armored T-28 Aircraft

33 **Spanner, Michael A.**, NASA/Ames Research Center; and Richard Waring, Oregon State University
Remote Sensing of the Seasonal Variation of Coniferous Forest Structure and Function

34 **Strapp, J.W.**, W.R. Leaitch, H.A. Wiebe, K.G. Anlauf, J.W. Bottenheim, K. Puckett, G.A. Isaac, Atmospheric Environment Service (Canada), C.W. Spicer, T. Kelly, J. Hubbe, N. Laulainen, Battelle Memorial Institute, F. Slemr, J. Werhahn, and H. Giehl, Fraunhofer-Institut
A Four Aircraft Intercomparison of Air Chemistry Measurements

35 **Taylor, John A.**, Lighter Than Air Technologies
Airship Support Services for Airborne Geoscience Applications

36 **Vance, Mike**, Gulfstream Aerospace
Gulfstream IV: The Productive Research Aircraft

37 **Wahlen, Martin**, Wadsworth Center for Laboratories and Research; Nori Tanaka, Yale University; Robert Henry, New York State Department of Environmental Conservation; and Harley Weyer, NASA/Johnson Space Center
Profiles of (gamma)^{13}C and (gamma)D in Methane from the Lower Stratosphere

38 **Way, JoBea**, Ron Kwok, John Holt, Jet Propulsion Laboratory; M. Craig Dobson, Kyle McDonald, and F. T. Ulaby, University of Michigan
Monitoring Forest Freeze-Thaw Cycles with Airborne SAR

39 **Wegener, Steven**, K. Roland Chan, Leonhard Pfister, and John Arvesen, NASA/Ames Research Center
High Altitude Aircraft Direction using Real-Time Scientific Analysis of Telemetered Data

Tuesday, January 29 **5:30 - 7:30 pm**

40 **Wu, Shih-Tseng**, NASA/Stennis Space Center
Polarimetric Radar for Assessing Subsurface Characteristics

41 **Angelici, Gary L.**, Lidia Popovici, Sterling Software; and Jay Skiles, Technicolor Government Services
The Pilot Land Data System (PLDS) at the Ames Research Center Manages Aircraft Data in Collaboration with an Ecosystem Research Project

42 **Baumgardner, Darrel**, National Center for Atmospheric Research
An Error Analysis Model for Aircraft Measurements

43 **Bowdle, David A.**, University of Alabama in Huntsville; Jeffry Rothermel, James E. Arnold, NASA/Marshall Space Flight Center; and Steven F. Williams, University of Alabama in Huntsville
GLObal Backscatter Experiment (GLOBE) Pacific Survey Mission

44 **Boyd, Janice D.**, NASA/Stennis Space Center
Air Deployed Expendable Probes in Oceanographic Research

45 **Weckler, Paul** and Charles Pruszynski, Aeromet, Inc.
High Altitude Observatory (HALO) Aircraft Capabilities

Thursday, January 31 **5:30 - 7:30 pm**

46-48 **Degreef, Leo H.**, NASA/Ames Research Center
NASA DC-8 Airborne Research Laboratory

49 **Browell, Edward V.**, NASA/Langley Research Center; Carolyn F. Butler, and Susan A. Kooi, ST Systems Corporation
Tropospheric Ozone and Aerosols Measured by Airborne Lidar During the 1988 Arctic Boundary Layer Experiment

50 **Burpee, Robert W.**, Joseph S. Griffin, James L. Franklin, and Frank D. Marks, Jr., NOAA/Hurricane Research Division
Analysis of Observations from a P-3 Aircraft in Support of Operational Hurricane Forecasting

51 **Cherniss, Susan C.**, Sterling Software; and Christine P. Scofield, NASA/Ames Research Center
NASA/Ames Research Center DC-8 Data System

Thursday, January 31 **5:30 - 7:30 p.m.**

52 **Flamant, Pierre H.**, CNRS
The French Airborne Backscatter LIDAR LEANDRE-1

53 **Garvin, James B.**, Jack L. Bufton, John F. Cavanaugh, NASA/Goddard Space Flight Center; William B. Krabill, Thomas D. Clem, Earl B. Frederick, and John L. Ward, NASA/Wallops Flight Facility
High-Resolution Measurements of Surface Topography with Airborne Laser Altimetry and the Global Positioning System

54 **Gregory, Gerald L.**, James M. Hoell, Jr., NASA/Langley Research Center; and Douglas D. Davis, Georgia Institute of Technology
Airborne Sulfur Trace Species Intercomparison Campaign: Sulfur Dioxide, Dimethylsulfide, Hydrogen Sulfide, Carbon Disulfide, and Carbonyl Sulfide

55 **Grossman, Robert L.**, University of Colorado
The Convection Waves Project: Cloud Street Experiment

56 **Hain, James H.W.**, Associated Scientists at Woods Hole
Whales and Ocean Habitats: Exploratory Research Using Airships

57 **Harris-Hobbs, Ray**, Arleen Lunsford, R. Lynn Rose, Aeromet, Inc.; Kathy L. Giori, Joel Kositsky, and Robert A. Maffione, SRI International
Airborne Field Mill Research Platform

58 **Hochstetler, Ron**, Airship Operation & Service
A New Look at the Airship as a Geoscience Research Platform

59 **Hoge, Frank E.**, NASA/Wallops Flight Facility; and Robert N. Swift, EG&G
Airborne Oceanographic Lidar Participation in the U.S. Joint Global Ocean Flux Study (JGOFS)

60 **Hood, Robbie E.**, Roy W. Spencer, and Mark W. James, NASA/Marshall Space Flight Center
The Advanced Microwave Precipitation Radiometer: A New Aircraft Radiometer for Passive Precipitation Remote Sensing

61 **Jedlovec, Gary J.**, Mark W. James, NASA/Marshall Space Flight Center; Matthew R. Smith, Universities Space Research Association; and Robert J. Atkinson, General Electric Company
A PC-Based Multispectral Scanner Data Evaluation Workstation: Application to Daedalus Scanners

Thursday, January 31 **5:30 - 7:30 p.m.**

62 **Kelly, Patrick**, Douglas Rickman, and Eric Smith, NASA/Stennis Space Center
End-to-End Remote Sensing at the Science and Technology Laboratory of John C. Stennis Space Center

63 **Krabill, William B.**, NASA/Wallops Flight Facility; Chreston F. Martin, and Robert N. Swift, EG&G
Applying Kinematic GPS to Airborne Laser Remote Sensing

64 **Lawless, James G.**, NASA/Ames Research Center; and Lisa J. Mann, TGS Technology, Inc.
Status Report on the Land Processes Aircraft Science Management Operations Working Group

65 **Luvall, Jeffrey C.**, NASA/Marshall Space Flight Center
The Use of Aircraft-Based Thermal Infrared Multispectral Scanner (TIMS) Data to Measure Surface Energy Budgets on a Landscape Scale

66 **Mascart, Patrick**, Meteo France, CNRM, Toulouse, France; M. Ravaut, INSU-DT, Paris, France; P. Flamant, LMD, Palaiseau, France; and A. Druilhet, LA, Toulouse, France
The New French ARAT Aircraft Program

67 **McIntosh, Robert E.** and Steve Carson, University of Massachusetts, Amherst
Geophysical Modeling of Backscatter from the Ocean Surface at C-Band

68 **Mollo-Christensen, Erik**, NASA/Goddard Space Flight Center; and J. David Oberholtzer, NASA/Wallops Flight Facility
The Surface Wave Dynamics Experiment (SWADE)

69 **Peterson, David L.**, NASA/Ames Research Center
Oregon Transect Ecosystem Research Project, A Multi-sensor Campaign (OTTER-MAC)

70 **Rothermel, Jeffry**, William D. Jones, NASA/Marshall Space Flight Center; Diana Hampton, Sverdrup Technology, Inc.; Vandana Srivastava, University Space Research Association; Maurice Jarzembski, NASA/Marshall Space Flight Center
Airborne Coherent Continuous Wave CO_2 Doppler Lidars for Aerosol Backscatter Measurement

Thursday, January 31 **5:30 - 7:30 p.m.**

71 **Russell, Philip B.**, NASA/Ames Research Center; David P. Lux, Dryden Flight Research Facility; R. Dale Reed, PRC Systems Services; Max Loewenstein, and Steven Wegener, NASA/Ames Research Center
Science Requirements and Feasibility/Design Studies of a Very-High-Altitude Aircraft for Atmospheric Research

72-73 **Shelton, Gary A.** and Bruce Coffland, NASA/Ames Research Center
The High Altitude Aircraft Program of NASA/Ames Research Center

74 **Smith, Dean S.**, University Research Foundation; and Jack L. Bufton, NASA/Goddard Space Flight Center
The Remotely Piloted Vehicle as an Earth Science Research Aircraft

75 **Smith, William L.**, Steven A. Ackerman, Hugh B. Howell, Allen H.-L. Huang, Robert O. Knuteson, Henry E. Revercomb, and Harold M. Woolf, University of Wisconsin, Madison
Cloud and Trace Gas Remote Sensing with the High-Resolution Interferometer Sounder (HIS)

76 **Spinhirne, James D.**, John F. Cavanaugh, NASA/Goddard Space Flight Center; S. Chudamani, Science Applications International Corporation; Jack L. Bufton, and Robert J. Sullivan, NASA/Goddard Space Flight Center
Visible and Near Infrared Observation on the Global Aerosol Backscatter Experiment (GLOBE)

77 **Portigal, Frederick P.**, James V. Taranik, and Christopher D. Elvidge, University of Nevada System
Extraction of Reflectance from 1989 AVIRIS Radiance Data using LOWTRAN 7 Atmospheric Models

78 **Tjernstrom, Michael**, Uppsala University
Airborne Observations of the Inhomogeneous Marine Boundary Layer in a Coastal Region

79 **Wachs, Peter**, P. Vorsmann, Aerodata FlugmeBtechnik GmbH
METEOPOD-An Airborne Module for Atmospheric Turbulence Measurements

80 **Walthall, Charles L.**, University of Maryland; James Irons, Phillip Dabney, Goddard Space Flight Center; David Peterson, NASA/Ames Research Center; Darrel Williams, NASA/Goddard Space Flight Center; Lee Johnson, TGS Technology, Inc.; and Jon Ranson, NASA/Goddard Space Flight Center
Advanced Solid-State Array Spectrometer (ASAS) Data Sets from the 1990 Field Season: A Unique Look at Two Forested Ecosystems

Thursday, January 31 **5:30 - 7:30 p.m.**

81 **Williams, Darrel L.**, NASA/Goddard Space Flight Center; Charles L. Walthall, University of Maryland; and Douglas Young, NASA/Wallops Flight Facility
A Pointable, Helicopter-Based Remote Sensing Data Acquisition System for Collecting Bidirectional Reflectance Data

82 **Williams, Darrel L.** and K. Jon Ranson, NASA/Goddard Space Flight Center
The 1990 Forest Ecosystem Dynamics Multisensor Aircraft Campaign

83 **Yoder, James A.**, University of Rhode Island; and Frank E. Hoge, NASA/Goddard Space Flight Center
Aircraft Remote Sensing of Phytoplankton Spatial Patterns during the 1989 Joint Global Ocean Flux Study (JGOFS) North Atlantic Bloom Experiment

84 **Orzel, George B.**, Micheal Miller, and Chris Higgins, Wright-Patterson Air Force Base
Availability of Air Force Aircraft and Support for Geoscience Research

Poster Presentations and Informal Reception

Tuesday and Thursday, January 29 & 31, 1991 • 5:30 to 7:30 PM*

*Poster Presenter Set-Up from 4:30 to 5:30 PM

Ida and Cecil Green
Faculty Club
University of California
San Diego

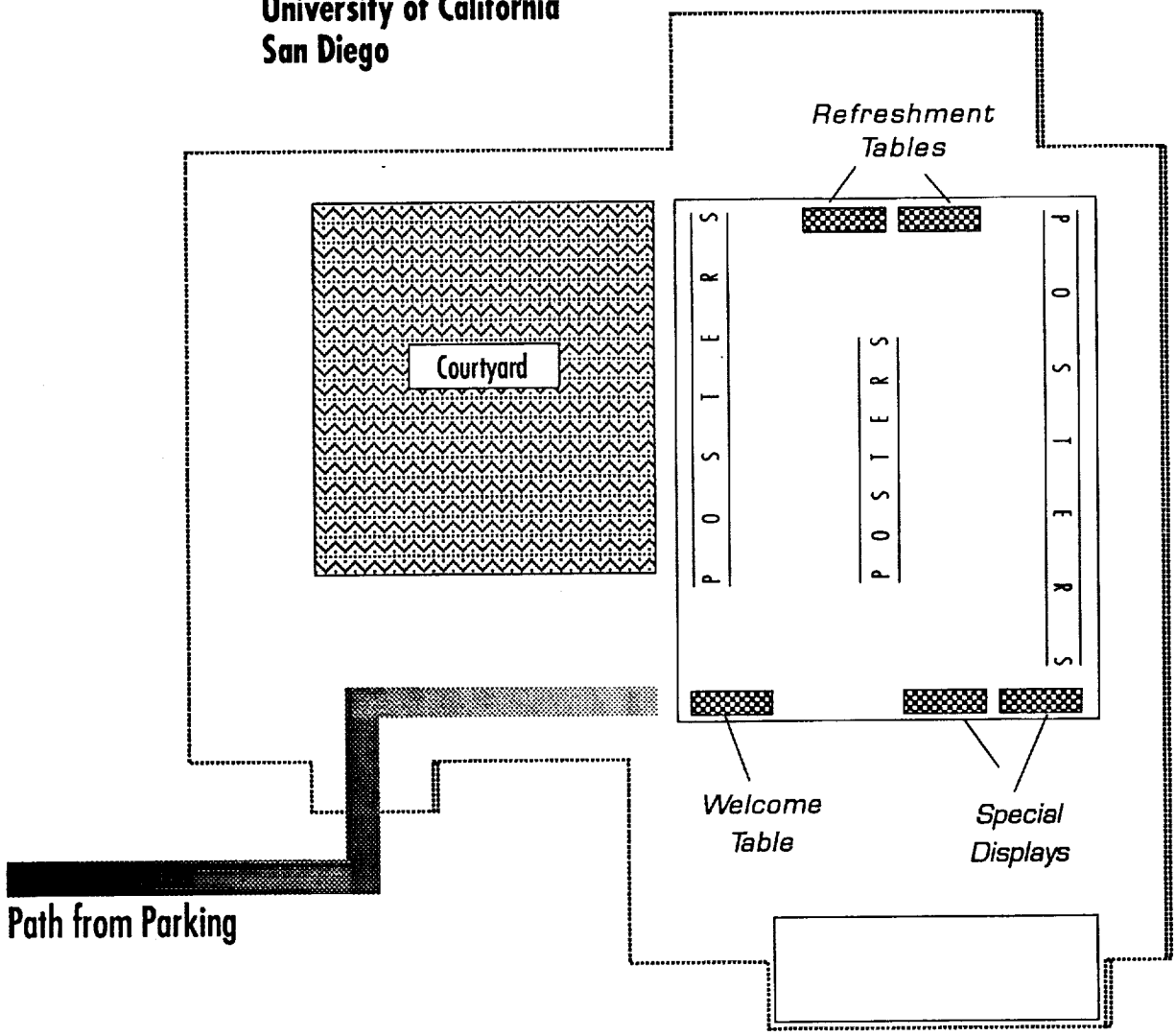

Special requirements for posters such as electric power, tables, etc. should be coordinated with
Andy Cameron or Dawn Cardascia
Earth Science Support Office
TEL: (202) 479-0360 • FAX: (202) 479-2743

Title: NCAR Activities and Plans in Airborne Atmospheric Research

Author: Robert Serafin, National Center for Atmospheric Research

Discipline: Atmosphere

Abstract will be available at the Workshop.

OMIT TO
P43

Title: Ocean Sciences at the Office of Naval Research

Author: Alan Weinstein, Office of Naval Research

Discipline: Oceans

Department of Defense (DoD) responsibility in basic oceanography research is vested primarily in the Ocean Science Directorate of the Office of Naval Research (ONR). This Directorate is the sponsor of fundamental studies in, on and above the Navy-unique environment - the world ocean. Twelve research programs span the diversity of science involved in understanding the ocean environment. The overreaching goal of this research is to sustain and enhance the operational capability of the U.S. Navy/Marine Corps team. Examples of these programs and specific research thrusts will be discussed. Of particular interest to this working group is ONR sponsored work in oceanography, sea ice, geology and geophysics, and meteorological research utilizing airborne remote sensors.

Title: The Department of Energy's Airborne Geoscience Programs

Author: Robert Leifer, U.S. Department of Energy

Discipline: Atmosphere

The Department of Energy (DOE) maintains a fleet of aircraft equipped for regularly scheduled research programs and to respond to national emergencies. These aircraft are either owned by various national laboratories or are contracted out to the laboratories for specific research programs. In addition to the programs using aircraft a limited number of research programs incorporate airborne balloons for atmospheric sampling and measurement of atmospheric motions.

Batelle/Pacific Northwest Laboratory (PNL), Sandia National Laboratories (SNL) and EG&G, Inc. have a combined fleet of 9 aircraft. These include:

PNL	Grumman Gulfstream 1 (G-1) aircraft
SNL	DeHavilland Twin Otter 20 aircraft
EG&G, Inc.	Convair 580-T aircraft
	Beechcraft Twin Bonanza E-50 aircraft
	2 Hughes H-500 helicopters
	2 Boeing BO-105 helicopters
	Beechcraft King A-100 aircraft

Brookhaven National Laboratory (BNL), Los Alamos National Laboratory (LANL) and Lawrence Livermore National Laboratory (LLNL) utilize aircraft from either the National Oceanographic and Atmospheric Administration (NOAA) or the National Aeronautical and Space Administration (NASA) for their research programs. Sandia has developed a special adjustable buoyancy balloon for atmospheric motion studies. The Environmental Measurements Laboratory (EML) works with the Air Force Geophysical Laboratory's balloon facility for periodic stratospheric balloon flights and with TCOM Inc. for sampling on tethered aerostats in the free troposphere.

Instrumentation on these platforms includes: 1) Particle Measuring Systems instrumentation for characterization of aerosol and droplet particles (diameters range from 0.1μm to 1.5 mm); 2) visible and IR radiation instruments; 3) downward looking optical systems; 4) aerial cameras, 5) experimental radars and lidar systems; 6) slant - range extinction instrumentation; 7) filter samplers; 8) continuous and grab gaseous samplers; 9) gamma radiation detectors.

A brief overview of the research efforts by these laboratories include:

Brookhaven National Laboratory
and
Environmental Measurements Laboratory

The study of "Continental and Oceanic Fates of Energy Related Air Pollutants".

EG&G Inc.

Assuring that all the U.S. energy "programs and operations are conducted in a manner that will protect the public, ensure occupational safety and health, and preserve the environment in accordance with nationally accepted norms".

Batelle/Pacific Northwest Laboratory

1) Research involving airborne cloud and radiation measurements which is part of the Atmospheric Radiation Measurements (ARM) program.
2) Collection of pollutant data from airborne sampling over sections of the northeastern United States for the the Acid Model Operational Diagnostic Evaluation Study of the National Acid Precipitation Assessment Program.

Batelle/Pacific Northwest Laboratory
and
Brookhaven National Laboratory

The study of transport and precipitation scavenging of atmospheric pollutants near frontal boundaries of extra-tropical cyclones.

Sandia National Laboratories

1) The characterization of the atmospheric radiation field.
2) The measurement of aerosol size distribution and gaseous atmospheric composition.
3) The characterization of clouds and ice particles in the troposphere and stratosphere.
4) Experiments involving a physical Lagrangian tracer (balloon) of atmospheric motions.

Los Alamos National Laboratory

1) The characterization of volcanic emissions.
2) The characterization of dust clouds produced from surface detonations using an ammonium nitrate-fuel oil blasting agent.

Lawrence Livermore National Laboratory

Understanding transport processes in the stratosphere through the measurement of ^{7}Be and ^{10}Be, cosmogenically produced radionuclides.

Title: Canadian Activities in Airborne Geoscience

Authors: Ian MacPherson, National Research Council (Canada)
Leon Bronstein, Canada Centre for Remote Sensing

Discipline: Multidisciplinary

The sensor research and development program at the Canada Centre for Remote Sensing (CCRS) covers the development and evaluation of new systems and new techniques for remotely sensing of the Earth's resources and environment. The airborne sensor developments have been accompanied by the parallel improvement of data processing and analysis systems, by advances in calibration and correction procedures for signature measurements, and by extensive data acquisition for remote sensing application development. An overview of the sensor developments will be presented.

In the area of microwave signature measurement, the CCRS Convair 580 is a unique research radar facility with its primary sensor a high-performance, fully digital, dual-frequency synthetic aperture radar (SAR). The radar provides choice of polarization, selectable swath (nadir, narrow or wide) and real-time processed image display. Recent advances include the implementation of phase measurements used in an experimental SAR polarimetric mode (in 1989) and an interferometric mode (in 1990). The CCRS radar has flown extensively for research projects across Canada and has participated in major international missions in Canada and Europe acquiring a unique set of radar data from oceans, ice and land to improve the understanding of microwave-target interaction and to prepare for the new range of radar satellites, including ERS-1, Radarsat and J-ERS-1.

In the electro-optical area, the high spectral and spatial resolution imagery available from the MEIS II airborne multispectral imager has led to improved discrimination of features in, for example, forested and coastal regions. Developments of hardware and of data processing systems have been accompanied by the development of an automated laboratory calibration facility suitable for high resolution array imagers and of atmospheric correction algorithms. An important advancement has been the WHIRL, the wide angle, high resolution line imager which was successfully flown in 1989 and which has performance exceeding that of any civilian line imager yet developed. It combines high spectral resolution and high spatial resolution with wide field of view.

The Flight Research Laboratory (FRL) of the National Research Council operates nine research aircraft, two of which are committed almost exclusively to airborne geoscience programs. A Twin Otter is instrumented as an atmospheric research aircraft for projects in cloud physics, atmospheric pollution, and the flux of trace gases. A Convair 580 is used to develop aeromagnetic instrumentation, precision navigation devices, and data interpretation methods in support of the Canadian geophysical exploration industry. It is also being outfitted with an extensive array of atmospheric sensing systems for participation in the Second Canadian Atlantic Storms Program in 1992. With this additional capability in its repertoire, the Convair 580 will join the Twin Otter as an important source of environmental data during the coming 'green decade'. The FRL has also just acquired a Falcon 20 jet aircraft for application in the areas of microgravity research and atmospheric sensing.

The FRL and the Cloud Physics Research Branch of the Atmospheric Environment Service (AES) continue their cooperation in cloud physics studies. This work has application in weather modification research and in the improved understanding and prediction of features such as precipitation bands in mesoscale storms. Part of this program involves instrumentation and software development to maintain the Twin Otter as a state-of-the-art cloud physics research aircraft. In particular, there is continuous effort to improve the accuracy of the wind measuring systems on the aircraft, and to understand the effects of airflow distortion on measurements made with cloud physics instruments.

The Air Quality and Cloud Physics Research Branches of the AES and the FRL are undertaking cooperative studies of cloud and precipitation scavenging of airborne pollutants. The main objective of these joint studies is to obtain a better understanding of the physical and chemical processes by which atmospheric pollutants, especially those contributing to acidic precipitation, are transported by, and ultimately removed from, the atmosphere and how these pollutants may inadvertently modify precipitation patterns. The Twin Otter has been used in a number of air pollution research projects at several North American locations, often in cooperation with U. S. agencies such as NOAA and the Dept. of Energy. These projects have addressed several important issues in air pollution research, including: the collection of data to test recently-developed computer models for the long-range transport of airborne pollutants; examination of the differences in the daytime and nighttime air chemistry; investigation of the constituents and sources of anthropogenic gases and aerosols in Arctic Haze; tracer experiments to identify individual sources of pollutants; the airborne collection of cloudwater and precipitation and supporting microphysical data to understand the role of clouds in the development of both acid rain and acid snow.

In cooperation with the Land Resource Research Centre of Agriculture Canada, the FRL has worked to develop the capability of accurately measuring carbon dioxide fluxes with an aircraft. Although this technique may find practical application in monitoring growth rates of crops and forests, it is in the field of climate change due to greenhouse gases that the most important contribution can be made. To make long range predictions of the effects of increased $C0_2$ levels in the atmosphere, scientists need quantitative information on the basic $C0_2$ exchange rates between the biosphere and the atmosphere. As a result of several years of careful development of instrumentation and analysis techniques, the NAE Twin Otter is now capable of making these important measurements for $C0_2$, water vapour, heat and momentum. Instrumentation is also being developed to measure the flux of methane. In cooperation with McGill University, analytical techniques are being studied to determine the so-called 'footprint corrections' to correct fluxes for downwind displacement and advective contributions. Development work is also under way to pioneer the application of the 'relaxed eddy accumulation technique' to measure the fluxes of gases for which fast-response analyzers do not exist. Recent project work has

included participation with NASA in the First ISLSCP[1] Field Experiment (FIFE) in central Kansas and the Northern Wetlands Study (ABLE-3B) in the Hudson Bay Lowlands. In the next several years, efforts will be concentrated on studies of the flux of toxic chemicals in the Great Lakes Basin and participation in BOREAS to measure biosphere-atmosphere interactions in the boreal forest.

The FRL of NRC has been a world leader in aeromagnetics for several decades. Achievements include early development of analog compensators and the oriented cesium magnetometer, which is recognized as the world's best for submarine detection. Other developments include techniques for using non-oriented magnetometers and algorithms for compensating geophysical survey aircraft. As a method for testing aeromagnetic instrumentation in an operational environment, the FRL carries out aeromagnetic surveys for Energy, Mines and Resources in remote areas of Canada and the Arctic Ocean using the Convair 580 as an aeromagnetics test bed. Current work involves advancement of aeromagnetic gradiometry techniques for both military and exploration applications, the development of a new generation of cesium vapour magnetometer, and continued improvements to the robustness of the compensation algorithms. Another area of endeavour, which finds application in both the aeromagnetic and atmospheric studies, is research on advanced navigation systems to precisely measure the motion of a research aircraft or recover its exact track over the ground. The research at the FRL emphasizes Kalman filter design for optimal use of redundant navigation information, and special attention is being given to the integration of GPS into the various motion sensing and positioning systems.

---

[1] International Setallite Land Surface Climatology Peoject

Title: Airborne Geoscience in Europe

Authors: Anne M. Jochum, German Aerospace Research Establishment
Patrick Mascart, Météo France, CNRM

Discipline: Atmosphere

A variety of platforms are available for airborne geoscience research in several European countries. An overview is given of the aircraft, their principal instrumentation, and main purpose. Particular emphasis is given to new research aircraft.

Airborne geosciences play a major role in many national and international research programs in Europe. Recent major field experiments with significant aircraft components are summarized, as well as future activities.

Title: **The Role of a Mid-Sized Jet in Atmospheric and Oceanic Research**

Authors: **Warren Johnson, National Center for Atmospheric Research**
Ronald Smith, Yale University

Discipline: **Atmosphere and Oceans**

Abstract will be available at the Workshop.

Title: **Developments and Possibilities for Very High Altitude Unmanned Aircraft in Atmospheric Research**

Author: **A.F. Tuck, NOAA/Aeronomy Laboratory**

Discipline: **Atmosphere**

Immediate past successes by the ER-2 manned aircraft are briefly outlined. The altitude, range, and payload requirements arising from atmospheric research tasks are presented. The ability of current and future aircraft to match these requirements is considered, and the conclusion reached that many important near-term requirements can be met by aircraft that currently exist or are under construction. There will remain a substantial challenge, posed by the need to combine long range (6000 nm) with high altitude (90,000 to 100,000 feet).

Title: The Use of an Airship to Make Improved Air-Sea Interaction Surface Flux Measurements

Author: Theodore V. Blanc, Naval Research Laboratory

Discipline: Atmosphere and Oceans

Because three-quarters of the Earth is covered by oceans, understanding the complex exchange process that occurs between the atmosphere and the ocean is essential to improving the forecasts of global weather, atmospheric pollution, and climate change. The fluxes of momentum, heat, and humidity must be measured to properly characterize the coupled two-way interaction that occurs at the surface of the sea. Up to the present, only a few thousand hours of direct, high-quality surface flux measurements have been made, and those have been from a small number of locations over a limited variety of oceanic environments. Many of these surface fluxes were measured with restricted upwind fetch lengths, most were measured over relatively shallow water, and only a few were measured with a full appreciation of the distortions induced by the observation platform. For these reasons, Bill Keller and myself of the Naval Research Laboratory (NRL) in conjunction with Bill Plant of the Woods Hole Oceanographic Institution (WHOI) have initiated a basic-research effort to make improved surface flux measurements over the ocean.

The need for improved meteorological measurements on a global scale has resulted in considerable effort being expended over the last two decades to develop various remote sensing techniques for possible use from Earth-orbiting satellites. In particular, the development of a satellite-based technique for remotely measuring the wind has received much attention because of the limited availability of measurements over large regions of the ocean not frequented by commercial shipping (Figure 1). The lack of uniformly distributed and timely observations over the sea has had a severe impact on the accuracy of global weather and sea-state forecasting. An active microwave system, called a scatterometer, presently seems to be the best candidate for the routine collection of oceanic surface wind measurements. A scatterometer operates by directing microwave radiation toward the surface of the ocean and by measuring the microwave power scattered back from the wind-roughened surface. From space, such a system could operate 24 hours a day to obtain uniformly distributed ocean wind information within a few hours of the observation. Both the Europeans and Japanese plan to launch spaceborne scatterometers within the next 2 years.

The manner in which the ocean surface backscatters microwave radiation is only partially understood and is a point of considerable debate. Experiments have shown that a large portion (50% to 80%) of the backscatter is the result of Bragg scattering, a resonant-type interaction between centimeter-long microwave radiation and the wind-induced, centimeter-size, gravity-capillary waves that are propagating in the direction of the radiation on the sea surface. A topic of keen interest within the scatterometry research community is whether the intensity of the backscattered signal is more directly the result of the wind-induced momentum flux (force per unit area) or the average wind speed. Although the surface momentum flux is largely (about 65%) a function of the wind speed, it is also influenced by the stability of the atmosphere, the ambient sea state, and the presence of biologically generated surface films. Different amounts of momentum, therefore, can be imparted to the ocean at a given wind speed. Heat and humidity flux measurements are required to determine the atmospheric stability.

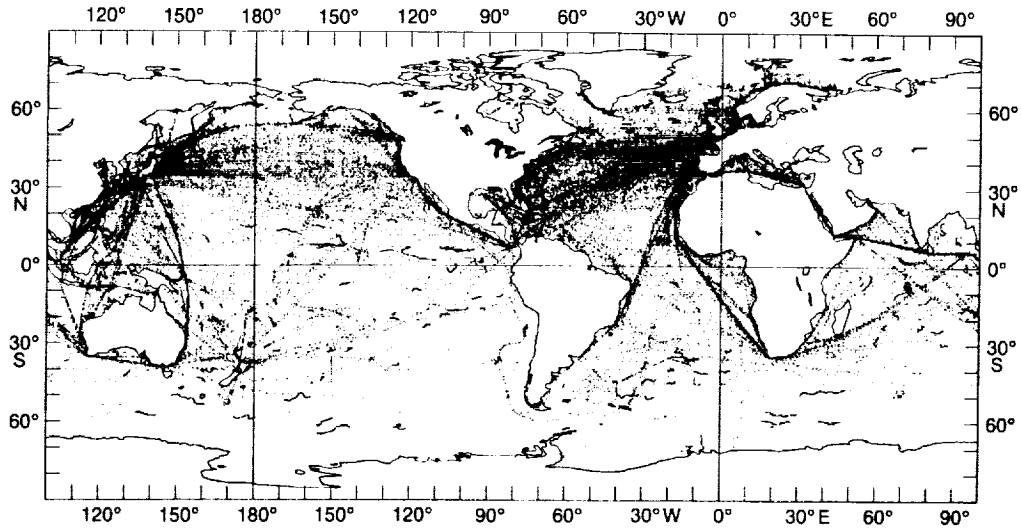

Figure 1. Distribution of marine meteorological surface observations reported within 10 hours of the observation for October 1986 as presented by R.W. Reynolds of the National Weather Services's Climate Analysis Center.

Accurate surface flux measurements are critical to the validation of the various proposed scatterometer theories. Such fluxes are difficult to measure over the ocean. Very few scatterometer measurements have been made simultaneously with direct, high-quality flux measurements. Much of the existing data consist of scatterometer results calibrated with indirect estimates of the fluxes, which are accurate to no better than about $\pm 35\%$. It is not surprising, then, that the relationship between the scatterometer backscatter signal and the air-sea surface fluxes is less exact than would be desirable. Direct flux measurements made from a distortion-free platform should be accurate to about $\pm 5\%$.

Until the current NRL/WHOI effort, only four basic types of Earth-based platforms had been used for air-sea flux measurements: fixed-wing aircraft, buoys, towers, and ships. Each imposes a particular set of limitations on the type and quality of the measurements. Because of safety and operational constraints, fixed-wing aircraft generally cannot be flown low enough to ensure that fluxes are measured within the marine atmospheric surface layer—the approximately 10- to 50-m-high region of the atmosphere that most influences the ocean. Buoys require highly ruggedized sensor packages that must survive unattended in the extremely hostile marine environment, and that can consume only a very limited amount of electrical power. High-accuracy, fast-response flux sensors usually cannot survive for long under such adverse conditions. Although considered mobile, buoys are not easily moved from place to place and require expensive logistical support such as oceangoing tugboats and divers. Buoy motion is also a problem. Towers are relatively immobile, are available in only a limited number of locations, and are typically situated in relatively shallow water. The upwind flow distortion produced by even the relatively open structure of a tower can make atmospheric flux measurements extremely difficult. Ships are not practical as flux-measurement platforms because of the massive obstruction they pose to the ambient wind and wave fields. Rotary-wing aircraft are unsuitable because of their highly turbulent "down-wash."

To overcome the difficulties associated with previous flux measurements, the joint NRL/WHOI effort uses an airship as a mobile "skyhook" for making nonintrusive surface measurements. The flux measurement instrumentation is suspended beneath the airship on an 80-m tether while simultaneous scatterometer and sea surface velocity measurements are made from the airship's gondola (Figures 2 and 3). We plan to use the Airship Industry's Model 1000 airship which is 68 m long, is 17 m in diameter, has a 34 m^3 main cabin, and has a payload lift capacity of 1900 kg. The airship can

achieve a maximum airspeed of 60 knots and, when equipped with an auxiliary fuel tank and flown at 40 knots, has a maximum range of about 2100 km or 1300 nmi. The current program calls for a series of experiments in fiscal years 1991 through 1993 in which coincident scatterometer and direct surface flux measurements are made over a variety of ocean environments. The airship will enable direct high-quality surface flux measurements to be made with a few meters of the sea surface, free from the distortions associated with conventional platforms. The work is funded by the Naval Research Laboratory and the Office of Naval Research.

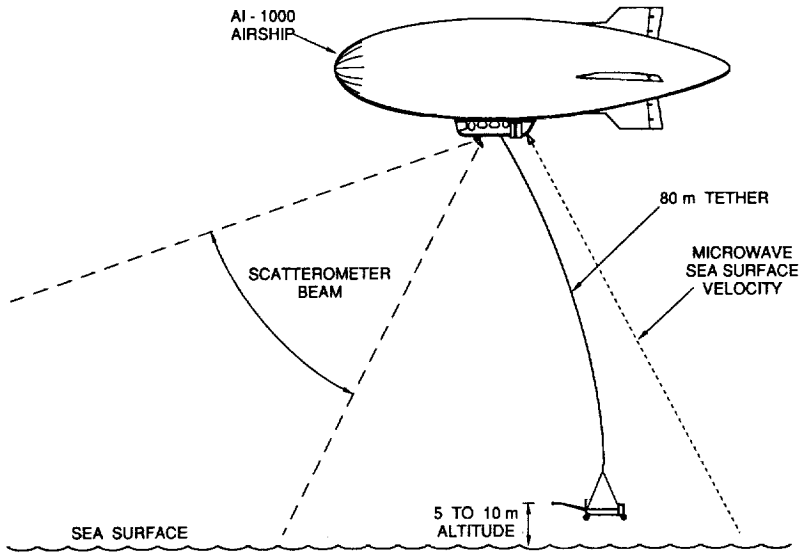

Figure 2. The airship enables direct high-quality surface flux measurements to be made within a few meters of the sea surface free of platform-induced distortions while coincident scatterometer and sea surface velocity measurements are made from the gondola.

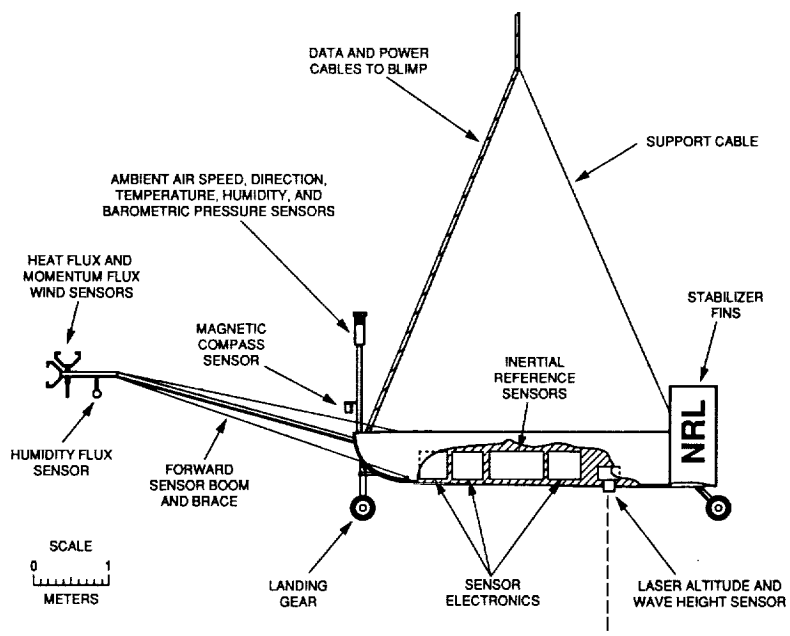

Figure 3. The surface flux sensor platform suspended beneath the hovering airship. The flux sensors are located on a long, forward boom so that the measurements are made upwind and are uninfluenced by any possible local flow distortion induced by the suspended platform.

Title: Multispectral Data Collected with an Ultralight Aircraft

Author: Rich McCreight, Oregon State University
Richard Waring, Oregon State University

Discipline: Land

An ultralight aircraft has provided a reliable, inexpensive platform for obtaining high quality spectral data throughout the year. In a NASA sponsored campaign in Oregon the ultralight supplemented data collected by seven other aircraft. It showed special advantages in being able to fly at speeds of 40-110 km/hr and at altitudes of 100 to 3000 meters (AGL) under varied sky conditions. Examples of data are provided that were collected with an eight-channel Barnes Modular Multiband Radiometer (Fig. 1), Spectron Engineering SE-590 (vis/ir) and SE-593 (mid-ir) spectrometers, an infrared thermometer, 35 mm camera, and color video camera.

The ultralight carries a calibration panel that is interrogated every 5 to 10 minutes during flight. This in-flight calibration allows for corrections for haze observed at specific altitudes (Fig. 2).

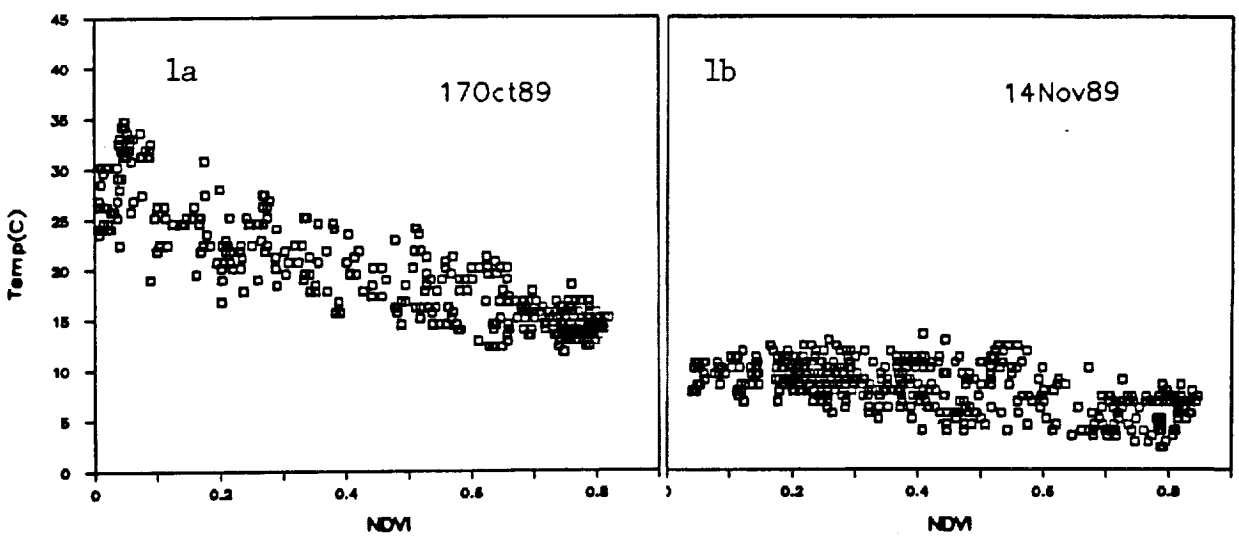

Fig. 1a When the potential for latent heat flux from soils and vegetation is low, the surface temperature(Y-axis) increases steeply as the vegetation cover, expressed as the Normalized Difference Vegetation Index (NDVI) decreases. When the potential for evaporation is high (Fig. 1b), the slope of the relationship is nearly flat, as predicted in theory developed by S.N. Goward and A.S. Hope (1989, Advances in Space Research 9:239-249).

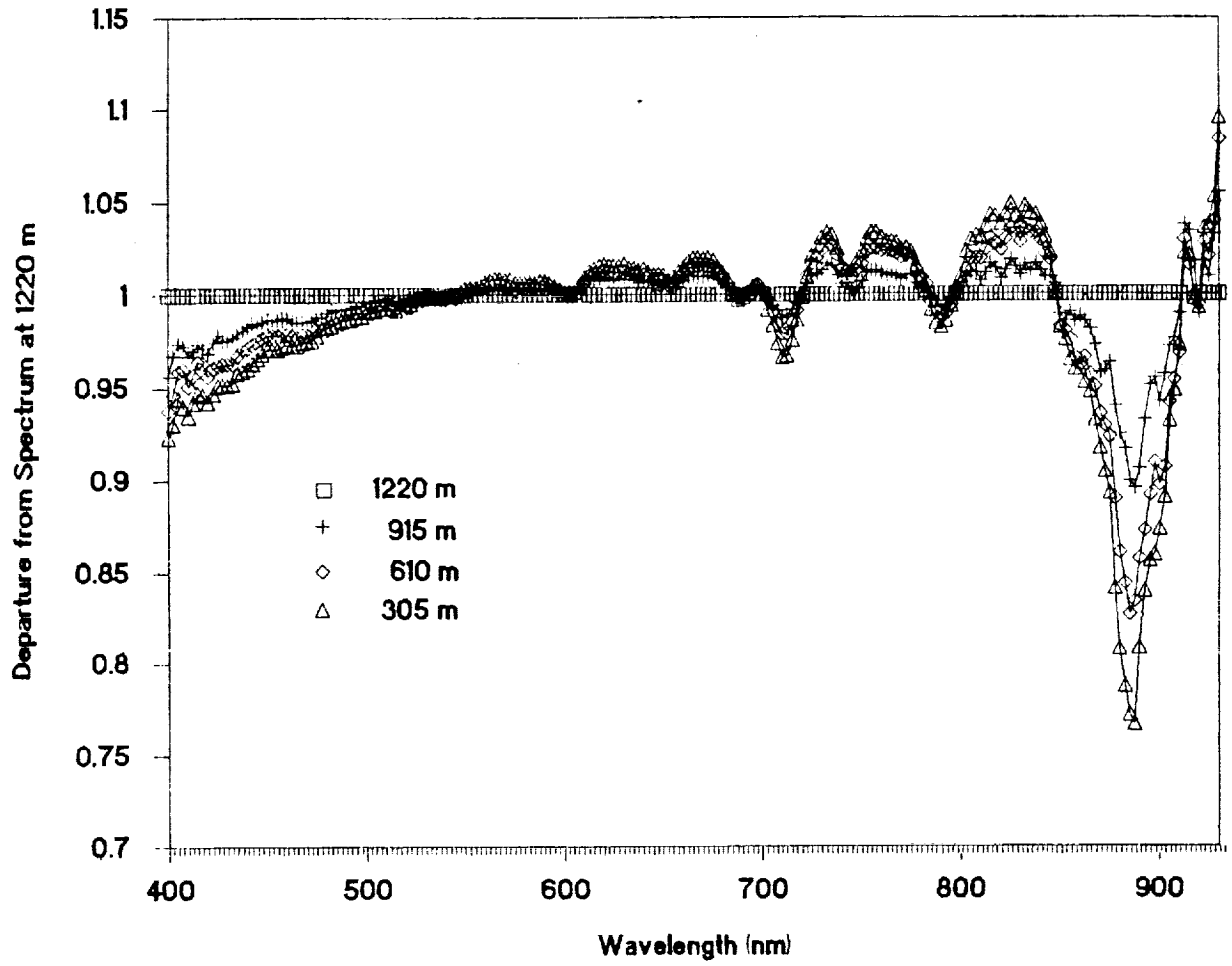

Fig. 2 In-flight calibration from an ultralight aircraft contrasts reference spectrum obtained above haze at 1220 m with spectral departures from this reference line as the plane drops through layers of haze down to an elevation of 305 m. To eliminate variation in brightness across the scene, the brightness value recorded in each wave band was first divided by the total brightness values for all wavelengths recorded in a given pixel.

Title: Airborne Oceanography: An Update

Author: John M. Bane, Jr., University of North Carolina

Discipline: Oceans

Oceanic measurements from aircraft are made with both remote sensors and deployable sensors. The suite of available aircraft oceanographic sensors is growing rapidly at present, with new deployable probes available (at least as prototypes) for profiling the ocean's temperature, salinity and light fields. Recent advances in the Global Positioning System (GPS) satellite constellation promises to provide significantly improved accuracy in the determination of aircraft absolute altitude. This determination is necessary for measuring the dynamic topography of the sea surface on horizontal scales of tens to hundreds of kilometers, the scales associated with ocean circulation.

This presentation will focus on the status of these new sensors and techniques, and it will highlight recent research programs that have utilized aircraft in oceanic measurements.

Title: New Techniques for Airborne Turbulent Flux Measurement

Author: Donald H. Lenschow, National Center for Atmospheric Research

Discipline: Atmosphere

Airborne flux measurements play a vital role in a variety of atmospheric research studies, from estimating surface deposition or emission of trace atmospheric constituents to measuring momentum flux in studies of momentum transport by convective cloud systems. The prime advantage of aircraft is their mobility. They can reach remote locations and take multi-level measurements in time intervals that are small compared to synoptic or diurnal variations. On the other hand, their mobility and response to turbulence add to the difficulty in obtaining accurate flux measurements. Since aircraft need to fly relatively fast compared to the mean wind speed in order to stay airborne, faster instrument response is required than for fixed-point measurements. Furthermore, corrections may have to be made for compressibility, adiabatic and frictional heating, and flow distortion induced by the aircraft.

The most direct means for estimating a turbulent flux involves measuring an air velocity fluctuation concurrently with the quantity whose flux is being measured, and averaging their product over a distance long enough to obtain a statistically stable estimate. The measurements required to resolve air motions must include measurement of both the airplane motion with respect to the earth and the velocity of the air with respect to the airplane. The velocity and attitude angles of the airplane are usually obtained from an inertial navigation system (INS), that has sufficient inherent accuracy for flux measurement under most conditions. In most cases, errors in air velocity measurements limit the accuracy of air motion for flux measurements. A major difficulty is that in situ flow sensors are measuring in a perturbed flow. This necessitates inflight calibration techniques which limits the accuracy of air velocity measurements. A solution to this may be a laser air motion sensing system which has the potential for obtaining absolute measurements of the air velocity far enough away from the airplane fuselage that flow distortion is negligible.

Since the flux is computed from a product of fluctuations, an accurate mean value of the constituent whose flux is being measured is not necessary; only the fluctuations need to be resolved. Furthermore, the constituent measurement can be noisy, as long as the noise is not correlated with the velocity. The standard deviation of uncorrelated noise can be as much as several times the ratio of the surface constituent flux to the convective velocity scale before the noise significantly affects the flux measurement. However, the sample length of the constituent measurement must be less than about ten meters in order to avoid significant errors in the measured flux. This can be accomplished by either (1)

using sensors with adequate frequency response to resolve 10 m wavelengths or, if that is not possible, (2) collecting a sample of air in less than ten meters flight distance and then measuring the constituent in the sample, that can be done over a longer period, or (3) conditionally sampling the air using vertical air velocity as an indicator function to determine where to store the sample (updraft air in one reservoir; downdraft air in another), and possibly also to determine the rate at which the air is collected.

Present aircraft systems are generally sufficiently accurate for measuring scalar fluxes for a wide range of meteorological problems. In the convective boundary layer (CBL), turbulence fluxes of temperature, humidity ozone, carbon dioxide, methane and carbon monoxide have been obtained with current aircraft systems. However, there are limitations: First, if the flux is small, errors in measurement due to flow distortion and compressibility may be significant. Second, in a stably-stratified boundary layer, the required frequency response is higher than in the CBL convective boundary layer, so that even if measurements are feasible in the CBL, they may not be in the stably-stratified boundary layer; furthermore, turbulent mixing processes tend to be intermittent there, so that sampling requirements are more difficult to estimate.

Measurement of momentum flux poses special problems. First, it is difficult to avoid contamination of the vertical and lateral velocity component measurements by the longitudinal component, and second, the required sampling length to obtain statistically significant measurements is usually longer than that required for scalar flux measurements in the boundary layer. It may be possible to alleviate the first problem by use of a laser-based velocity measuring technique. The second could, perhaps, be best addressed by use of some remote sensing area-averaging technique. Although area-averaging seems a difficult challenge for momentum flux, lidar technology does have the potential to measure an along-beam velocity component. Combining this with remote measurement of species concentration with, for example, Differential Absorption Lidar (DIAL) offers the possibility of remote measurement of some trace species fluxes (e.g., water vapor and ozone). Measurements of flux profiles throughout the boundary layer while flying at one level would then be possible.

N91-25446

Title: Airborne Lidar Research

Author: S. Harvey Melfi, NASA/Goddard Space Flight Center

Discipline: Atmosphere

The planetary boundary layer (PBL) is the lowest layer of the atmosphere in contact with the Earth's surface. It plays an important role in atmospheric circulation and dynamics by influencing surface fluxes of moisture, heat, and momentum. It also provides an important reservoir of readily available moisture to fuel deep convective development. The PBL is characterized by its temperature, moisture and wind profiles, its height, and most importantly, by its turbulence structure. Organized convection within the PBL may generate gravity waves within the free troposphere. These waves can propagate vertically, modifying global circulation. Remote sensing of the PBL using a downward-looking lidar is providing new insight into dynamic processes of this important layer and its connection with wave generation. An airborne lidar is an ideal tool to study the PBL since aerosols are frequently trapped in this layer.

The lidar is installed on the NASA Electra aircraft. It consists of a frequency doubled Nd:YAG laser aligned with a 40-cm diameter telescope. As the laser beam propagates downward from the aircraft toward the surface, it is scattered by the aerosols and molecules in the atmosphere. Generally, there is a sharp gradient of aerosol scattering associated with the PBL top, with high aerosol scattering from within the PBL, and generally very low scattering from the free atmosphere above. It is this gradient in aerosol scattering that is used to visualize the structure of the PBL. A small portion of the scattered radiation is collected by the telescope, filtered, detected by a photomultiplier, and digitized at 100 nsec rate (corresponding to 15-m vertical resolution). The horizontal resolution is typically around 13 m, using a 10 Hz laser and a nominal aircraft speed of 130 m/sec. In other words, with the laser continuously firing as the aircraft moves, the resolution of features in the atmosphere below the aircraft is about 15 x 13 m.

Results from several recent studies will be presented and discussed.

Title: Update on the NASA/JPL AIRSAR System

Author: Jacob van Zyl, Jet Propulsion Laboratory

OMIT TO P71

Discipline: Land

Abstract will be available at the Workshop.

Title: A Dual-Beam Technique for Deriving Wind Fields from the NOAA P-3's Airborne Doppler Radar

Author: David P. Jorgensen, NOAA/National Severe Storms Laboratory

Discipline: Atmosphere

A new technique for deriving horizontal and vertical air motions using the NOAA P–3's airborne Doppler radar is presented and discussed. This technique utilizes the horizontal scanning ability of the current NOAA P–3 tail-mounted radar antenna to view a region of space from two vantage points along a single straight-line flight track. Because the antenna is alternately looking forward and then aft of the flight track on alternate vertical scans (Fig. 1) this technique is termed the "Fore/Aft Scanning Technique" or FAST. The major advantage of FAST over the previous technique of flying two quasi-perpendicular flight tracks with the antenna scanning in a vertical plane normal to the flight track is that the data are collected in roughly half the time. However, accuracy of the resulting wind field is compromised slightly because the beam intersection angle is reduced from 90° to about 50°. Fig. 2 illustrates the two approaches. A wind vector is calculated at the intersection of the two beams. The effective horizontal data density of observations using FAST is roughly half of what can be obtained by flying 2 perpendicular flight legs if the antenna is operated in a 360° vertical sweep mode. However, if data from only one side of the aircraft is desired then the antenna can be operated in a sector-scanning mode yielding nearly the same horizontal data density as the previous method (~1 km). One major complication that arises when the FAST method is used is the substantial contamination of the observed radial velocity due to the component of the aircraft's motion seen by the forward (or aft) looking beam. At typical P–3 ground speeds of ~125 m s^{-1}, the contamination component is ~53 m s^{-1}. Evidence will be shown that demonstrates that this contamination velocity can be removed by examination of the ground velocity. The reduction of area covered because of the drift angle is also discussed. To show the utility of the method, analyses of data collected using this technique are compared to conventional dual-Doppler-derived wind fields constructed from data collected simultaneously by S-band ground-based Doppler radars from a highly stratiform weather system that occurred in central Oklahoma in June 1989.

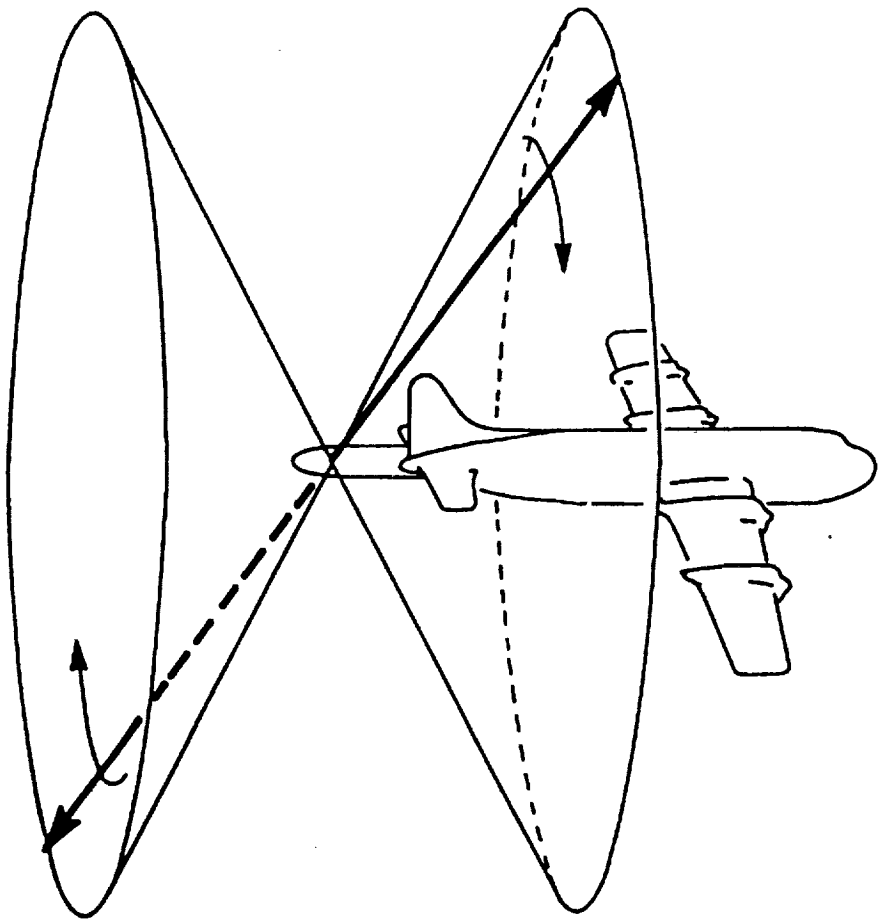

Fig. 1 Schematic illustration of the NOAA P-3's tail Doppler radar FAST scan capability. The antenna sweeps through a vertical plane first pointed forward ~25° and then aft ~25° from a vertical plane normal to the flight track. The rotation rate can be as high as 60° s^{-1} (10 RPM).

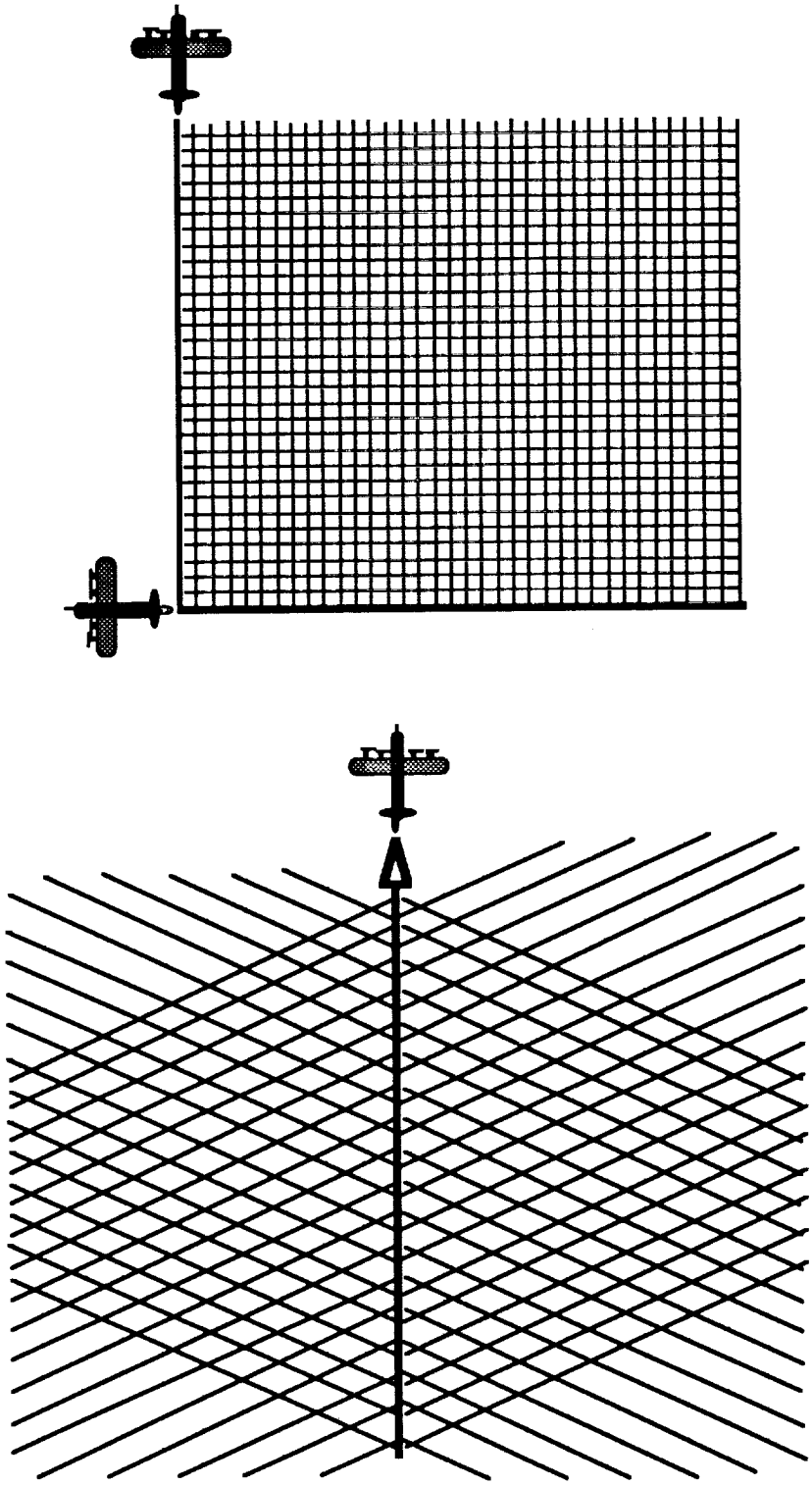

Fig. 2 Horizontal projection of the radar beams from the airborne Doppler radar for the case of two quasi-perpendicular flight legs (top diagram) and for the FAST technique (bottom diagram).

PRECEDING PAGE BLANK NOT FILMED

PAGE 48 INTENTIONALLY BLANK

Title: ALIAS ER-2 Laser Measurements of Atmospheric Composition and Chemistry

Author: Christopher Webster, Jet Propulsion Laboratory

Discipline: Atmosphere

Abstract will be available at the Workshop.

Title: Airborne Hyperspectral Imaging: Applications and Analysis Methods

Author: Alexander F.H. Goetz, University of Colorado

Discipline: Atmosphere, Land, and Oceans

Hyperspectral imaging carried out by imaging spectrometers, at present airborne but in the future spaceborne, provides a wealth of new information about the Earth and makes quantitative remote sensing possible. The single most important advantage of an imaging spectrometer over a multispectral scanner is the contiguous nature of the spectral channels. This fact makes possible deterministic types of processing for data analysis instead of only statistical inferential approaches with multispectral sensors. In turn, the complete information content of the data makes it possible to address problems based on the underlying physical principles in a quantitative way, a more fundamental and ultimately more satisfying approach.

A number of data analysis techniques have been developed that make it possible to directly identify materials on the surface from the reflectance spectra and in addition make it possible to determine the relative abundance of the different materials found within a single pixel.

The applications range from water vapor determination in the atmosphere, to new techniques for cloud cover determination, to determination of chlorophyll and accessory pigments in Class I and Class II marine and fresh waters to biochemistry of vegetation canopies. In each case, the contiguous nature of the spectral channels and the full wavelength coverage in the solar reflected region of the spectrum provides the basis for quantitative information extraction.

Title: Airborne Passive Microwave Measurements: The Electronically Steered Thinned Array Radiometer

Author: Calvin T. Swift, University of Massachusetts

Discipline: Atmosphere

Abstract will be available at the Workshop.

Title: Matching Recording Techniques with Aircraft Data Collection Requirements

Author: Alan Goldstein, NOAA/Aircraft Operations Center

Discipline: Aircraft Data Management

Abstract will be available at the Workshop.

Title: Airborne Geoscience Activities in DoD

Author: Alan Weinstein, Office of Naval Research

Discipline: Aircraft Applications

Abstract will be available at the Workshop.

Title: **Tropical Ocean Global Atmosphere/Coupled Ocean Atmosphere Response Experiment (TOGA/COARE)**

Author: **Joachim P. Kuettner, University Corporation for Atmospheric Research**

Discipline: **Atmosphere and Oceans**

TOGA/COARE addresses the coupling processes over the "West-Pacific warm pool," responsible, among others, for the El Niño events. It will take place from November 1992 to February 1993, preceded by a 1-year enhanced monitoring period.

The multi-scale experiment requires the participation of the NASA DC-8 (equipped with Omega-Dropwindsonde capability, SST and microwave sensors), the NCAR-Electra (equipped with "ElDORA"-Doppler Radar and airmotion system), and two NOAA P-3s (equipped similarly, plus an Omega-Dropwindsonde capability). They will probe the intensive "Super cluster" convective systems over the "Primary Flux Array," an octagon ship array with Dual-Doppler capability carrying Integrated Sounding Systems.

A key to the field operation will be a voice and data communication system connecting the platforms and operation bases via satellite. Ten countries are expected to participate.

Title: Polar Ozone

Author: J.J. Margitan, Jet Propulsion Laboratory

Discipline: Atmospheric and Oceanographic Sciences

Since the identification of the Antarctic ozone hole by Farman in 1985, the polar stratosphere has been a major focus of study by the atmospheric science community. In the last five years, there have been several ground-based campaigns and two major aircraft expeditions: the 1987 Airborne Antarctic Ozone Experiment (AAOE) and the 1989 Airborne Arctic Stratospheric Expedition (AASE), both of which utilized the NASA DC-8 and ER-2 aircraft equipped with a suite of instruments from several NASA Centers, other government laboratories, and universities in undertakings jointly sponsored by NASA, NOAA, NSF, and the Chemical Manufacturers Association (CMA), as well as several participating foreign agencies. As a result of this intense study, we now understand that the isolated, cold airmass of the polar vortex sets up the conditions leading to denitrification (sometimes dehydration) and the conversion of inactive chlorine reservoirs (HCl and $ClONO_2$) into active Cl and ClO. These conditions of perturbed chemistry exist sufficiently long in the Antarctic so that large depletions of ozone have occurred. While the Arctic stratosphere has been seen to be "primed" for ozone depletion, and some studies have inferred depletion, the early breakup of the Arctic vortex has prevented the formation of an Arctic hole on the scale of the Antarctic. The results of these campaigns, our understanding of polar ozone, and outstanding questions for future missions will be discussed.

Title: **The Atlantic Stratocumulus Transition Experiment (ASTEX)**

Author: **Bruce A. Albrecht, Pennsylvania State University**

Discipline: **Atmosphere**

The representation of boundary layer clouds (stratocumulus and trade cumulus) in large-scale and mesoscale models continues to be an unresolved problem. These clouds have, however, a pronounced effect on the earth's radiation budget and on the visibility in the lower layers of the atmosphere. Their representation in models is complicated by the fact that they are frequently less than 500 m thick and are intimately connected to the boundary layer turbulence. Thus in large-scale or mesoscale models their effects must be parameterized or represented as functions of the resolvable fields.

The development of parameterizations requires an understanding of the processes that generate, maintain, and dissipate boundary layer clouds. This development is currently impeded by a lack of understanding of the transition from stratocumulus clouds to trade cumulus clouds and the factors that control cloud type and amount in the boundary layer. The Atlantic Stratocumulus Transition Experiment (ASTEX) will address key issues associated with stratocumulus to trade-cumulus transition and cloud mode selection. This experiment will involve intensive measurements from several platforms and is designed to study how the transition and mode selection are affected by 1) cloud-top entrainment instability, 2) diurnal decoupling and clearing due to solar absorption 3) patchy drizzle and a transition to horizontally inhomogeneous clouds through decoupling 4) mesoscale variability in cloud thickness and associated mesoscale circulations, and 5) episodic strong subsidence lowering the inversion below the lifting condensation level.

From a broader perspective, ASTEX is designed to provide improved dynamical, radiative, and microphysical models and an improved understanding of the impact of aerosols, cloud microphysics, and chemistry on large-scale cloud properties. ASTEX is part of the First ISSCP Regional Experiment (FIRE) and has multiagency support with the Office of Naval Research (ONR) as the lead agency. In addition, scientists from the United Kingdom, France and Portugal will be participating in ASTEX.

ASTEX will involve coordinated measurements from aircraft, satellite, ships, islands and moored buoys in the area of the Azores and Madeira Islands. This area is shown in Fig. 1 and was selected since 1) this area is favorable for low-level cloud conditions ranging from solid stratocumulus decks to broken trade cumulus, 2) the islands in this region provide suitable sites for surface observations and aircraft operations, and 3) the ASTEX efforts will be coordinated with an oceanographic investigation, the Subduction Accelerated Research Initiative (SARI) of ONR.

ASTEX is scheduled for June of 1992. Climatologies based on several years of satellite analyses, ECMWF analyses, and surface measurements from the islands indicate that during June this region is typically dominated by subsiding trade-

wind flow (Fig. 2) associated with a maximum in low-cloud amount. The satellite studies indicate a wide range of cloud amounts and types between Madeira and the Azores during June and July.

The goals of ASTEX will be pursued by combining measurements from several platforms. Continuous wind profiling with frequent radiosonde measurements will be made from Santa Maria in the Azores, Porto Santo in the Madeiras, and an anchored ship. These points will form a triangle (see Fig. 1) approximately 800 km on a side. Large-scale mass, energy, and moisture budgets will be calculated using the data collected from the vertices of the triangle. In addition, a French ship, which is part of Surface of the Ocean Fluxes and Interaction with the Atmosphere (SOFIA), will be anchored in the triangle to make surface flux and upper-air measurements. With this ship a set of smaller triangles can be used for budget calculations. Remote sensing of cloud properties from Santa Maria and Porto Santo will be used to examine the time evolution of the clouds in different convective regimes. The instrumentation planned for both islands includes a microwave radiometer, a ceilometer, a cloud radar, a wind profiler, and RASS. Moored buoys that will be deployed as part of the ONR SARI program will be used to define ocean and surface meteorological conditions in the area of interest.

Aircraft will be invaluable for investigating the transition from stratocumulus to cumulus and cloud mode selection during ASTEX since they provide the mobility needed to study events as they occur in the triangular area defined by the two islands and the ship. They will be used to describe the cloud microphysical, turbulent, radiative, chemical, and aerosol properties both in and above the boundary layer. In addition, aircraft observations will be compared directly with those from satellite and in situ and remote sensors on the islands and ships. At least four aircraft will be required to minimize the difficulty of separating time and space variations that is inherent with aircraft measurements. Two aircraft must be equipped to measure turbulent fluxes and the thermodynamic properties in and above the boundary layer. A third is needed to measure cloud and radiative properties while a fourth will be operated at high levels to map cloud-top height, cloud radiative properties, and serve as a platform from which low-level aircraft could be directed to study features of interest.

The preferred platforms for boundary layer and cloud measurements are the UK C-130, the National Center for Atmospheric Research (NCAR) Electra, and the U. of Washington C-131A. The UK C-130 and the NCAR Electra have comparable turbulence and cloud microphysical instrumentation. In addition, the Electra has a Doppler lidar system that can be used to map cloud-base and cloud-top variations and motions near and above the inversion. A fast response ozone sensor and a suite of instruments for various aerosol and chemistry measurements will also be included on the Electra. It is anticipated that the chemistry measurements made during ASTEX will contribute to the International Atmospheric Chemistry Program. The University of Washington C-131A is equipped to make detailed cloud physics, cloud radiation, and cloud chemistry measurements. The NASA DC-8 is the platform of choice for the radiation measurements and cloud-top mapping. It will link the low-level aircraft and surface-based measurements to satellite observations. It may also be used to launch dropwindsondes to supplement the measurements from the islands and the ships.

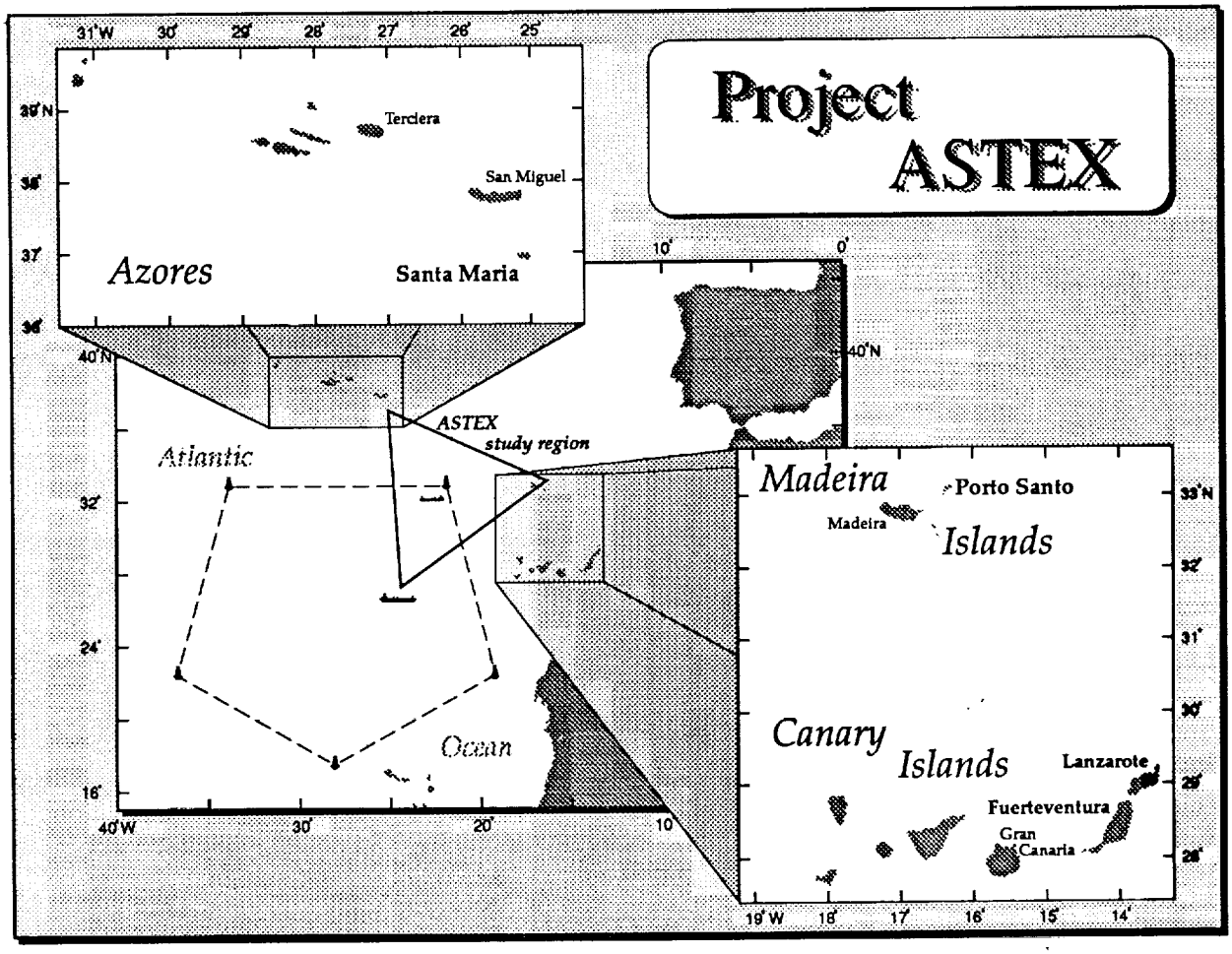

Figure 1. Map of ASTEX region showing location of proposed wind profiler/upper-air network and buoys during the subduction experiment.

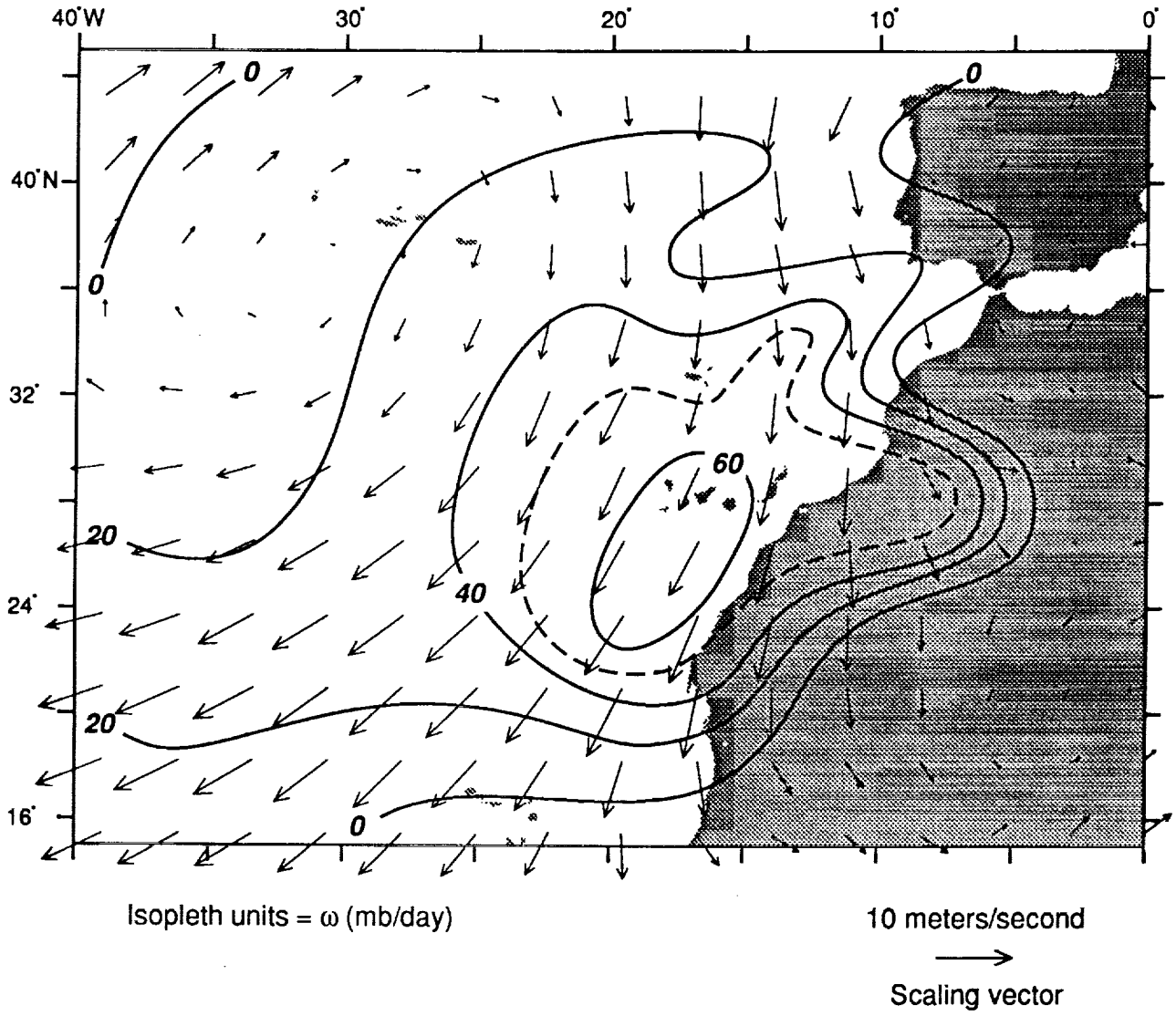

Figure 2. Resultant-wind vectors at 1000 mb and vertical velocity (omega) at 850 mb for June of 1984 from ECMWF analyses.

Title: **High-Resolution Remote Sensing**

Author: **Frank L. Herr, Office of Naval Research**

Discipline: **Atmosphere and Oceans**

In order to properly extract geophysical information from airborne and satellite sensors and to interpret high-resolution radar imagery of the ocean, the Office of Naval Research (ONR) has developed a series of multidisciplinary research initiatives to investigate precisely how the marine boundary layer and the upper ocean affect backscatter and emission. These field efforts have involved airborne remote sensing assets used in close coordination with *in situ* sensing of key geophysical parameters. Elements of two of these initiatives, SAXON-FPN and High Res ARI, will be discussed.

The SAR and X-Band Ocean Nonlinearities Experiment (SAXON-FPN) was a joint German/American experiment taking place in November 1990 in the North Sea German Bight on and near the German Forschungsplattform Nordsee (FPN). SAXON-FPN was the fourth in a series of remote sensing experiments centered around ocean platforms and aimed at understanding radar backscatter from the sea surface and SAR imagery of the surface. The Co-Principal Investigators are William J. Plant of the Woods Hole Oceanographic Institution and Werner Alpers of Universitaet Hamburg.

The primary objective of SAXON-FPN was to investigate radar backscatter and SAR imagery at a variety of microwave frequencies under high sea state conditions which try critical aspects of the theories. In particular, the steep waves typically found in the North Sea during the fall allow such investigations under extremely nonlinear hydrodynamic and imaging conditions. For instance, the limits of applicability of specular and composite Bragg scattering theories, the most viable theories of how the ocean surface scatters microwaves, are presently unknown. Similarly, while present SAR imaging theories unanimously predict nonlinear dependences of the final image on sea surface conditions, the degree to which these nonlinearities are present under different surface conditions is not known.

Aircraft measurements made during SAXON-FPN included fully polarimetric synthetic aperture imagery at L, C, X and Ka bands; dual polarized real aperture imagery at C, X, and W bands; laser profilometer measurements; quasi-simultaneous scatterometry at five frequencies from 1 to 15GHz; measurements of directional wave spectra; and sea surface temperature measurements. Measurements from the FPN during SAXON-FPN included the following: meteorological determination of fluxes and ambient conditions; measurements of directional wave spectra; stereophotography of small-scale structure on the sea

surface; surface tension measurements; wave height, slope, and curvature measurements by laser techniques; microwave measurements of the normalized radar cross-section of the sea; ocean wave-radar modulation transfer functions; polarization matrices; and scattering statistics. Buoys provided additional meteorological and directional wave spectral measurements.

The High Resolution Remote Sensing ARI is a joint project between ONR and the Naval Research Laboratory (NRL) to predict the modulations in radar backscatter developed by interactions of surface waves and ocean currents at open ocean submesoscale features. The Hi-Res project seeks to develop and improve the physical models used to predict a SAR image of a two-dimensional open ocean feature such as a front under weak to moderate wind forcing. Field experiments are planned for September 1991 and summer 1993 near the Gulf Stream off Cape Hatteras; the latter date will hopefully take advantage of SIR-C and ERS-1. Principal Investigators are George Marmorino/NRL and Donald R. Thompson/Johns Hopkins University, Applied Physics Laboratory.

In recent years, efforts directed toward interpreting SAR images of the ocean have concentrated on developing a series of models to codify the physics involved in upper ocean current fields, surface wave-current interactions, radar backscatter, and SAR imaging mechanisms. Modeling efforts are underway to extend the applicability of 2-D SAR image reconstruction to increasingly complex ocean features involving curvilinear flows and current shears. Atmospheric boundary layer dynamics will be explicitly considered in future models. Multidisciplinary field experiments are planned to collect data sets useful for constraining the above models, allowing quantitative prediction of backscatter intensity variations in the radar images. Currently, 1-D features such as internal wave convergence-divergences can be quantitatively modeled with some precision, but it is not clear how realistically the models treat 2-D variability of model parameters such as surface current fields, wind stress and wave growth, air-sea temperature differences, and surface wave spectra at the boundaries of the region of interest.

Aircraft measurements to be made during the Hi-Res field experiments include three-frequency, fully polarimetric SAR imagery using the P-3 flown by Naval Air Development Center; dual polarized real aperture imagery at C and X bands; and laser profilometer measurements flown on the NRL P-3. In addition, airborne meteorological flux measurements will be made in coordination with radar imagery and scatterometer measurements by a fixed wing aircraft and an airship using a tethered meteorological sled.

N91-25447

Title: NASA 1990 Multisensor Airborne Campaigns (MACs) for Ecosystem and Watershed Studies

Authors: Diane E. Wickland, NASA Headquarters
Ghassem Asrar, NASA Headquarters
Robert E. Murphy, NASA Headquarters

Discipline: Ecology and Hydrology

The Multisensor Airborne Campaign (MAC) focus within NASA's former Land Processes research program was conceived to achieve the following objectives: 1) to acquire relatively complete, multisensor data sets for well-studied field sites, 2) to add a strong remote sensing science component to ecology-, hydrology-, and geology-oriented field projects, 3) to create a research environment that promotes strong interactions among scientists within the program, and 4) to more efficiently utilize and compete for the NASA fleet of remote sensing aircraft. The successes of the first MAC, the 1989 Geologic Remote Sensing Field Experiment (GRSFE), were reported on at the last Airborne Geoscience Workshop. Four new MACs were conducted in 1990: 1) the Oregon Transect Ecosystem Research (OTTER) project along an east-west transect through central Oregon, 2) the Forest Ecosystem Dynamics (FED) project at the Northern Experimental Forest in Howland, Maine, 3) the MACHYDRO project in the Mahantango Creek watershed in central Pennsylvania, and 4) the Walnut Gulch project near Tombstone, Arizona.

The OTTER project is testing a model that estimates the major fluxes of carbon, nitrogen, and water through temperate coniferous forest ecosystems. The focus in this project is on short time-scale (days-year) variations in ecosystem function. Four intensive field campaigns (IFCs) were conducted in 1990 to capture the seasonal variability along the transect. Data from the following airborne sensors were acquired in at least one of the IFCs: Daedalus Airborne Thematic Mapper, Airborne Visible-Infrared Imaging Spectrometer (AVIRIS), Advance Solid-state Array Spectrometer (ASAS), Airborne Synthetic Aperture Radar (AIRSAR), Airborne Tracking Sunphotometer (ASTP), Thermal Infrared Multispectral Scanner, NS-001 thematic mapper simulator (TMS), the Fluorescence Line Imager (FLI), and the Compact Airborne Spectrographic Imager (CASI). A novel component of the project was the use of an ultralight aircraft carrying several spectrometers for low altitude remote sensing. The Pilot Land Data System is being used to receive, archive, and distribute OTTER aircraft data to project participants. Much of the field data for OTTER is being archived at OSU in cooperation with the NSF Long-Term Ecological Research (LTER) program.

The FED project is concerned with modeling vegetation changes of forest ecosystems using remotely sensed observations to extract biophysical properties of forest canopies. The focus in this project is on long time-scale (decades to millenia) changes in ecosystem structure. The first FED IFC was conducted in September, 1990, and another is planned for June, 1991. Data from the following airborne sensors are being acquired: ASAS, AVIRIS, AIRSAR, NS-001 TMS, TIMS, ASTP, Push-Broom Microwave Radiometer (PBMR), and Electronically Scanned Thinned Array Radiometer (ESTAR). A helicopter mounted with spectrometers, the Airborne Laser Polarimeter System (ALPS), and a scatterometer was used for low altitude remote sensing. A geographic information system (GIS) will be used to integrate of all these data sets.

The MACHYDRO project is studying the role of soil moisture and its regulating effects on hydrologic processes. The focus of the study is to delineate soil moisture differences within a basin and their changes with respect to evapotranspiration, rainfall, and streamflow. The emphasis will be on measurements of soil moisture in a spatial and temporal context by using a combination

of *in situ* and remote sensing techniques in a small basin in Pennsylvania. The usefulness of AIRSAR and passive microwave radiometers for measuring the distribution and changes in soil moisture are being assessed. A combination of remotely sensed and traditional point measurements of hydrologic variables are used in conjunction with distributed hydrologic model(s) in two different ways: 1) to use these data as input to the model(s) to close the water balance equation; or 2) to compare model simulation results (i.e. soil moisture) with remotely sensed estimates.

The Walnut Gulch project is focused on the effects of soil moisture on the energy and water balance of arid and semiarid ecosystems and their feedbacks to the atmosphere via thermal forcing. The main objective of this study is to assess the usefulness of multispectral remotely sensed data in providing estimates of surface soil moisture, albedo, and radiative temperature at different spatial and temporal scales that can be used in conjunction with simple process-based hydrologic models for studying the land-surface-atmosphere exchange in these ecosystems. Measurements of land-surface and atmospheric properties were obtained with the aid of ground-based and airborne sensors over a three week period during the "monsoon" season in Arizona. These data sets will be distributed among the participating scientists for further analysis.

The 1990 MACs have produced some of the most complete airborne multisensor data sets ever assembled for ecological and hydrological research. Once they are suitably prepared for analysis and quality controlled, these data sets will be made available to the scientific research community through PLDS and other agency data systems. It is hoped that these data will be used by many scientists outside of the projects which generated them to better understand the biophysics of remote sensing, to simulate EOS data, and to begin the sorts of Global Change analyses that will be done with EOS data.

omit to p.79

Title: Global Energy and Water Cycle Experiment (GEWEX)

Authors: Deborah Vane, Jet Propulsion Laboratory
Moustafa Chahine, Jet Propulsion Laboratory

Discipline: Multidisciplinary

The Global Water and Energy Cycle Experiment (GEWEX) is a core component of the World Climate Research Programme (WCRP). The scientific objectives of GEWEX are:

-- to determine the hydrological cycle and energy fluxes by means of global measurements of observable atmospheric and surface properties;

-- to model the global hydrological cycle and its impacts on the atmosphere and ocean;

-- to develop the ability to predict the variations of global and regional hydrological processes and water resources, and their response to environmental change; and,

-- to foster the development of observing techniques and data management and assimilation systems, suitable for operational applications to long-range weather forecasts, hydrology and climate predictions.

Within this context, a central goal of the GEWEX program is to develop and improve macroscale hydrological models to integrate surface and groundwater processes on the catchment scale into fully interactive representations of the global ocean-land-atmosphere system. The Joint Scientific Committee (JSC) has endorsed the concept of a GEWEX Continental-Scale International Project (GCIP) whose objectives would be to: (1) develop and validate macroscale hydrological models and coupled hydrological/atmospheric models, (2) develop and validate information retrieval schemes incorporating existing and future satellite observations and in-situ measurements, and (3) provide a capability to translate the effects of a future climate change into impact on water resources on a regional basis.

The GCIP is a major project requiring international collaboration. The Mississippi Basin has been proposed as the location primarily because of the availability of very good three-dimensional rainfall data expected to be available through the NEXRAD system, and because of the exploitation and quality control of the existing surface and subsurface hydrological data. The GCIP will be implemented in stages, beginning as early as Fiscal Year 1992, and is expected to have a duration of approximately five years.

Title: National STorm-scale Operation and Research Meteorology (STORM) Program Field Experiments

Author: Richard A Dirks, National Center for Atmospheric Research

Discipline: Atmosphere

The National STORM Program (a.k.a. U.S. Weather Research Program) is a broad interagency initiative on mesoscale weather with the goal of advancing weather observing capabilities and fundamental understanding of the nature of weather and to use this understanding to improve numerical weather prediction and enhance weather services provided to the Nation.

This decade-long program capitalizes on the current modernization of the nation's weather observing systems (NEXRAD radar, GOES-NEXT, Automated Surface Observing Systems, wind profilers) which form a vastly improved base for conducting research on mesoscale weather.

A series of special field observing programs utilizing research aircraft is planned. The first set of experiments, STORM I (Central U.S.), consists of a systems test (STORM-FEST, February-March 1992), a spring/summer multiscale experiment (April-July 1993) and a winter/spring multi-scale experiment (January-April 1994). Later phases of STORM (1995-2000) will extend the observing domain to include the continental United States and coastal regions.

The STORM Field Experiments will require several new capabilities:

1. Over the horizon communications (via satellite), both voice and data, between ground and aircraft.

2. Dropwindsondes deployable (safely) from high altitude (45,000 feet) over land.

3. Dual beam scanning airborne Doppler radar.

4. Improved moisture measurements (liquid water, humidity)

5. GPS aircraft navigation and positioning.

6. Mid-sized jet aircraft with high altitude capability.

Title: Airborne Facilities of the National Center for Atmospheric Research

Author: Lawrence F. Radke, National Center for Atmospheric Research

Discipline: Atmosphere and Oceans

The Research Aviation Facility (RAF) operates four aircraft in direct support of observational research studies of atmospheric chemistry, cloud physics, mesoscale meteorology, boundary-layer dynamics, air-sea interactions, oceanography, and other fields within the atmospheric sciences. The aircraft and their typical performance characteristics are listed below:

RAF #	Type	Endurance (h)	Range (n mi)	Maximum Altitude (ft)	Maximum Payload (lb)	Cabin Volume (ft^3)
29J	Schweitzer	unpowered	glider	–	600	–
312	King Air	7.3	1,800	35,000	2,340	360
307	Sabreliner	2.5	1,300	43,000	2,250	480
308	Electra	8.5	2,400	28,000	20,800	4,700

The powered aircraft are equipped to measure atmospheric state parameters, turbulent fluxes up to 10 Hz equivalent wavelength, cloud physics parameters, and atmospheric trace gases. Radiometers (shortwave, longwave, and ultraviolet), remote radiometric surface-temperature sensors, and video cameras are available. The King Air and Electra aircraft are also equipped for dropwindsonde and oceanographic dropsonde dispensing and data acquisition. The glider is an extremely rugged specialty platform available for electric field and cumulus cloud research.

Currently the RAF is in the midst of a major expansion of its active remote sensing capabilities with both a 10 μm Doppler lidar and an extremely sophisticated Doppler radar soon to be deployed. In addition to NCAR-provided instrumention, the facility is committed to support the adaptation and installation of user-supplied equipment on the RAF aircraft.

The aircraft are equipped with computer controlled data systems, which also provide a friendly real-time data display in user selectable formats within a workstation environment. Data tapes generated during flights are processed by the RAF Computing Group to produce a standard output tape containing measured and derived parameters. For quick-look analysis and planning future missions, near real-time processing of the raw data tapes can be done on site, using RAF hardware and software. Some data analysis software are available to users.

The RAF scientific, engineering and technical staff can advise, assist or join users in the aeronautical, chemical and electrical engineering design and fabrication of specialized airborne research equipment. Guidance in sampling and measurements can also be provided. Aviation and science staffs will help project scientists with experimental design and operational and flight planning.

Title: NASA/Ames Research Center's Science and Applications Aircraft Program

Author: G. Warren Hall, NASA/Ames Research Center

Discipline: Aircraft Operations

NASA-Ames Research Center operates a fleet of seven Science and Applications Aircraft, namely the C-141/Kuiper Airborne Observatory (KAO), DC-8, C-130, Lear Jet and three ER-2s. These aircraft are used to satisfy two major objectives, each of equal importance. The first is to acquire remote and in situ scientific data in astronomy, astrophysics, earth sciences, ocean processes, atmospheric physics, meteorology, materials processing and life sciences.

The second major objective is to expedite the development of sensors and their attendant algorithms for ultimate use in space (shuttle and free-flying satellites) and to simulate from an aircraft, the data to be acquired from spaceborne sensors.

NASA-Ames Science and Applications Aircraft are recognized as national and international facilities. They have performed and will continue to perform, operational missions from bases in the United States and worldwide. Historically, twice as many investigators have requested flight time than could be accommodated. This situation remains true today and is expected to increase in the years ahead.

A major advantage of the existing fleet of aircraft is their ability to cover a large expanse of the earth's ecosystem from the surface to the lower stratosphere over large distances and times aloft. Their large payload capability allows a number of scientists to use multi-investigator sensor suites to permit simultaneous and complementary data gathering. In-flight changes to the sensors or data systems have greatly reduced the time required to optimize the development of new instruments. It is doubtful that spaceborne systems will ever totally replace the need for airborne science aircraft. This presentation addresses the operations philosophy and capabilities of the Science and Applications Aircraft as they currently exist at NASA-Ames Research Center.

N91-25449

20117

P3

Title: Goddard Space Flight Center/Wallops Flight Facility Airborne Geoscience Support Capability

Author: Roger L. Navarro, NASA/Wallops Flight Facility

NE 200400

Discipline: Aircraft Operations

Goddard Space Flight Center's Wallops Flight Facility (GSFC/WFF), located on Virginia's Eastern Shore, operates six aircraft which are used as airborne geoscience platforms. The aircraft complement consists of two UH-1B helicopters, one twin engine Skyvan, one twin jet T-39, and two four-engine turboprop aircraft (P-3 and Electra) offering the research community a wide range of payload, altitude, speed, and range capabilities.

WFF's support to a principal investigator includes mission planning of all supporting elements, installation of equipment on the aircraft, fabrication of brackets, adapters, etc., as required to adapt payloads to the aircraft, and planning of mission profiles to meet science objectives. The flight regime includes local, regional, and global missions.

The WFF aircraft serve scientists at GSFC, other NASA centers, other government agencies, and universities. The WFF mode of operation features the "walk on" method of conducting research projects. The principal investigator requests aircraft support by letter to WFF and after approval is granted, works with the assigned mission manager to plan all phases of project support. The instrumentation is installed in WFF electronics racks, mounted on the aircraft, the missions are flown, and the equipment is removed when the scientific objectives are met. The principal investigator reimburses WFF for each flight hours, any overtime and travel expenses generated by the project, and for other mission-related expenses such as aircraft support services required at deployment bases.

For information pertaining to the use of the WFF aircraft, contact Roger L. Navarro (804-824-1448) or Peter N. Bradfield (804-824-1292).

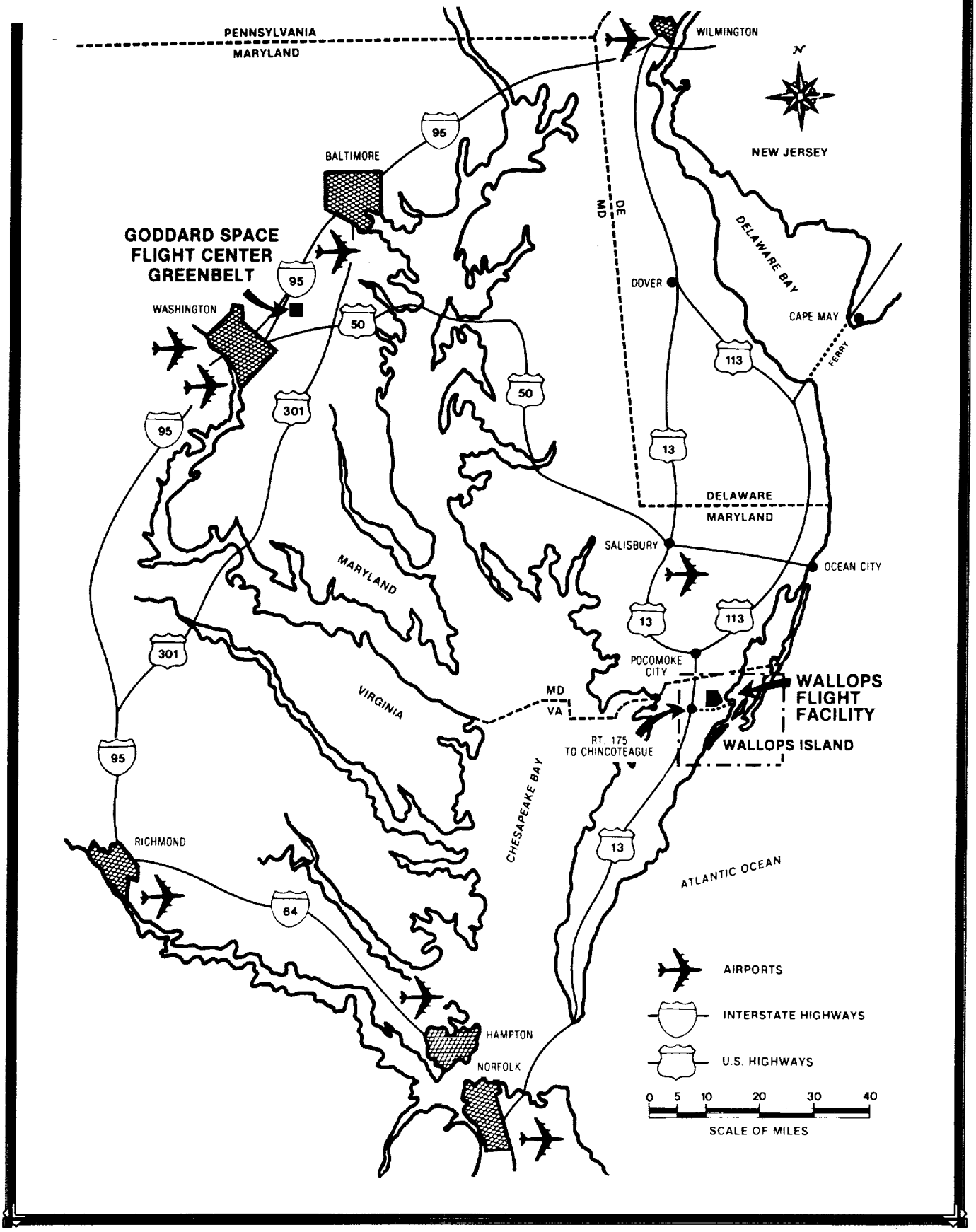
PENNSYLVANIA
MARYLAND
WILMINGTON
NEW JERSEY
BALTIMORE
GODDARD SPACE FLIGHT CENTER GREENBELT
WASHINGTON
DE
MD
DELAWARE BAY
DOVER
CAPE MAY
FERRY
DELAWARE
MARYLAND
SALISBURY
OCEAN CITY
MARYLAND
POCOMOKE CITY
WALLOPS FLIGHT FACILITY
WALLOPS ISLAND
MD
VA
VIRGINIA
RT 175 TO CHINCOTEAGUE
CHESAPEAKE BAY
RICHMOND
ATLANTIC OCEAN
HAMPTON
NORFOLK
95
50
301
113
13
64
AIRPORTS
INTERSTATE HIGHWAYS
U.S. HIGHWAYS
0 5 10 20 30 40
SCALE OF MILES

ORIGINAL PAGE
BLACK AND WHITE PHOTOGRAPH

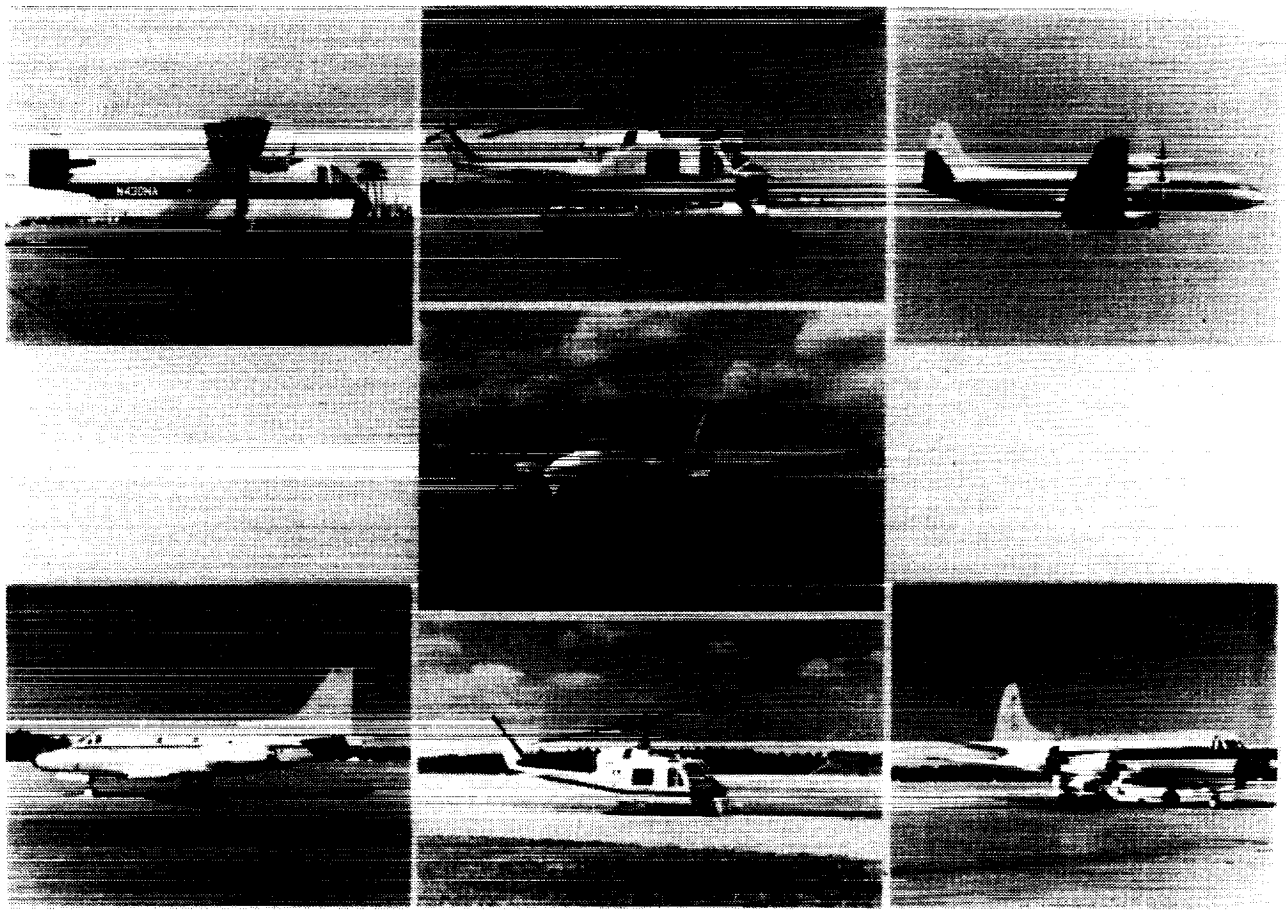

GSFC/Wallops Flight Facility Aircraft

ORIGINAL PAGE IS
OF POOR QUALITY

P93

Title: NOAA Aircraft Operations Center, A Facility Overview

Author: F.D. Moran, NOAA/Aircraft Operations Center

Discipline: Aircraft Operations

The NOAA Aircraft Operations Center (AOC) was established in October 1983, to consolidate the management of all aircraft used by the U.S. Department of Commerce. Operating from its headquarters in Miami, Florida, AOC utilizes three basic types of aircraft to accomplish NOAA's missions; helicopters, twin-engine light aircraft, and four-engine, turbo-prop transport type aircraft. The helicopters are operated for transportation and logistical support for marine mammal surveys, hyudrographic and geodetic studies and fisheries law enforcement. The light aircraft support snow surveys, aeronautical charting and mapping projects, air chemistry studies and fish and marine mammal surveys. The WP-3D Lockheed Orion aircraft are instrumented platforms which particpate in atmospheric and oceanic research programs worldwide. Each of the aircraft will be discussed along with a short explanation of the programs they support.

Title: CCRS Airborne Program Planning for ERS-1 and Radarsat

Author: Leon Bronstein, Canada Centre for Remote Sensing (CCRS)

Discipline: Aircraft Applications

Abstract will be available at the Workshop.

Title: French Activities in Airborne Geoscience

Author: Jean-Pierre Chalon, Centre National de Recherches Météorologiques

Discipline: Aircraft Operations

Abstract will be available at the Workshop.

Title: University Facilities for Airborne Geoscience

Author: Paul L. Smith, South Dakota School of Mines and Technology

Discipline: Atmosphere

University facilities (that is, platforms) for airborne geoscience are, as far as can be determined, confined to the atmospheric sciences. Two such facilities are operated under cooperative agreements with the National Science Foundation (NSF), and are made available to users in essentially the same manner as the Research Aviation Facility aircraft from the National Center for Atmospheric Research (NCAR). These are:

King Air B200T (University of Wyoming). The King Air is a medium twin-turbine-powered aircraft intended for a large variety of atmospheric research studies. Inboard fuel tanks are available for over-ocean ferry. The aircraft is fully deiced and R-NAV equipped. Winds are measured with a deiced gust probe and inertial navigation system. Many of the instruments are located on pylons attached to the wing tips. The core of the data system is a multi-processor VME bus that controls data acquisition, recording, and real-time displays consisting of digital channels, a high-resolution color display, and two electro-luminescent panels. In addition to the standard data system, the user may add up to 200 kg of instruments (pending available space and power). The aircraft is operated by a single pilot so the scientist can direct the research from the right seat.

T-28 (South Dakota School of Mines and Technology). The T-28 is a special-purpose aircraft intended mainly for penetrations of mature convective storms. It has a single radial engine, is armored for penetrations of hail-bearing storms, and is equipped primarily for cloud physics observations. Unique instrumentation includes an optical-array hailstone spectrometer and an experimental hailstone catcher. Work to develop a calibrated electric field mill system is in progress. Capacity is available for up to 70 kg of user-suppled instrumentation. The T-28 is operated in a single-seat configuration and flights into mature storms must be directed from the ground on the basis of meteorological radar observations. Air-to-ground telemetry is available to transmit data to the ground during research flights.

Two other university aircraft facilities are operated independently:

Citation II (University of North Dakota). The Citation is a twin fanjet with performance characteristics well suited for atmospheric research. It is radar-equipped and certified for flight into known icing conditions. Cloud physics instruments are mounted on wing-tip

pylons and an inertial navigation system (INS) and nose-boom-mounted flow angle sensors provide three-dimensional wind data. A computer-based "pointer" system permits following the three-dimensional motion of a designated air parcel. The aircraft has mounts for upward and downward-looking radiometers as well as optically-flat windows for side-looking cameras. An inlet port brings air samples into the cabin region and various instruments are available for aerosol and trace-gas measurements (including SF_6 tracer gas). A pilot and co-pilot are required, but a special observer's jump seat has been installed.

Convair C-131A (University of Washington). The C-131 is a twin-engine, propeller-driven aircraft that carries a large instrumentation payload and a crew of up to eight persons. It is particularly well instrumented to carry out aerosol, trace gas, cloud physics, cloud chemistry and atmospheric radiation measurements. Unique instruments include a cloud condensation nucleus spectrometer, an 8.6 mm wavlength radar, a dual-wavelength (0.532-1.604 um) lidar and a multi-wavelength (0.5-2.3 μm) scanning radiometer for atmospheric radiation studies. Computer terminals and color graphic displays of real-time measurements are available at four stations aboard the aircraft. Space is available for user-supplied instruments and guest scientists.

The previous presentations indicate that a much wider array of aircraft facilities is available through federal or quasi-federal agencies. This situation contrasts with that in oceanographic (ship) facilities, which are heavily concentrated in academic institutions and coordinated through the University National Oceanographic Laboratory System. As noted by a gentleman named Knauss (1988):

"Meteorology chose an alternate route, setting up NCAR ... in Colorado which operates most of the major facilities for the university meteorology departments of this nation. Others may disagree, but I believe oceanography chose the correct course. For one thing, it added a bit of competition, which, in turn improved both the effectiveness and the efficiency of the operation. As Director of the Rhode Island program, I was made acutely aware by scientists at my institution and elsewhere if our facilities were not as effective and as "user friendly" as those they could find elsewhere. One result is a UNOLS fleet that is generally considered very cost effective."

His assessment might well encompass the aircraft facilities operated by the universities discussed here today.

Acknowledgments. The assistance of John Marwitz, Jeffrey Stith, and Peter Hobbs in providing information about their aircraft facilities is appreciated. Preparation of this manuscript was supported by the NSF under Cooperative Agreement No. ATM-86-20145.

Reference

Knauss, J. A., 1988: Academic oceanography: How we got from there to here. Marine Technol. Soc. Journal, 22:1, 5-11.

N91-25450

20118

p.3

Title: **The Pilot Land Data System (PLDS) at the Ames Research Center Manages Aircraft Data in Collaboration with an Ecosystem Research Project**

Authors: Gary Angelici, Sterling Software
Lidia Popovici, Sterling Software
Jay Skiles, Technicolor Government Services

S 2516923

TF 389378

Discipline: **Aircraft Data Management**

The Pilot Land Data System (PLDS) is a data and information system serving NASA-supported investigators in the land science community. The three nodes of the PLDS, one each at the Ames Research Center (ARC), the Goddard Space Flight Center (GSFC) and the Jet Propulsion Laboratory (JPL), cooperate in providing consistent information describing the various data holdings in the PLDS and other data systems. Each of the nodes operate computer hardware and software (accessible via network and modem) that provide information about and access to PLDS-held data, which is available for distribution. Information is available at each of the nodes about a wide range of land science data, from meteorological data to remote sensing imagery. A large percentage of the data types handled by PLDS is data collected from sensors mounted on low, medium and high altitude aircraft.

A major new activity of the PLDS node at the Ames Research Center involves the interaction of the PLDS with an active NASA ecosystem science project, the Oregon Transect Ecosystem Research (OTTER) project. The collaboration between OTTER and PLDS involves the management of, access to, and distribution of the large volume of widely-varying aircraft data collected by OTTER from different sensors flown on several aircraft.

The OTTER project, funded through NASA Headquarters Codes SEL and SBR, is managed by researchers at the Ames Research Center and Oregon State University. Its principal objective is to estimate major fluxes of carbon, nitrogen, and water of forest ecosystems using an ecosystem process model driven by remote sensing data. Ten researchers at NASA centers and universities are analyzing data for six sites along a temperature- moisture gradient across the western half of central Oregon (called the Oregon Transect). Several types of remotely sensed and ground data, totalling over 13 gigabytes of storage, have been collected mainly during the 1990 growing season.

Sensors mounted on six different aircraft have acquired data over the Oregon Transect in support of the OTTER project. The Daedalus Thematic Mapper Simulator (TMS), the Advanced Visible Infrared Imaging Spectrometer (AVIRIS), the Thermal Infrared

Imaging Spectrometer (TIMS) sensors and a color infrared camera were all mounted on the high altitude ER-2 aircraft. The C-130 Medium Altitude aircraft carried the Advanced Solid State Array Spectrometer (ASAS), the NS001 Thematic Mapper Simulator, an airborne sun photometer, and cameras. The DC-8 aircraft, flown for the OTTER project in the summer of 1990 only, has acquired data from the Synthetic Aperture Radar (SAR) instrument. The Fluoresence Line Imager (FLI) was flown on an Apache, and a Spectron SE590 spectrometer and a Compact Airborne Spectrographic Imager (CASI) were flown on Cessna aircraft. Flights on the small low altitude Ultralight aircraft yielded spectrometer data from the Spectron and Barnes instruments, surface temperature measurements, and video tapes. A summary table listing the sensors by aircraft type is offered in Table 1.

In this collaboration, the PLDS node staff at the Ames Research Center have been and will continue to work closely with OTTER project scientists from both NASA centers and universities to place the information about the aircraft data (as well as other data sets) collected by the OTTER project into an inventory on the ARC PLDS computer and database system. Scientists have access to the data and information via normal PLDS-developed software and procedures which allow flexible database query and data ordering. For most aircraft data, which are stored offline on magnetic tape, the PLDS staff at ARC provides timely tape duplication and distribution services.

Additional capabilities and services for OTTER scientists have been identified for future work. For example, derived data from the OTTER project-selected ecosystem model and from scientist algorithms may be characterized and stored in the PLDS data base. The meteorological and chemical data currently stored at Oregon State University may be integrated into the PLDS data base to complete the full suite of data. Finally, useful OTTER data, including aircraft data, may be published on CD-ROMs for future use by ecosystem scientists.

While this collaboration is important by itself in the verification of the PLDS as a useful data and information system for the management of aircraft data, there are implications that extend beyond the scope of this effort. Optimized techniques for the management of aircraft data in support of the NASA science community by a major NASA data system will be developed. In addition, demonstrated effectiveness here by the PLDS node at Ames could allow PLDS to serve as a model information system for those providing information services to scientists involved in Earth Observing System (EOS) projects. Lessons learned and effective capabilities from this aircraft data-based testbed could enhance the future design and implementation of the EOS Data and Information System.

Table 1

OTTER Aircraft Data Sets
Managed By
PLDS at the Ames Research Center

Aircraft	Data Set Name
ER-2	Daedalus TMS, AVIRIS, TIMS, Color Infrared Photos
C-130	ASAS, NS001-TMS, TIMS, Sun photometer, Photos
DC-8	SAR
Apache	FLI
Cessna	CASI, Spectron SE590
Ultralight	Spectron SE590, Barnes MMR, Temperature, Video

N91-25451

ABS ONLY

120119

p.1

Title: Aircraft Laser Derived Chlorophyll Distribution Across the Iceland-Faeroe Front

Authors: Robert A. Arnone, NASA/Stennis Space Center
Paul E. La Violette, NASA/Stennis Space Center

ND 103456

Discipline: Oceans

The ocean surface color (water-leaving radiances) and thermal structure across the Iceland - Faeroe Front under both clear and cloudy conditions were measured from a NASA research aircraft on 25 May 1989. The measurements were made along four north-south lines that were 125 km in length and spaced 35 km apart. The color measurements were made with a 14 channel, non-polarized Multispectral Airborne Radiometer System (MARS) while the thermal data were collected by a thermal radiometer and aircraft bathythermographs. The satellite imagery (NOAA AVHRR) sequence show the development of meanders through the frontal region. These aircraft ocean color and thermal data characterize the biological distribution and are closely coupled to the physical processes occurring in the frontal systems. The ratio of several channels of the ocean color data are used to determine the surface chlorophyll. The retrieved data correlate well with (a) laser-induced chlorophyll fluorescence obtained at the same time and (b) historical chlorophyll data.

The observed chlorophyll patchiness appearing across the Iceland - Faeroe Front is believed to be directly and indirectly related to primary and secondary circulation processes in ocean frontal systems. High chlorophyll concentrations were observed on the north side of the front and are inferred to be the result from the advection of Icelandic Coastal Water into the region. The sharp chlorophyll decline at and south of the thermal frontal boundary is clearly related to the subsurface thermal structure.

OMIT TO P 107

Title: An Error Analysis Model for Airborne Measurements

Author: Darrel Baumgardner, National Center for Atmospheric Research

Discipline: Atmosphere

Aircraft measurements are used to evaluate the behavior of the atmosphere for in order to gain a better understanding of the physics and chemistry of our environment and how changes and interactions of the fundamental elements produce changes in weather. The instrument packages used to make these measurements are designed to sense and record as accurately as possible. However, these measurements will have a certain degree of uncertainty that depends upon numerous factors that must be determined for the individual instrument.

The atmosphere can be largely characterized by measurements of the spatial and temporal structure of pressure, temperature, humidity, and air motion. However, numerous other parameters are often used to evaluate atmospheric conditions, e.g. potential temperature, mixing ratio, heat and moisture fluxes, and other variables that are derived from the fundamental measurements. The uncertainties in the basic measurements will be propagated into the derived parameters and must be taken into account when interpreting aircraft measurements.

A technique is proposed here that provides a means of modeling uncertainties in both primary and derived atmospheric variables. This error analysis model has important applications in three areas of research.

- Facilities that provide airborne measurements can use the results of the error model to evaluate present measurement capabilities and obtain guidance with regards to which areas of sensor technology require higher priority for new developments.
- The error model provides scientists who use airborne measurements with a guide when analyzing data and interpreting the measurements in the context of expected uncertainties.
- The error model can be used in comparisons between theoretical climate models and observations.

The error model is based upon the technique described by Merceret (1982) who studied the effect of measurement fluctuations on a variety of derived variables. The basic premise is that the uncertainty, σ_y^2, of a measured variable, y, can be expressed as

$$\sigma_y^2 = [\sigma_u \frac{dy}{du}]^2 + [\sigma_v \frac{dy}{dv}]^2 + \ldots + [\sigma_w \frac{dy}{dw}]^2$$

where u,v,..w represent independent variables and σ_u, σ_v,.... σ_w are the respective uncertainties. In this formulation the uncertainties in the independent variables are assumed to be uncorrelated. The derivatives of the function with respect to the independent variables provide a means of assessing the significance of the errors associated with each of the variables and the degree with which they affect the total error. These derivatives are what Merceret termed the "sensitivity coefficients" and are useful in assessing where more accurate measurements are needed and where additional accuracy would provide little improvement.

At this point it is necessary to offer a brief discussion of the nature of measurement errors and their components. An excellent summary of this topic is found in the handbook by Abernathy *et al* (1973). The uncertainty of a measurement is the maximum error which might reasonably be expected and is a measure of the closeness of the measurement to the true value. There are two components to the measurement: a fixed error and a random error. The random error, often referred to as the precision error, is the error that can be minimized but not eliminated by repeated measurements. The fixed error, referred to as the bias, is a systematic error that is the same throughout repeated measurements and could be nearly eliminated through comparison with a standard instrument if such existed.

The distinction between these two types of error is important when applying error analysis to the measurements since in some cases, both errors must be included in the analysis, while in others, the bias error can be neglected. Thus, error values should have random and bias components expressed separately. The total error is just the square root of the sum of squares of the two components, often referred to as the "root sum square" (RSS). Establishing the sources and magnitudes of these errors is not trivial and has only recently received the attention that it deserves. At this time, the only airborne measurements that have been adequately evaluated are pressure (Brown, 1988) and temperature (Cooper, 1988). The NCAR Research Aviation Facility (RAF) has embarked on a major project to characterize all of its airborne measurements with the uncertainty reporting method reported by Abernathy *et al* (1973) and hope to encourage other facilities to emphasize a similar approach.

The error model has been used to make a preliminary analysis of the RAF wind measurement capabilities. Figures 1 and 2 summarize the results of using the model to derive horizontal and vertical wind at several pressure altitudes and air speeds. The uncertainties have been stratified by total error (solid lines) and random error (dashed lines). These figures show that the uncertainty in wind measurements increases with air speed and with altitude. These results, while not surprising, show that the expected accuracy of horizontal and vertical wind measurements are probably never better than 0.5 ms^{-1}. Thus, this area of measurement deserves more attention since accuracies of this magnitude are too large for many scientific applications.

In summary, the error model described can be a valuable tool for instrument users and instrument developers, alike. Even more importantly is the need for aircraft facilities to reach a consensus on the importance of determining measurement errors and finding a common means of reporting them. The error model discussed here provides a method of using these estimates of measurement uncertainty in a practical application.

References

Abernathy, R.B. and J.W. Thompson, 1973: Handbook on uncertainty in gas turbine measurements. Arnold Engineering Development Center Report AEDC-TR-73-5, 172pp.

Brown, E.N., 1988: Position error calibration of a pressure survey aircraft using a trailing cone. *NCAR Technical Note NCAR/TN-313+STR*, 29pp.

Cooper, W.A., 1987:The Ophir radiometric thermometer: Preliminary evaluation. *NCAR Technical Note, NCAR/TN-292+STR*, 54pp.

Merceret, F.J., 1982: The sensitivity of variables computed from RFC WP3D flight data to fluctuations in the raw data inputs. *NOAA Technical memorandum ERL RFC-8*, 43pp.

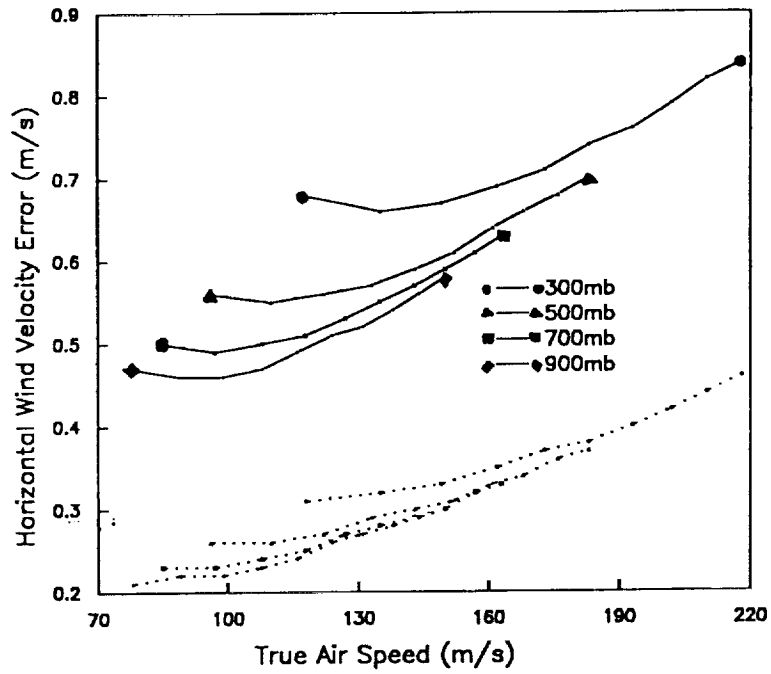

Figure 1. The estimated error in horizontal velocity is shown as a function of air speed and pressure. Both the total (solid line) and random (dotted) errors are shown.

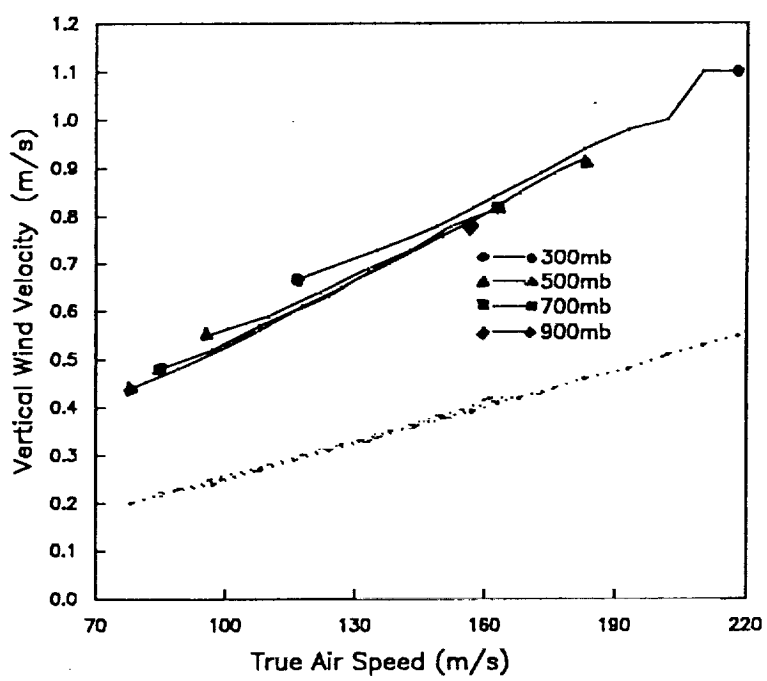

Figure 2. Vertical velocity error as a function of airspeed and pressure.

Title: An Aircraft-Deployed Rawinsonde for Use in Remote or Hazardous Areas

Authors: Michael A. Bellmore, Aeromet, Inc.
Dan J. Rusk, Aeromet, Inc.
R. Lynn Rose, Aeromet, Inc.
D. Ray Booker, Aeromet, Inc.

Discipline: Atmospheric Sensing

1. INTRODUCTION

Atmospheric soundings over remote oceanic areas have traditionally been limited. Investigators with a data requirement in an area not coincident with an island have often been frustrated. To address this need, Aeromet, Inc., under subcontract to the Applied Physics Laboratory at Johns Hopkins University, developed the Air-Launched Meteorological Sounding System (**ALMET**). ALMET produces a standard rawinsonde sounding and can obtain data into the stratosphere, a clear advantage over the limited altitude coverage of dropsondes.

The ALMET is designed to deploy a modified Vaisala RS-80 omega rawinsonde that is borne aloft by a 500 gm meteorological balloon. The rawinsonde and balloon package is launched from an aircraft and descends to the ocean surface by parachute. The launch and deployment sequence is depicted in **Figure 1.** The descending balloon, parachute, helium tank, and rawinsonde are depicted in **Figure 2.** When the ALMET nears the ocean surface, a water sensor causes the balloon and rawinsonde to be separated from the descent module. The balloon and rawinsonde then ascend, with the rawinsonde transmitting temperature, pressure, humidity, and omega wind data until the balloon bursts at altitudes between 60,000 to 100,000 ft.

Data transmitted from the rawinsonde are received and processed aboard the launch aircraft with a MARWIN unit, manufactured by Vaisala, Inc. The modified MARWIN has demonstrated its capability to receive and record data while installed in an aircraft. It has received and processed sounding data well over 250 nm from the rawinsonde.

2. ALMET SYSTEM DETAILED DESCRIPTION

The ALMET is placed in the aircraft launch tube (or stores rack) and a lanyard is attached between the aircraft and the probe. Upon launch, the lanyard pulls taut and releases the probe's decelerator cover, deploying a drogue parachute. When the drogue fills, a switch is actuated that initiates the timing sequence and activates the rawinsonde. Under the drogue parachute, the ALMET descends at approximately 70 mph (6160 ft/min).

Depending on the launch altitude, the descent module separates from the deployment canister 12 to 40 seconds after launch by means of a pyrotechnic cutter that releases the descent module restraint straps, allowing gravity to deploy it (see Figure 1). The descent module then descends under the main parachute at approximately 11 mph (1000 ft/min).

Descent module deceleration extends the water sensor, which is on a 50-foot lead. The center conductor of its three conductor lead is the auxiliary Very Low Frequency (**VLF**) omega antenna, and the remaining conductors are the water sensing circuitry. The auxiliary VLF antenna is used to synchronize the MARWIN to the omega system before balloon release, allowing wind data to be processed and recorded beginning at the surface.

Release of helium into the balloon begins 12 seconds after the descent module separates from the deployment canister, by means of a pyrotechnic cutter that releases a spring-operated valve. The 500 gm balloon is packed so as to fill from the top down. The balloon inflates against a protective cap and pushes it off. It immediately stretches to its full length and lays on the parachute as the gas continues to flow in. The balloon takes shape quickly; in 30 to 40 seconds, 90% of the gas is in the balloon.

The descent module is now configured for balloon release. After an approximate four minute descent on the main parachute, the descent module approaches the surface. When the water sensor enters the water, an electrical circuit is completed that actuates the final cutter which releases the balloon and rawinsonde. Upon balloon release, its valve core seats on the balloon flange, seals it, and then lifts the rawinsonde. The VLF antenna and string, stored on the unwinder, slowly extend to their full length so that the rawinsonde does not touch the water.

Nominal ascent rate for the balloon is 1000 ft/min. Data are transmitted to the MARWIN using a switch cycle varying between 1.2 and 1.8 seconds. Pressure, temperature, and humidity data are filtered and 10-second data are recorded. Omega winds are also recorded on the 10-second data file, which corresponds to the 10-second repeat cycle of the omega transmitter system. Sounding data are later processed and put into Range Standard, WMO, or user specified format. Various graphical plots are also produced.

3. CONCLUSION

The ALMET can be deployed from a variety of aircraft including the NKC-135 (Boeing 707), P3-A/B/C Orion, Learjet 36, Cessna 182, and Aeromet's Autonomous Unmanned Reconnaissance Aircraft (AURA), a remotely piloted vehicle. ALMET has been proven in the operational arena since 1987 by providing soundings for reentry vehicle flight evaluations. However, any application with a need for accurate soundings extending from the surface into the stratosphere can benefit from ALMET.

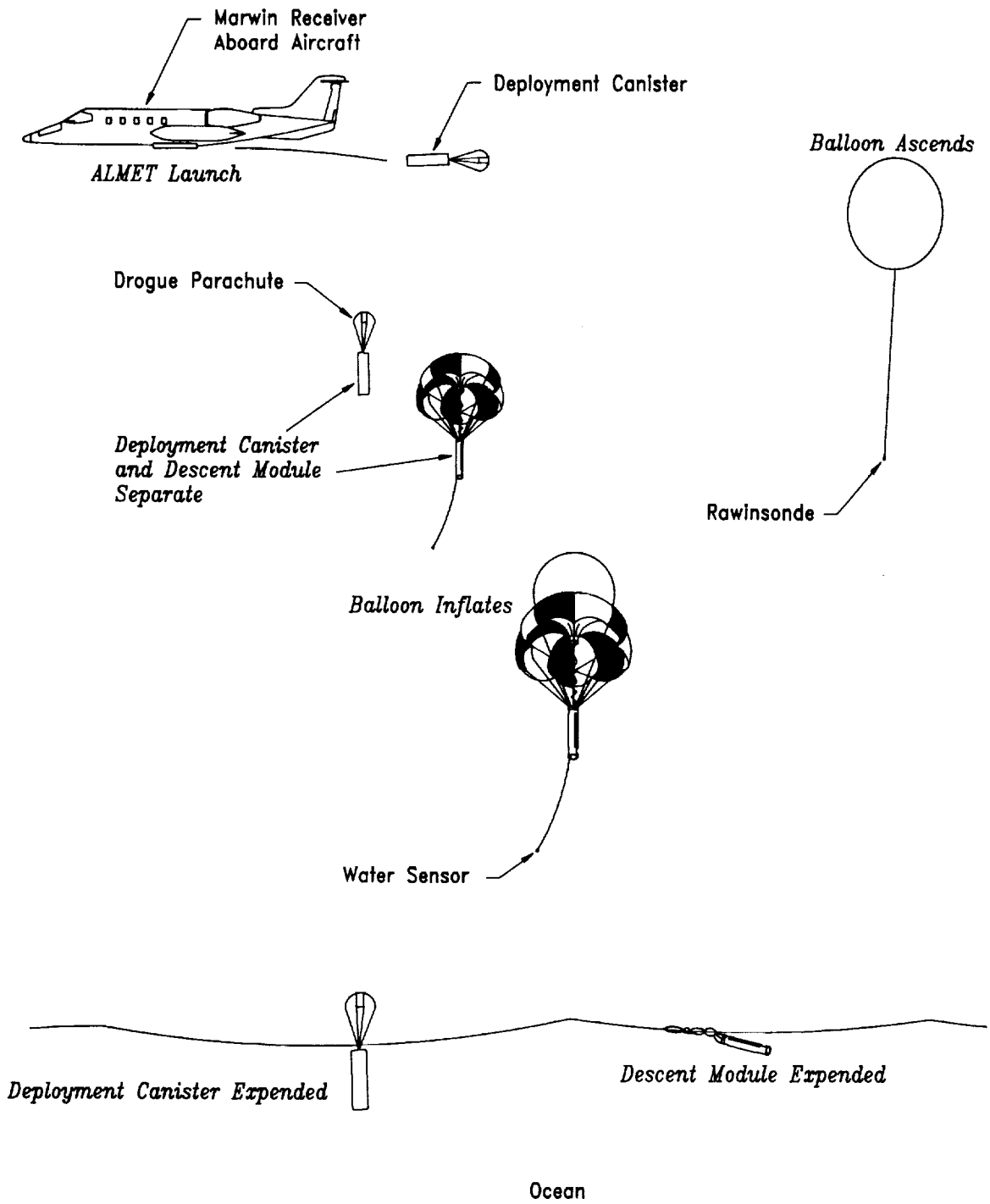

Figure 1 ALMET Deployment from Learjet

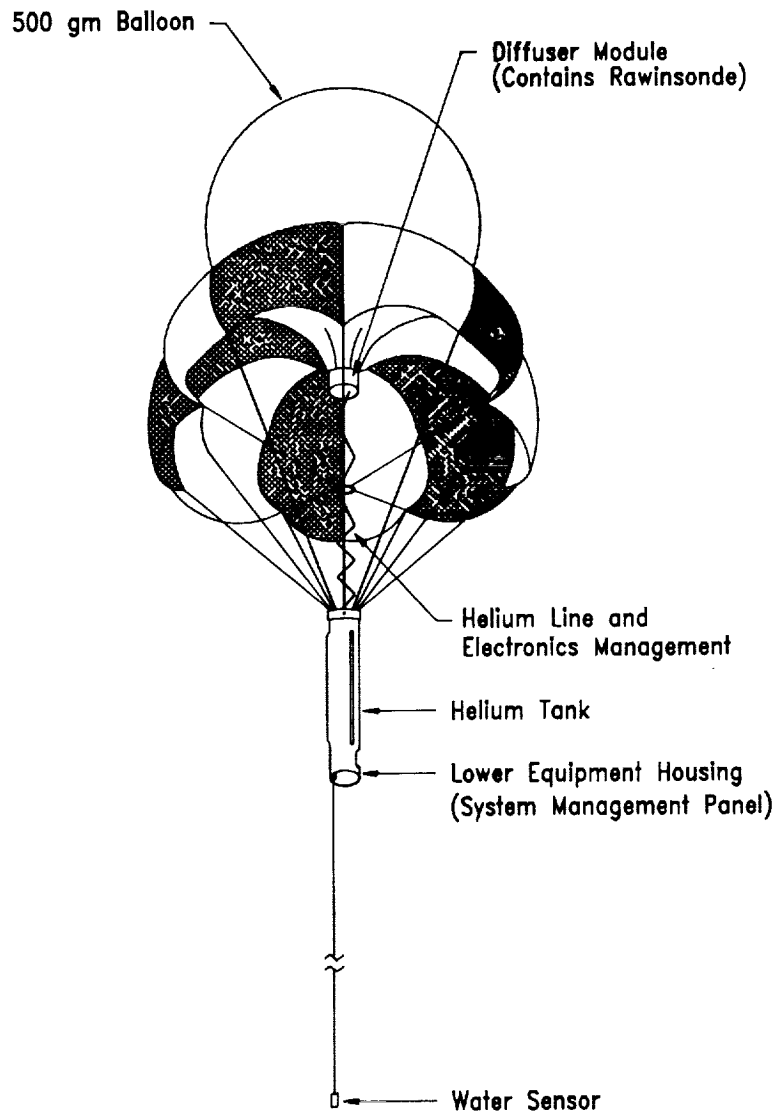

Figure 2 ALMET Descent Module Prior to Ocean Contact

N91-25452

p.4

Title: GLObal Backscatter Experiment (GLOBE) Pacific Survey Mission

Authors: David A. Bowdle, University of Alabama in Huntsville
Jeffry Rothermel, NASA/Marshall Space Flight Center
James E. Arnold, NASA/Marshall Space Flight Center
Steven F. Williams, University of Alabama in Huntsville

ND736801
AM584056

Discipline: Atmosphere

The National Aeronautics and Space Administration (NASA) conducted the GLObal Backscatter Experiment (GLOBE) Survey Missions on a NASA DC-8 aircraft over the near-coastal and remote Pacific Ocean during November 6 - 30, 1989 (GLOBE I) and May 13 - June 5, 1990 (GLOBE II). These missions were designed to study the optical, physical, and chemical properties of atmospheric aerosols. Particular emphasis was given to the magnitude and spatial variability of aerosol backscatter coefficients (β, $m^{-1}sr^{-1}$) at mid-infrared (9-11 μm) wavelengths, and to the remote middle and upper troposphere, where these aerosol properties are poorly understood.

Survey instruments (Table 1) were selected to provide either direct β measurements at the key wavelengths, empirical links with long-term or global-scale aerosol climatologies, or aerosol microphysics data required to model any of the above quantities. The core instruments included three lidar systems, a pulsed coherent CO_2 lidar, a pulsed incoherent Nd:YAG lidar, and two focused continuous-wave (CW) CO_2 Doppler lidars. The pulsed lidars provided β profiles above and below the aircraft, while the CW lidars provided complementary flight-level β measurements. The lidar instruments were supported by flight-level instruments for aerosol microphysical and optical properties. Some of the supporting instruments were mounted on aerodynamic pylons below the wingtips, to characterize aerosol concentrations and size distributions as nearly *in situ* as possible, with minimal interference from the aircraft boundary layer. Other sensors were mounted in the DC-8 cabin, where they sampled isokinetically from nozzles mounted on the aircraft fuselage, to provide detailed information on aerosol chemical, morphological, and visible-wavelength optical properties. Supporting meteorological data on the Survey aircraft were obtained from a microwave moisture sounder, video camera cloud monitors, and standard meteorological sensors. In addition, satellite imagery, rawinsonde soundings, weather analyses, and calculated air-mass trajectories were obtained to augment Survey aerosol data analyses.

The Survey deployment included both long-distance 6-8 hour transit flights and detailed 4-6 hour local flights (Fig. 1). Transit flight altitudes were usually near 8 km, except when higher altitudes were required to avoid extensive cloud fields. Overall, the transit flights provided relatively rapid and nearly pole-to-pole coverage, along with important seasonal, hemispheric, and airmass contrasts. Local flights usually involved multiple passes over the same test area at varying altitudes. These flights were conducted before and after deployment for engineering check-out and measurement validation, and during deployment for additional validation and for empirical links with key aerosol climatologies. Overall, approximately two-thirds of mission flight

hours were used for transit, and the remainder for validation experiments and aerosol climatology intercomparisons.

Several general features have been observed from preliminary Survey data analyses. Validation and intercomparison results have shown good agreement, usually better than a factor of two. Atmospheric aerosols frequently exhibited a three-layer vertical structure, with: (1) high and fairly uniform backscatter in the shallow cloud-capped marine boundary layer; (2) moderate and highly variable backscatter in a deeper overlying "cloud-pumped" layer; and (3) low, regionally uniform, but seasonally and latitudinally variable backscatter in the middle and upper troposphere. Frequent clouds and cloud residues were observed, often with lidar returns from deep within visually opaque cirrus shields. CO_2 β values were correlated with aerosol composition, even when subtle chemical changes were not accompanied by changes in aerosol concentration or size distribution. CO_2 β values were also correlated with water vapor concentration. Detailed statistical and case study analyses are underway to quantify these observations.

Three major uncertainties remain in the characterization of the global aerosol system for the middle and upper troposphere over the Pacific Ocean. The first concerns identification and quantification of the physical mechanisms that produced the observed low backscatter conditions. The second concerns the representativeness of the low backscatter regimes, including backscatter magnitude and seasonal / latitudinal variability. The third concerns the validity of a quasi-steady-state "background" aerosol model concept. Exploration of these issues will require detailed analyses of the comprehensive Survey data base, including the extensive validation data from both missions -- initially to quantify sensor sensitivities, sampling biases, and correction factors, and ultimately to develop robust estimates of "background" backscatter properties. The results of these analyses will provide important new insights into the dynamics of the global aerosol system.

The Survey Missions represent two isolated snapshots of a small portion of the global aerosol system. Consequently, Survey results can best be understood by synthesizing them with the more comprehensive GLOBE data base, which is being compiled at NASA Marshall Space Flight Center, Huntsville, AL. This data base will include key aerosol climatologies, as well as results from the Survey Missions and smaller GLOBE-related field programs. The overall GLOBE data base is being incorporated into a global-scale aerosol backscatter model at MSFC. The model results, in turn, are being used for design and simulated performance studies on MSFC's Laser Atmospheric Wind Sounder (LAWS), one of several NASA Facility Instruments planned for the Earth Observing System (EOS) in the late 1990's. GLOBE results will also be useful in the design of other lidar-based systems that use atmospheric aerosols as passive scattering targets for measurements of primary atmospheric variables.

Acknowledgments The authors acknowledge the assistance of numerous individuals and research groups in the conduct of the GLOBE Survey Missions. Special acknowledgment is due to Dr. Ramesh Kakar, GLOBE Program Manager at NASA Headquarters, and to the Mission Management and Mission Operations personnel for the DC-8 aircraft at NASA Ames Research Center. Research contributions from two of the authors (DAB and SFW) were supported under NASA contract NAS8-37585; this support is gratefully acknowledged.

TABLE 1 – GLOBE SURVEY MISSION INSTRUMENTATION

INSTRUMENT	MEASUREMENT	REMARKS	INVESTIGATOR	AFFILIATION
Pulsed CO_2 Lidar	9.25 micrometer backscatter	coherent detection	R.T. Menzies	Jet Propulsion Laboratory (NASA)
Pulsed Nd:YAG Lidar	0.53, 1.06, 1.54 micrometer backscatter	incoherent detection 1.54 is Raman–shifted	J. Spinhirne	Goddard Space Flight Center (NASA)
CW CO_2 Doppler Lidars	9.11 and 10.6 micrometer backscatter	coherent detection 9.11 is CO_2 isotope	W.D. Jones	Marshall Space Flight Center (NASA)
Optical Particle Counters Wire Impactors	size distribution, concentration chemistry, morphology	pylon–mounted in–situ sampling	R. Pueschel	Ames Research Center (NASA)
Optical Particle Counters Condensation Nuclei Counters Filters / Impactors	size distribution, concentration size–distributed chemistry airmass source monitoring	cabin–mounted aspirated sampling thermal pretreatment	A.D. Clarke	University of Hawaii
Optical Particle Counter Filters / Impactors Integrating Nephelometer	size distribution, concentration elemental / molecular chemistry 0.69 micrometer scattering	cabin–mounted aspirated sampling batch chemistry	E.M. Patterson	Georgia Institute of Technology
Integrating Nephelometer	0.45, 0.55, 0.70 micrometer scattering	cabin–mounted aspirated sampling GLOBE I only	B. Bodhaine	Geophysical Monitoring for Climatic Change (NOAA)
Advanced Microwave Moisture Sounder	water vapor column content	GLOBE I only	J. Wang	Goddard Space Flight Center (NASA)
Data Acquistion and Distribution System (DADS)	meteorological and navigational data	data broadcast to DC–8 experimenters	D. Jaynes	Ames Research Center (NASA)
DC–8 Aircraft	instrument platform	high–altitude, long–distance, large payload	D. Jaynes	Ames Research Center (NASA)

FIGURE 1 – GLOBE SURVEY MISSION FLIGHT TRACKS

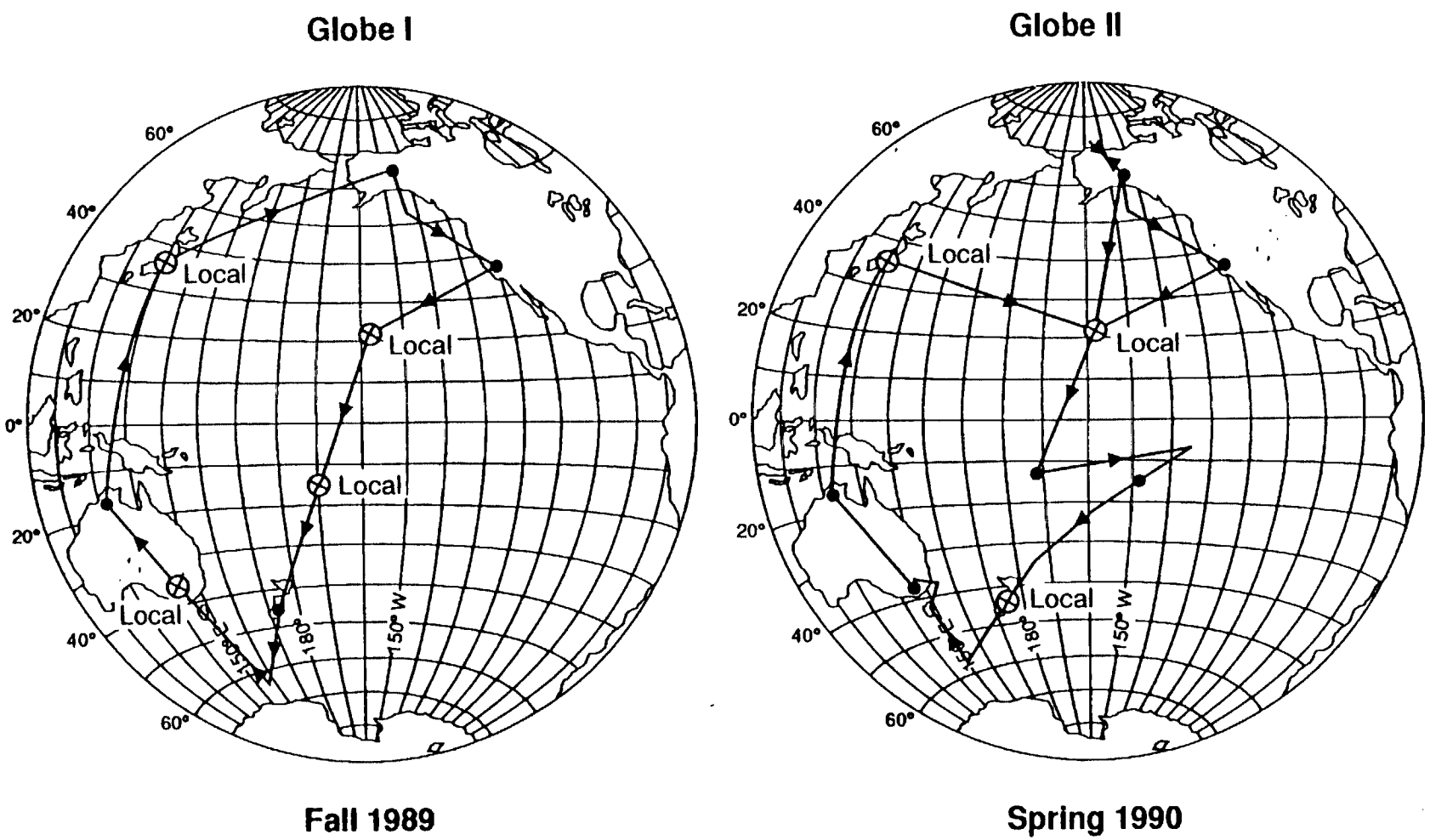

N91-25453

20121

Title: Calibration of the ER-2 Meteorological Measurement System

Authors: Stuart W. Bowen, San Jose State University
K. Roland Chan, NASA/Ames Research Center
T. Paul Bui, NASA/Ames Research Center

p. 2
NC 47365
SB 413975

Discipline: Atmosphere

The Meteorological Measurement System (MMS) on the high-altitude ER-2 aircraft was developed specifically for atmospheric research. The MMS provides accurate measurements of pressure (p), temperature (T), the wind vector (u, v, w), position (longitude, latitude, altitude), pitch (θ), roll (ϕ), heading (ψ), angle of attack (α), angle of sideslip (β), true airspeed, aircraft eastward velocity ($\dot{x}$), northward velocity ($\dot{y}$), vertical acceleration ($\ddot{z}$), and time (t) at a sample rate of 5 s^{-1}. MMS data products are presented in the form of either 5-Hz time series or 1-Hz time series. The 1-Hz data stream, generally used by ER-2 investigators, is obtained from the 5-Hz data stream by filtering and desampling.

The instrumentation of the MMS was described by *Scott et al.* [1990]. MMS data have been used extensively by other ER-2 investigators in studying the polar ozone chemistry, and applications of the MMS data on atmospheric dynamics are discussed in a companion poster paper by *Chan et al.* [1991]. The accuracies of the MMS primary products are:

	Typical value at ER-2 altitude	Accuracy		
Pressure	60 mb	± 0.3 mb	or	0.5%
Temperature	180 K	± 0.3 K	or	0.2%
Wind vector	30 m s^{-1}	± 1 m s^{-1}	or	3.3%
		(resolution: 0.1 m s^{-1})		

Accurate measurements of pressure and temperature require judicious choice of sensor location, repeated laboratory calibrations, and proper corrections for compressibility, adiabatic heating and flow distortion of these measurements. Accurate determination of the wind vector, computed from the true airspeed and ground speed vectors, is a difficult problem because the vertical wind ($\approx \pm 0.1$ m s^{-1}) is several orders of magnitude smaller than the aircraft velocity and true airspeed (≈ 200 m s^{-1}), and simultaneous measurements of about 20 independent variables are needed in order to compute the winds. If the variables are not simultaneously measured and properly calibrated, computed winds will exhibit undesirable "feedthrough" or "leakages" from the motion of the aircraft.

The calibration of the MMS consists of (1) individual sensor calibration, (2) system and transducer response tests, (3) laboratory determination of the dynamic behavior of the inertial navigation system (INS), (4) inflight calibration, and (5) comparison with radiosondes and radar-tracked balloons.

Particular attention has been given to the dynamic response of the MMS measurements. Both time shifts and the frequency response of various measurements have been determined by

direct measurement and/or by calculations. The calibrations include effects due to active anti-aliasing filters used on analog data and the inherent response of the INS outputs, pressure transducers (including plumbing) and temperature sensors. Power spectra of MMS products yielding useful system resolution and noise figure will be illustrated and discussed.

Individual pressure transducers were calibrated inhouse using a coiled quartz system accurate to $\pm$ 0.07 mb. The airflow angles (α, β) are determined by the differential pressure system at the nose cone. The Mach number dependence and angular offsets were calibrated by requiring that the observed winds show no dependence on induced pitch and yaw maneuvers or on aircraft heading in a uniform airmass. The position error for static pressure taps as a function of β was determined to be zero. However, a small α-dependent correction was found to be necessary.

Two temperature sensors (with different time constants) and matching amplifiers were calibrated by the manufacturer (Rosemount) over the range from -100°C to 0°C. Corrections for recovery factor, Mach number and time shift are then applied. Results of intercomparing the two sensors and intercomparing them with Vaisala radiosondes give $\pm$ 0.3 K accuracy.

The information of pitch, roll, heading, $\dot{x}$, $\dot{y}$, and $\ddot{z}$ from the INS are used for the wind computation, and the signal time delays of these variables are of primary importance. A simple physical pendulum was constructed. With the INS on the pendulum platform, the INS outputs and the swing angle (measured by a 16-bit x 8-synchro converter) were recorded. Variations in $\ddot{z}$ are generated as a function of the swing angle. By orienting the swing axis $\approx$ 45° from the north-south direction, $\dot{x}$ and $\dot{y}$ are generated during the swinging. By tilting the swing axis $\approx$ 20° from the horizontal, heading variation is generated during the swinging. By twisting the INS $\approx$ 45° on the platform, pitch and roll variations are generated during the swinging. From the Lissijous plots, the time delay of each variable can be determined to an accuracy of <0.01 s. For pitch, roll, heading, $\dot{x}$ and $\dot{y}$, only the swing angle (A) data were needed in the Lissijous plots. For the variable $\ddot{z}$, appropriate function such as $\{\ddot{A}\sin A+(\dot{A})^2\cos A\}$ was computed for comparison in the Lissijous plots. For the INS (Litton LTN-72RH unit) we use, we found that pitch and roll have zero time delay, heading has 0.045 s delay, $\dot{x}$ and $\dot{y}$ have 0.08 s delay, and $\ddot{z}$ has 0.39 s delay (including the active filter delay of 0.27 s).

MMS inflight calibration is a self consistency test, requiring that the computed winds have minimum leakage from the aircraft motion (θ, ϕ, ψ). Comparison of MMS measurements with Vaisala radiosondes and radar tracking of balloons and the ER-2 aircraft was conducted in 1986 [*Gaines et al.*, 1991], and comparison of the MMS real-time wind profiling capability via telemetry with radar-tracked "Jimsphere" balloons was conducted in 1989. In both cases, the results of the intercomparisons support the accuracy of MMS measurements stated above.

References

Chan, K. R., L. Pfister, T. P. Bui, S. W. Bowen, and J. Dean-Day, Applications of the ER-2 Meteorological Measurement System, poster paper submitted to the *Fourth Airborne Geoscience Workshop*, La Jolla, CA, January 29 to February 1, 1991.

Gaines, S. E., R. S. Hipskind, S. W. Bowen, T. P. Bui, and K. R. Chan, Comparisons of the NASA ER-2 Meteorological Measurement System with radar tracking and radiosonde data, *in preparation*, 1991.

Scott, S. G., T. P. Bui, K. R. Chan, and S. W. Bowen, The Meteorological Measurement System on the NASA ER-2 aircraft, *J. Atmos. and Oceanic Technol.*, *7*, 525-540, 1990.

Title: Air Deployed Expendable Probes in Oceanographic Research

Author: Janice D. Boyd, NASA/Stennis Space Center

Discipline: Oceans

Physical oceanographic instrumentation is both nonexpendable and expendable. Nonexpendable instrumentation has the advantage of yielding measurements that are typically both highly accurate and highly precise, but taken as a group it has the disadvantage of having a high unit cost and of being cumbersome and complicated to deploy even in good weather, requiring trained personnel on specialized platforms which are not underway. Expendable instruments for both shipboard and aircraft use have been developed which yield moderate accuracy and precision at a low or moderate unit cost and which may be deployed by less trained personnel on less specialized platforms both in more extreme environmental conditions and while underway.

While shipboard expendables are familiar to many researchers, most are not familiar with the variety of air deployable expendables available, although the quasi-synoptic, 3-dimensional view of the ocean that aerial studies yield can be very valuable in oceanographic research. As well as acoustics-oriented probes, air deployed sensors exist for the measurement of temperature (AXBT), sound speed (AXSV), currents (AXCP), and optical properties (AXKT), and work is underway to develop probes measuring simultaneous conductivity and temperature (AXCTD). In addition, low-cost drifting buoys with both oceanographic and meteorological sensors are available, and ice-penetrating probes are being developed for arctic research. Characteristics of these instruments are presented, along with examples of their use and a discussion of some of their not so well publicized shortcomings.

SMIT 70
P. 119

Title: A New Electronics for the FSSP PMS Probe

Author: J.L. Brenguier, Meteorologie Nationale, CNRM

Discipline: Atmosphere

Abstract will be available at the Workshop.

Title: Airborne Lidar Studies of Arctic Hazes

Authors: Charles A. Brock, University of Washington
Lawrence F. Radke, University of Washington
Peter V. Hobbs, University of Washington
Bruce M. Morley, SRI International

Discipline: Atmosphere

Pollution hazes found in the arctic troposphere are often extensively layered. Ground-based measurements of pollutants may indicate that no hazes are present when, in fact, hazes are present aloft. While remote sensing studies of the hazes have potential, radiometric measurements are impossible in the arctic night and ground-based lidar observations are often obscured by clouds and ice crystals as well as being geographically limited. *In situ* airborne measurements are inherently one-dimensional, and have provided an incomplete picture of the haze structure and spatial variability. However, an airborne, active remote sensing instrument, such as lidar, avoids many of these problems.

During studies of arctic hazes over Greenland and the Canadian Arctic in March and April 1986, a downward-pointing Nd:YAG lidar system at 1064 nm wavelength was used aboard the University of Washington's C-131A research aircraft to map the distribution of pollutants in two episodes of layered arctic hazes. The details of fine structures in the hazes were clearly detected with the lidar. By comparing the observed profiles of the backscattering coefficient due to particles (β_p) with *in situ* measurements of particle size distributions and bulk particle chemistry, we have derived a satisfactory quantitative relationship between β_p and the airborne concentration of sulfur in the particles, (S_p). Backscattering and scattering coefficients determined from the measured aerosol size distributions, using the hygroscopic and optical properties of H_2SO_4, agree well with the remotely sensed lidar-derived values.

The techniques developed in this study may be used in the future to determine the total masses and mass fluxes of particles within highly layered arctic hazes.

Title: Tropospheric Ozone and Aerosols Measured by Airborne Lidar during the 1988 Arctic Boundary Layer Experiment

Authors: Edward V. Browell, NASA/Langley Research Center
Carolyn F. Butler, ST Systems Corporation
Susan A. Kooi, ST Systems Corporation

Discipline: Atmosphere

Ozone (O_3) and aerosol distributions were measured from an aircraft using a differential absorption lidar (DIAL) system as part of the 1988 NASA Global Tropospheric Experiment--Arctic Boundary Layer Experiment (ABLE-3A) to study the sources and sinks of gases and aerosols over the tundra regions of Alaska during the summer. The airborne DIAL system made measurements of O_3 and aerosols above and below the NASA Wallops Electra aircraft to obtain data from the surface to above the tropopause. These measurements comprise the first extensive set of simultaneous nadir and zenith observations of tropospheric ozone and aerosols. They were made in a broad range of atmospheric conditions over the tundra, ice, and ocean regions near Barrow and Bethel, Alaska, from July 10 to August 12, 1988.

The tropospheric O_3 budget over the Arctic was found to be strongly influenced by stratospheric intrusions. Regions of low aerosol scattering and enhanced O_3 mixing ratios were usually correlated with descending air from the upper troposphere or lower stratosphere. In the vicinity of Barrow, Alaska, O_3 was generally in the range of 20-30 ppbv below 2 km; however, air with O_3 >40 ppbv and low aerosol scattering was found as low as 1 km with continuity in air mass characteristics to above 3 km. These increases could be followed back to large-scale stratospheric intrusions that affected the distribution of O_3 in the upper troposphere. Ozone mixing ratios of >100 ppbv were found as low as 6 km in the presence of strong intrusion events. The variability in O_3 in the mid to upper troposphere affects the O_3 distribution in the lower troposphere, and due to the frequency of the observed intrusions, this process plays an important role in the tropospheric O_3 budget at high latitudes.

Several cases of continental polar air masses were examined during this experiment. The aerosol scattering associated with these air masses was very low,

and the atmospheric distribution of aerosols was quite homogeneous for those air masses that had been transported over the ice for ≥ 3 days. The average O_3 profile derived from three cases of continental polar air masses had a nearly constant gradient of 7 ppbv/km from 30 ppbv at 600 m to 55 ppbv at 4 km. This distribution reflects the influence of downward transport of O_3 from the upper troposphere at high latitudes.

Five cases were studied to determine the average background O_3 profile over the tundra region of southwestern Alaska. Near the surface, the tundra and continental polar O_3 levels are about the same; however, the average O_3 value above 1.5 km is 10-20% less than for the continental polar cases. This is thought to be due to the influence of more frequent stratospheric intrusions at the higher latitudes associated with the continental polar air masses. Zenith O_3 profiles in the region of 56-62°N showed good agreement from 2.5-10.0 km in altitude with a 5.5 ppbv/km gradient determined below 2.5 over the tundra.

The transition in O_3 and aerosol distributions from tundra to marine conditions was examined on several occasions during this experiment. The aerosol data clearly show an abrupt change in aerosol scattering properties within the mixed layer from lower values over the tundra to generally higher values over the water. The distinct differences in the heights of the mixed layers in the two regions was also readily apparent. The O_3 distribution above 1 km, which is above the mixed layers over both regions, did not change along the transect; however, there was an apparent reduction of O_3 in the mixed layer over the tundra that was not present over the water. This is consistent with the tundra being more of a sink for O_3 than the water surface.

Several cases of enhanced O_3 were observed during ABLE-3A in conjunction with enhanced aerosol scattering in layers in the free troposphere. These layers were coming from regions where biomass burning was occurring. In some cases, the enhancement in O_3 was found to be more than 50% larger than the average background O_3 distribution over the tundra region. The products of biomass burning can significantly alter the O_3 concentrations in the troposphere in the Arctic as was shown to happen over the Amazon Basin during the dry season.

This poster presents examples of the large-scale variations of O_3 and aerosols observed with the airborne lidar system from near the surface to above the tropopause over the Arctic during ABLE-3A. These results are related to atmospheric dynamical and chemical processes that determine the distribution of O_3 and aerosols in the troposphere at high latitudes during the summer.

S41-45
N91-25456
p. 2

Title: **Airborne Lidar Measurements of Ozone during the 1989 Airborne Arctic Stratospheric Expedition**

Authors: Edward V. Browell, NASA/Langley Research Center
Marta A. Fenn, ST Systems Corporation
Susan A. Kooi, ST Systems Corporation

ND210491
SY768289

Discipline: **Atmosphere**

The NASA/NOAA Airborne Arctic Stratospheric Expedition (AASE) was conducted during the winter of 1988-89 to study the conditions leading to possible ozone (O_3) destruction in the wintertime Arctic stratosphere. The mission was based near Stavanger, Norway, and aircraft flights into the polar vortex were conducted between January 6 and February 15, 1989. As part of this experiment, the NASA-Langley Research Center's airborne differential absorption lidar (DIAL) system was configured for operation on the NASA Ames Research Center's (ARC) DC-8 aircraft to make measurements of O_3 profiles from about 1 km above the aircraft to altitudes of 22-26 km.

The airborne DIAL system remotely sensed ozone above the DC-8 by transmitting two laser beams at 10 Hz using wavelengths of 301.5 and 311 nm. Large-scale distributions of ozone were obtained on 15 long-range flights into the polar vortex during the AASE. Each flight lasted for an average of about 10 hours and covered about 8000 km. Over 150 hours of lidar data were collected on these flights which were conducted between Stavanger (59°N, 5°E) and the North Pole and between about the 40°W and 20°E meridians. These measurements were displayed in real time as false color images of ozone concentrations along the flight path. This poster presents selected data samples of O_3 observed during these flights, general trends observed in O_3 distributions, and correlations between these measurements and meteorological and chemical parameters.

The O_3 distribution observed on the first flight of the DC-8 into the polar vortex on January 6 reflected the result of diabatic cooling of the air inside the vortex during the winter compared to the warmer air outside the vortex. On a potential temperature (PT) surface, the O_3 mixing ratio generally increases when going from outside to inside the vortex. The trends in the O_3 mixing ratio and potential vorticity (PV) distributions were generally well correlated over the entire atmospheric cross section. Based on the location of the maximum gradient in PV on the 440-K PT surface on January 6, the edge of the vortex was estimated to be

near 69°N, which also corresponded closely to the location of the maximum wind speed. The O_3 mixing ratio also showed a sharp gradient at this same location. Because of the good correlation in the gradients of O_3 and PV, the DIAL-derived O_3 distribution was used to determine the location of the edge of the polar vortex on each mission.

Post mission analysis of DIAL data extended the altitude range of ozone measurements at least an additional 3 km in range to provide data up to 30 km altitude. The extension technique utilized a single wavelength of lidar data, 311 nm, along with a modeled molecular return. Comparisons with ozonesonde data agree within 20%. These higher altitude data will be useful to investigators interested in mapping other chemical species on the ozone field.

The last AASE mission to be flown deep into the polar vortex was made on February 9. The O_3 distribution at latitudes above 80°N on the 460-K PT level was essentially constant to the Pole; however, between 71-80°N the O_3 mixing ratio was lower than at the higher latitudes within the vortex. This region of lower O_3 extended in the vertical across the PT range from ~420 to 580 K. The magnitude of the decrease was at a maximum at about 500 K (~20 km in altitude), and it represented a decrease of about 17% over the O_3 levels farther inside the vortex. A second large region of low O_3 was also observed on the transit flight from Stavanger to California across the polar vortex on February 15. It was also located near the edge of the vortex, and it had about the same relative O_3 decrease compared to O_3 levels farther inside the vortex, as was observed on February 9. Measurements of O_3 and nitrous oxide from the NASA ARC high-altitude (ER-2) aircraft on February 9 showed that the O_3 decrease at the bottom of this region was due to an in situ loss of O_3 and not due to transport processes. The O_3-depleted region observed by the lidar was correlated in vertical extent with the polar stratospheric cloud observations. This O_3 depletion is thought to be directly related to the chemical perturbation of the Arctic polar vortex that was observed during the AASE.

Acknowledgments

The authors would like to thank Syed Ismail, Patricia Robinette, Shane D. Mayor, Noah S. Higdon, James H. Siviter, Jr., M. Neale Mayo, Robert J. Allen, William J. McCabe, Jerry A. Williams, Loyd W. Overbay, Byron L. Meadows, Jaye A. Moen, and Ricky L. Martin of the Lidar Applications Group in the Atmospheric Sciences Division at the NASA Langley Research Center for their assistance in developing the comprehensive measurement capabilities of the airborne DIAL system, integrating the system into the DC-8, operating the lidar in the field, and reducing the lidar data after the mission. This research was supported by NASA's Upper Atmospheric Research Program.

Title: Analysis of Observations from a P-3 Aircraft in Support of Operational Hurricane Forecasting

Authors: Robert W. Burpee, NOAA/Hurricane Research Division
Joseph S. Griffin, NOAA/Hurricane Research Division
James L. Franklin, NOAA/Hurricane Research Division
Frank D. Marks, Jr., NOAA/Hurricane Research Division

Discipline: Atmosphere

The structure of the hurricane core has become increasingly clear during the last 15 years as a result of research with the National Oceanic and Atmospheric Administration's (NOAA) P-3 aircraft observations. During hurricane flights, meteorologists onboard the P-3's are able to synthesize the information displayed by the data system and develop an accurate depiction of the storm structure. Although limited subsets of the aircraft data have been transmitted to the National Hurricane Center (NHC) for more than 10 years, forecasters sometimes prepare their advisories without being aware of significant aspects of storm structure observed by the aircraft. Real-time access to more comprehensive aircraft data sets that depict the mesoscale kinematic and precipitation structure of tropical cyclones would enable forecasters to issue more accurate warnings and forecasts.

During the 1990 Atlantic hurricane season, the Hurricane Research Division (HRD) installed a workstation on a P-3 aircraft operated by NOAA's Aircraft Operations Center and began real-time, interactive processing of radar, Omega dropwindsonde (ODW), and flight-level data in the core of tropical cyclones. This paper describes the workstation and provides examples of analyses computed on the aircraft during the 1990 season.

The workstation, which weighs 85 kgm, currently consists of a Hewlett-Packard 9000/825 CH system with a 670 Mbyte disk drive, a 40 cm high color monitor (with a resolution of 1280 by 1024 pixels), and a laser printer. The computer has 32 Mbytes of RAM and a CPU capable of 8 MIPS. A hardware two-dimensional transform box, solely for graphics, supports HP's Starbase graphics package. The workstation captures data from the output busses that are being written to tape by the flight-level and radar data systems. A data line from the dropwindsonde computer system provides the ODW observations. Operator interaction is via keyboard and trackball. Besides hardcopy output from the laser printer, the workstation communicates data to the aircraft-satellite data link (ASDL) computer for transmission to NHC.

The 5 cm lower fuselage radar provides an overall perspective of the horizontal patterns of precipitation within which flight-level observations can be analyzed. Interpretation of reflectivity patterns from single rotations is difficult, however, because of aircraft motion, intervening attenuation, and inadequate filling of the 4.1° vertical beamwidth with precipitation particles. These problems can be overcome by combining a number of radar scans in a composite map centered on the storm position.

Real-time compositing combines single radar sweeps stored at intervals of about 5 minutes and includes periods of 1-2 h. The operator marks the approximate center in the inital sweep. The image processing software uses an objective procedure for estimating the center of the rain-free, quasicircular eye. It attempts to refine the operator's position and follow the center as a function of time. The operator may override the software when the objective procedure determines an inaccurate position. Poor center estimates tend to occur in weak storms that don't have an eye or at low aircraft altitudes. If the objective procedure for tracking the radar center is inadequate, another algorithm is available to estimate the center based upon time series of the horizontal wind along the flight track.

Interactive software on the workstation allows for real-time processing of ODW wind and thermodynamic data, and for automatic dissemination of mandatory and significant level data in the standard World Meteorological Organization TEMP DROP code. ODW data are received from the P-3's ODW computer as the ODW's descend and are stored by the workstation. Meteorologists onboard can then recall the data for any ODW for interactive processing. Objective algorithms are available to scan the sounding for suspicious observations; in addition, the sounding can be displayed on a skew-T log-p thermodynamic diagram for subjective detection of erroneous data. After bad observations have been flagged, algorithms to fill data gaps, filter the sounding, and calculate geopotential heights are run. The software then identifies mandatory and significant levels and encodes the TEMP DROP message, which is sent electronically to the P-3's ASDL computer for transmission to NHC and the National Meteorological Center.

The real-time availability of composite radar analyses and ODW mandatory and significant-level data near the end of the 1990 hurricane season demonstrated the potential value of workstations on the P-3's. Plans for the 1991 hurricane season include the purchase of a workstation for the second P-3, development of additional software estimates of the surface windspeed from the stepped-frequency microwave radiometer, and installation of a new ASDL computer with expanded capacity for data transmission. With the implementation of these plans, NHC will receive two-dimensional analyses of the mesoscale wind structure of the storm core and improved estimates of the location and recent motion of tropical cyclones. As forecasters learn to interpret this diagnostic information, we anticipate improvements in the accuracy of their track forecasts and warnings.

N91-25457

20125

Title: Applications of the ER-2 Meteorological Measurement System

Authors: K. Roland Chan, NASA/Ames Research Center
Leonhard Pfister, NASA/Ames Research Center
T. Paul Bui, NASA/Ames Research Center
Stuart W. Bowen, San Jose State University
Jonathan Dean-Day, San Jose State University

NC473657
SB413977

Discipline: Atmosphere

The NASA ER-2 aircraft is used as a platform for high-altitude atmospheric missions. The Meteorological Measurement System (MMS) was developed specifically for atmospheric research to provide accurate high-resolution measurements of pressure (±0.3 mb), temperature (±0.3°C), and the 3-dimensional wind vector (±1 m s^{-1}) with a sampling rate of 5 s^{-1}. Operational since 1986, the MMS participated in three scientific expeditions: the Stratospheric-Tropospheric Exchange Project (STEP) in Australia during January and February of 1987, the Airborne Antarctic Ozone Experiment (AAOE) in Chile during August and September of 1987, and the Airborne Arctic Stratospheric Expedition (AASE) in Norway during January and February of 1989.

The MMS consists of three subsystems: (1) an air motion sensing system to measure the velocity of the air with respect to the aircraft, (2) a high-resolution inertial navigation system (INS) to measure the velocity of the aircraft with respect to the earth, and (3) a data acquisition system to sample, process and record the measured quantities. The instrumentation of the MMS was reported in detail by *Scott et al.* [1990], and the calibration of the MMS will be discussed in a companion poster paper by *Bowen et al.* [1991].

MMS data have been used extensively by ER-2 investigators in elucidating the polar ozone chemistry. In this paper applications on atmospheric dynamics are emphasized. Large-scale (polar vortex, potential vorticity, model atmosphere), mesoscale (gravity waves, mountain waves) and microscale (heat fluxes) atmospheric phenomena are investigated and discussed.

With the aircraft cruising on isentropic surfaces along a north-south path during the AASE and AAOE, features of the Arctic and Antarctic vortexes (boundary, position, strength, variance, shape) are best depicted by latitudinal variations of the horizontal wind. The 1989 Arctic vortex during the AASE is weaker (wind speed), smaller (in areal extent) and more variant (shape and jet stream fluctuations) than the 1987 Antarctic vortex during the AAOE. The 1987 Antarctic vortex in mid-winter was dominated by a strong circumpolar circulation with small meridional amplitudes and the 1989 Arctic vortex in late winter and early spring was composed of several synoptic scale waves imbedded in two planetary waves with separated low pressure centers.

The potential vorticity on isentropic surfaces is a quasi-conservative quantity and important dynamical tracer. Large-scale features of the potential vorticity distribution computed from the horizontal wind and temperature gradient (lapse rate) data agree with those of observed nitrous oxide, also a quasi-conservative tracer (*Hartmann et al.*, 1989). The aircraft

data provide temporal and spatial detail that is not currently achievable with other measurement techniques. In principle, this resolution allows the study of fine structure in the potential vorticity distribution and offers added insight into the details of the mixing processes.

The ER-2 can climb and descend rapidly, and measurements during aircraft takeoff, landing, mid-flight descent and ascent provide near-vertical profiles. MMS temperature profiles are used in developing model atmospheres (*Chan et al.*, 1989; *Chan et al.*, 1990). An AAOE or AASE model atmosphere (an idealized temperature profile) is a reference atmosphere at a specific latitude for the duration of the expedition. For a specific flight, concurrent synoptic or in situ meteorological data should be used. However, for investigations requiring the mean meteorological environment as the boundary condition during the expedition, the model atmosphere (substantially different from the standard atmosphere) is needed.

Small and periodic variations in the vertical wind data ($\approx \pm 1$ m s^{-1}) are the first indications of atmospheric wave phenomena. Coherence and phase relationships of the temperature and wind data by cross-spectral analyses provide the evidence of gravity waves and their physical properties. Gravity waves, generated by Cyclone Jason in Australia (2/8/87), will be discussed and illustrated.

Large and periodic variations in the wind data ($\approx \pm$ 2-6 m s^{-1}) are the indications of waves of different origin. Mountain waves over the Palmer Peninsular of Antarctica (9/22/87) and near Iceland in the northern polar region (2/10/89) are the best examples of orographically generated waves observed by the MMS.

Small and irregular variations in the temperature and vertical wind data are analyzed and heat fluxes computed. Episodic downward heat fluxes during the STEP (1/31/87) are identified and illustrated. Evidence of turbulence is supported by the comparison of power spectra of vertical wind and temperature during quiet and disturbed periods.

Real-time wind profiling (30 s lag) capability of the ER-2 MMS via telemetry was demonstrated at Kennedy Space Center during the Space Shuttle STS-28 launch on 8 August 1989. In addition to providing the quick access to the wind profiles, the quality and high resolution of the wind shear information measured by the MMS on a controlled platform offer advantages over the "Jimsphere" balloon system currently used in the support of Space Shuttle launch operation.

References

Bowen, S. W., K. R. Chan, and T. P. Bui, The calibration of the ER-2 Meteorological Measurement System, poster paper submitted to the *Fourth Airborne Geoscience Workshop*, La Jolla, CA, January 29 to February 1, 1991.

Chan, K. R., S. G. Scott, T. P. Bui, S. W. Bowen, and J. Day, Temperature and horizontal wind measurements on the ER-2 aircraft during the 1987 Airborne Antarctic Ozone Experiment, *J. Geophys. Res.*, *94*, 11573-11587, 1989.

Chan, K. R., S. W. Bowen, T. P. Bui, S. G. Scott, and J. Dean-Day, Temperature and wind measurements and model atmospheres for the 1989 Airborne Arctic Stratospheric Expedition, *Geophys. Res. Lett.*, *17*, 341-344, 1990.

Hartmann, D. L., K. R. Chan, B. L. Gary, M. R. Schoeberl, P. A. Newman, R. L. Martin, M. Loewenstein, J. R. Podolske, and S. E. Strahan, Potential vorticity estimates in the south polar vortex from ER-2 data, *J. Geophys. Res.*, *94*, 11625-11640, 1989.

Scott, S. G., T. P. Bui, K. R. Chan, and S. W. Bowen, The Meteorological Measurement System on the NASA ER-2 aircraft, *J. Atmos. and Oceanic Technol.*, *7*, 525-540, 1990.

N91-25458

26126

Title: NASA/Ames Research Center DC-8 Data System

Authors: S.C. Cherniss, Sterling Software
C.P. Scofield, NASA/Ames Research Center

Discipline: Aircraft Data Management

NC473657
S2516923

In-flight facility data acquisition, distribution, and recording on the NASA Ames Research Center (ARC) DC-8 are performed by the Data Acquisition and Distribution System (DADS). Navigational and environmental data collected by the DADS are converted to engineering units and distributed real-time to investigator stations once per second. Selected engineering units data are printed and displayed on closed circuit television monitors throughout flights. An in-flight graphical display of the DC-8 flight track (with barbs indicating wind direction and magnitude) has recently been added to the DADS capabilities. Logging of data run starts/stops and commentary from the mission director are also provided. All data are recorded to hard disk in-flight and archived to tape medium post-flight. Post-flight, hard copies of the track map and mission director's log are created by the DADS.

The DADS is a distributed system consisting of a Data subsystem, an Avionic Serial Data-to-VMEbus (ASD2VME) subsystem, and a Host subsystem (see DC-8 DADS System Block Diagram). Each subsystem has a dedicated central processing unit (CPU) and is capable of stand-alone operation. All three subsystems are housed in a single 20-slot VME chassis (6U form factor) and communicate with each other over the VMEbus (see the DC-8 DADS Internal Configuration diagram).

The Data subsystem is dedicated to acquiring and processing data from aircraft support systems, sensors and the ASD2VME subsystem; transmitting processed data to an external Data Distribution subsystem; and displaying processed data on video monitors. Information about data formats and transmission rates are available through the Medium Altitude Missions Branch at ARC. The Data subsystem is a real-time, turn key subsystem in which custom software is combined with the pSOS-68K Real-time, Multi-tasking Operating System Kernel.

The ASD2VME subsystem collects data from two inertial navigation systems plus radar altitude data. The ASD2VME subsystem converts this

data to engineering units, thus reducing processing on the Data subsystem. It is a real-time, turn key subsystem consisting of two custom-built avionics receiver boards controlled by a CPU board running custom software.

The Host subsystem performs functions that have no rigid real-time requirements, such as printing engineering units data on a character printer, recording data to disk files, logging mission director commentary, and post-flight data archival. Unlike the Data and ASD2VME subsystems, the Host subsystem is not turn key. The Host subsystem consists of custom software running under the UniFLEX Operating System.

Displayed and printed DADS data are configurable based on mission requirements. Calculated values, such as sun and moon azimuth and elevation, specific humidity and potential temperature, are available from the DADS. The majority of the avionics and environmental parameters that are displayed remains fairly constant from mission to mission.

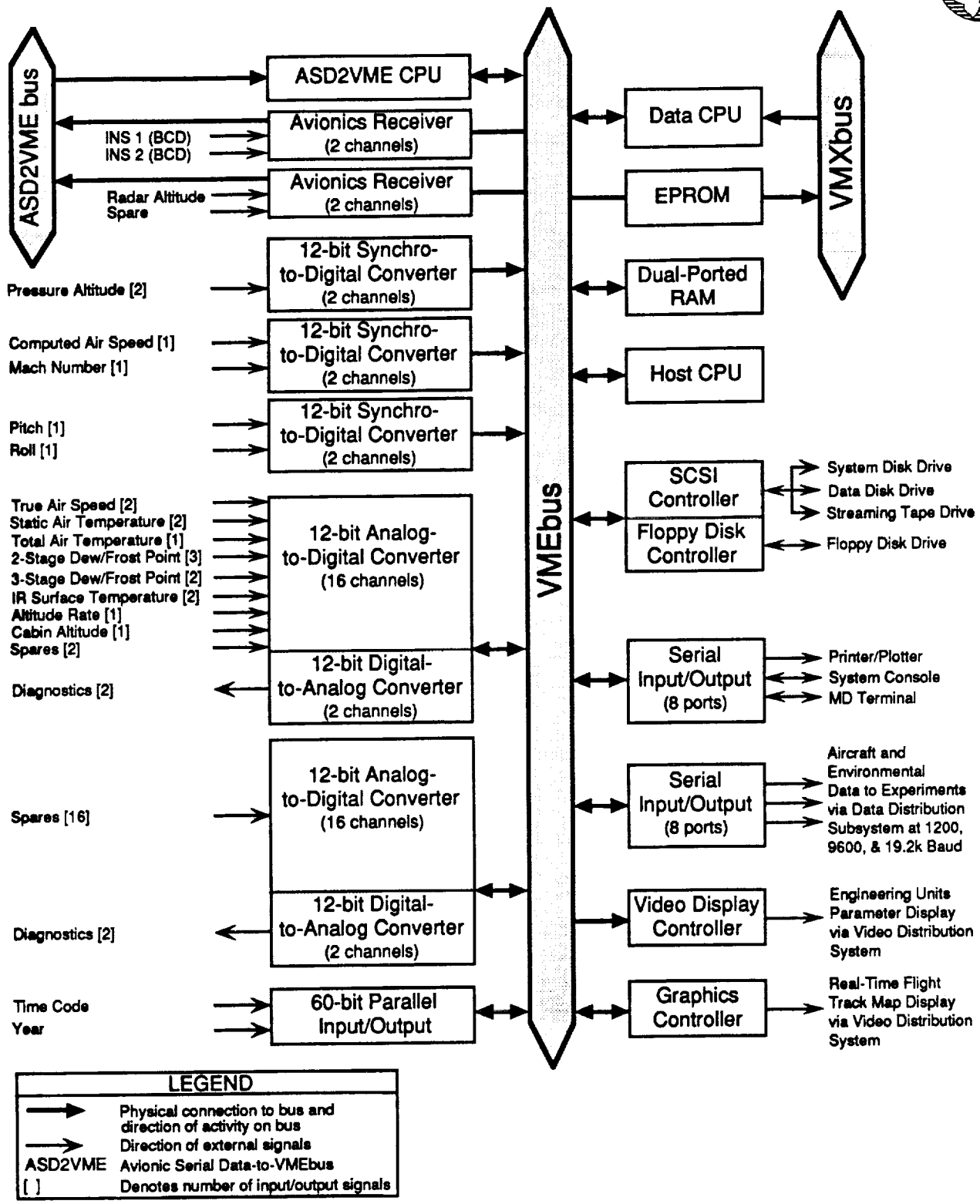

DC-8 DATA ACQUISITION AND DISTRIBUTION SYSTEM (DADS)

INTERNAL CONFIGURATION

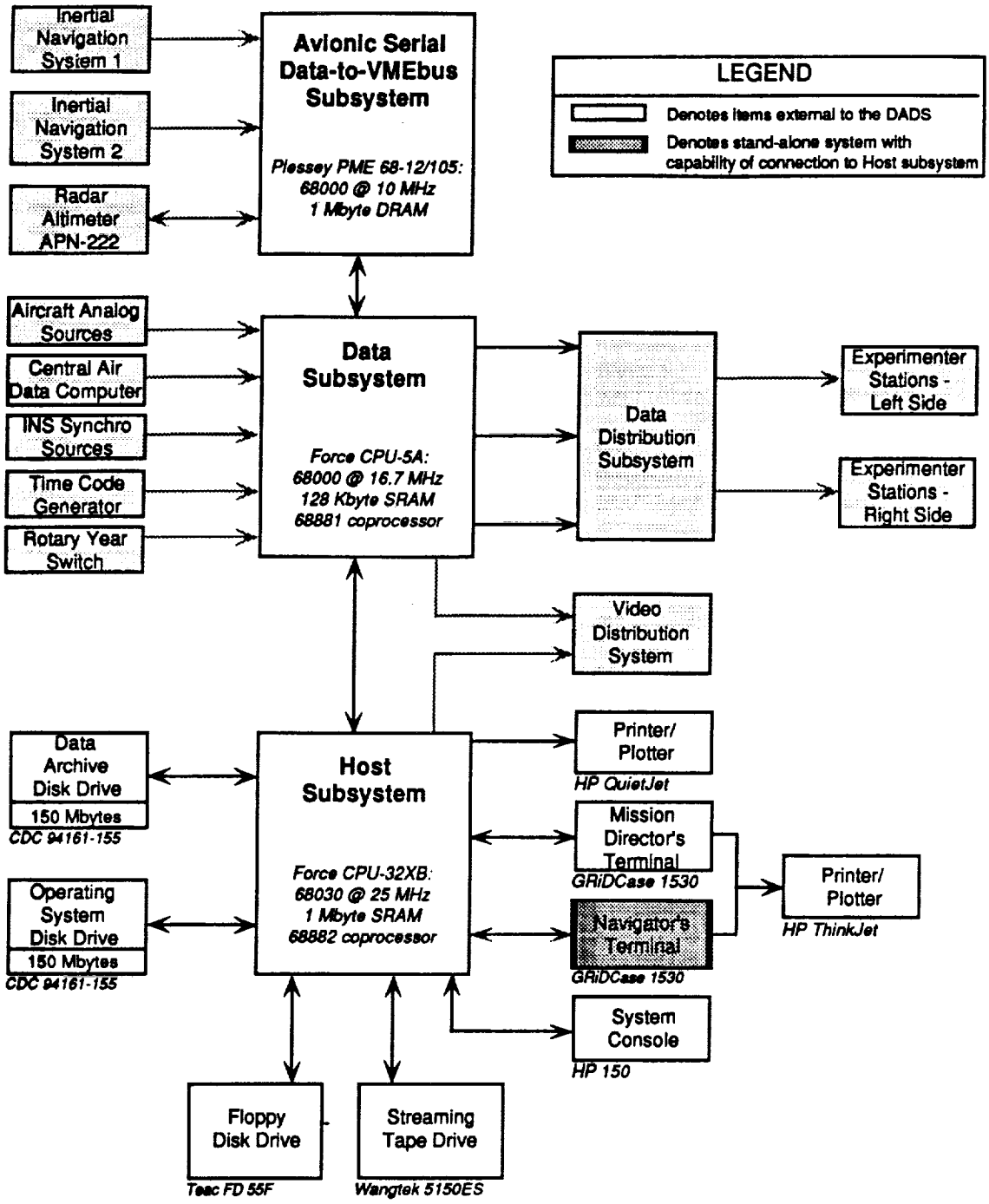

DC-8 DATA ACQUISITION AND DISTRIBUTION SYSTEM (DADS)
SYSTEM BLOCK DIAGRAM

Title: ^{36}Cl in the Stratosphere

Authors: Bruce Deck, Wadsworth Center for Laboratories and Research
Martin Wahlen, Wadsworth Center for Laboratories and Research
Harley Weyer, NASA/Johnson Space Center
Peter Kubik, Nuclear Structure Research Laboratory
Pankaj Sharma, Nuclear Structure Research Laboratory
Harry Gove, Nuclear Structure Research Laboratory

Discipline: Atmospheric Chemistry

Initial measurements of the cosmogenic radionuclide ^{36}Cl in the lower stratosphere have been made by Accelerator Mass Spectrometry. Samples were obtained using the large volume LASL air sampling pods on a NASA WB-57F aircraft. Untreated (for collection of particulates only) and Tetrabutylammoniumhydroxide treated (for collection of particulates and HCl) IPC-1478 filters have been flown on three flights in the lower stratosphere, following techniques by (1).

Cl and Cl compounds are important trace constituents for stratospheric chemistry, in particular with respect to O_3 destruction. Stratospheric Cl chemistry has recently received increased attention with the observation of strong O_3 depletion in the Antarctic winter vortex and in the weaker and more complex Arctic winter vortices.

Cosmogenic ^{36}Cl is produced by spallation reactions from Ar mainly in the stratosphere, and has had several applications as a geochemical tracer. The large amounts of ^{36}Cl introduced by nuclear weapon testing have been removed from the stratosphere by now, and measurements in the stratosphere to obtain cosmogenic production rates and concentration distributions is now possible.

We are investigating the use of cosmogenic ^{36}Cl as a tracer for stratospheric Cl chemistry and for stratospheric/tropospheric exchange processes. In a first attempt we are trying to determine stratospheric and tropospheric production rates, the partitioning of ^{36}Cl among particulate and gaseous Cl compounds, and the respective inventories and removal rates.

Results from a flight at 13.7 km, 30-33°N, 97-107°W, (1.8-2.4 km above the tropopause) and results from a second flight at 17.7 km, 43-45-36°N, 92-94°W, (7.6 km above the tropopause) for the untreated and treated filters respectively are presented below.

Samples	$^{36}Cl/Cl x10^{-15}$	^{36}Cl m^{-3} air STP	HCl (ppbV)
#1 particulate	63±7	1.45±0.16 $x10^3$	
HCl	655±52	1.99±0.18 $x10^4$	0.26±0.5
#2 particulate	350±20	3.0±0.2 $x10^4$	
HCl	3260±130	2.9±0.2 $x10^5$	2.0±0.2

These results show that about 90% of ^{36}Cl atoms are associated with HCl, the main stratospheric gaseous Cl compound. More data will be available at the time of the conference for comparison to the calculated production rates and to the measured deposition rates (2,3). ^{10}Be (another cosmogenic isotope entirely associated with the particulate phase) has not been measured in these samples yet but $^{10}Be/^{36}Cl$ ratios can be inferred from numerous data in the stratosphere at many latitudes and altitudes (M.Wahlen et al., unpubl. data), and can be compared to $^{10}Be/^{36}Cl$ in polar deposition (3). This comparison suggests that Cl might at times be strongly removed in polar regions.

Ref.: 1: Lazarus et al., JGR (1976) 1067. 2: Elmore et al., Nucl. Instr. and Meth. B29 (1987) 207. 3: N. Conard, MS thesis, University of Rochester, 1986.

N91-25460

Title: NASA DC-8 Airborne Research Laboratory

Author: Leo H. DeGreef, NASA/Ames Research Center

Discipline: Medium Altitude Airborne Research

Since the summer of 1987 NASA Ames Research Center has been operating a DC-8 equipped with CFM 56 engines as a flying research laboratory. In this relatively short time the DC-8, with its tremendous capabilities, has made significant contributions to numerous scientific fields. Capable of staying aloft for over 12 hours, the DC-8 has flown directly over both the North and South Poles, gathering data relating to the Ozone Hole. Operating from a few thousand feet to over 40,000 feet above sea level the interchangeable payload capability of the DC-8 has made it a versatile scientific tool. In its short time in the operational mode, the DC-8 has been based at the following locations: Punta Arenas, Chile; Stavanger, Norway; Tokyo, Japan; Stuttgart, Germany; Melbourne, Australia; Prestwick, Scotland; and Christchurch, New Zealand to name just a few. The DC-8 also plays a vital role in the development of new satellite-borne sensors as very often those sensors are test-flown on the DC-8 before they are launched into space. The tremendous range and instrument carrying capability make the DC-8 an ideal flying laboratory. A few of the programs the DC-8 has participated in as well as a sampling of the instruments carried are outlined below.

OZONE HOLE

To aid in understanding the Ozone Hole problem the DC-8, in coordination with the NASA ER-2, has conducted two extensive field campaigns in order to better understand the ozone mystery. The first mission, the Airborne Antarctic Ozone Experiment (AAOE), conducted from the Southern tip of Chile in August and September of 1987, flew missions over the Antarctic continent. The second major campaign, the Airborne Arctic Stratospheric Expedition (AASE), was conducted in January and February of 1989 from Stavanger, Norway. The DC-8 carried a payload of ten separate experiments over the Norwegian and Greenland Seas as far north as the North Pole in order to investigate the ozone destruction phenomenon.

SYNTHETIC APERTURE RADAR (SAR)-JPL

The ability to "SEE" through clouds using C-, L-, and P- Bands gives the JPL-SAR a tremendous advantage over other sensors that are interfered with by science-hindering cloud cover. The range of the DC-8 gives the JPL-SAR the capability to cover even the remotest reaches of our planet and to map wide areas for evaluation of the biological processes in forests

and croplands, the hydrology of drainage basins, the geology of erosion and tectonic activity, the condition and motion of glaciers and sea-ice packs, and the motion of major ocean circulation patterns. The JPL-SAR has been flown extensively over Shuttle Imaging Radar (SIR) test sites in preparation for the upcoming SIR-C Shuttle flight.

LASERS

The use of lasers onboard the DC-8 has notably extended the aircraft's utility as a research platform. By looking directly up and down simultaneously an atmospheric profile can be obtained. When combined with in-situ measurements the lasers make the atmospheric picture much clearer. Lasers that have already flown on the DC-8 include: The Differential Absorption Lidar (DIAL) - LaRC, the Airborne Backscatter Lidar Experiment - JPL, Visible-Near IR Lidar - GSFC, Continuous Wave CO_2 Lidars - MSFC, and the Aerosol Lidar - LaRC.

Additional Instruments Carried Include: Measurement of Air Pollution from Satellites (MAPS) - LaRC, Airborne Backscatter Lidar Experiment (ABLE) - JPL, Loran-C Dropsonde - NCAR, Whole Air Sampler - ARC/NCAR, Lyman Alpha Hygrometer - NOAA, F.T. Interferometer - JPL, F.T. Spectrometer - NCAR, UV/Blue Spectrograph - NOAA, Microwave Radiometers - GSFC, Rain Mapping Radar (RMR) - Japan/GSFC and many others. It is the ability to vary the sensors it carries depending on the science required that gives the DC-8 its tremendous flexibility and utility as an airborne research laboratory.

Additional Major Programs Supported Include: SAR/DARPA, Global Backscatter Experiment - GLOBE, Tropical Cyclone Motion - TCM, Tropical Rain Measuring Mission - TRMM, and Global Tropospheric Experiment - GTE.

Additional Fields Studied Include: Volcanology, Hydrology, Geology, Oceanography, Atmospheric Sciences, Meteorology, and many others.

With its host of on-board sensors, extraordinary range, and dedicated operators, the DC-8 stands ready to meet the scientific challenges posed by the research community well into the 21st Century.

ORIGINAL PAGE
BLACK AND WHITE PHOTOGRAPH

DC-8-72, McDonnell Douglas

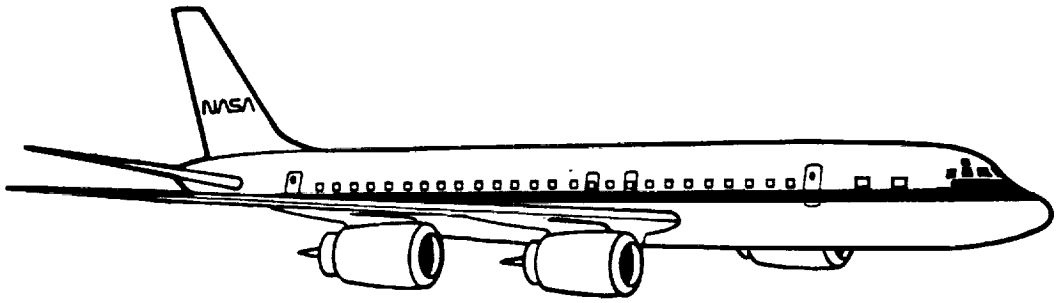

DC-8-72, McDonnell Douglas

Description:

Crew:	Two Pilots, Flight Engineer, Navigator
Length:	157 feet
Wingspan:	148 feet
Engine:	Four CFMI CFM56-2-C1 High Bypass Ratio Engines
Base:	Ames Research Center, Moffett Field, CA

Performance:

Altitude:	30,000-40,000 feet (Cruise), 42,000 feet (Maximum)
Range:	5400 nautical miles (Nominal 2700 nautical miles)
Duration:	12 hours (Nominal 6.0 hours)
Speed:	425-490 knots True Air Speed (Nominal 450 knots)
Payload:	30,000 lb

Accommodations:

Sensor Viewports at Nadir, 8° and 62° Elevations, and Zenith
Wing Pylons (2)
Optical Windows
19-inch Panel Equipment Racks
Liquid Nitrogen Supply
Heliostate: Gyro Stabilized Mirror System
Dropsonde Delivery Tube
Air and Aerosol Sampling Probes
Laser Chiller Unit

Support:

Navigation Flight and Environmental Data: Distributed and Recorded for Each Flight By Central Computer System
Weather Radar
Inertial Navigation with DME update
Time Code Generator
Closed Circuit Television
Dual Intercom System
60 Hz and 400 Hz Power

Sensors:

Dew/Frost Point Hygrometer
Radar Altimeter
Surface Temperature Radiometer
Metric, Panoramic, and Video Cameras
Walk-on: Ten to Twelve Stations Provided for Investigators Supplied and Operated Sensors

S16-43

N91-25461

p. 1

Title: The Geologic Remote Sensing Field Experiment (GRSFE): The First Geology Multisensor Airborne Campaign

Authors: Diane L. Evans, Jet Propulsion Laboratory
Raymond E. Arvidson, Washington University

JJ574450
WF835159

Discipline: Land

The primary objective of the Geologic Remote Sensing Field Experiment (GRSFE) is to acquire relevant data for geological sites that can be used to test models for extraction of surface property information from remote sensing data for Earth, Mars and Venus in support of the Earth Observing System (EOS), Mars Observer, and Magellan, respectively. Over forty scientists from eight universities and three NASA centers are participating in GRSFE which is co-sponsored by the NASA Planetary Geology and Geophysics Program and the NASA Geology Program. Highlights of the airborne campaign included the first simultaneous acquisition of Airborne Visible and Infrared Imaging Spectrometer (AVIRIS) and Thermal Infrared Multispectral Scanner (TIMS) data on September 29, 1989, and acquisition of Advanced Solid-State Array Spectroradiometer (ASAS), Polarimetric Synthetic Aperture Radar (AIRSAR), and Airborne Terrain Laser Altimeter System (ATLAS) data all within 3 months months of each other. The sites covered were Lunar Crater Volcanic Field and Fish Lake Valley in Nevada; and Cima Volcanic Field, Death Valley and Ubehebe Crater in California. Coincident field measurements included meteorological and atmospheric measurements, visible/near-infrared and thermal spectra, and characterization of geology and vegetation cover. GRSFE airborne and field data will be reduced to a suite of standard products and submitted, along with appropriate documentation, to the Planetary Data System (PDS) and the Pilot Land Data System (PLDS). These data will be used for a variety of investigations including paleoclimatic studies in the arid southwestern United States, and analysis of Magellan data (specifically those aimed toward understanding remote sensing signatures of basalt flows of varying ages and depth of aeolian fill, developing models for crater degradation, and understanding the correlation between radar roughness and aerodynamic roughness). GRSFE data will also be used to support Mars Observer Laser Altimeter (MOLA) and Mars Rover Sample Return (MRSR) simulation studies.

Title: The French Airborne Backscatter Lidar LEANDRE-1

Author: Pierre H. Flamant, CNRS

Discipline: Atmosphere

omit to P145

Abstract will be available at the Workshop.

PRECEDING PAGE BLANK NOT FILMED

Title: Fast-Response Aircraft Temperature Sensors

Authors: Carl A. Friehe, University of California, Irvine
Djamal Khelif, University of California, Irvine

Discipline: Aircraft Instrumentation

1. Introduction

Fast-response aircraft air temperature sensors are required for many applications: measurement of turbulent heat flux, temperature spectra, calculation of true airspeed, and accurate measurement of transients, such as inversions. The standard sensor has been the Rosemount total air temperature probe, although early in its use, it became apparent (McCarthy (1973a)) that the sensor suffered from two time constants. The shorter time constant is attributed to that of the 25 micron diameter Pt wire, whereas the longer time constant is attributed to the "housing" (Rodi and Spyers-Duran (1972)). Acheson (1973) criticized McCarthy's approach as having no physical basis; McCarthy (1973b) responded that the two time constants determined empirically from in-flight data appeared to adequately describe the response. Since then, the approaches to the measurement of fast temperature have been to use the Rosemount, and perhaps correct it for time response, as Ritter, et al. (1987) have done, or develop new sensors, as NCAR (see Spyers-Duran and Baumgardner (1983)) and Lawson (1990, personal communication) have done. These new sensors are characterized, however, by low recovery factors of about 0.8. This is of some concern, as Wyngaard (1988) has shown that low recovery-factor temperature probes can give erroneous fluctuating air temperature measurements when used in regions of high flow distortion, such as around an aircraft fuselage. Therefore it seems desirable to keep with the proven Rosemount design as much as possible since it has a high recovery factor (0.95-0.98). We believe that this is possible because the long time constant of the Rosemount probe is not due to the "housing", but rather due to the internal mounting of the Platinum wire inside the housing. In order to achieve a nominal resistance of 50 ohms of $d = 25$ micron Platinum wire inside the housing, Rosemount winds the wire around four mica supports in a compact "bobbin", with about $l = 1.5$ mm of unsuspended wire between supports (see Figure 1). This results in the Pt wire contacting a mica support about every 60 wire diameters. Paranthoen et al. (1982) have shown that such small l/d ratios give an undesirable second time constant due to the effect of lagged support temperature on the measured temperature. We believe that it is the slow temperature response of the mica supports, and not the "housing", which is responsible for the longer time constant. For measurements unaffected by supports, the l/d should be at least 1000, preferably 2000, according to Paranthoen et al. Since this is not possible for the 25 micron wire in the small space in the present housing, we merely replaced the internal Platinum element by a single thermistor bead in order to avoid the second time constant.

2. Modified Sensor

The modification of the standard temperature probe was straight-forward: the internal Pt element sub-assembly was removed and replaced with a similar sub-assembly with a $d = 75$ micron thermistor (see Figure 1). The non-deiced Rosemount Model 102 housing was used. For ease of installation, mounting of the thermistor and replacement, a TSI (St. Paul, MN) hot-wire anemometer probe was used. This terminates in two gold-plated stainless needles about 1.5mm apart, across which the thermistor bead (Thermoelectric Co.) was soldered. The TSI probe plugs into a TSI

probe support shaft which has BNC connector at the end for connection to the circuit. We replicated the brass shield of the Rosemount sub-assembly around the TSI probe support, as this must be an integral part of the flow control inside the housing.

A simple DC-Wheatstone bridge was used with the nominal 5Kohm thermistor. The output was slightly non-linear, due to the exponential response of the thermistor to temperature. The thermistor and bridge was calibrated in a constant-temperature bath of de-ionized water. The non-linear calibration was accounted for in the data reduction.

The modified sensor, along with a standard Rosemount 102EAL was mounted on the NCAR King Air just behind the radome. The data from all the probes were recorded at 50 Hz with a 14-bit analog-to-digital convertor and anti-aliasing filters at 20 Hz. The data were processed at NCAR to a final rate of 20 Hz. Comparison with the Rosemount sensor indicated that the recovery factor of the modified probe was unchanged.

The aircraft flew approximately 120 hours in the Shelf Mixed Layer Experiment (SMILE) off of the west coast of northern California. Most of the research flights were conducted at low levels in the marine boundary layer at altitudes of 30m. Occasional soundings were made to about 1200m. All temperature sensors remained intact for the duration of the program.

3. Data Analysis

From the flight data, portions were selected for both spectral analysis and transient response. Long flight tracks at low levels in the turbulent boundary layer were chosen for the spectral analysis. Soundings through inversions were used to assess the transient response.

The results of the transit through a reasonably sharp inversion are shown in Figure 2. Some adjustments were made to account for slight differences in gains (1 to 2 %) and offsets (approx. 0.5C) of the UCI-modified probe compared to the Rosemount by performing a least-squares fit of the measured UCI temperatures versus the Rosemount for a 5 min period around the transient feature. In the traverse through the inversion, the thermistor appears to have better response than the Rosemount. It appears that the Rosemount sensor takes about 10 sec to fully respond to the temperature change, considerably longer than the approximately 1 sec reported in the previous studies of Spyers-Duran and Baumgardner and McCarthy.

Spectral analysis was performed on approximately 8 min of data obtained in the marine boundary layer at 30m altitude. The spectra from the standard Rosemount and UCI-modified probe are shown in Figure 3, where there is some evidence for slightly more spectral variance between 0.1 and 3 Hz with the thermistor. This is shown in more detail in Figure 3, where the ratio of the two spectra are plotted. The thermistor probe has about 20% more spectral energy from 1 to 3 Hz, above which its response falls off due to its relatively large size. The sensible heat flux, obtained by correlation with the vertical velocity, was about 5% greater for the thermistor signal.

4. Conclusions

These tests demonstrate that some improvements in fast-response aircraft air temperature can be made by replacement of the Pt wire element in the Rosemount housing. The slow second time constant due to sensor wire support effects appears to be reduced by the use of a small thermistor bead in place of the multiply-supported Pt wire. Further improvement appears possible with the use of smaller elements in the housing.

5. Acknowledgements

This work was supported by the Office of Naval Research Marine Meteorology Program and the Division of Ocean Sciences of the National Science Foundation. We would lie to thank the

Research Aviation Facility of the National Center for Atmospheric Research for their support. Jim Perez fabricated the sensor and Todd Sutton built the electronics.

6. References

Acheson, D.T. 1973: *J. Appl. Meteor., 12*, 1089-1090.
McCarthy, J., 1973a: *J. Appl. Meteor.,12*, 211-214.
McCarthy, J. 1973b: *J. Appl. Meteor., 12*, 1090-1091.
Paranthoen, P., C. Petit and J.C. Lecordier, 1982: *J. Fluid Mech.,124*, 457-473.
Ritter, J.A., G.L. Smith and D.R. Cahoon, 1987: *Sixth Symposium on Meteorological Observations and Instrumentation,* New Orleans, Jan 12-16, 1987, American Meteor. Soc., Boston, MA, 261-264.
Rodi, A. R. and P. A. Spyers-Duran, 1972: *J. Appl. Meteor., 11*, 554-556.
Spyers-Duran, P. and D. Baumgardner, 1983: *Fifth Symposium on Meteorological Observations and Instrumentation,* Toronto, April 11-15, 1983, American Meteor. Soc., Boston, MA, 352-357.
Wyngaard, J.C. 1988: *J. Atmos. Sci., 45*, 3400-3412.

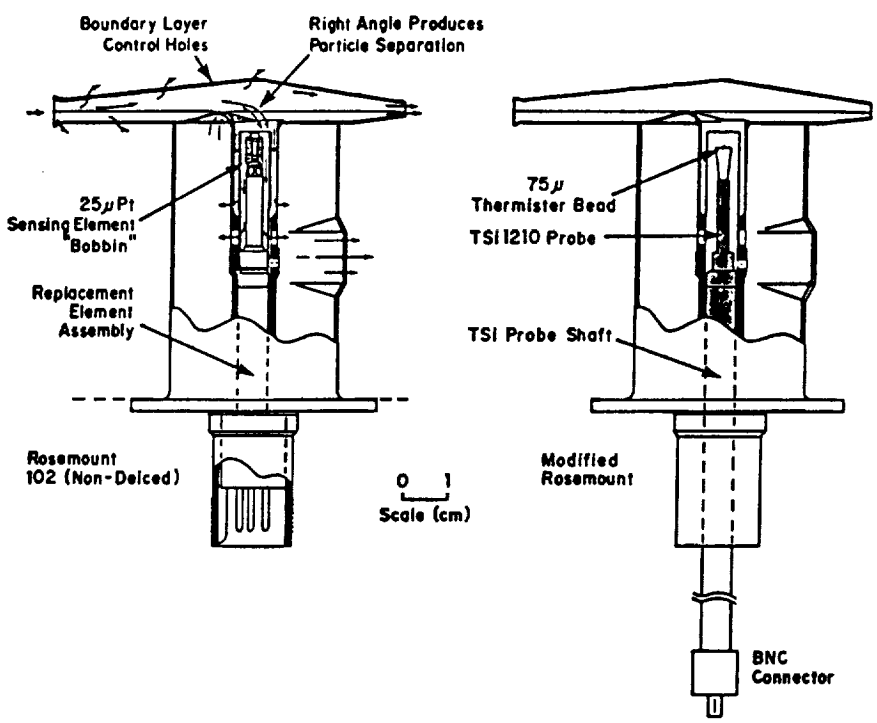

Figure 1. Standard Rosemount 102 Sensor (left); Modified Sensor (right).

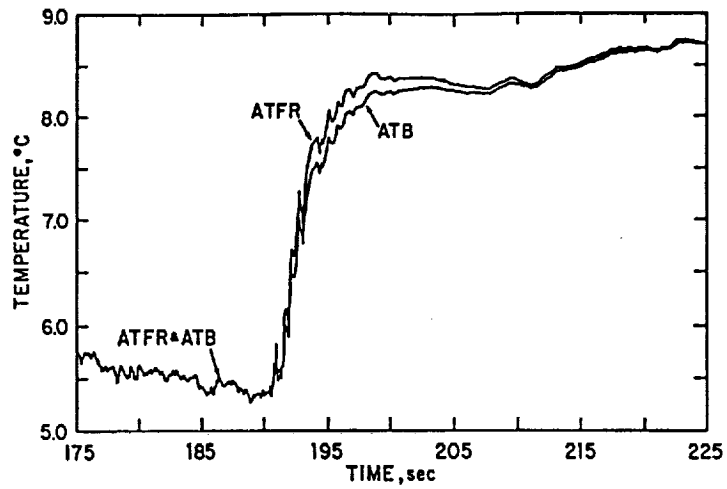

Figure 2. Time Series of the Standard Rosemount (ATB) and Modified Sensor (ATFR) Through an Inversion.

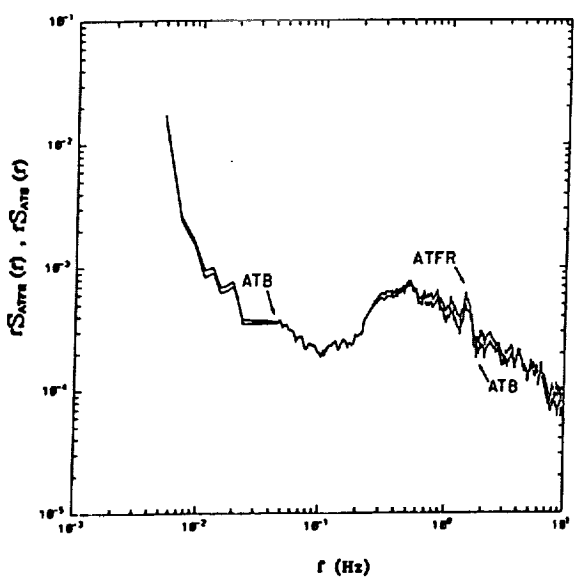

Figure 3.
Power Spectra (multiplied by frequency) for Standard Rosemount (ATB) and Modified Sensor (ATFR) in the Marine Boundary Layer.

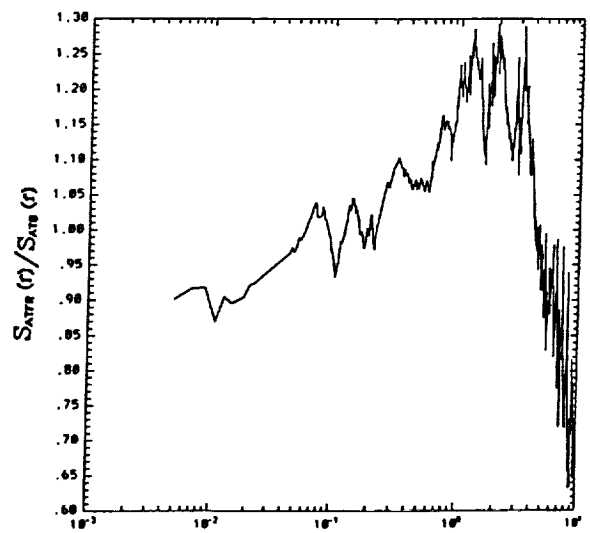

Figure 4.
Ratio of Power Spectra of Figure 3: ATFR/ATB.

N91-25462

Title: High-Resolution Measurements of Surface Topography with Airborne Laser Altimetry and the Global Positioning System

Authors: James B. Garvin, NASA/Goddard Space Flight Center
Jack L. Bufton, NASA/Goddard Space Flight Center
John F. Cavanaugh, NASA/Goddard Space Flight Center
William B. Krabill, NASA/Wallops Flight Facility
Thomas D. Clem, NASA/Wallops Flight Facility
Earl B. Frederick, NASA/Wallops Flight Facility
John L. Ward, NASA/Wallops Flight Facility

Discipline: Land

We have recently developed and are now operating an airborne lidar system that measures laser pulse time-of-flight and the distortion of the pulse waveform upon reflection from Earth surface terrain features. This instrument is combined with Global Positioning System (GPS) receivers and a two-axis gyroscope for accurate recovery of aircraft position and pointing attitude. The laser altimeter system is mounted on a high-altitude aircraft platform and operated in a repetitively-pulsed mode for measurements of surface elevation profiles at nadir. The laser transmitter makes use of recently developed short-pulse diode-pumped solid-state laser technology in Q-switched Nd:YAG operating at its fundamental wavelength of 1064 nm. A reflector telescope and silicon avalanche photodiode are the basis of the optical receiver. A high-speed time-interval-unit and a separate high-bandwidth waveform digitizer under microcomputer control are used to process the backscattered pulses for measurements of terrain.

Accurate recovery of the surface topography to the 10 cm level and understanding of the laser waveform data require 3-axis position knowledge and 2-axis pointing knowledge for the aircraft platform. These data are primarily provided by an on-board Global Positioning System (GPS) receiver and roll and pitch gyroscope sensors. Aircraft position in three-dimensions is measured to sub-meter accuracy by use of differential Global Positioning System receivers. An eight-channel, single frequency GPS receiver is located inside the aircraft and operated to provide one-half of the required aircraft position data set. Differential GPS position recovery results by utilizing a second, ground-based receiver, identical to the airborne unit. The ground-station is usually located at the airbase operations center or in the remote target area at a survey marker or other geodetic reference point. Aircraft roll and pitch attitude are obtained to the resolution of ~ 1.5 mrad by orthogonal-mounted 12-bit

gyroscopes and the associated synchro/resolver electronics.

The lidar system, position-determination sensors, and pointing-attitude sensors are packaged into a relatively compact and low-power interface to a NASA turbojet research aircraft, a T-39 Sabreliner, that is based at Wallops Flight Facility (WFF), Wallops Island, Virginia. Laser altimeter measurements are typically acquired along the nadir track of the WFF T-39 aircraft. Data acquisition is possible over the entire operational envelope of the T-39 aircraft. This extends under clear atmospheric conditions from approximately 150 m to 12.5 km altitude. The laser divergence slightly overfills the receiver field-of-view of 2.5 mrad. Thus, the laser footprint on the surface is 2.5 m diameter per kilometer of altitude. At an aircraft speed of 100 m/sec, typical for the T-39 during straight & level VFR data acquisition, the 55 Hz ranging rate of the laser altimeter will produce contiguous data at altitudes of 730 m or above. This is the standard operational mode and can accommodate data runs from a single pulse to 5 minutes of data (16,500 pulses covering 30 km of horizontal distance).

This airborne lidar instrument was developed during the period 1986-1990 under sponsorship of the Land Processes Program of NASA Headquarters for topographic profiling studies of dynamic geology. It has been employed to date in five airborne topography campaigns in the Western U.S. from which data sets are now becoming available. The airborne instrumentation described here has been developed to provide the capability for ranging and waveform studies of Earth surface topography at high resolution as a precursor to the development and application of spacecraft instruments and as a means to acquire local-scale geological data. Both this airborne instrument and the spacecraft instruments are designed with laser pulse timing and waveform capability for geodetic quality (~ 10 cm) topography data.

N91-25463

Title: The Millimeter-Wave Imaging Radiometer (MIR)

Authors: A.J. Gasiewski, Georgia Institute of Technology
D.M. Jackson, Georgia Institute of Technology
R.F. Adler, NASA/Goddard Space Flight Center
L.R. Dod, NASA/Goddard Space Flight Center
J.C. Shiue, NASA/Goddard Space Flight Center

Discipline: Atmosphere

The Millimeter-Wave Imaging Radiometer (MIR) is a new instrument being designed for studies of airborne passive microwave retrieval of tropospheric water vapor, clouds, and precipitation parameters. The MIR is a total-power cross-track scanning radiometer for use on either the NASA ER-2 (high-altitude) or DC-8 (medium altitude) aircraft. The current design includes millimeter-wave (MMW) channels at 90, 166, 183±1,3,7, and 220 GHz. An upgrade for the addition of submillimeter-wave (SMMW) channels at 325±1,3,7 and 340 GHz is planned. The nadiral spatial resolution is approximately 700 meters at mid-altitude when operated aboard the NASA ER-2.

The MIR consists of a scanhead and data acquisition system, designed for installation in the ER-2 superpod nose cone (Fig. 1). The scanhead (Fig. 2) will house the receivers (feedhorns, mixers, local oscillators, and preamplifiers), a scanning mirror, hot and cold calibration loads, and temperature sensors. All channels will have nearly identical beamwidths (3°). The $\pm 50^o$ field-of-view will be scanned every $\sim$ 2.5 seconds. Particular attention is being given to the characterization of the hot and cold calibration loads through both laboratory bistatic scattering measurements and analytical modelling.

The data acquisition system consists of a PC/AT compatible computer with 200 MB optical WORM disk drive, a 12-bit 32-channel opto-isolated A/D converter, IF and video circuitry, and power conditioning module. Automatic offset and gain controls (AOC and AGC) provide *in situ* compensation for inevitable system offset and gain fluctuations. (Such fluctuations are expected for non-Dicke type radiometers. An optional chopper-wheel Dicke switch will be installed if necessary.) A watch-dog timer and IRIG-B time decoder are included in the PC/AT.

The high spatial resolution MMW brightness imagery will be useful for 1) verifying MMW radiative transfer models in clear air and precipitation, 2) constructing and evaluating MMW precipitation parameter (e.g., rainfall rate, particle size), cloud parameter (e.g., liquid and cirrus water content), and water vapor retrievals, 3) studying convective raincell and atmospheric gravity wave structure, and 4) evaluation of AMSU, TRMM, EOS, ESGP and joint IR-microwave retieval algorithms. Future imagery using both MMW and SMMW channels will be useful for 1) verification of SMMW radiative transfer models (particularly for cirrus clouds), 2) initial evaluation of water vapor profiling using 183 and 325 GHz channels, and 3) evaluation of cloud parameter retrieval and precipitation mapping using the SMMW channels. Most of the MIR science objectives will require complementary data from other airborne instruments (e.g., AMPR, EDOP, MTS, MAMS, weather radars, optical and infrared satellites, and radiosondes).

The MIR is a joint effort between NASA GSFC and the Georgia Tech School of Electrical Engineering. Meteorological data flights aboard the NASA ER-2 using the MIR MMW channels are tentatively scheduled for August and September 1991 during CAPE. The data will have potential impact on the design of future polar and geosynchronous passive microwave satellite missions.

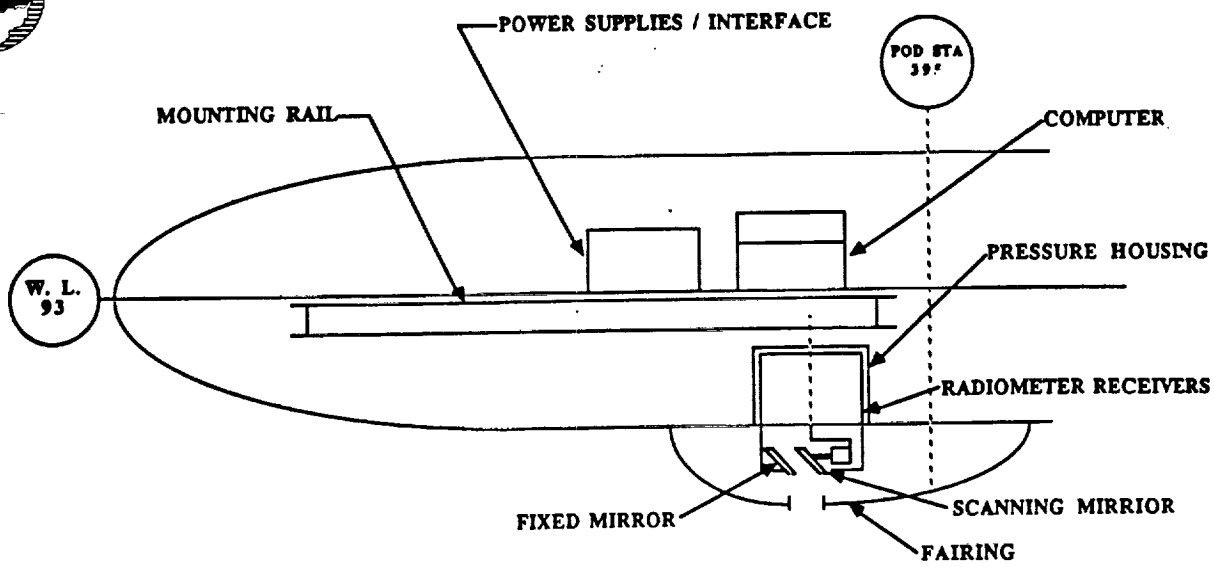

Figure 1: Location of the MIR in the ER-2 superpod nosecone.

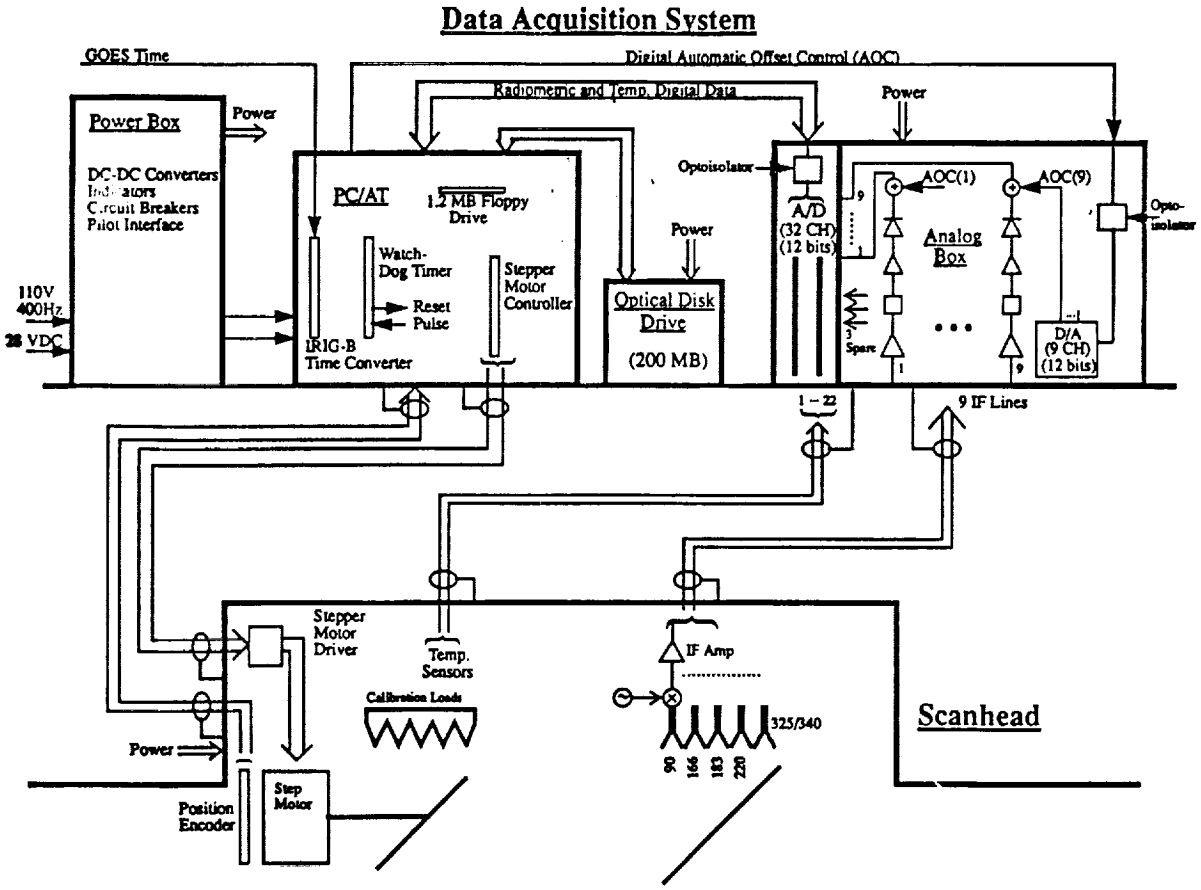

Figure 2: Block diagram of the MIR scanhead and data acquisition system.

N91-25464

20132

P4

Title: Airborne Sulfur Trace Species Intercomparison Campaign: Sulfur Dioxide, Dimethylsulfide, Hydrogen Sulfide, Carbon Disulfide, and Carbonyl Sulfide

Authors: Gerald L. Gregory, NASA/ Langley Research Center
James M. Hoell, Jr., NASA/Langley Research Center
Douglas D. Davis, Georgia Institute of Technology

NT210491

GW167534

Discipline: Atmosphere-Instrumentation Intercomparison

Results from an airborne intercomparison of techniques to measure tropospheric levels of sulfur trace gases are presented. The intercomparison was part of the National Aeronautics and Space Administration (NASA) Global Tropospheric Experiment (GTE) and was conducted during the summer of 1989. The intercomparisons (Chemical Instrumentation Test and Evaluation--CITE-3) were conducted on the Wallops Electra aircraft during flights from Wallops Island, Virginia, and Natal, Brazil. Sulfur measurements intercompared included sulfur dioxide (SO_2), dimethylsulfide (DMS), hydrogen sulfide (H_2S), carbon disulfide (CS_2), and carbonyl sulfide (OCS). Measurement techniques ranged from filter collection systems with post-flight analyses to mass spectrometer and gas chromatograph systems employing various methods for measuring and identifying the sulfur gases during flight. Sampling schedules for the techniques ranged from integrated collections over periods as long as 50 minutes to 1- to 3-minute samples every 10 or 15 minutes. Several of the techniques provided measurements of more than one sulfur gas. As was the case for earlier CITE-1 and -2 tests, instruments employing different detection principles were involved in each of the sulfur intercomparisons. Intercomparison of measurements obtained by instruments employing different detection principles is one approach to add credibility to the measurement of low levels of trace gases as well as to provide confidence in both new and existing technology. The majority of the intercomparison results were for mixing ratios below 200 parts-per-trillion (pptv) and, thus, are important to validating current measurement capabilities at low concentrations normally encountered in clean and remote areas of the troposphere. Sulfur dioxide intercomparisons included mixing ratios to the ppbv levels. Carbonyl sulfide results were at the 300 to 600 pptv level; i.e., nominal ambient values. Also included in the intercomparison measurement scenario were a host of supporting measurements (i.e., ozone, nitrogen oxides, carbon monoxide, total sulfur, aerosols, etc.) for purposes of (1) interpreting the intercomparison results (i.e., correlation of any noted instrument disagreement with the chemical composition of the measurement environment) and (2) providing supporting chemical data to meet CITE-3 science objectives of studying ozone/sulfur photochemistry, diurnal cycles, etc.

Results show good agreement among techniques for DMS, H_2S, and CS_2, from near the detection limit of the instruments (few ppt) to 100 to 200 pptv (upper limits of the intercomparisons). For example, DMS instrument agreement was on the average about 10 pptv among the instruments and was within stated accuracy and precision of the techniques (typically about 20%). Figure 1 shows the DMS results where data from different techniques are plotted versus the average DMS. The average is the arithmetic mean of the values reported from all the techniques. Plotted with the data point are the 1-sigma values for the average. Linear regression results are also given for each panel of the figure. Carbonyl sulfide results also showed good agreement for the 300- to 600-pptv range of concentrations investigated. Results suggest that each technique, regardless of its sampling period, provides equally valid measurements of the respective species. Apparently, such is not the case for SO_2. The initial analyses of the SO_2 intercomparison data suggested that ambient variability of SO_2 combined with the different temporal sampling schedules of the techniques were influencing the results and that, in many cases, differences between SO_2 values reported by the various techniques may be the result of SO_2 ambient variability. Additional analyses are being performed to separate ambient variability/temporal overlap influences from instrument intercomparison results. While these analyses are not yet complete, results suggest that there are some significant biases among one or more of the techniques which cannot be attributed to ambient variations and sample temporal overlap. On the other hand, results also suggest that for equally valid measurement techniques (i.e., no bias between techniques), the different sampling schedules combined with ambient variations can result in significantly different reported values of SO_2.

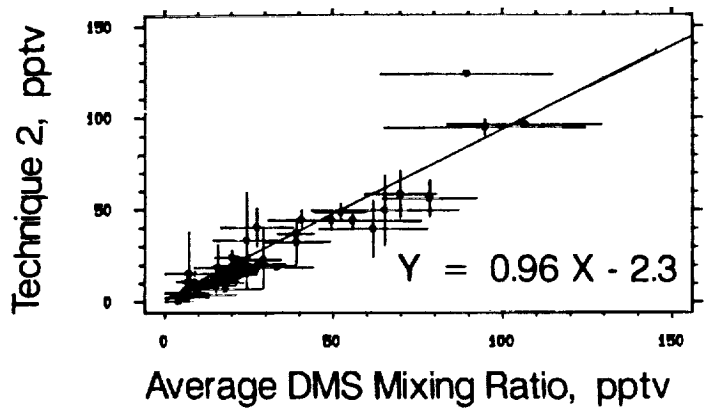

a) Technique 2

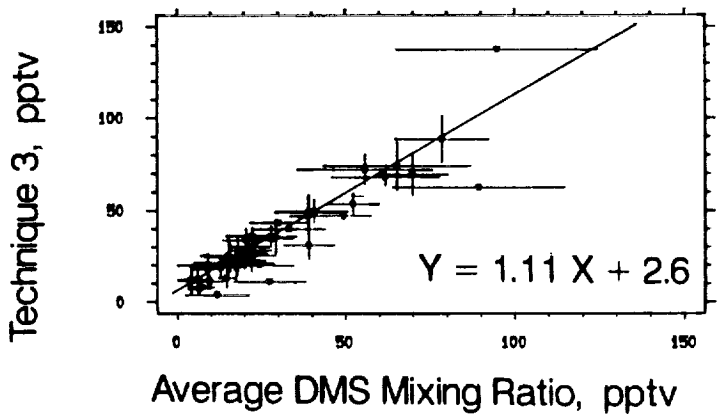

b) Technique 3

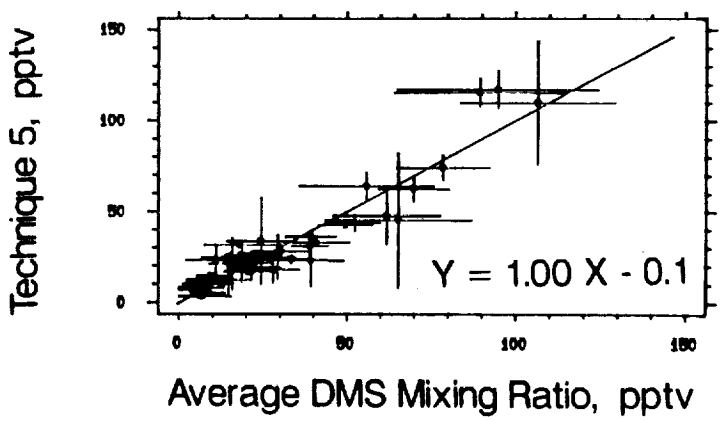

c) Technique 5

Figure 1. - Results of DMS Intercomparisons

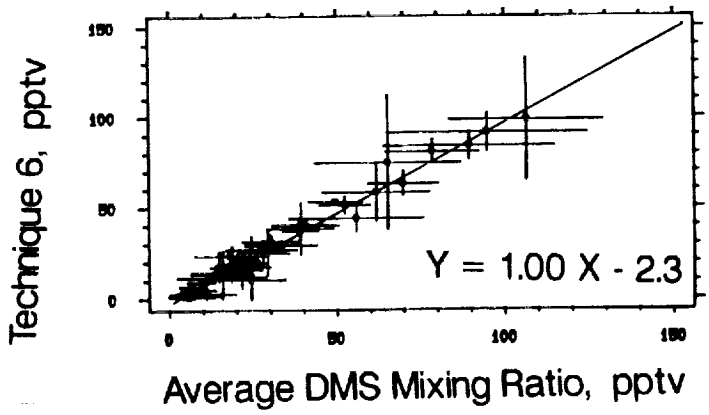

d) Technique 6

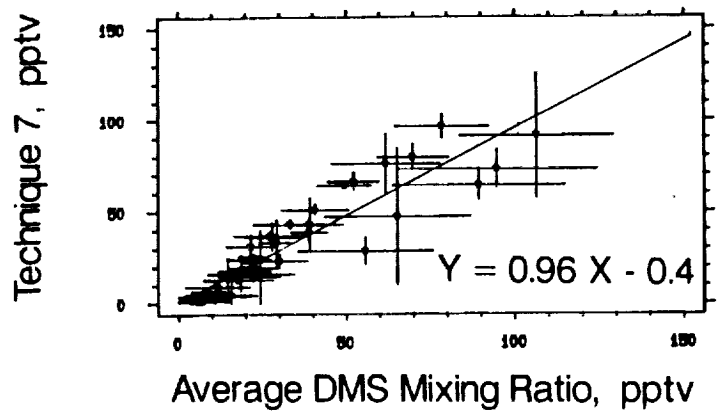

e) Technique 7

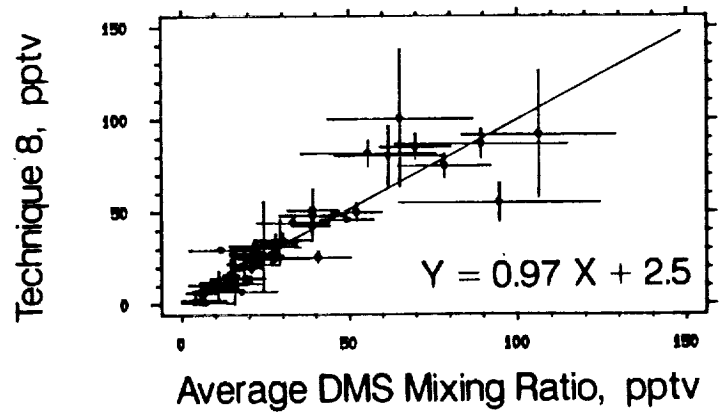

f) Technique 8

Figure 1. - Concluded.

Title: An Electrically Scanned Thinned Array Radiometer for Earth Remote Sensing

Authors: Andrew J. Griffis, University of Massachusetts
Calvin T. Swift, University of Massachusetts
David LeVine, Goddard Space Flight Center

Discipline: Microwave Remote Sensing—Soil Moisture and Ocean Salinity

Interferometric aperture synthesis is being investigated as an alternative to real aperture measurements of the brightness temperature of the Earth from low Earth orbit. Aperture synthesis allows for the realization of space borne microwave systems with attractive spatial resolution characteristics. Radio astronomers have performed aperture synthesis by cross-correlating spatially separated antenna element pairs for some time [1]. The application of this technique to the observation of a distributed source, as opposed to a point source in radio astronomy, presents a novel and challenging application of aperture synthesis. The demonstration of this geophysical application of aperture synthesis was carried out by constructing and flight testing a prototype instrument, the Electrically Scanned Thinned Array Radiometer (ESTAR). The subsequent data analysis and image reconstruction yielded an image of the eastern shore of Virginia [2]. In the past year, more data of the same region have been taken and analyzed, as well as for other regions of Virginia, Pennsylvania and Maine.

Improvements have been made in the image reconstruction technique and in the system electronics for the current and upcoming instruments (ESTAR00 and ESTAR0, respectively), particularly in terms of calibration instrumentation and techniques. The authors will be presenting the prototype system schemata, inversion algorithm and reconstructed brightness temperature images (both early and recent) in the poster session.

[1] Brown, R. and R. Twiss, "A New Type of Interferometer for Use in Radio Astronomy," Phil. Mag., vol. 45, p. 663, 1954.

[2] LeVine, Kao, Tanner, Swift and Griffis, "Performance of a Proposed Spaceborne Synthetic Aperture Microwave Radiometer," IEEE Trans. Rem. Sens. and Geosc., Vol. 28, No. 4, pp. 614–619, 1990.

Title: The Convection Waves Project: Cloud Street Experiment

Author: Robert L. Grossman, University of Colorado

Discipline: Atmosphere

omit to p. 161

Abstract will be available at the Workshop.

PRECEDING PAGE BLANK NOT FILMED

PAGE 154 INTENTIONALLY BLANK

Title: A Small, Lightweight Integrated Flight Data System (IADS) for Flight Testing

Author: Jorg M. Hacker, Flinders University

Discipline: Atmosphere

Abstract will be available at the Workshop.

Title: Whales and Ocean Habitats: Exploratory Research Using Airships

Author: James H.W. Hain, Associated Scientists at Woods Hole

Discipline: Oceans

Several thousand hours of survey time from fixed-wing aircraft have been conducted on whales, dolphins, and their ocean habitats. These studies have provided a valuable dataset and a perspective that complements and expands on what had been learned from many years of more traditional ship-based studies. The experience has also pointed the way to the next major data requirement: fine-grain, site-specific studies on time/space variability, behavior, and habitat characteristics.

Much of this "next generation" research will require slow-flight or station-keeping capabilities. Spatial scales will be 1 to 20 miles, and time scales from several hours to complete days—with emphasis on replicate sampling.

In 1989, Associated Scientists expanded its AirBorne Science Project to include lighter-than-air vehicles. Attention was focused on the new generation of airships now becoming available. A multi-year study is now underway to demonstrate, evaluate, and refine the use of airships—specifically for whale and ocean habitat research, but also more generally for a wide range of oceanographic studies and environmental monitoring. A flight program began in December 1989.

To date, 10 days of flying have taken place. Studies have been conducted off Cape Cod, Massachusetts; Cape Hatteras, North Carolina; and the east coast of Florida. The airship as a research platform has met expectations. A "carry-on" science/instrument package continues to be refined and developed, as do positioning and survey techniques. Still- and video-photography have been successful. Observations on whale distribution, behavior, individual recognition, and habitat use are continuing.

N91-25466
20134
p2

Title: Remote Sensing of Earth's Atmosphere and Surface using a Digital Array Scanned Interferometer—A New Type of Imaging Spectrometer

Authors: Philip D. Hammer, NASA/Ames Research Center
Francisco P.J. Valero, NASA/Ames Research Center
David L. Peterson, NASA/Ames Research Center
William Hayden Smith, Washington University

NC473657
WF835159

Discipline: Atmosphere/Land/Remote Sensing

We have been evaluating the capabilities of the DASI (digital array scanned interferometer) class of instruments for measuring terrestrial radiation fields over the visible to mid-infrared. DASIs are capable of high throughput, sensitivity and spectral resolution and have the potential for field-of-view spatial discrimination (an imaging spectrometer). The simplicity of design and operation of DASIs make them particularly suitable for field and airborne platform based remote sensing. Our long term objective is to produce a versatile field instrument which may be applied toward a variety of atmospheric and surface studies.

The basic principle behind the operation of the DASI is similar to that for conventional scanned interferometers. The detected signal results from two-beam interference. The wavelength spectrum of the incident radiation is obtained by Fourier transforming this recorded interferogram. However, unlike a conventional interferometer, the DASI operates with its mirrors fixed in position. The range of path differences between the recombined beams is achieved by means of the configuration of the optical components so that fringes of equal inclination are formed at the image plane. This comprises the interferogram which can be resolved spatially by a detector array. Fig. 1 shows a particular DASI configuration using a tilted grating to obtain a variable range of path differences across the detector [1].

The advantages of DASIs may best be described by comparison with other commonly used spectrometers. In general Fourier transform spectrometers (FTS) have several advantages over grating spectrometers [2]. These include enhanced throughput (particularly at higher spectral resolution) and superior signal linearity and dynamic range. DASIs have additional advantages over conventional Michelson interferometers [3]: 1) *Simplicity of design and operation* - interferograms are acquired with the optics stationary; 2) *Capability of Observing transient events* - the entire interferogram is measured simultaneously; 3) *Spatial imaging* - the redundant coordinate at the image plane can be used for one-dimensional imaging of the field of view; 4) *Enhanced throughput potential* - certain DASI optical configurations result in field widening, eliminating the aperture size constraint of Michelson interferometers [4]; 5) *Reduction of background radiation by cooling* - The absence of moving optical components facilitates cryogenic operation of the entire spectrometer which can greatly reduce ambient background radiation in the infrared. Although this is achievable with scanning interferometers [5,6], such instruments are complex and expensive.

There is much information which can be retrieved from spectrally as well as spatially resolved remote sensing data which would be applicable to both global and regional problems. At lower resolution ($> 10\ cm^{-1}$), surface albedo and emissivity, and aerosol and cloud properties may be derived. For example radiative transfer theory may be applied to remote sensing measurements of clouds to retrieve microphysical properties of the constituent ice crystals [7] which is important for understanding the heat budget of the atmosphere, and measurements of infrared solar reflectance from plant canopies may be used to study biogeochemical processes [8].

Higher resolution instruments ($< 0.1\ cm^{-1}$) can reveal molecular transition features. This permits superior discrimination, detection, and quantization of specific molecular species which may serve as tracers or indicators of important atmospheric chemical and dynamical processes. The derivation of altitude profiles of the atmosphere can be done in principle based on pressure effects on the line shapes and temperature effects on relative line intensities. The nadir viewing ER-2 based HIS (High resolution In-

terferometer Sounder) is a Michelson interferometer developed for such purposes [9]. Two high resolution infrared Michelson Fourier spectrometers were flown on the NASA DC-8 aircraft during the polar ozone expeditions [10]. Observations of the sun were made to measure column densities of numerous atmospheric molecules. A higher sensitivity instrument capable of measuring molecular thermal emissions in the absence of sunlight (i.e. a cryogenic field widened interferometer) would be a major advancement for future polar missions.

For the reasons revealed above there is currently a vital need for a versatile instrument having high spectral resolution, sensitivity and tunability as well as imaging capabilities. DASIs show promise of meeting these criteria: they have many of the positive characteristics of conventional FTS instruments and the additional features described above. The ease of construction and operation due to the absence of actively scanning optical components provides a relatively inexpensive alternative to other interferometer designs.

References

[1] Butcher, H., N. Douglas, S. Frandsen, F. Maaswinkel, "A Practical Non-scanning FTS for Astronomy", Abstracts of OSA Topical Meeting on High Resolution Fourier Transform Spectroscopy, Santa Fe, NM, Feb., (1989).

[2] Connes, P. "Astronomical Fourier Spectroscopy", *Ann. Rev. Astron. Ap.*, **8**, 209, (1970).

[3] Caulfield, H. J., "Holographic Spectroscopy" in Advances in Holography, (N. Farhat ed.), Vol. 2, p. 139, Marcel Dekker, New York, (1976).

[4] Smith, W. H. and W. V. Schempp, "Digital Array Scanned Interferometers", *J. Exp. Astron.*, in press, (1990).

[5] Beer, R. and T. A. Glavich, "Remote Sensing of the Troposphere by Infrared Emission Spectroscopy", Abstracts of OSA Topical Meeting on High Resolution Fourier Transform Spectroscopy, Santa Fe, NM, Feb., (1989).

[6] Kunde, V. G. et al., "Infrared Spectroscopy of the Lower Stratosphere with a Ballon-borne Cryogenic Fourier Spectrometer", *Appl. Opt.* **26**, 545, (1987).

[7] Hammer, P. D., F. P. J. Valero, and S. Kinne, "The 27-28 October 1986 FIRE IFO Case study: A comparative study of infrared radiance measurements by an ER-2 based radiometer and the Landsat 5 thematic mapper (TM6)", *Mon. Wea. Rev.*, submitted, (1990).

[8] Peterson, D. L. et al., "Remote Sensing of Forest Canopy and Leaf Biochemical Contents", *Rem. Sens. Environ.*, **24**:85-108 (1988).

[9] Smith, W. L., R. Frey, "On Cloud Altitude Determinations from High Resolution Interferometer Sounder (HIS) Observations", *J. Appl. Meteor.*, **29**, 658, (1990).

[10] AASE, "Airborne Arctic Stratospheric Expedition", Project Office, NASA Ames, Oct., 1988.

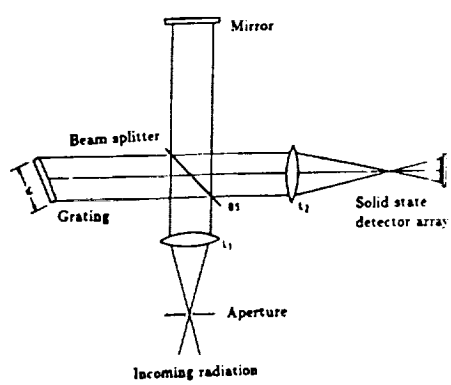

FIG 1 - DASI configuration using a tilted grating. Lens L2 images the grating onto the detector array so that the path difference varies across the array (in plane of paper). The orthogonal axis (perpendicular to plane of paper) is available for spatial imaging.

Title: Airborne Field Mill Research Platform

omit to p. 167

Authors: Ray Harris-Hobbs, Aeromet, Inc.
Arleen Lunsford, Aeromet, Inc.
R. Lynn Rose, Aeromet, Inc.
Kathy L. Giori, SRI International
Joel Kositsky, SRI International
Robert A. Maffione, SRI International

Discipline: Atmospheric Sciences

Space launch vehicles have historically been subject to triggered lightning strikes as they pass thorough or near clouds that might not otherwise discharge. Examples are the Apollo 12 in 1969, which triggered two lightning discharges, and in 1987 an Atlas/Centaur launched from Cape Canaveral Air Force Station triggered a lightning strike which resulted in its demise. Consequently, the launch criteria which are based upon little data and limited understanding of the development of electrified clouds are quite restrictive. To gain the knowledge that will enable the safe launch of vehicles without undue delays, the Air Force Space Division (**AFSD**) initiated a program to directly measure the development and dissipation of electric fields in convective cloud systems. This program is called the Airborne Field Mill (**ABFM**) program.

The purpose of the ABFM program is to better specify and identify atmospheric conditions conducive to triggered lightning. In addition, this program is designed to aid in formulating a space launch weather criteria that properly balances launch availability and safety concerns. This effort was initiated by using electric field mills designed and built by SRI on the High Altitude Research Platform (**HARP**), a Lear 36A operated by Aeromet, with other meteorological instrumentation. The HARP is supported by the Ballistic Missile Organization (**BMO**) through a contract with the U. S. Army Strategic Defense Command.

This abstract provides a preliminary summary of the theory, operation, and data analysis as applied specifically to estimate the accuracy of the ABFM system installed and operated during the summer of 1989.

The HARP is a high performance jet capable of operating between sea level and 45,000 ft and staying on station for 4.5 hours. Figure 1 shows the location and type of meteorological instruments and field mills on the HARP. The aircraft went through two lightning protection reviews, concluding with the Engineering Report, Lightning Protection Improvements for Aeromet Lear 36 (Rupke 1989).

The ABFM system used on the HARP employed electric field mills designed by SRI to minimize size, weight, and complexity of use. The design uses the chopped static field between two plates to produce an alternating current signal proportional to the electrostatic field intensity as shown in Figure 2 and 3. In using an aircraft platform for measuring ambient electric fields, it is essential to recognize that the aircraft itself is a part of the sensor system. The presence of the aircraft, like any other probe, perturbs the ambient field as shown in Figure 4. Under the uniform field hypothesis, the scalar field magnitude measured at a point perpendicular to the aircraft surface is related to the ambient field vector by a linear sum of the field components and the aircraft potential. The scalar field magnitude at a point on the aircraft may be written as

$$F_i = a_{ix}E_x + a_{iy}E_y + a_{iz}E_z + a_{iv}V.$$

The enhancement factors $(a_{ix},\ldots,a_{iv})$ for each field mill location are measured from a scale-model charge-transfer of the Lear 36. The eight by four matrix defined by A with measured fields F can be minimized, and E can be estimated by

$$E = (A^TA)^{-1}A^TF$$

which is the least-squares solution for the ambient vector electric field.

Preliminary analyses indicate that the laboratory measurements of the airframe enhancement matrix, A, were accurate to within 6%. This precision, together with a properly weighted least-squares estimate (a more complicated solution than presented here) of the system of field equations, provide a viable and accurate method of resolving the ambient vector electric field. It has been demonstrated that the aircraft could be artificially charged while the ABFM system continued to correctly measure zero ambient field conditions. For the cases analyzed, clear air errors were typically less than 7%. The only exceptions to this accuracy were the cases of heavy aircraft charging which occurred in cloud. Such conditions require further analytical and experimental studies to determine the accuracy of the ABFM system in cloud.

REFERENCES

Harris-Hobbs, R., K. Giori, R. Adamo, J. Kositsky, and R. Maffione, "Preliminary Calibration of the Airborne Field Mill System," Submitted to USAF/Space Systems Division Los Angeles AFB, Aeromet, Tulsa, OK, April 1990.

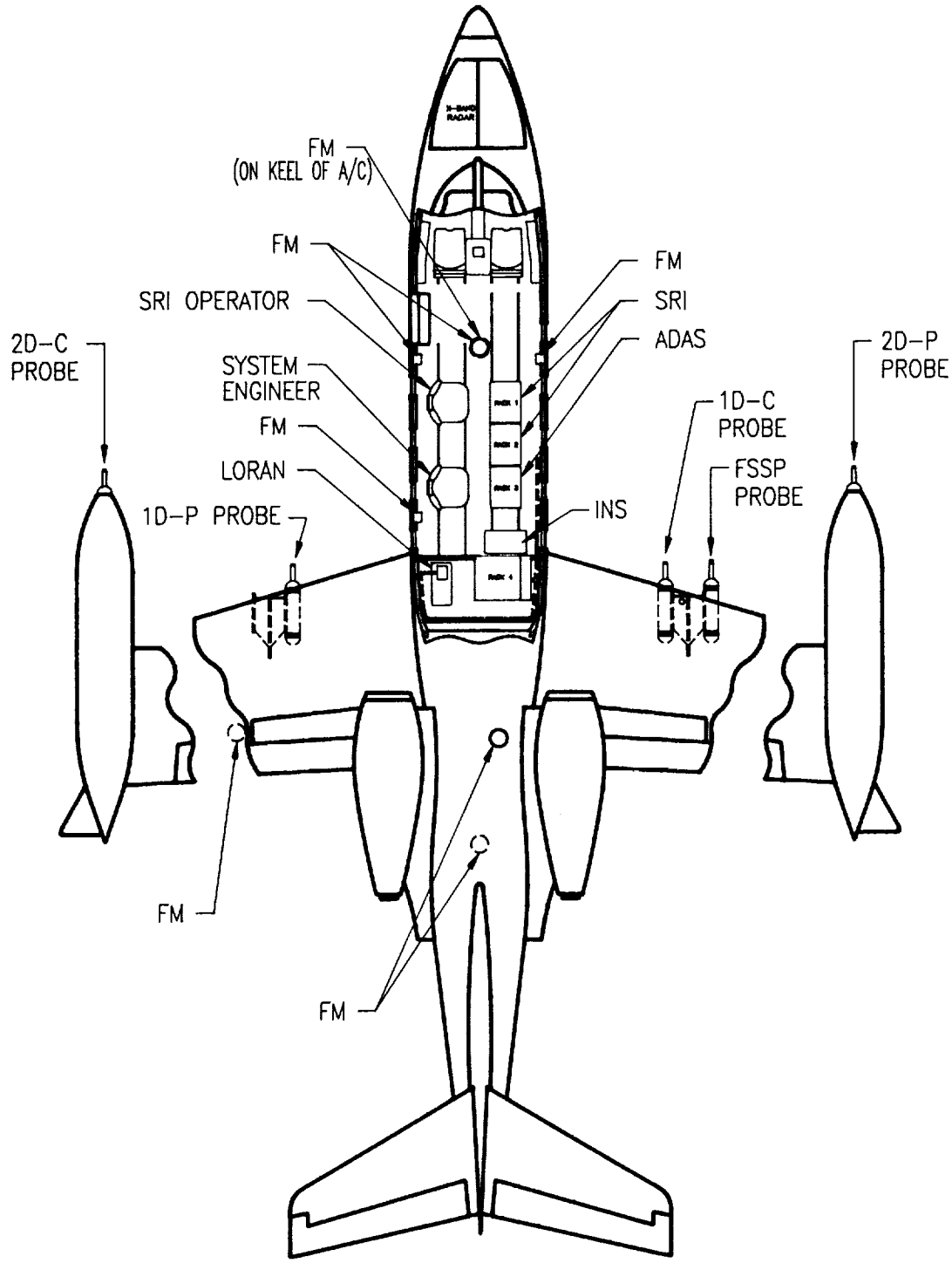

Figure 1 Instrumentation on the HARP

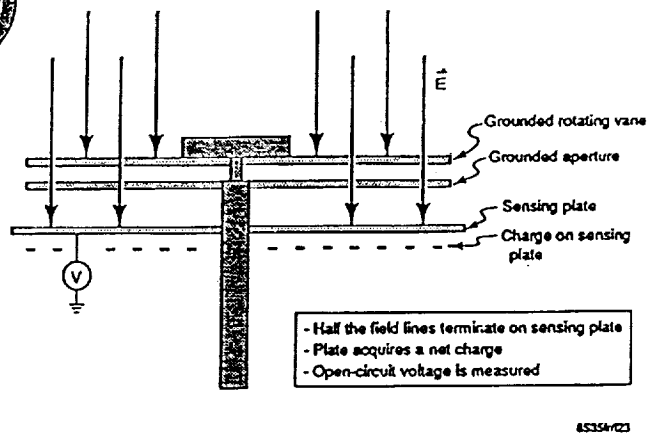

Figure 2 Vanes in Open Position

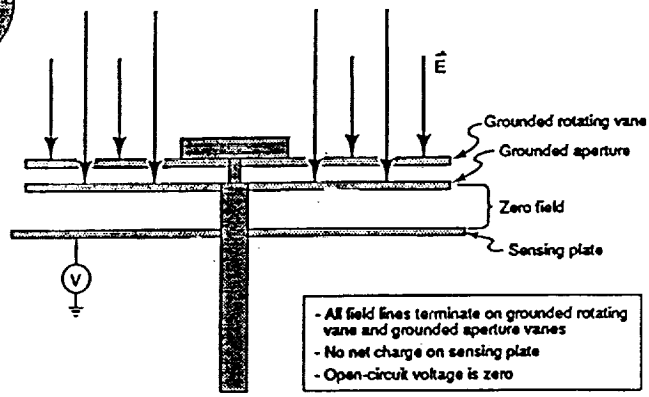

Figure 3 Vanes in Closed Position

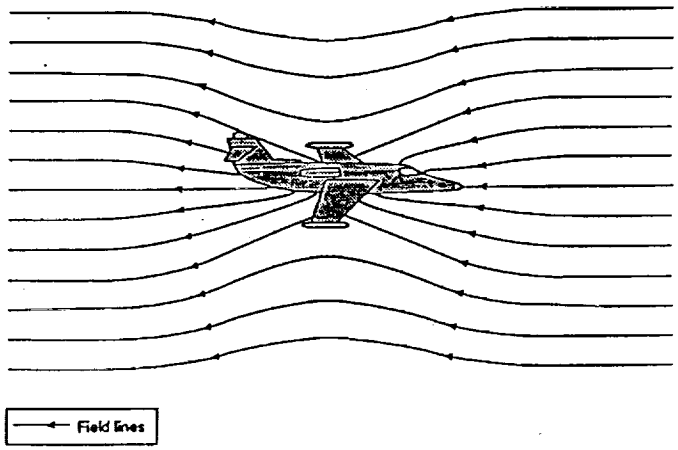

Figure 4 Conducting Aircraft in Uniform Electric Field

N91-25467

Title: Airborne Wator Vapor DIAL System and Measurements of Water Vapor and Aerosol Profiles

Authors: Noah S. Higdon, NASA/Langley Research Center
Edward V. Browell, NASA/Langley Research Center

Discipline: Atmosphere

The Lidar Applications Group at the NASA Langley Research Center has developed a differential absorption lidar (DIAL) system for the remote measurement of atmospheric water vapor (H_2O) and aerosols from an aircraft. The airborne H_2O DIAL system is designed for extended flights to perform mesoscale investigations of H_2O and aerosol distributions. This DIAL system utilizes a Nd:YAG-laser-pumped dye laser as the off-line transmitter and a narrowband, tunable Alexandrite laser as the on-line transmitter. The dye laser has an oscillator/amplifier configuration which incorporates a grating and prism in the oscillator cavity to narrow the output linewidth to approximately 15 pm. This linewidth can be maintained over the wavelength range of 725-730 nm, and it is sufficiently narrow to satisfy the off-line spectral requirements. In the Alexandrite laser, three intracavity tuning elements combine to produce an output linewidth of 1.1 pm. These spectral devices include a five-plate birefringent tuner, a 1-mm thick solid etalon and a 1-cm air-spaced etalon. A wavelength stability of ±0.35 pm is achieved by active feedback control of the two Fabry-Perot etalons using a frequency stabilized He-Ne laser as a wavelength reference. The three tuning elements can be synchronously scanned over a 150 pm range with microprocessor-based scanning electronics.

For accurately positioning the on-line laser to the center of the H_2O line, we utilize a 1-meter monochromator and a multipass absorption cell. The monochromator incorporates an optical multichannel analyzer to achieve a measurement resolution of 20 pm. This system is used to set the output wavelength close to the H_2O absorption line of interest. The absorption cell is heated to 60°C and filled with approximately 40 torr of pure H_2O. With these environmental conditions and a 100 m pathlength, there is sufficient optical depth to accurately center the wavelength on any H_2O line with a line strength greater than 10^{-24} $cm^{-1}(cm^2/molecule)$. An energy ratiometer is then used to measure the amount of absorption through the multipass cell as the laser wavelength is scanned

across the line. When the maximum absorption is reached, the laser is locked on the line by the active wavelength control.

The receiver system has a 14-inch-diameter, f/7 Celestron telescope to collect the backscattered laser light and focus it into the detector optics. An adjustable field stop is placed in the focal plane of the telescope to provide a variable field-of-view. The detector optics consist of a collimating lens, a beamsplitter, and an interference filter, which has a bandwidth of 0.38 nm (FWHM) and a transmission of 32 percent. After transmission through the filter, the return signals are directed to the detector, which can be either a photomultiplier (PMT) tube or an avalanche photodiode.

After the return signals are converted to electrical signals by the optical detector, they are sent to the digitizers contained in the data acquisition system (DAS). The signals are then digitized to 12 bits at 10 MHz over 4096 words and stored on magnetic tape. The HV power supply for the PMT is housed in the DAS so that the dynamic range of the measurement can be controlled from there. In addition, the DAS has computers and monitors for signal processing and data display, which facilitate real-time experiment control. The aerosol and H_2O distributions derived by the DAS are plotted in real time on color printers.

The airborne H_2O DIAL system was flight tested in July 1989 on board the Electra aircraft at the NASA Wallops Flight Facility. Preliminary H_2O distributions were obtained during these flight tests, and comparison in situ H_2O measurements were in good agreement with the DIAL H_2O measurements.

The first extensive observations of H_2O and aerosols in the lower troposphere were made during March and April 1990 with the DIAL system operating in a nadir mode from the NASA Wallops Electra aircraft. Water vapor measurements were made on flights at night over the ocean, during the day over land and ocean, and across a cold front. Daytime DIAL measurements clearly showed the decrease in the mixed layer depth from about 1.7 km over land to less than 500 m over the Atlantic. The dry atmospheric conditions above the moist mixed layers were readily apparent in the DIAL H_2O data. Regions with enhanced H_2O concentrations were also found to have higher aerosol backscattering. The airborne DIAL measurements showed for the first time the detailed H_2O and aerosol structure that occurs in the free troposphere and in the mixed layer over different land and marine regimes. In addition, the first high-spatial resolution distribution of H_2O was obtained across a cold front. The transition from the very dry conditions behind the front to the very moist conditions ahead of the front was seen in detail. These experiments have provided new insights into atmospheric processes involving H_2O, and they will serve as a basis for future H_2O investigations, including studies of cloud formation and the effect of H_2O on the Earth's climate system.

Title: **A New Look at the Airship as a Geoscience Research Platform**

Author: **Ron Hochstetler, Airship Operations and Services**

omit To P.175

Discipline: **Airship Logistical Support**

It has been proposed by some in the airborne geoscience research community that the airship would be a valuable complement to conventional research aircraft. The purpose of this poster will be to examine how currently available airships have been employed for such work and how they could be optimized for use as airborne geoscientific platforms.

Unique Features of the Airship

Lighter-than-air balloons were the first aircraft to fly and are still used today in metrology and for gathering data at very high altitudes. Over the years, airships have been recognized as optimum observational platforms because of their unique performance features.

Because of its design, the airship incorporates several of the qualities of both airborne and seaborne research vessels. Its large size provides ample area for locating bulky sensors or large lightweight arrays. And since the airships flight speeds are 60 kts and below, there are far fewer aerodynamic constraints placed on external instrument installations.

With its ability to fly very slowly or even to hover over a spot, the airship is the ideal platform for deploying *and recovering* dropsondes, bathythermographs, or virtually any expensive and otherwise expendable device.

The airship is an excellent vehicle for carrying out traditional oceanographic research. It can easily cover the land/sea interface as well as the air/sea interface, and has the capability of performing direct sea surface/subsurface duties.

With speeds far higher than most sea-going ships, the airship provides relatively rapid access to deep water sites, shallow coastal areas, or rough terrain inland locations. And once onsite, the airship can carry out extended observations for tens of hours.

The airship's stability permits high resolution for sensitive instruments and the low vibration environment required for such activities as airborne gravity mapping. The airship's ability to drift along with an air mass permits long-duration *in situ* studies of air pollution, low-level cloud dynamics, and other atmospheric processes. Three-dimensional profiles of plume dispersions, air mass movements, and mixing patterns of targeted chemicals could be compiled.

Atmospheric missions can take advantage of the airship's ability to tether sensor packages below the ship so as not to disturb the air mass under observation. For example, this feature can permit the study of vertical properties of the atmospheric boundary layer while at the same time onboard doppler radar and lidar systems study environments horizontally or overhead.

The long wavelengths associated with airship movements during flight make it attractive as a platform for geophysical work, primarily airborne gravity mapping. Because the airship can operate slow and low over otherwise inaccessible areas (dense forest, sea cliffs, coral reefs, and ice packs), it can obtain high-resolution gravity and electromagnetic (EM) measurements from locations that are poorly mapped. In a typical airship gravity/EM mission, the airship would fly to the study area and follow very accurately a grid plotted over the study site. As the airship moves along, it can obtain continuous gravity measurements rather than just point measurements at grid intersections. At the same time the gravity work is occurring, other sensors can be measuring the EM environment around the study site.

The airship could be deployed from most any small airport or unprepared remote field site. The ship's transit times, though slower than a helicopter's, would be faster than surface vehicles and still permit hovering over sites, but with far greater dwell time on each station.

Some specific tasks for which the airship is well-suited:

- Lower and recover survey personnel, instruments, or dropsondes
- Towing lightweight arrays or collection drags
- Carrying radars, scatterometers, radiometers, laser altimeters
- Performing coastal pollution monitoring, airborne bathymetry, biomass studies, and fisheries management
- Carrying large wind profilers, outsized radar arrays, gas and particle sniffers
- Performing lower tropospheric and boundary layer studies (ozone radon, industrial pollution, etc.), *in situ* photochemistry measurement and monitoring, look-down lidar surveys
- Carrying magnetic anomaly detectors, large-diameter induction coils, airborne laser altimeters
- Performing gravimetric surveys over inaccessible areas, high-resolution spectrometry, radiometric surveys, and stereo photography.

Title: **An Airborne Measurement System for Mass Fluxes of Air Pollutants**

Authors: **A.M. Hoff, Aerodata FlugmeBtechnik GmbH**
W. Muller, Niedersachsisches Landesamt f. Immissionsschutz
J. Werhahn, Fraunhofer-Inst. f. Atmospharische Umweltforschung

Discipline: **Atmosphere**

Atmospheric transport and deposition of anthropogenic trace substances cannot be derived only by ground-based measurements. *In situ* measurements by aircraft are very efficient tools to detect plumes, even under complex meteorological conditions, or to determine the lateral transport of air pollutants.

There are numerous scenarios like smog warning, source detection, or turbulent mass flux measurement to which such a system could be applied. One of the most interesting applications is the measurement of mass fluxes of gaseous air constituents across boundaries. Provided the source strength of industrial areas, high precision onboard wind and trace gas concentration data can be determined by mass flux balancing.

A system designed for these tasks has to satisfy the following demands.

- Low detection limits to measure large-scale transport of strongly diluted constituents
- Short response times of the instruments (1 sec or less) to resolve structures of the convective scale at an aircraft speed between 50 and 100 m/sec
- Devices to eliminate the cross-sensitivity of the instruments to the atmospheric pressure for measurements during arbitrary altitude changes
- Instrumentation for meteorological parameters, including the onboard wind vector determination which is indispensable for precise mass flux calculation.

Equipment with these features are presently used onboard a Beechcraft King Air B200T, as shown in Figure 1.

Other carriers prepared for operation of the equipment are a Hawker Siddeley HS 125 and a Dornier Do 128. The parameters measured routinely on these platforms include:

- Continuous measurements (1 Hz sampling rate maximal).
  - Mixing ratios of SO_2, NO, NO_Y, NO_2, O_3, CO, H_2O_2
  - Meteorological parameters such as pressure, temperature, humidity, and wind vector
  - Navigational and flight mechanical data

- Discontinuous measurements
  - Aerosol and grab samples.

The two-dimensional patterns of trace gas distributions, vertical as well as horizontal, are typically measured by saw tooth-shaped flight paths. In the vertical sections, pollution is found covering large horizontal areas but only a few tens or hundreds of meters vertically. Regional wind systems (e.g., low level jets, which are hardly detectable from ground level) may cause a powerful long-range transport of pollutants. *In situ* measurement of the wind vector together with simultaneous trace gas analytics provide reliable means to calculate the mass flux of gaseous constituents.

A typical pattern of the SO_2 distribution over a vertical cross section is shown in the middle of Figure 2. The maxima of the mixing ratio can be found in about 300 to 400 m above MSL. The upper part of Figure 2 shows the simultaneously measured wind field. Obviously, the structure in the lateral transport (i.e., the mass flux density in the lower part of Figure 2) is not necessarily identical to that of the concentration. Another strong maximum in the distribution of the mass flux occurs in 600 m above MSL. The biggest transport of pollutants often happens within levels above the top of the actual mixing layer. A weak concentration maximum coupled with a strong orthogonal wind component through the cross-section surface results in a powerful contribution to the lateral transport.

In contrast to previous aircraft-based flux determinations depending on wind data of the synoptic network, this system provides the local wind information. The accuracy of the wind vector measurement is mainly limited by the quality of the navigation data. The system actually based on an inertial platform leads to an accuracy of ±1 m/sec. The intended combination with the satellite navigation (GPS) will end up with ±0.2 m/sec.

Another interesting aspect of this aircraft system is the turbulence measurement. It enables the determination of the horizontal and vertical diffusion of plumes. By means of a five-hole probe system, the aircraft will be able to provide the turbulent fluctuations of the wind vector and the appropriate stochastic parameters.

ORIGINAL PAGE
BLACK AND WHITE PHOTOGRAPH

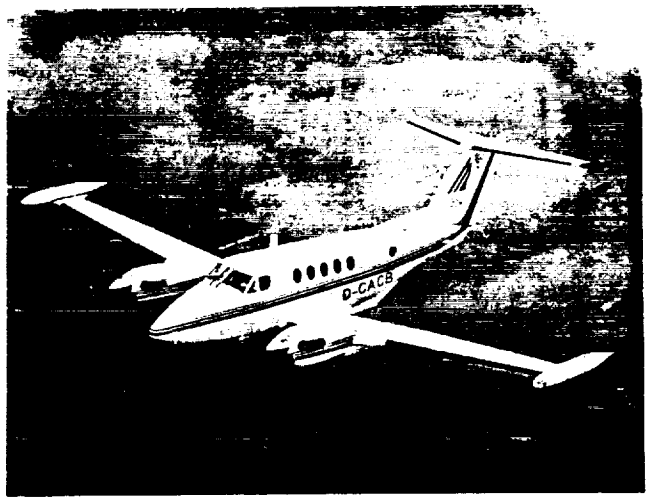

Fig. 1.
Beechcraft King Air B 200 T operated by the "Avionik Zentrum Braunschweig" in Germany. The inlets for the air analytics system are integrated in the upper cabin section of the fuselage behind the cockpit.

ORIGINAL PAGE IS
OF POOR QUALITY

Fig. 2. Wind field, SO_2 mixing ratio, and SO_2 mass flux density within a meridional vertical cross section along the eastern boundary of Lower Saxony. The dotted lines indicate the flight path. (Campaign under contract of the Ministry of Environmental Control of Lower Saxony).

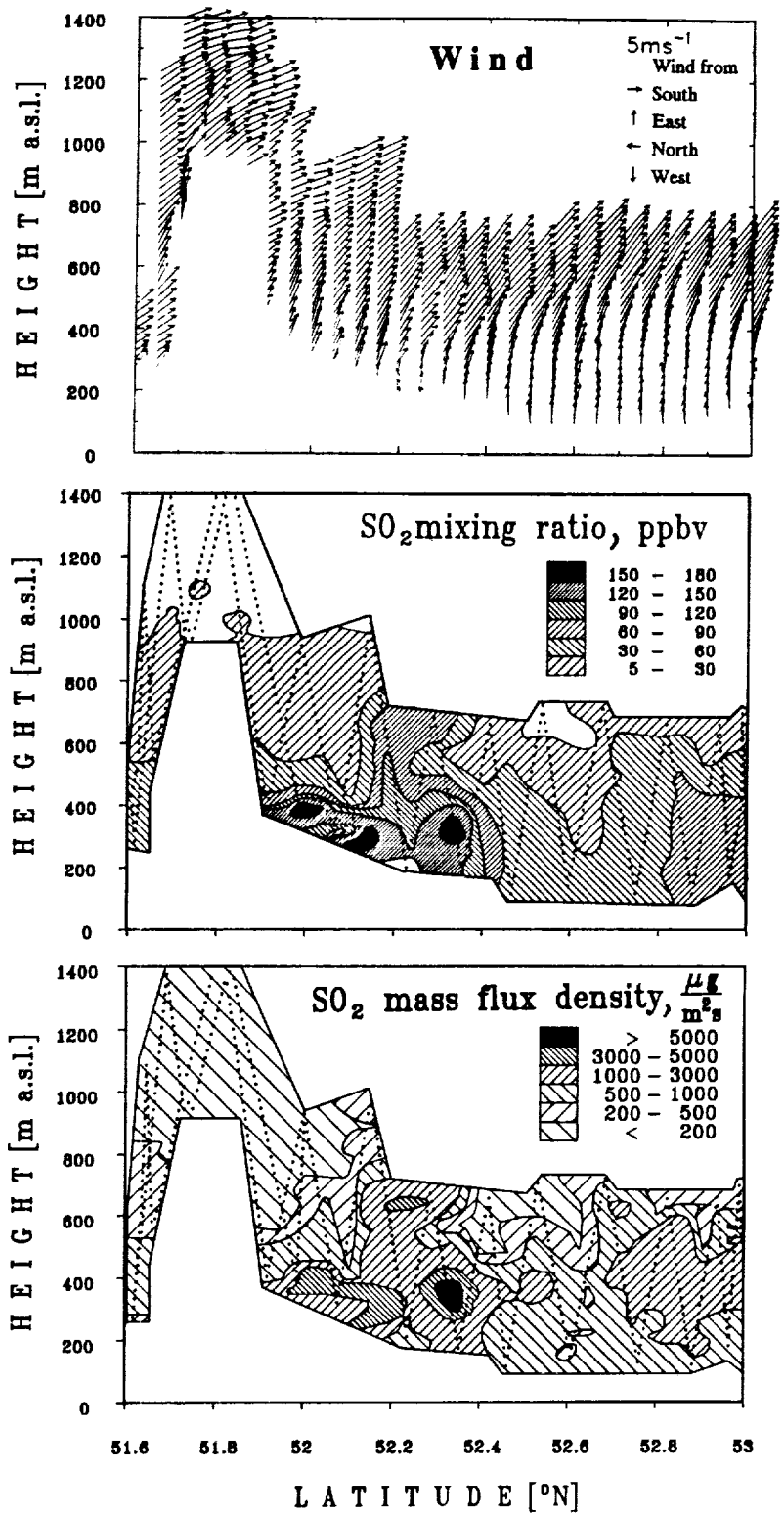

In contrast to previous aircraft based flux determinations depending on wind data of the synoptic network, this system provides the local wind information. The accuracy of the wind vector measurement is mainly limited by the quality of the navigation data. The system actually based on an inertial platform leads to an accuracy of ± 1 m/s . The intended combination with the satellite navigation (GPS) will end up with ± 0.2 m/s.

Another interesting aspect of this aircraft system is the turbulence measurement. It enables the determination of the horizontal and vertical diffusion of plumes. By means of a five-hole probe system the aircraft will be able to provide the turbulent fluctuations of the wind vector and the appropriate stochastic parameters.

N91-25468

ABS. ONLY

20136

Title: Airborne Oceanographic Lidar Participation in the U.S. Joint Global Ocean Flux Study (JGOFS)

P.1

Authors: Frank E. Hoge, NASA/Wallops Flight Facility
Robert N. Swift, EG&G

ND200400
EG921409

Discipline: Oceans

The U.S. JGOFS is part of a major international field experiment which the National Science Foundation (NSF) is conducting during the decade. It will combine ship and aircraft data collected in both the Atlantic and Pacific oceans. The primary data collected by the Airborne Oceanographic Lidar (AOL) is laser-induced chlorophyll fluorescence together with the concurrent laser-induced water Raman backscatter and phycoerythrin fluorescence. Passive solar-induced up-welling radiances and down-welling solar irradiance are also acquired. Results from the 1989 Atlantic mission as well as plans for use of the new long-range Wallops P-3 during the upcoming Equatorial Pacific mission will be presented.

Title: Airborne Stabilized Optical Systems

Authors: LaMont Holmes, Pacific Missile Test Center
Jim Hochstetler, Pacific Missile Test Center

Discipline: High-Resolution Airborne Imagery

The Pacific Missile Test Center (PMTC), Code 4032 at Point Mugu, California, has developed a series of airborne stabilized optical systems known generically as "CAST GLANCE". Since the mid 1970's, these versatile stabilized optical systems have been installed on a wide variety of military and civilian aircraft and have provided high resolution photodocumentation of aerial and spaceborne events. Organizations which have used these systems include NASA, U.S. Navy, U.S. Air Force, and the Strategic Defense Initiative Organization.

These optical systems use gyro-stabilized gimballed mirrors to direct light through telescopes and lenses into video and high-speed film sensors. The effective optical aperture of these systems is either 4 inches or 7 inches, depending on the gimballed mirror used in the system. The large aperture of these systems allows multiple, concentrically-boresighted sensors to be installed on each system. Each sensor may then have a different effective focal length. A typical configuration for the 7" system would include three separate fields-of-view, wide, medium, and narrow with focal lengths of 2 inches, 40 inches and 120 inches respectively.

During September 1990 two of our optical platforms were used on the Combined Release and Radiation Effects Satellite (CRRES) experiment in the South Pacific. PMTC supplied the optical platforms used to point sensors which observed chemical releases from the CRESS satellite, in the Earth's magnetic field. The configuration of the systems on this mission was coordinated with the principle investigator in that only one, large-aperture sensor was installed on each platform.

These systems have proven themselves to be reliable and versatile. They are easily integrated into different airborne platforms and readily modified to accept new and unique sensors for a wide variety of applications.

N91-25469

Title: The Advanced Microwave Precipitation Radiometer: A New Aircraft Radiometer for Passive Precipitation Remote Sensing

Authors: Robbie E. Hood, NASA/Marshall Space Flight Center
Roy W. Spencer, NASA/Marshall Space Flight Center
Mark W. James, NASA/Marshall Space Flight Center

Discipline: Atmosphere

Past studies of passive microwave measurements of precipitating systems have yielded broad empirical relationships between hydrometeors and microwave transmission. In general, these relationships fall into two categories of passive microwave precipitation retrievals. A radiometer measures radiances emitted in the microwave by the Earth's surface and atmosphere. These radiances can be in turn converted to brightness temperatures. Emission-based methods of precipitation retrievals rely upon the observed effect of liquid precipitation to increase the brightness temperature of a radiometrically cold background such as an ocean surface. A scattering-based method is based upon the effect that frozen hydrometeors tend to decrease the brightness temperature of a radiometrically warm background such as land.

One step toward developing quantitative brightness temperature-rain rate relationships is the recent construction of a new aircraft instrument sponsored by National Aeronautics and Space Administration/Marshall Space Flight Center (NASA/MSFC). This instrument is the Advanced Microwave Precipitation Radiometer (AMPR) designed and built by Georgia Tech Research Institute to fly aboard high altitude research aircraft such as the NASA ER-2. The AMPR and its accompanying data acquisition system are mounted in the Q-bay compartment of the NASA ER-2.

AMPR is a cross-track scanning microwave radiometer with a unique combination of four total power channels centered at 10.7, 19.35, 37.1, and 85.5 GHz. It has a dual lens antenna to accommodate two separate feedhorns. One horn is a copy of the Special Sensor Microwave/Imager spaceborne multi-frequency feedhorn designed and built by Microwave Engineering Corporation. This horn feeds the 19.35, 37.1, and 85.5 GHz channels while the other AMPR feedhorn is for the 10.7 GHz channel. The sum of the two lenses of the dual antenna is less than 15 inches which is the maximum the ER-2 hatch opening could accommodate. Other design features of the AMPR system include surface resolutions of the nadir-viewing footprints ranging in size from 2.8 km for the 10.7 and 19.35 GHz channels down to 0.64 km at 85.5 GHz. All channels achieve a minimum sampling temperature resolution of less than 0.5°C.

The wide range of channel frequencies the AMPR possesses will be extremely useful in future field studies of precipitating systems. Further understanding of the vertical structure of thunderstorms should be gained since the higher frequency measurements such as 85.5 GHz tend to be greatly affected by ice particles above the freezing level while lower frequency data such at 10.7 GHz exhibit a greater influence by liquid hydrometeors below the freezing level. Other research topics of special interest include the quantitative correlation of brightness temperature and rain rate over the entire rain rate range, over the life cycle of a precipitation system, and between precipitation systems in differing atmospheric environments.

N91-25470

20138

P2

Title: Lidar Measurements of Polar Stratospheric Clouds during the 1989 Airborne Arctic Stratospheric Expedition

Authors: Syed Ismail, NASA/Langley Research Center
Edward V. Browell, NASA/Langley Research Center

Discipline: Atmosphere

The Airborne Arctic Stratospheric Expedition (AASE) was conducted during January-February 1989 from the Sola Air Station, Norway (59°N, 5°E). As part of this expedition, the NASA Langley Research Center's multiwavelength airborne lidar system (Browell, 1989) was flown on the NASA Ames Research Center's DC-8 aircraft to measure ozone (O_3) and aerosol profiles in the region of the polar vortex.

The lidar system simultaneously transmitted laser beams at 1064, 603, 311, and 301.5 nm to measure atmospheric scattering, polarization and O_3 profiles. Long range flights were made between Stavanger, Norway, and the North Pole, and between 40°W and 20°E meridians. Eleven flights were made, each flight lasting an average of 10 hours and covering about 8000 km. Atmospheric scattering ratios, aerosol polarizations, and aerosol scattering ratio wavelength dependences were derived from the lidar measurements to altitudes above 27 km. Details of the measurements at 1064 nm (IR) and 603 nm (VIS) have been given by Browell et al. (1990), and their aerosol optical properties have been discussed by Toon et al. (1990).

Polar stratospheric clouds were observed in the polar vortex on 10 of 11 flights between January 6 and February 2, 1989. The altitude range of the PSC observations was from 14 to 27 km, and the altitude of the most frequent PSC occurrence was near 20 km. On the missions conducted in the first half of January, two types of large-scale PSCs (depth >2 km and horizontal extent >200 km) with distinctly different optical characteristics were observed for aerosols thought to be composed of nitric acid trihydrate (NAT). These PSCs were present at temperatures between 190-198 K, where it is expected that aerosols containing NAT will form at ambient vapor pressures for nitric acid and water vapor in the wintertime polar stratosphere. Within the general category of NAT PSCs (Type 1), two sub-types of NAT PSCs were found. Type 1a PSCs had low atmospheric scattering ratios (≈1.35 VIS) and high depolarizations (>30 %), and Type 1b PSCs had high scattering ratios (3-8 VIS) and low depolarizations (<4%). Water ice PSCs (Type 2) were observed in isolated

regions on January 24 and February 2 and over a wide area on January 31. Type 2 PSCs were observed in regions of very low temperatures <190 K. The optical characteristics of the PSCs, observed during the AASE, are given in Table 1 where α is the aerosol scattering ratio wavelength dependence parameter and β is the aerosol depolarization wavelength dependence parameter (Browell et al., 1990).

In this paper the details of the aerosol scattering properties of lidar observations in the IR, VIS, and UV regions will be presented along with correlations with the National Meteorological Center's temperature profiles.

Table 1. Optical Characteristics of PSCs Observed During AASE

TYPE	SCAT. RATIO		α	AERO. DEPOL. (%)		β
	VIS	IR		VIS	IR	
1a	1.2-1.5	2-5	0.4	30-50	30-50	≈0
1b	3-8	5-20	2-3	0.5-2.5	<4	--
2	>10	>20	<0.8	>10	>10	≈0

Acknowledgements

The authors would like to thank Patricia Robinette and Greg Nowicki of ST Systems Corporation for extensive computer programming associated with the lidar data reduction.

References

Browell, E. V., Differential absorption lidar sensing of ozone, Proc. of the IEEE, 77, 419-432, 1989.

Browell, E. V., C. F. Butler, S. Ismail, P. Robinette, A. F. Carter, N. S. Higdon, O. B. Toon, M. R. Schoeberl, and A. F. Tuck, Airborne lidar observations in the wintertime Arctic stratosphere: 1. Polar stratospheric clouds, Geophys. Res. Lett., 17, 385-388, 1990.

Toon, O. B., E. V. Browell, S. Kinne, and J. Jordan, An Analysis of lidar observations of polar stratospheric clouds, Geophys. Res. Lett., 17, 393-396, 1990.

N91-25471

20139

p.2

Title: A PC-Based Multispectral Scanner Data Evaluation Workstation: Application to Daedalus Scanners

Authors: Gary J. Jedlovec, NASA/Marshall Space Flight Center
Mark W. James, NASA/Marshall Space Flight Center
Matthew R. Smith, Universities Space Research Association
Robert J. Atkinson, General Electric Company

ND 736801

U1341676

GH 550250

Discipline: Interdisciplinary

In late 1989, a personal computer (PC)-based data evaluation workstation was developed to support post flight processing of Multispectral Atmospheric Mapping Sensor (MAMS) data. The MAMS Quick View System (QVS) (Jedlovec *et al.*, 1989a) is an image analysis and display system designed to provide the capability to evaluate Daedalus scanner data immediately after an aircraft flight. Even in its original form, the QVS offered the portability of a personal computer with the advanced analysis and display features of a mainframe image analysis system. It was recognized, however, that the original QVS had its limitations, both in speed and processing of MAMS data. Recent efforts, documented here and visually displayed at the workshop, focus on overcoming earlier limitations and adapting the system to a new data tape structure. In doing so, the enhanced Quick View System (QVS2) will accommodate data from any of the four spectrometers used with the Daedalus scanner on the NASA ER2 platform (the MAMS, AOCI, TMS, and WILDFIRE (under development)).

The QVS2 is designed around the AST 486/33mhz CPU personal computer and comes with 10 EISA expansions slots, keyboard, and 4.0 mbytes of memory. Specialized PC-McIDAS software provides the main image analysis and display capability for the system. Additional hardware features for the QVS2 include 3-$^1/_2$ and 5-$^1/_4$ disk drives, expansion board with 4 mbytes memory (additional), a 1.2 gbyte hard disk and controller which is accessible through a SCSI interface, an AST/VGA color monitor and adapter card with 512 kbytes memory, and a Kensington bus mouse. AST OS/2 (version 1.2) and DOS 4.01 are also required as basic software packages.

Image analysis and display of the digital scanner data is accomplished with PC-McIDAS software. PC-McIDAS is the personal computer version of an imaging software package created for mainframe systems by the University of Wisconsin/ Space Science and Engineering Center. The mainframe package runs on an IBM host and provides many enhanced hardware and software capabilities for the analysis and display of all types of geophysical data (Suomi, et al., 1983). In 1985 SSEC produced a DOS version of McIDAS with much of the functionality of the mainframe package while running on IBM PC's. Early in 1989, UW/SSEC released a version for the PC which runs under the OS/2 operating system. This change allowed for greater compatibility between mainframe and PC software and for multiple task applications. With a VGA video interface and the power of the 80386 processor (IBM PS2/80 standard), PC-McIDAS now has impressive capabilities, similar to those of a mainframe McIDAS workstation.

In addition to the basic computer system, other hardware components are a necessary part of the QVS2. A frame grabber card and supporting software

should allow for windowing and scrolling of image data, features which were unavailable with the previous QVS. This allows for more useful displays of scanner data in the preview mode. The use of an OS2 supported frame grabber card allows for the immediate collection of digital data on the PC. It also allows for instantaneous switch to McIDAS to calibrate and display the image data. Communications with a host McIDAS system are possible from off-site with an external modem for real-time weather data. This capability has been demonstrate for both the UW/SSEC and MSFC/EADS/WetNet (Goodman *et al.*, 1990; and Young *et al.*, 1990) systems and will allow access to the entire real-time weather data bank available on these systems. This capability will provide invaluable during deployments in support aircraft flights and for flight planning.

The QVS2 system will allow for greater capability and more flexibility in the evaluation of scanner data after each aircraft flight. The first step in this evaluation is to get a preview of the image data throughout the flight. The QVS2 allows for the preview and side-by-side display of any two (of the twelve) channels in a moving window mode as the data is read from the flight recorder. The QVS2 will support a preview-to-collection speed of 8-1 (at 30 ips). Thus two channels can be previewed from a four hour flight in 30 minutes (factor of 8 increase over the original QVS). The preview mode will be used to verify the general performance of the scanner and to select specific scenes for more detailed evaluation. For detailed analysis of Daedalus scanner data, the data is ingested from the flight recorder through the SCSI interface using a menu drive set of panels. The user inputs the desired time or scanline for the data, the channels and number of scanlines to collect, and the destination file name. One to twelve channels can be collected and saved to disk. Additional processing is available with PC McIDAS for the analysis of image data (Jedlovec *et al.*, 1989a,b). The 1.2 gbyte of disk space will allow for the storage of data from one or more flights.

References

Goodman, H. M., R. Spencer, J. Dodge, and J. Star, 1990: The WetNet Project. Preprints Sixth International Conference on Interactive Information and Processing Systems for Meteorology, Oceanography, and Hydrology, February 1990, Anaheim, California, AMS, Boston, 149-152.

Jedlovec, G. J., R. J. Atkinson, M. W. James, and M. R. Smith, 1989a: The MAMS Quick View System (QVS): A PC based field evaluation workstation. Presentation and summary paper to the McIDAS Users Group Meeting, November 1989, Madison, Wisconsin, 9 pgs.

Jedlovec, G. J., K. B. Batson, R. J. Atkinson, C. C. Moeller, W. P. Menzel, and M. W. James, 1989b: Improved capabilities of the Multispectral Atmospheric Mapping Sensor (MAMS). NASA Technical Memorandum 100352, Marshall Space Flight Center, Huntsville, AL, 80 pgs.

Suomi, V. E., R. Fox, S. S. Lemaye, and W. L. Smith, 1983: McIDAS III: A modern interactive data access and analysis system. J. Climo. Appl. Meteor., 22, 765-778.

Young, J. T., R. Dengel, and D. A. Santek, 1990: WetNet System. Preprints Sixth International Conference on Interactive Information and Processing Systems for Meteorology, Oceanography, and Hydrology, February 1990, Anaheim, California, AMS, Boston, 57-60.

N91-25472

P. 2

Title: Hyperspectral Data Analysis for Estimation of Foliar Biochemical Content along the Oregon Transect

Authors: Lee F. Johnson, TGS Technology, Inc.
David L. Peterson, NASA/Ames Research Center

NC473657
TV743199

Discipline: Land

The NASA Oregon Transect Ecosystem Research (OTTER) project (described elsewhere in these proceedings by D. Peterson) completed a data acquisition phase during the period March-October, 1990. Data were acquired with several airborne imaging spectrometers. Included were the Airborne Visible and Infrared Imaging Spectrometer (AVIRIS) aboard the ER-2, the Advanced Solidstate Array Spectrometer (ASAS) aboard the C-130, and the Fluorescence Line Imager (FLI) and Compact Airborne Spectrographic Imager (CASI), both aboard light aircraft. In addition, Spectron™ visible and near-infrared data were acquired in transects across study areas from a low-altitude ultralight craft. Sunphotometer data were taken approximately coincident with each overflight for atmospheric correction of the aircraft data.

A primary goal of the OTTER project is the remote estimation of canopy nitrogen and lignin content. Past research with the Airborne Imaging Spectrometer (AIS) has shown sensitivity to foliar nitrogen and lignin absorption in the near-infrared region between 1200-2400 nanometers. During the data analysis phase, AVIRIS data will be used to build upon the AIS findings, and to extend the study into the 400-1200 nanometer region. AVIRIS spectra will be statistically related to laboratory assays of chemical content from foliage samples at each site. Estimation equations will be developed by use of both waveband selection (stepwise multilinear regression) and data compression (partial least squares regression) techniques. The sensitivity of AVIRIS data to foliar nitrogen and lignin will be

evaluated in light of three main variables: stage of the growing season, environmental conditions (temperature, rainfall, elevation), and artifically-induced fertility gradients. Biochemical indicators in the visible region will be compared with data from the ASAS, CASI, and FLI. Ultimately, remotely-derived measures of biochemical content will be input to the FOREST-BGC forest ecosystem model.

Another OTTER objective is the remote estimation of chlorophyll pigmentation in coniferous ecosystems. The primary instruments for this effort are the high spectral resolution (~2 nm.) CASI and FLI. Chlorophyll-induced red edge position and depth of the chlorophyll absorption well will be examined. The feasibility of characterizing these parameters with the coarser resolution AVIRIS (~10 nm.) and ASAS (~15 nm.) instruments will be addressed by comparison with FLI and CASI. Laboratory chemical assays of chlorophyll A/B concentration will be available for verification.

Spectra of fresh foliage samples were acquired in the laboratory with Spectron™ and LICOR™ portable spectroradiometers during the June, August, and October field campaigns. These data will be useful in establishing the nominal spectral response of foliage at each site in the absence of confounding atmospheric and background effects associated with the aircraft data.

N91-25473

20141

P2

Title: End-to-End Remote Sensing at the Science and Technology Laboratory of John C. Stennis Space Center

Authors: Patrick Kelly, NASA/Stennis Space Center
Douglas Rickman, NASA/Stennis Space Center
Eric Smith, NASA/Stennis Space Center

ND103456

Discipline: Land and Oceans

The Science and Technology Laboratory (STL) of Stennis Space Center (SSC) has been developing an expertise in remote sensing for more than a decade. Capabilities at SSC/STL include all major areas of the field. STL includes: the Sensor Development Laboratory (SDL), Image Processing Center, a Learjet 23 flight platform and on staff scientific investigators.

Sensor Development - The Sensor Development Laboratory (SDL) at SSC/STL is responsible for research, development, maintenance and calibration of multispectral scanners used in remote sensing. In the area of airborne sensors the SDL has designed and developed the Calibrated Airborne Multispectral Scanner (CAMS), the Airborne Multispectral Pushbroome Scanner (AMPS), and the Airborne Bathymetric Scanner (ABS). Also, the Thermal Infrared Multispectral Scanner (TIMS) and the Thematic Mapper Simulator (TMS) were modified at the SDL to the current state of operation. The SDL also develops ground based sensor systems. The Shuttle Thermal Imager (STI) was conceived and integrated at SSC using off the shelf technology. Currently, there are seven STI units installed at KSC with eight more to be installed in the next fiscal year. It is projected more units will follow. As a follow on to the STI an Ice Detection System (IDS) has been developed and is currently being tested. The IDS will be used along with the STI to monitor conditions on the Space Shuttle prior to commit to launch.

Data Acquisition - STL maintains a Learjet 23 (LJ23) for acquiring airborne remotely sensed data. The aircraft is equipped with instrumentation necessary to provide the housekeeping information for locational and attitude data used in the analysis of the images acquired. Basic operating parameters for the aircraft are altitudes from 3,000 to 41,000 FT ASL, range approximately 1,000 nautical miles and speeds up to 400 knots. The sensor system is installed in an open bay area of the aircraft and is accompanied by a Zeiss 9in square format aerial photographic camera. With the sensor systems available on this platform data has been acquired with resolutions from 2.5 to 30 meters. The LJ23 has been deployed to acquire data throughout the USA, Canada, Central and South America. Data acquired by STL is decomutated and processed on the in house computer systems. Key to STL's data acquisition program is the rapid response status in which the LJ23 is operated. In the past mission have been requested scheduled and flown in less than 24 hours. Secondly, because of the low cost to operate the LJ23, STL has the unique capability to stay deployed on target and wait for optimal weather conditions and accomplish the mission.

Data Analysis - To meet research objectives STL has developed ELAS, an image processing software package. Originally created to process digital images acquired by the Multi-Spectral Scanner (Landsat MSS) for NASA, ELAS developed into a very flexible, general purpose tool. ELAS has been used to process data from satellite and aircraft images, images of Egyptian tomb paintings, fish scales and turtle flippers, Magnetic Resonance Imaging (MRI) images of the human head, breast and heart, aerial photographs, soil maps, gravity potential fields, topographic data, and submarine sonar images. It has been used to extract information for studies on topics such as wetlands productivity, forest stress due to drought, thermal response of forests, remote analysis of rock's silica content, compiled geographic information system/data base applications at a wide range of scales for many sites, relationship of mychorrizal involvement and the health of pine trees, and the transport of sediment in the near shore marine environment. This flexibility is inherent in the design and creation of the ELAS software.

STL has found the concept and execution of ELAS so successful and useful that over a period of more than 7 years approximately 140 man-years of programmer effort has been expended in its continuing development. Today more than 100 other organizations, federal, state, academic and private, now use the software. Also at least four companies utilize it as the basis of their commercially available image processing software.

ELAS is designed primarily to process data sets which form two or three dimensional arrays. Although there are no limitations in the software that make this a basic premise, it is convenient to conceive of these arrays as forming images or pictures. The package also has extensive ability to define and manipulate data defined in a vector format (polygons, line segments, points). There are several elements in the design of ELAS that are key to understanding its flexibility and general utility. Major features include utilization of FORTRAN for all application programs, a standard library of subroutines and single set of routines which all application programs must use to interface with the host computer, a master and slave task structure, a single format interface for the storage of almost all data, retention of intermediate results and process for the storage of almost all data, retention of intermediate results and process control information in user accessible files, and a directive and parameter driven user interface. All application programs, referred to as modules, are accomplished by single functions. Only when practical utilization of the module's primary function so requires are multiple functions placed within a single module. The modules are also order independent. In a real sense one can consider ELAS to be a very high level programming language which is designed to process arrays (images) of data.

FORTRAN is used for the application modules because of its wide spread availability and the transportability of code from one machine to another. While not perfect, FORTRAN has demonstrated longevity. To implement ELAS on a new type of computer requires creation of programs which act as the interface between the operating system and the application code. These interface programs will handle the actual I/O. These programs, which form the master task, are machine specific and should be written in a form that maximizes speed. The remainder of ELAS, which is over 99% of the software, is therefore shielded from machine variations and can be transferred on to the new computer with minimal difficulty.

N91-25474

20142

p.3

NC473657

Title: Ames Research Center C-130

Author: Mark A. Koozer, NASA/Ames Research Center

Discipline: Atmosphere, Land, and Oceans

The C130 Earth Resources Aircraft is based at Ames Research Center, Moffett Field, California. The aircraft provides a platform for a variety of sensors that collect data in support of terrestrial and atmospheric projects sponsored by NASA in coordination with federal, state, university, and industry investigators. This data is applied to research in the areas of forestry, agriculture, land use and land cover analysis, hydrology, geology, photogrammetry, oceanography, meteorology, and other earth science disciplines.

The C130 is a platform aircraft flying up to 25,000 feet above sea level at speeds between 150 and 330 knots True Air Speed. The aircraft is capable of precise flight line navigation by means of an optical borescope from which line guidance is provided to the pilots. The aircraft and its complement of on-board sensors provide a readily deployable remote sensing platform that supports scientific research throughout the conterminous United States, Alaska, and Hawaii. Additionally, the aircraft has been deployed in support of research in Australia, Bermuda, France, Germany, Austria, and Italy.

Sensors regularly carried on board are the NS001 Thematic Mapper Simulator (TMS); the Thermal Infrared Multispectral Scanner (TIMS); the Advanced Solid State Array Spectroradiometer (ASAS); the Pushbroom Microwave Radiometer (PBMR); the C-Band Radar Scatterometer (CSCAT); the K-Band Radar Scatterometer (NUSCAT); the Precision Thermal Radiometer (PRT-5); two Zeiss 9 inch format cameras; a Frost-Dew Point Hygrometer; and a C130 Aircraft Data Distribution System (CADDS) which distributes real time navigation and environmental data to experimenter and other stations throughout the aircraft. TIMS, ASAS, PBMR, CSCAT, and NUSCAT are experimenter provided instruments. The rest are a standard part of the aircraft.

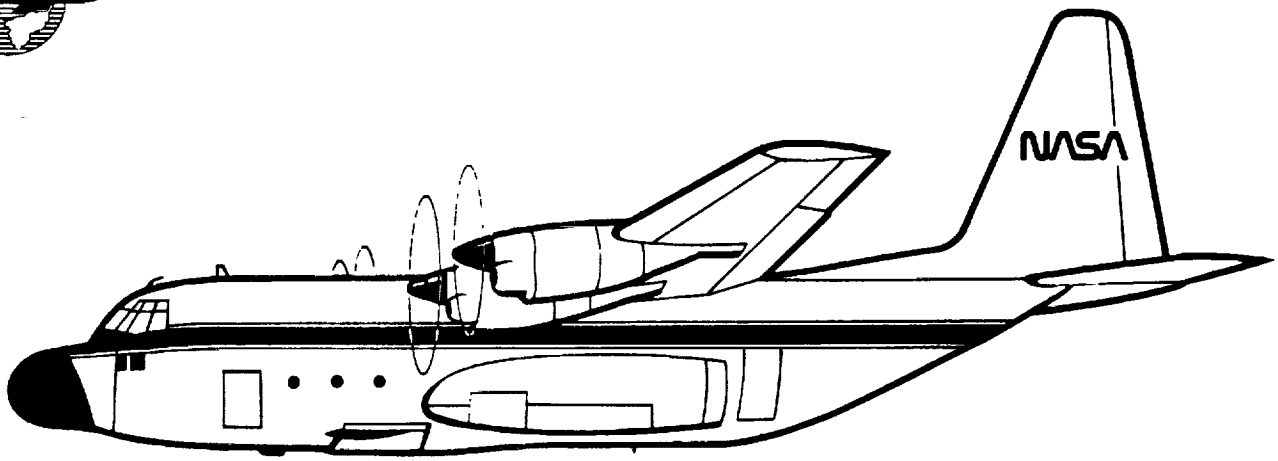

C-130B, Lockheed

Description:

Crew:	Two Pilots, Flight Engineer, Navigator
Length:	97 feet, 9 inches
Wingspan:	132 feet, 7 inches
Engine:	Four Allison T56-A-15 Turboprop
Base:	Ames Research Center, Moffett Field, CA

Performance:

Altitude:	25,000 feet (max)
Range:	2200 nautical miles
Duration:	8 hours at 22,000 feet
Speed:	150-330 knots True Air Speed
Payload:	20,000 lb

Accommodations:

Zenith and Nadir Viewports
External Antenna Attachment Mounts
Optical Windows
19-inch Panel Equipment Racks

Support:

Navigation Flight and Environmental Data: Recorded Automatically and Available to Investigator
Dew/Frost Point Hygrometer
Radar Altimeter
Weather Radar
Inertial Navigation
Time Code Generator
Housekeeping Distribution

Sensors:

Metric Cameras
Multispectral Scanner
Walk-on: Eight Stations Provided for Investigator Supplied and Operated Sensors

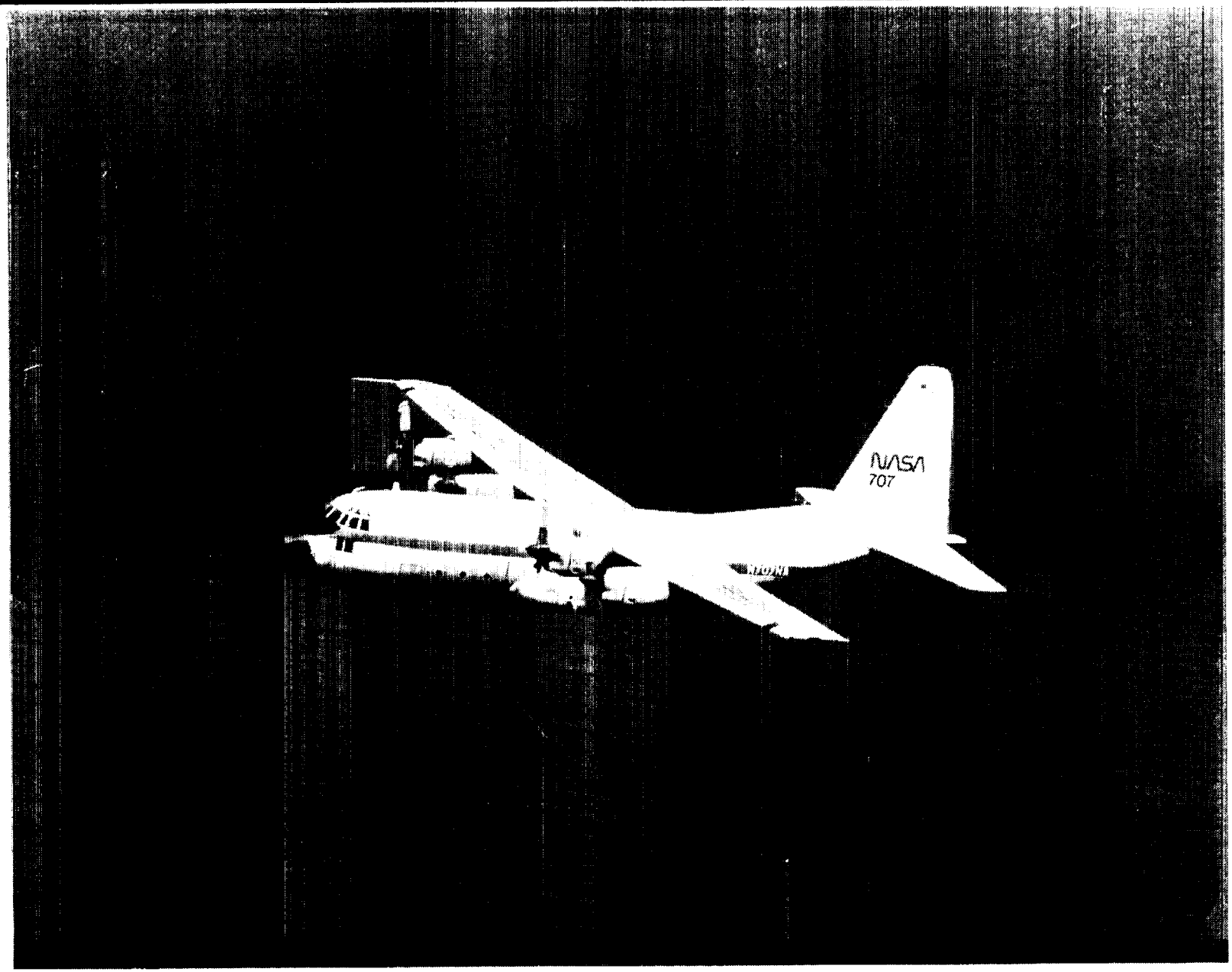

C-130B, Lockheed

Title: The USGS Side-Looking Airborne Radar (SLAR) Program: An Update—SLAR Data on CD-ROM

omit

Authors: Allan N. Kover, U.S. Geological Survey
James W. Schoonmaker, Jr., U.S. Geological Survey
Clark H. Cramer, U.S. Geological Survey

Discipline: Land

Side-looking airborne radar (SLAR) data have been collected systematically for the United States Geological Survey (USGS) since 1980. SLAR image strips (37 to 45 km swath width) are compiled into quadrangle mosaics using the USGS 1:250,000-scale topographic map series for title, format, and control. One-time coverage (X-band) of over 3.75 million km^2 has been mosaicked, but the amount of data collected is considerably larger because of quadrangle overruns, special missions, and 60 percent sidelap of image strips. The latter provides stereoscopic images and permits mosaicking of the part of the SLAR image with the best terrain detail.

The SLAR data collected since FY86 are available on computer compatible tapes (CCTs) as well as photographic products. In 1989, the USGS began compiling data on CD-ROM (compact disc-read-only memory). This makes a large volume of data easily and quickly available to users of any computers, including personal computers, equipped with CD-ROM readers. A number of experimental CD-ROMs have been prepared that include text, radar raster image files, and other selected image data sets. SLAR scenes with varied geologic features in Alaska, Arizona, Arkansas, California, Louisiana, Michigan, Missouri, and Washington have been chosen to demonstrate the versatility of using CD-ROMs to display and analyze SLAR and other images. The success of these demonstration discs encouraged the USGS to prepare SLAR CD-ROMs as standard products. The first disc contains five western 1° x 2° quadrangle SLAR mosaics: Ritzville, Walla Walla, Pendleton, Mariposa, and Las Vegas. Beginning with FY90, all USGS procurements for SLAR data will include delivery of the data on CD-ROMs.

The poster session will demonstrate the utility of using a CD-ROM reader-equipped portable personal computer to examine SLAR and correlative data, and will display some recent photographic prints of SLAR mosaics.

N91-25475

530-43

ABS. ONLY

P.1

Title: Applying Kinematic GPS to Airborne Laser Remote Sensing

Authors: William B. Krabill, NASA/Wallops Flight Facility
Chreston F. Martin, EG&G
Robert N. Swift, EG&G

ND 200400

Discipline: Land and Oceans

Results from the application of differential carrier phase tracking of the Global Positioning System (GPS) constellation of satellites to precise positioning (sub-10 cm) of and aircraft are presented. These aircraft positions are utilized in the process of providing geodetic quality position information for airborne laser "footprint" locations on the surface of the earth. The combination of these techniques provides a rapid, cost effective means for collecting geodetic and topographic data, including sea surface topography. Operational techniques and constraints, along with results from recently collected data, are presented.

Title: The PERSEUS Unmanned Scientific Research Aircraft

omit to p. 201

Authors: John S. Langford, Aurora Flight Sciences Corporation
James G. Anderson, Harvard University

Discipline: Atmosphere

Recent advances in computational aerodynamics, lightweight structures, energy sources, and microelectronics have made possible a new class of semi-autonomous unmanned aircraft. Since May of 1989, Harvard University and Aurora Flight Sciences have been jointly developing Perseus, a lightweight aircraft designed to carry a 50 kg payload to altitudes of at least 25 km for use in stratospheric chemistry experiments. During the course of this development, it has become clear that there are other potential uses for such a platform in such areas as radiation, dynamics, and meteorology. The purpose of our presentation is to introduce the Perseus and its capability with the goal of entraining new investigators to use this technology.

There are two versions of Perseus under development (see Table 1). The Perseus A is designed to reach extremely high altitudes for short durations. The Perseus B is designed for longer duration and lower altitudes, and places a premium on low operating costs. Both versions share common tooling and flight control systems. Performance is summarized in Figure 1.

Perseus A. Perseus A uses a unique closed-cycle internal combustion engine operating on methane and oxygen, both of which are stored onboard in liquid form. The aircraft is designed to carry a 50 kg payload to an altitude of 30 km for a few minutes, or to 25 km for a few hours. The Perseus A configuration is shown in Figure 2.

Perseus B. Perseus B uses a turbocharged internal combustion engine to achieve longer durations at altitudes up to 18 km. As seen in Figure 1, the Perseus B can carry 150 kg payloads at 18 km altitudes for over 24 hours or at 11 km for almost 100 hours.

Payloads. Harvard University is developing a lightweight self-contained payload for use in polar stratospheric chemistry research. The complete payload, including power supply and data logging equipment, weighs approximately 50 kg and measures chlorine monoxide, bromine monoxide, ozone, temperature, and pressure. The ClO radical is detected using a kinetic-spectroscopic technique in which the oxygen atom is extracted from the ClO radical by nitric oxide, leaving the naked Cl atom, which in turn is detected by atomic resonance scattering. BrO is detected in a similar manner. The payload is housed in the forward section of the aircraft, which is easily adapted for the carriage of other payloads.

Table I
Perseus Data

	A Version		B Version	
	(SI)	(Eng)	(SI)	(Eng)
Wing span	17.9 m	58.7 ft	17.9 m	58.7 ft
Wing area	16.0 m^2	172 ft^2	16 m^2	172 ft^2
Length	7.3 m	23.9 ft	7.3 m	23.9 ft
Prop diameter	4.5 m	14.7 ft	2.4 m	7.8 ft
Empty weight	236 kg	521 lb	245 kg	541 lb
Gross weight	399 kg	880 lb	695 kg	1,534 lb

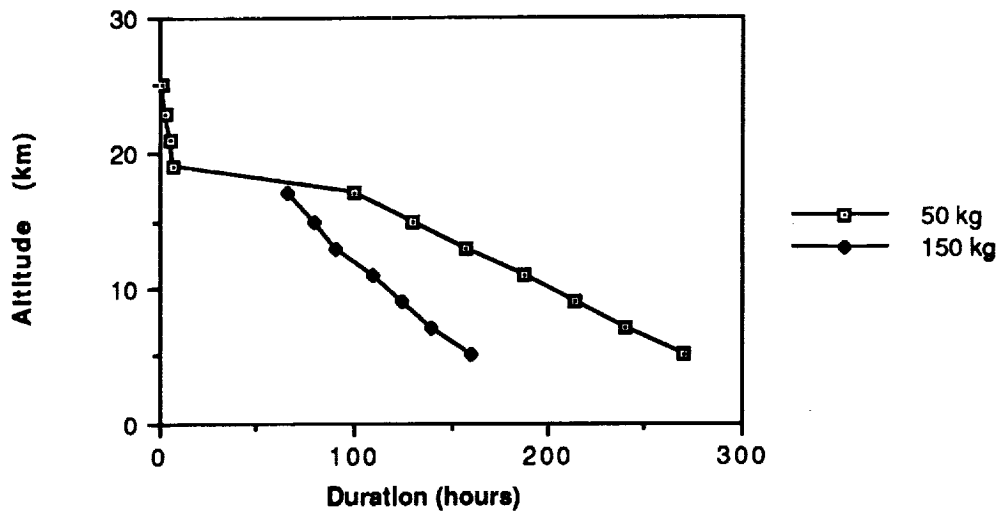

Figure 1. Summary of Perseus performance data. Altitudes above 18 km use the Perseus A configuration, while those below 18 km assume the Perseus B configuration.

PERSEUS

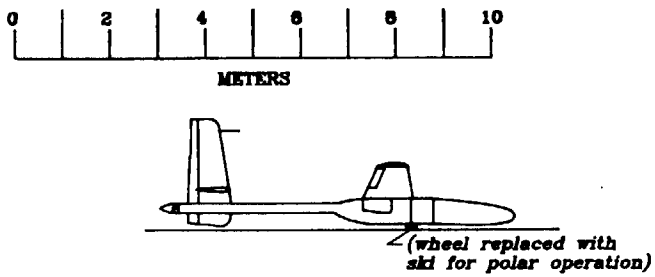

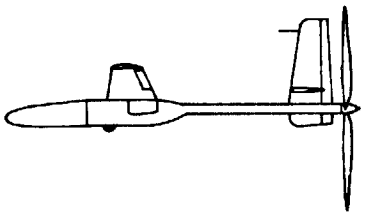

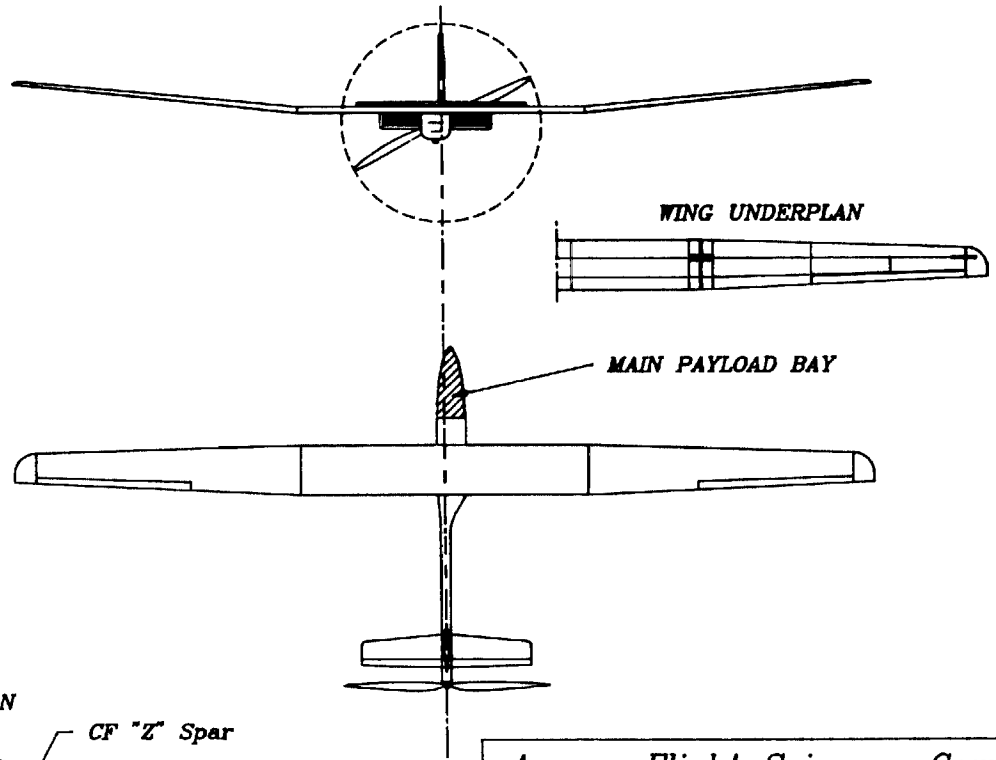

PHYSICAL CHARACTERISTICS	
Span	17.9m
Wing Area	16.0m
Empty Weight	240kg
Gross Weight	400kg

WING CROSS SECTION

Aurora Flight Sciences Corp.
3107 Colvin St. Alexandria, VA 22314

PERSEUS AU-002

3-View

DRAWN BY	DATE	REV.
		9/14/90

N91-25476

Title: Status Report on the Land Processes Aircraft Science Management Operations Working Group

Authors: James G. Lawless, NASA/Ames Research Center
Lisa J. Mann, TGS Technology, Inc.

Discipline: Land

Since its inception three years ago, the Land Processes Aircraft Science Management Operations Working Group (MOWG) has provided recommendations on the optimal use of the Agency's aircraft in support of the Land Processes Science Program. Recommendations have covered topics such as aircraft and sensor usage, development of long-range plans, Multisensor Airborne Campaigns (MAC), program balance, aircraft sensor databases, new technology and sensor development, and, increased University scientist participation in the program. Impacts of these recommendations have improved the efficiency of various procedures including the flight request process, tracking of flight hours and aircraft usage.

The group has also created a bibliography focused on publications produced by Land Processes scientists from the use of the aircraft program, surveyed NASA funded PI's on their participation in the aircraft program, and developed a planning template for multi-sensor airborne campaigns. Benefits from these activities will be summarized in the poster session.

omit

Title: Tethered Aerostat Sampling over Grand Bahama Island

Authors: Robert Leifer, U.S. Department of Energy
Ronald H. Knuth, U.S. Department of Energy
Lawrence E. Hinchliffe, U.S. Department of Energy

Discipline: Atmosphere

This program is testing the feasibility of using tethered aerostat sampling platforms (TASP) in atmospheric chemistry experiments. TASP uses large and highly stabilized balloons to lift heavy payloads to altitudes as high as 3 km. Compact aerosol equipment has been developed at EML to be "piggy-backed" onto an existing tethered aerostat.

EML's environmental package contains 12 stacked filter cassettes, a drum impactor and a mini computer. The design of the instrument allows us to collect, unattended, aerosol samples for periods of up to 3 weeks. Using the stacked filter packs we have been able to characterize the collected aerosol into a fine and coarse fraction for elemental composition, mass concentration and optical absorption using the respective techniques of Particle Induced X-ray Emission spectroscopy (PIXE), gravimetric methodologies and the Laser Integrating Plate System (LIPS). The fine fraction was analyzed for elements lighter than Na using Forward Alpha Scattering Techniques (FAST).

We have measured the composition of maritime and continental aerosols in the free troposphere over the island of Grand Bahama, and have related these variations to atmospheric transport from the continental U.S. and the Atlantic Ocean. Mass concentrations ranged from $2 \pm 0.2\ \mu gm^{-3}$ to $10 \pm 1\ \mu gm^{-3}$. Sulfur and H were the most abundant elements measured on the fine filter fraction. If we assume that the S was part of $(NH_4)_2SO_4$ then we are able to account for up to 50% of the total mass. On many of the fine fraction filters there were elements associated with marine aerosol (Na) and soil (Si, Fe, Ca, K). Excess K could also be associated with smoke. In addition, results of the analysis of our impactor by PIXE, with a time resolution of 8 hours, are discussed.

S32-43
N91-25477
20145
p. 1

Title: The Use of Aircraft-Based Thermal Infrared Multispectral Scanner (TIMS) Data to Measure Surface Energy Budgets on a Landscape Scale

Author: Jeffrey C. Luvall, NASA/Marshall Space Flight Center

Discipline: Land

A series of Thermal Infrared Multispectral Scanner Data (TIMS) was collected over the H.J. Andrews experimental forest in western Oregon and at the Coweeta Hydrologic Laboratory (USDA Forest Service) in North Carolina. Flight lines were overlapped with an 8 to 28 minute time difference between flight lines. Concurrent radiosonde measurements of atmospheric profiles of air and dew point temperatures provided inputs to LOWTRAN6 for atmospheric radiance corrections of the TIMS data. Surface temperature differences over time between flight lines allowed the development of thermal response numbers (TRN) which characterized the thermal response (KJ m^{-2} $^{o}C^{-1}$) of the different surface types. The polygons containing mostly soil and bare rock had the lowest TRN whereas the forested polygons were the highest.

Remotely sensed forest canopy temperatures were used to estimate evapotranspiration (ET) from a coniferous stand at the Coweeta Hydrologic Laboratory. The use of intense, concurrent, ground based measurements of the physical (net and solar radiation; needle temperatures; vapor pressure deficits; wind) and physiological (stomatal conductance, leaf area index, canopy structure) parameters important for forests in controlling ET allowed for the comparison with the results obtained from a surface temperature (TIMS) model to those obtained using energy balance techniques (Penman-Monteith). Results indicate that forest canopy temperatures measured by the TIMS are comparable to needle thermocouples temperatures. ET models developed from the TIMS data obtained similar ET rates as those using energy balance techniques.

Title: Recent Developments in Airborne Flux Measurement

Author: Ian MacPherson, National Research Council (Canada)

OMIT TO P.219

Discipline: Atmosphere

To make long range predictions of the effects of increased $C0_2$ levels in the atmosphere, scientists need quantitative information on the basic $C0_2$ exchange rates between the biosphere and the atmosphere. As a result of several years of careful development of instrumentation and analysis techniques in cooperation with Agriculture Canada, the NRC Twin Otter (Fig. 1) is now capable of making these important measurements for $C0_2$, water vapour, heat and momentum. Participation in First ISLSCP[1] Field Experiment (FIFE) has brought the Twin Otter international recognition in the flux-measuring field.

This paper will serve as a progress report on current development work to enhance the capabilities of the Twin Otter as a flux-measuring aircraft. This work includes:

- an integrated inertial sensing algorithm, based on the Kalman filtering technique, to improve accuracy of the wind measuring system.
- a fast-response methane analyzer
- application of the so-called relaxed eddy accumulation technique (REA) to measure the fluxes of gases, aerosols, etc., for which fast-response analyzers do not exist.

The research work on the Kalman filter design for the Twin Otter navigation sensor suite (Litton-90 IRS, Loran-C and Doppler radar) was presented at the Oberpfaffenhofen workshop sponsored by DLR (Leach and MacPherson, 1991). Since then, the design has been further refined using specialized flight test data, and a subroutine has been added to the Twin Otter playback software to derive corrections to the geographical position and the three inertial velocity components. This will result in improved measurement of mean winds and momentum fluxes, but is unlikely to have a major effect on the computed vertical fluxes of sensible and latent heat and $C0_2$. Application of the Kalman filter algorithm to the real-time, airborne software will have to await installation of a more powerful microprocessor in the aircraft.

The focus of the 1990 Northern Wetlands Study (NWS) and ABLE-3B was the exchange of methane and $C0_2$ between the atmosphere and the surface of the Hudson Bay wetlands. The Twin Otter carried a prototype fast-response methane analyzer developed by Unisearch Associates. It was based on tuneable diode laser technology with a test cell

[1] International Satellite Land Surface Climatology Project

operating at 1/10 atmosphere fed by an inlet and pump drawing 50 litres/min. Including pump, the device weighed about 100 kg. The analyzer was completed by the contractor only days before the NWS, so its development unavoidably extended into and through the field project. At this writing, analysis of the data is continuing, but the findings to date can be summarized here.

The methane analyzer did appear to achieve the frequency response (> 5 Hz) required to compute methane fluxes using the eddy correlation (EC) technique with the Twin Otter vertical wind component, w′. Also, the lag between measurement of w′ and the CH_4 signal was found to be an acceptable 1/4 sec. The analyzer did require a considerable warm-up time prior to flight, and continuous monitoring and retuning during flight. Its accuracy was also severely degraded by VHF radio transmissions, which had to be avoided during flux runs. Transfer of its digital output to the aircraft microprocessor for real-time flux estimation and recording was achieved without problem.

Nevertheless, it appears that the instrument did not meet the sensitivity and resolution tolerances required to measure the low CH_4 fluxes experienced during the NWS. For a flux of 50 mg m^{-2} d^{-1}, for example, the expected σ_m of the methane signal would be about 3 ppb. To measure the flux to an accuracy of 20 percent would require a resolution of 0.6 ppb. It appears that the instrument was subject to errors an order of magnitude larger than this due to accelerations caused by aircraft motion and turbulence. Attempts to correct the methane signal by parameterization using measured aircraft accelerations have not met with success, because the effects on the analyzer were not consistent. The sign and amplitude of the disturbance to the methane signal depended on how well the laser was tuned to the particular methane line of the spectrum being used. Another correction technique that offers promise, is to examine the cospectrum for the methane flux for peaks associated with aircraft motion, then eliminate this peak during the integration to compute the mean flux for a run. Analysis continues. In the meantime, internal components of the instrument are being stiffened by the contractor and further flight tests are planned for 1991.

The relaxed eddy accumulation technique (Businger and Oncley, 1990) involves the partitioning of the gas sample into two separate reservoirs based on whether the real-time wind-measuring system senses ascending or descending air. The gas sampled can be analyzed later by a slow response analyzer, such as a gas chromatograph. The conceptual simplicity of the technique is attractive, because the vertical flux estimate $\overline{w'c'}$ for a trace gas is a simple function of the standard deviation of the vertical gust velocity, σ_w, the mean concentration difference of the gas samples, $(\overline{c^+ - c^-})$, and an empirical constant A:

$$\overline{w'c'} = A\ \sigma_w(\overline{c^+ - c^-}) \qquad (1)$$

To investigate the application of the relaxed eddy accumulation method (REA) on an aircraft, a number of computer simulations have been performed on data collected by the NRC Twin Otter during FIFE. The findings from these simulations are summarized in MacPherson and Desjardins, 1991. Table 1 and Fig. 2 give examples of these computations. The reference also discusses the important effects of biases in w′, filtering, gust thresholds and lag between measurement of w′ and activation of the sampling valves.

Agriculture Canada has developed a prototype REA device which was interfaced to the Twin Otter by the Flight Research Laboratory of NRC. A schematic of the device is shown in Fig. 3, details of which are given in MacPherson and Desjardins, 1991. One of the main difficulties in the use of the eddy accumulation technique is attaining the required resolution in the analysis of the gas concentrations in the bags (small difference between two large numbers). This REA device was flown on the Twin Otter during the NWS to serve as a alternative method to measure methane fluxes. However, the required resolution of about 0.5 ppb was not attained by the gas chromatograph used in the field. This work showed that it is preferable to analyze the bags with a differential analyzer, of one exists for the species being studied. Consequently, an Agriculture Canada differential $C0_2$ analyzer, with a resolution of 0.3 ppm, was used to analyze $C0_2$ samples collected on a series of four test flights. As can be seen from Table 2, the results were disappointing, with reasonable agreement between REA and EC fluxes achieved on only about a third of the test cases.

The experience gained on using the prototype REA system in the Twin Otter has led to several suggestions for improvement, and the development of a Mk.2 device that is currently being tested on a tower. It will be flown in the Twin Otter in the spring of 1991.

REFERENCES

Businger, J.A., and S.P. Oncley, 1990: Flux measurement with conditional sampling. *J. Atmos. Oceanic Technol.*,7, 349-352.

Leach, B.W., and J.I. MacPherson, 1991: Application of Kalman filtering to airborne wind measurement. *J. Atmos. Oceanic Technol.*, (in press).

MacPherson, J.I., and R.L. Desjardins, 1991: Airborne tests of flux measurement by the relaxed eddy accumulation technique. *Proceedings of the seventh AMS symposium on meteorological observations and instrumentation,* New Orleans, Jan. 13-18, 1991.

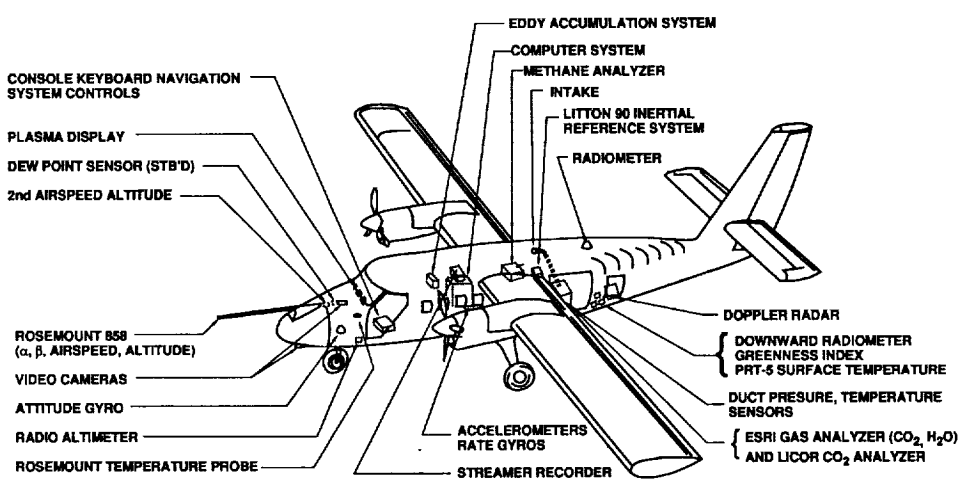

Fig. 1: NRC Twin Otter atmospheric research aircraft as instrumented for gaseous exchange measurement

Flt	# Runs	A_{WT}	A_{WC}	A_{WQ}	Z/L
08	08	0.603	0.589	0.592	-5.2
08	08	0.612	0.602	0.597	-3.7
11	16	0.596	0.591	0.592	-0.2
24	16	0.591	0.569	0.576	-0.2
26	06	0.592	0.578	0.604	-1.5
36	12	0.591	0.573	0.608	-0.9
37	10	0.589	0.554	0.620	-21.6
Means		**0.596**	**0.579**	**0.598**	

Table 1: REA empirical constants computed from FIFE-87 data for sensible heat (A_{WT}), $C0_2$ (A_{WC}) and latent heat (A_{WQ}). The threshold level used for w' was 0.05 ms^{-1}. Z/L is height over Obhukhov length and is a measure of atmospheric stability. Results are in excellent agreement with those of Businger and Oncley (1990) using tower data.

Date 1990	Runs	Dist km	σ_w ms^{-1}	Δc ppm	REA kg/hectare/h	EC
June 15	6	82	0.60	-1.96	-37.2	-28.3
June 19	4	55	0.59	-0.65	-11.7	-20.6
	4	52	0.75	-1.01	-24.9	-23.0
June 20	1	61	0.84	-0.36	-8.0	-19.4
	1	60	0.95	-0.53	-13.9	-26.9
July 27	1	48	0.77	-0.11	-2.8	0.7
	1	52	0.89	1.06	33.9	-8.6
	1	52	0.86	-0.21	-5.5	-4.5
	1	53	0.88	0.32	9.1	3.5
	1	53	0.99	0.07	3.3	-3.8
	1	53	0.84	0.18	5.6	-19.8
	1	53	0.90	-0.41	-14.0	-20.2
	1	54	0.86	-0.64	-18.6	-16.1
	1	55	0.98	-0.13	-4.0	-20.4
	1	55	0.77	-0.19	-4.9	-12.4
	1	54	0.77	-0.94	-25.4	-14.1
	1	54	0.64	-0.55	-12.2	-10.5
	1	54	0.70	-0.46	-9.0	-13.3

Table 2: $C0_2$ fluxes measured by the prototype eddy accumulation device (REA) compared with those using eddy correlation (EC). σ_w is the rms vertical gust velocity and Δc is the $C0_2$ concentration difference between the 'up' and 'down' bags. Aircraft altitude was approximately 100 m.

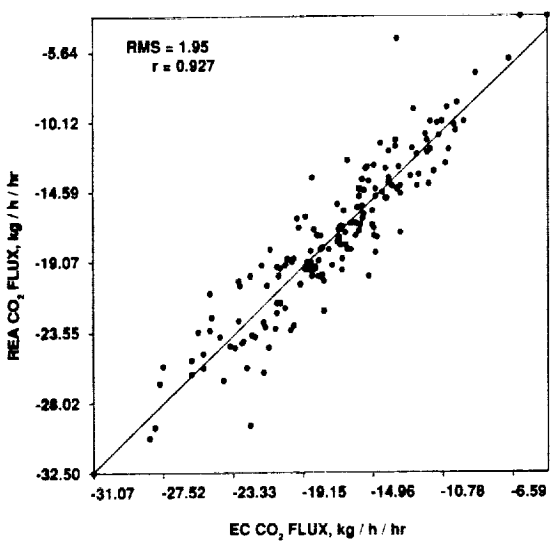

Fig. 2: Results of simulation of eddy accumulation $C0_2$ fluxs (REA) versus eddy correlation (EC). Computations used Twin Otter data collected in FIFE 1989.

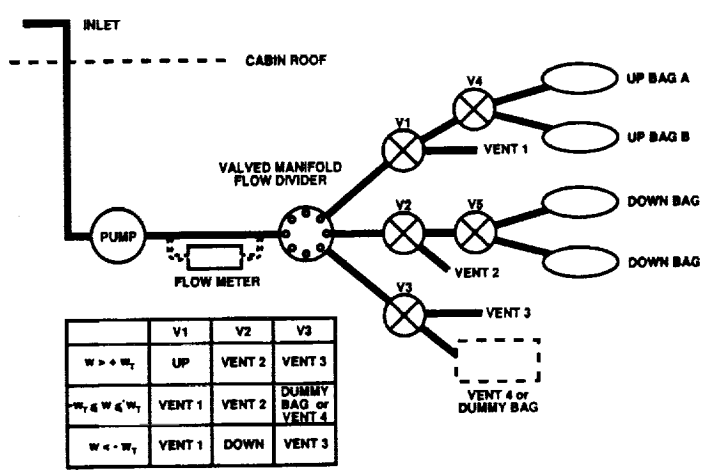

Fig. 3: Schematic of prototype eddy accumulation device flown on NRC Twin Otter in 1990.

Title: **The New French ARAT Aircraft Program**

Authors: **P. Mascart, Météo France, CNRM, Toulouse, France**
M. Ravaut, INSU-DT, Paris, France
P. Flamant, LMD, Palaiseau, France
A. Druilhet, LA, Toulouse, France

Discipline: **Atmosphere**

Four French institutes—Institut Géographique National (IGN), Institut National des Sciences de l'Univers (INSU), Centre National d'Etudes Spatiales (CNES), and Météo France (DMN)—have joined forces in a cooperative ARAT (Avion de Recherche Atmosphérique et de Télédétection) program of instrumented aircraft for atmospheric sciences and remote sensing research.

The ARAT aircraft is a Fokker-27 (Model 700) modified to accommodate a wide variety of meteorological instrumentation used for mesoscale dynamics, cloud physics, radiation, and air/cloud chemistry. Onboard equipment can also include a vertically scanning lidar, the LEANDRE system, and an extensive remote sensing payload for visible, infrared, or microwave investigations.

The poster gives a description of the scientific payload, and illustrates the aircraft capabilities using examples taken from the Pyrenean Range Atmospheric Experiment (PYREX) field program, flown from October through November 1990, to investigate the wave and turbulence generation mechanisms over a mountain ridge in southwestern France.

Title: MISERS GOLD Dust Collection and Cloud Characterization

Authors: Allen S. Mason, Los Alamos National Laboratory
David L. Finnegan, Los Alamos National Laboratory
Gregory K. Bayhurst, Los Alamos National Laboratory
Robert Raymond, Jr., Los Alamos National Laboratory
Roland C. Hagan, Los Alamos National Laboratory
Gary Luedemann, Los Alamos National Laboratory
Kenneth H. Wohletz, Los Alamos National Laboratory

Discipline: Atmosphere

MISERS GOLD was a surface detonation of 2445 tons of ammonium nitrate-fuel oil blasting agent conducted by the Defense Nuclear Agency for a variety of research purposes. This report presents the results of an experiment designed to study the dust cloud over the 24-hour period following the detonation.

The cloud was sampled by aircraft to obtain material needed to characterize the quantity of dust lofted, the source regions of the cloud, and the size, shape, and mineralogical characteristics of the particles. Elemental tracers and organic dyes were emplaced in the charge and in surrounding areas. Analyses were done by instrumental neutron activation analysis (INAA), fluorimetry, scanning electron microscopy (SEM), and energy-dispersive spectrometry (EDS). Tracer data define the source regions of the dust cloud. Extensive particle size distribution data were obtained.

The major emphases placed on the dust cloud study were determination of the total mass lofted, its density and distribution with altitude, tracking of the cloud, characterization of the source regions and size, shape, and mineralogy of the dust particles in various portions of the cloud. These objectives were addressed by the emplacement of one elemental tracer within the charge and five buried in the surrounding terrain, and by collecting airborne dust samples. Samples were collected by a well-characterized filter sampler carried by the WB-57F aircraft shown in figure 1.

The amount of dust collected on each pass through the cloud was determined by weighing of the filters. Figure 2 shows the dust density *vs.* height. The estimated dust inventory at sampling time was calculated by

assuming that the cloud is composed of cylindrically symmetrical layers, that the aircraft flew the diameters of the cylinders, and that each sample was representative of the height range between the half-distances to the adjacent samples. The uncorrected estimate of total dust aloft at sampling time is 3.08 x 10^9 g. However, the indium tracer results discussed below indicate that the cloud geometry used overestimated the extent of the cloud, and a more plausible estimate would be 1.8 x 10^9 g.

The indium tracer density was determined by INAA, and is shown as a function of height in figure 3. The tracer was inventoried by the same approach used for the dust in the preceding paragraph after the local soil background and filter blank were subtracted. The percentage recovered was calculated from the known amount emplaced. The indium, which is relatively volatile, was located toward the upper portion of the cloud but was recovered to the extent of 172%. This is attributed to the errors in cloud geometry as discussed above, and this value has been used to correct the dust lofting estimate.

Figure 4 shows an overview of the diagnostic cloud trajectory and sampling flights conducted at 5 and 24 hours following the detonation. Indium tracer and location data from those flights are presented in figures 5 and 6.

Particles were removed from the filters by destroying the cellulose filter material and the organic ester with which it was impregnated in a low temperature asher. This procedure, done directly on the SEM slide, has been shown to have negligible losses or effects on particle characteristics. The particles were then embedded in epoxy directly on the slide and the preparation polished for examination. The SEM-EDS analysis is automated such that particle sizes, shapes, and semi-quantitative compositions are determined in a single scan of a section. Particle mass distributions from shortly after detonation and from 5 and 24 hours later are shown in figures 7 through 9. Corresponding mineralogy is shown in figures 10 through 12.

This work was sponsored by the Defense Nuclear Agency under IACRO 89-830, task code and title: RA/RY, Aerospace Systems V&H Above Ground Testing, work unit code and title: 00014, Dust Collection and Cloud Characterization MISERS GOLD, work unit manager: Maj D. Wade, USAF.

Title: Geophysical Modeling of Backscatter from the Ocean Surface at C-Band

Authors: Robert E. McIntosh, University of Massachusetts, Amherst
Steve Carson, University of Massachusetts, Amherst

Discipline: Atmosphere

The reflection of microwaves by the ocean surface increases as surface winds generate ocean roughness. Empirical relations measured at Ku-band were used to interpret Seasat scatterometer data in 1978. The magnitude and direction of the wind over the ocean was inferred from the Seasat data to an estimated accuracy of $\pm$ 2 ms^{-1} in magnitude, and $\pm$10 degrees in direction. This has motivated the European Space Agency (ESA) to include a C-band scatterometer to remotely sense the ocean surface in the European Research Satellite (ERS-1), which will be flown next year.

In this poster presentation, we describe a C-band Scatterometer (C-SCAT) that was developed at the University of Massachusetts for the purpose of measuring the relationship that microwave backscatter at 5-5.7 GHz has with surface winds. This sensor flew on the NASA-Ames Research Center's C-130B aircraft in a series of flights with JPL's NuSCAT. Additional data will be collected during the planned participation in the Surface Wave Dynamics Experiment (SWADE), and during verification underflights of the European Space Agency's ERS-1 satellite.

C-SCAT is divided into four subsystems: the transmitter and receiver, the antenna and spinner, the computer and data acquisition hardware, and the digital interface electronics. All of these subsystems, with the exception the spinner and the antenna, are mounted in a standard rack.

The antenna is a frequency-steered microstrip patch array laminated onto a four foot diameter aluminum disk positioned horizontally beneath the fuselage of the airplane. The antenna is bolted to a hollow drive shaft which passes through a pressure seal in the fuselage skin. The drive shaft is coupled to an 1/8 hp dc motor. This assembly makes it possible to rotate the antenna at speeds ranging from 0 to 35 RPM.

The off nadir pointing angle of antenna can be varied from 20 to 50 degrees by varying the operating frequency from 5.7 GHz to 4.98 GHz. Rotating the antenna with its main beam pointed off nadir produces a conical scan of the ocean surface. This conical scan provides full azimuthal coverage of the radar incidence angle relative to the direction of the wind. A 10 bit optical encoder is coupled the the drive shaft, providing instantaneous measurement to the antenna azimuth angle to an accuracy of 0.3 degrees.

Previous flights with JPL's NuSCAT have yielded data with ground truth provided by NOAA buoy 46012. This data covers a range of wind speeds ranging from 6.9 to 11.2 m/s. This data set has enabled the construction of a preliminary model function.

In SWADE, an extensive set of ground truth will be available, and different sea state conditions are anticipated. The data set resulting from this experiment will enable the refinement of the C–Band model function.

Although the basic model function has been established, the influence of other factors must be accounted for. For instance, capillary wavelets are superimposed on longer gravity waves, whose wavelength is on the order of tens of meters. The height and slope of these gravity waves influence the backscatter from the ocean surface. The functional dependence of the ocean backscatter upon these factors will be identified and accounted for as we develop a model function that relates the radar backscatter from the ocean at C–band to the magnitude and direction of the wind vector at the ocean surface.

Title: **Aerosol and Cloud Backscatter Measurements in the Thermal Infrared using an Airborne Backscatter Lidar**

Authors: Robert T. Menzies, Jet Propulsion Laboratory
David M. Tratt, Jet Propulsion Laboratory
Alan M. Brothers, Jet Propulsion Laboratory
Stephen H. Dermenjian, Jet Propulsion Laboratory
Carlos Esproles, Jet Propulsion Laboratory

Discipline: **Atmosphere**

An airborne CO_2 lidar developed at JPL was flown on the NASA Ames Research Center DC-8 research aircraft in 1989-90 to measure vertical profiles of aerosol and cloud backscatter throughout the vertical extent of the troposphere, with emphasis on coverage of a wide range of latitudes, including the equatorial region and portions of the southern hemisphere. The acquisition and interpretation of atmospheric backscatter data over large geographical regions, using a direct measurement technique as exemplified by the range-gated CO_2 lidar approach, is key to the evaluation of the coherent Doppler lidar technique for the measurement of global wind fields from an Earth-orbiting platform. The CO_2 laser technology is the technology of choice for an Earth-orbiting Doppler lidar, and a wavelength near 9 μm is the optimum wavelength assuming a CO_2 coherent lidar is used. Although aerosol extinction measurements at visible and near-IR wavelengths with an instrument such as SAGE can provide insight into the global aerosol climatology, there is limited value in attempting to extrapolate to aerosol backscatter in the thermal infrared using these data. In addition, the SAGE data are biased toward cloud-free regions in the mid and upper troposphere because the solar occultation technique requires clear line-of-sight for several hundred km near the tangent altitude. There is much interest in assessing the performance of the NASA LAWS (Laser Atmospheric Wind Sounder) instrument near clouds, e.g., cirrus and convective cumulus. A measurement program involving airborne lidar greatly expands the data base for aerosol backscatter at infrared wavelengths in regions for which there is presently a severe shortage of data, with high spatial resolution in both the vertical and horizontal.

The Airborne Backscatter Lidar (ABL) instrument first flew on the DC-8 with the JPL Synthetic Aperture Radar during the summer of 1989, and then again with several other aerosol science instruments on the NASA DC-8 in November/December 1989 and May/June 1990 as part of the NASA GLOBE (Global Backscatter Experiment) Missions. Participation in the SAR/DARPA/ESA Mission provided experience in calibration procedures and permitted an extended engineering checkout of the instrument. The instrument proved to be robust and durable under actual deployment conditions. An overflight of the NOAA/WPL CO_2 lidar in Boulder, Colorado during the transit flight from Moffett Field to Bangor Maine on August 3, 1989 resulted in an excellent opportunity for an intercomparison of aerosol backscatter profiles obtained with the two lidars.

The GLOBE 1989 Pacific Mission consisted of 15 flights, which geographically extended from 66-degrees north latitude to 66-degrees south latitude. In addition to the transit flights from one location to another, local flights included one in the Hawaii area, two south of Australia, three in the Japan area, and one north of Pt. Barrow, Alaska.

The GLOBE 1990 Pacific Mission consisted of 13 flights, three of which were local flights out of Hickam AFB, Hawaii, Christchurch, New Zealand, and Yokota Air Base in Japan.

Much of the data from both GLOBE missions has been processed in high resolution mode using false color display plotting. These plots indicate vertical profiles of backscatter in calibrated absolute units, with vertical resolution of approximately 100 m and horizontal resolution of approximately 500 m. This "quick-look" data display format permits the recognition of both vertical layering and the extent of horizontal homogeneity at a given altitude, which can then be used for judging the relevance of spatial averaging over larger scales.

N91-25478

Title: The Surface Wave Dynamics Experiment (SWADE)

Authors: Erik Mollo-Christensen, NASA/Goddard Space Flight Center
J. David Oberholtzer, NASA/Wallops Flight Facility

Discipline: Oceans

The Surface Wave Dynamics Experiment is designed to provide the basic data needed to understand the wind-wave interactions in the open ocean. During the period of October 1990 through March 1991 two discus, four meteorological buoys, and several other specialized buoys will collect continuous in-situ data. During three intensive periods of study, several aircraft and an airship will collect synoptic data from the study area in the Atlantic east of the Wallops Flight Facility. Data from the buoys will be collected by aircraft and ARGOS data links. Instrumentation descriptions as well as preliminary data from the first intensive study period will be presented.

Title: **Availability of Air Force Aircraft and Support for Geoscience Research**

Authors: George B. Orzel, Wright-Patterson Air Force Base
Michael Miller, Wright-Patterson Air Force Base
Chris Higgins, Wright-Patterson Air Force Base

Discipline: **Aircraft Operations**

AIRBORNE RESEARCH RESOURCES: Our organization with 38 unique research Aircraft is perfectly suited to support airborne geoscience research. We also have the capability to design, fabricate, and install extensive structural modifications on our/your aircraft. Additionally, we can design and fabricate sophisticated instrumentation systems and can reduce and process your data. We are the 4950th Test Wing located at Wright-Patterson AFB, Ohio, a unit of Air Force Systems Command's (AFSC) Aeronautical Systems Division (ASD).

AIRCRAFT: The 4950th Test Wing has two flying squadrons, one dedicated to C-135 and C-18 aircraft, and the other to the C-141, and T-39 aircraft. Most of the Wing's aircraft have one-of-a-kind configurations for flight testing electronic countermeasures, advanced navigation systems, satellite communications, new radars, electro-optical and surface-to-air detection systems, and for environmental research. Our aircraft can be modified to accommodate any requirements. Three maintenance squadrons provide the necessary support to carry out the World wide flying commitment. We are the large aircraft testbed manager for AFSC. Our aircraft include:

	C-135	C-18	C-141	T-39
SERVICE CEILING	*39,000 ft*	*39,000 ft*	*41,000 ft*	*41,000 ft*
DURATION (Endurance)	*11 hours*	*12 hours*	*12 hours*	*3.5 hours*
RANGE (Endurance)	*5,000 nm*	*5,880 nm*	*6,000 nm*	*1,575 nm*
LENGTH	*136 ft*	*152 ft*	*145 ft*	*43 ft*
WINGSPAN	*130 ft*	*145 ft*	*159 ft*	*44 ft*
MAX GROSS WEIGHT	*299,000 lb*	*331,600 lb*	*323,100 lb*	*18,650 lb*

WORLD WIDE DEPLOYMENT: The 4950th Test Wing has extensive experience deploying world wide. Last year, the Wing had 75 deployments to 27 countries such as Diego Garcia, Brazil, Singapore, Kenya, Iceland, Australia and other far and remote locations.

MODIFICATION: The 4950th Test Wing design, fabrication, and modification facility is a large complex, utilizing the personnel, manufacturing skills, and equipment similar to that found in any large aircraft plant. It includes a 220,000 Sq Ft fabrication facility, and 3 modification hangars totaling 114,000 Sq Ft. The Computer Aided Engineering/Computer Aided Manufacturing (CAD/CAM) capability provides high productivity, rapid response, and accuracy required for producing one-of-a-kind test articles.

INSTRUMENTATION: The 4950th Test Wing can design, fabricate, install, and operate sophisticated custom airworthy and ground instrumentation, real-time data acquisition/processing/display, and telemetry systems which are tailored to meet your needs. Out capabilities and unique expertise allow us to design and fabricated from the circuit level up to complete systems.

DATA REDUCTION AND ANALYSIS: The 4950th Test Wing can design and write software in support of post flight data analysis. It has extensive experience in the merging of multiple asynchronus data streams recorded on tapes using diverse formats, processing large amounts of flight test data, and performing numerical and statistical analysis.

OUR PEOPLE: Our most important assets, nearly 1900 military and civilian people, are highly trained professionals with a can-do, customer oriented attitude.

PROGRAM MANAGEMENT: The 4950th Test Wing offers a matrix approach to flight test program management. Once a customer identifies the test requirements, the Commander appoints a Test Program Manager (TPM) and a test team to manage the project. The TPM functions as the team leader, serving as the single point of contact to the customer, with total responsibility for coordinating the entire Wing effort. This team approach along with a highly motivated work force, is the key to the Test Wing providing timely and successful results for our customers.

RECENT NASA SUPPORT: The most recent example of 4950th performance was demonstrated in the fast reaction support of the Combined Release and Radiation Effects Satellite (CRRES) program. In mid-May 1990 NASA requested the 4950th to support the Critical Velocity Experiments of the CRRES program. The most appropriate aircraft was selected (NKC-135A), modified, and was operationally ready for deployment on 4 Sep 1990, less than four months from the initial request.

The modification encompassed the installation of cameras, movable mirrors, associated electronics, video recorders and video monitors which were provided by NASA. The Test Wing provided and installed three 28-inch diameter optical windows through which low light cameras could view the event. The windows were evaluated for transmissivity at the important wavelengths and were found to be acceptable. The necessary racks, tables, seats, and other instrumentation were also provided by the Test Wing. The complete modification effort was performed by the Special Programs Branch of the Modification Center. See Figure 1.

Additionally, the 4950th Test Wing prepared the operations plan which outlined how the aircraft was going to meet the required test objectives. This encompassed designing aircraft flight profiles which maximized the data collection opportunity of the sensors, flying the aircraft in the proper position at the right time to observe the event, and coordinating other support and operational activities that related to the deployment of the aircraft to the South Pacific. **RESULT:** Two very successful missions were flown, one on 10 Sept 90 departing from and returning to American Samoa and one on 14 Sept 90 departing from American Samoa and landing in Brisbane, Australia.

OTHER RELATED PROGRAMS: The 4950th Test Wing supports the Argus airborne photodocumentation aircraft and has supported the Air Force Geophysics Laboratory (AFGL) with two testbed aircraft for over 15 years: 1) Aerospace Radiation Propagation (ASRP) aircraft and 2) Infrared (IR) Properties aircraft.

SUMMARY: The 4905th Test Wing has the capability to support your airborne research requirements. From flying world wide deployments to aircraft modification, customer satisfaction is our #1 objective. If you have any further questions or would like more information, please contact Mr. George Orzel at (513) 257-6344 or Mr. Micheal Miller at (513) 257-3242.

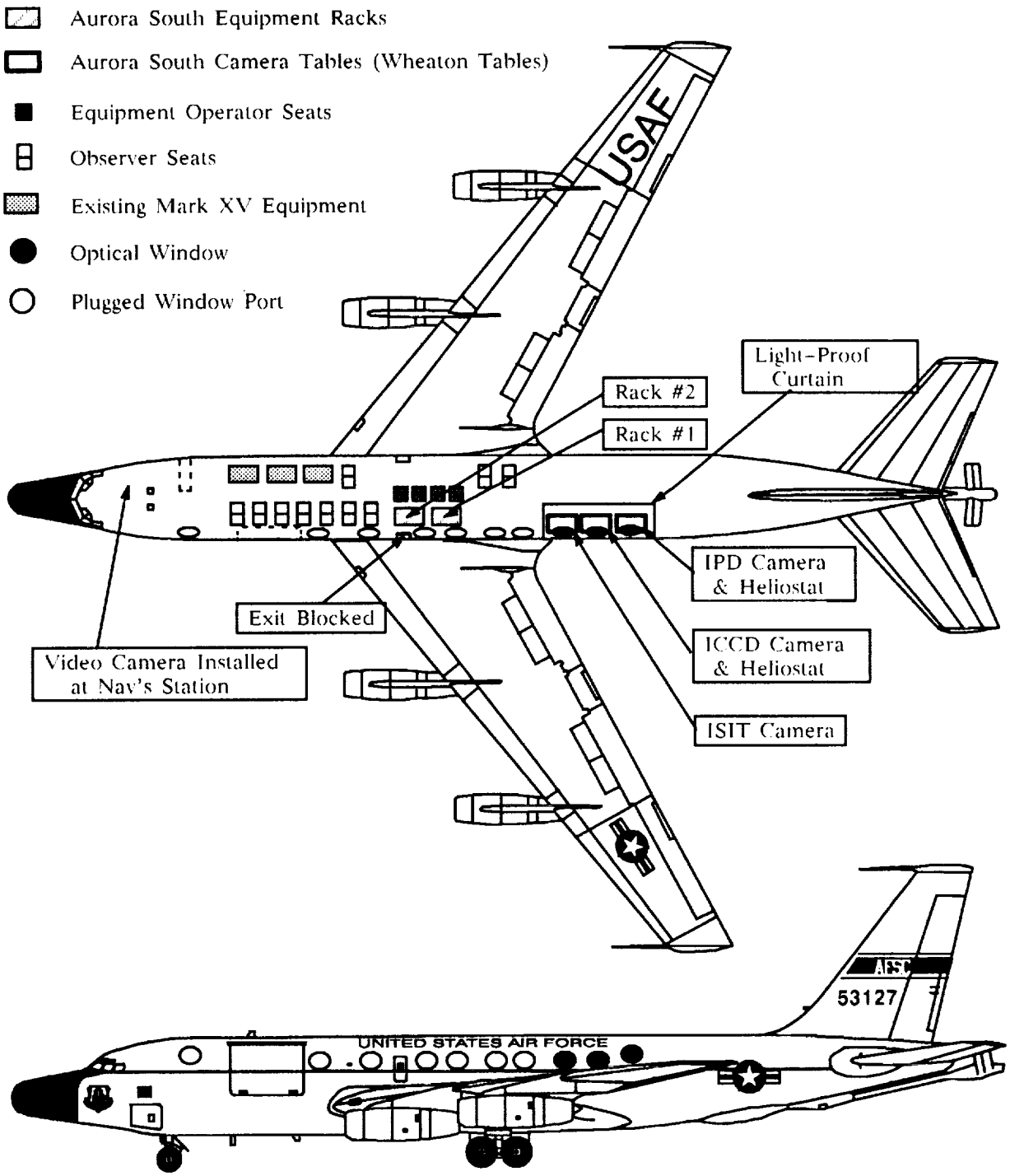

Figure 1. NKC-135A Aircraft Modification Layout

N91-25479

Title: Airborne Ground Penetrating Radar (GPR) for Peat Analyses in the Canadian Northern Wetlands Study

Author: Ramona E. Pelletier-Travis, NASA/Stennis Space Center

Discipline: Land

This study was conducted as part of the NASA Biospherics Research on Emissions from Wetlands (BREW) program in conjunction with the Global Tropospheric Experiment/Atmospheric Boundary Layer Experiment 3B (GTE/ABLE) of the Canadian Northern Wetlands in the Summer of 1990. An important aspect of the program is to investigate the terrestrial production and atmospheric distribution of methane and other gases contributing to global warming. High latitude wetlands are important ecosystems to consider because of their significant production of these gases, their global extent and, the anticipated severity of impact to these ecosystems if global warming occurs. Since the production of many of these gases is biogenic and originates in the soil it is valuable to understand the various soil parameters that impact this production. The distribution and the amount of the carbon source available for microbial metabolism are some of these parameters. In this study we attempted to determine peat depth and to characterize some of the stratigraphy within the peat profile using Ground Penetrating Radar (GPR).

The focal test site of the study was in the Hudson Bay Lowlands - near Moosonee, Ontario. Data was collected from an area extending from James Bay on the east, westward across the coastal marsh, further extending across a predominantly fen environment, and onward to a predominantly bog environment about 100 km inland. Over this distance the peat depth ranged from 0m at the coast to approximately 3m at the 100 km inland bog site.

Multi-kilometer transects of airborne (helicopter) GPR data were collected periodically along the 100 km distance from the coast inland so as to obtain a regional trend in peat depth and related parameters. Global Positioning System (GPS) data was simultaneously collected from the helicopter to properly georeference the GPR data. Additional 50m ground-based transects of GPR data were also collected as a source of ground truthing, as a calibration aid for the airborne data sets and, as a source of higher resolution data for characterizing the strata within the peat. In situ peat depth probing and soil characterizations from excavated soil pits were used to verify GPR findings.

Results from the ground-based data are quite good. Peat depth was determined with the GPR by identifying the interface between the peat and the older marine clays below due to the conductivity differential between them. GPR-determined peat depths corresponded very closely with in situ probing. The greatest discrepancy, yet minor, between GPR-determined depths

and probing occurred in areas with significant above ground, unsaturated moss growth. Preliminary analysis demonstrated that the GPR was also able to delineate stratifications within the peat indicative of denser layers. These occurrences were generally supported by in situ probing and examination of the soil pits dug.

Airborne GPR data acquisition is very experimental but proved promising from preliminary analysis. GPR did a fair job in determining peat depth depending upon the helicopter height. When the sensor was within 3m-5m of the ground surface the data was fairly good; above that height the data decreased significantly in its capability to delineate peat depth. Airborne GPR however provided minimal within-peat strata characterization. Occasionally, peat depth responses and in many cases the within-peat strata responses were confounded by responses from ground surfaces, the helicopter or some other source. Shielding and other improvements in the engineering of the system will decrease these sources of interference in the future.

Various trends in peat depth persisted across differing spatial scales. On the regional scale, GPR data affirmed a trend with increasing peat depth from the coastal marsh environment to the bog. Within the bog environment it was difficult, from preliminary analyses, to discern a significant change in peat depth as we traveled further inland. There may be a controlling factor in the natural ecosystem preventing bog peat depth from increasing or we may not have sampled far enough inland. (This sampling was hindered by logistics and remoteness.) On a local scale, peat depth was much more spatially variable. Still, a trend persisted of relatively shallow peat depths near water bodies changing to greater depths as the landscape progressed to fen and bog and possibly to tree islands. This sequence of change may occur over distances of 50m but usually over greater distances. When these vertical determinations of peat depth are integrated with lateral classifications of land cover from more traditional forms of remotely sensed data models can be developed to estimate carbon source in these northern wetlands from peat volume calculations.

Some paleoecologists believe that the Hudson Bay Lowlands have undergone a series of plant community successions, especially on a local scale, over the past 5000 years. Evidence of denser material and woody tissue indicating forest growth can be identified at various depths in the peat from the soil pits dug. In many cases the GPR was able to identify changes in response with depth that were correlated with these strata. Therefore, GPR may prove to be a beneficial tool in paleoecological studies.

Title: Oregon Transect Ecosystem Research Project Multisensor Airborne Campaign (OTTER-MAC)

Author: David L. Peterson, NASA/Ames Research Center

omit to A 235

Discipline: Land

Abstract will be available at the Workshop.

Title: Extraction of Reflectance from 1989 AVIRIS Radiance Data using LOWTRAN 7 Atmospheric Models

Authors: Frederick P. Portigal, University of Nevada System
James V. Taranik, University of Nevada System
Christopher D. Elvidge, University of Nevada System

Discipline: Atmosphere

The development of the Airborne Visible/Infrared Imaging Spectrometer (AVIRIS) has provided the scientific community a window into the future of hyper - spectral remote sensing. The AVIRIS sensor measures upwelling radiance from the Earth in 224 spectral bands from 400 to 2500 nm. This measured radiance is a function of solar irradiance, path scattered, atmospheric, attenuated ground reflected radiance and ground albedo. To become a practical tool for environmental monitoring, ground reflectance must be retrieved from imaging spectrometer data with little or no field work. Statistically based methods which employ the image data alone have been shown to be useful for extraction of absorption features in terrain materials, however they are generally not suitable for quantitative work. Empirical line methods are based on the use of a range of bright and dark ground targets of known reflectance. These targets are used to develop a series of linear equations which map the radiance data to reflectance thereby removing the atmospheric and solar irradiance effects. The empirical techniques are of limited value because they require the existence of suitable targets as well as extensive field and laboratory work. This paper investigates the use of atmospheric models for extraction of ground reflectance from a September 20, 1989 AVIRIS image over Stanford University's Jasper Ridge Biological Preserve, along the Central California coast. The results of the LOWTRAN 7 modelled reflectance have been compared with those of the empirical line method. Preliminary results indicate that atmospheric models may ultimately provide the means for extraction of ground albedo from hyper - spectral radiance data.

Title: The Structure of a Stable Internal Boundary Layer over the Coastal Ocean

Authors: David P. Rogers, Scripps Institution of Oceanography
Douglas W. Johnson, Royal Aerospace Establishment (England)
Carl A. Friehe, University of California, Irvine

Discipline: Atmosphere

The coastal environment is characterized by small scale variations in the structure of the ocean and the atmosphere. This variability is due to the topography of the coastline and the land-sea thermal contrast that contributes to a number of important effects, including the land-sea breeze, the formation of coastal atmospheric fronts, and atmospherically induced coastal ocean currents and upwelling. Downwind of large horizontal temperature gradients, caused either by the land-sea discontinuity or ocean fronts, an internal boundary layer (IBL) can develop with a distinctly different structure from the overlying planetary boundary layer (PBL). If the thermal transition is from a cold to a warm surface, the IBL may be unstable and may rapidly erode the overlying PBL. Alternatively, if the air flow is from a warm to a cool surface, a stable IBL may develop. The latter was observed during the Frontal Air-Sea Interaction Experiment (FASINEX) where a sharp discontinuity in sea surface temperature (SST) caused the formation of a shallow, stable IBL over the cooler water downwind of the front (Rogers 1989, Friehe et al. 1990). The most significant result was the sudden decrease in the wind stress over the colder water in response to an increase in stability of the air near the surface and a decrease in the transfer of momentum from higher altitude. In this case the IBL was about 100 m deep with the top of the layer coincident with the level at which the momentum flux was negligible.

To investigate these effects in more detail, we conducted a number of aircraft flights at various locations around the coast of Britain during 1990 as part of the Internal Boundary Layer Experiment (IBLEX). A major goal of this work is to understand the vertical exchange of heat, moisture, and momentum between the surface layer and boundary layer clouds. The present study focuses on the variability of the structure of the boundary layer close to the sea surface. Measurements were obtained using the U.K. Meteorological Research Flight's C-130 (Hercules) aircraft.

Here we present some preliminary results from a flight over the Irish Sea where the airflow was from the west, blowing across the Irish coast from the land to sea. The flight pattern consisted of short across wind horizontal legs at various heights within and above the marine boundary layer to determine the turbulent fluxes of heat, moisture and momentum. The upwind stacks were flown close to the Irish coast and the downwind stacks were flown close to the English coast. Shallow vertical profiles were also obtained along the wind direction to determine the mean structure of the entire marine atmospheric boundary layer (MABL).

This MABL is characterized by four distinct layers, a stable IBL below about 200 m, a transition region between the top of the stable layer and cloud base, a cloud layer between about 600 and 900 m, and a shallow, stable capping inversion layer about 100 m deep (Fig. 1). The MABL is stable at all levels, except close to cloud base where it appears to be nearly neutral or well-mixed. The top of the stable IBL coincides with the top of the region of strongest horizontal wind shear.

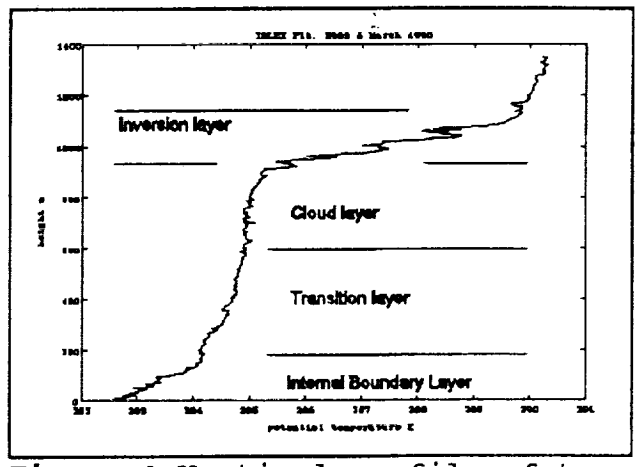

Figure 1 Vertical profile of temperature

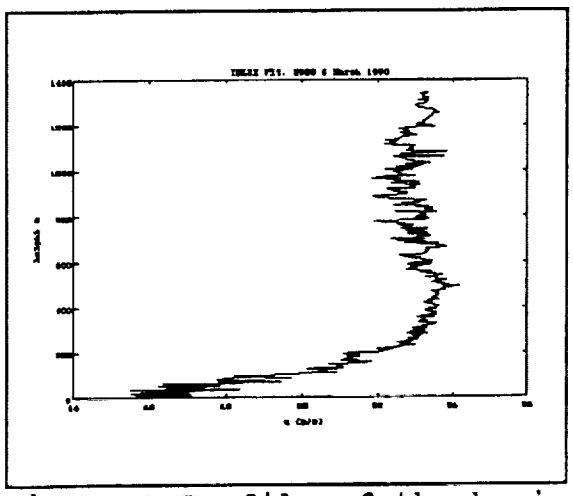

Figure 2 Profile of the horizontal wind component, u.

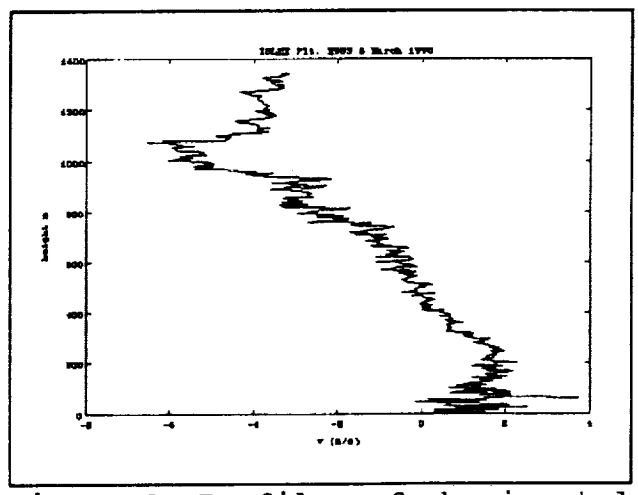

Figure 3 Profile of horizontal wind component, v.

High winds were observed throughout this flight with speeds increasing from about 15 m s^{-1} near the sea surface to about 24 m s^{-1} at the top of the stable IBL (Figs. 2 &3). There is negligible directional shear within the stable layer. Above the IBL, the wind speed remains high, but veers with height up through the base of the inversion.

The most striking feature of this boundary layer is the vertical variability of the moisture field. In particular, there is a maximum of 6.2 g kg^{-1} in the water vapor mixing ratio at 100 m above the sea surface (Fig. 4). At the lowest flight level (15 m), the mixing ratio is about 6.1 g kg^{-1}. Above the IBL, the mixing ratio decreases to a minimum in the MABL of about 5.8 g kg^{-1}, just below cloud base. The water vapor gradient in the stable IBL may be simply due to differential advection of the air from a dryer source close to the surface, or, possibly, aerosol scavenging. The latter explanation is consistent with a large aerosol gradient associated with the high winds within the IBL. Unfortunately, direct aerosol measurements were not available on this flight.

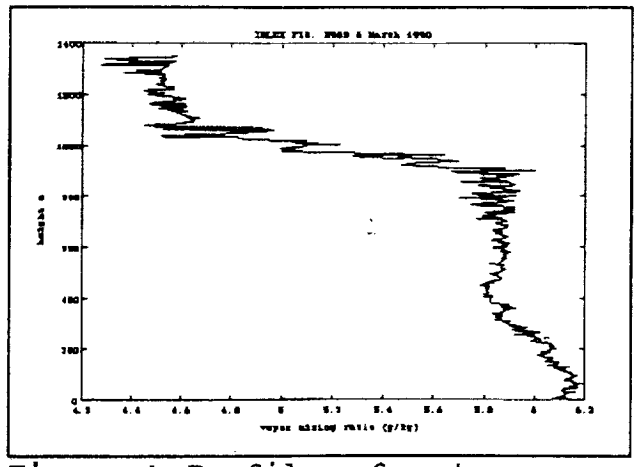

Figure 4 Profile of water vapor mixing ratio.

The turbulent fluxes of moisture at the 100 m level are generally small, and negative, consistent with the observed water vapor gradient below 100 m. The wind stress at this level is about 0.05 $m^2 s^{-2}$, which is similar to the values obtained over cold water downwind of an SST front in FASINEX (Friehe et al. 1990).

ACKNOWLEDGEMENTS

This work was supported by the Office of Naval Research under award N00014-90-J-1265.

REFERENCES

Friehe, C.A., W.J. Shaw, D.P. Rogers, K.L. Davidson, W.G. Large, S.A. Stage, G.H. Crescenti, S.J.S. Khalsa, G.K. Greenhut, and F. Li, 1990: Air-Sea Fluxes and Surface-Layer Turbulence Around a Sea Surface Temperature Front. *J. Geophys. Res.*, accepted for publication.

Rogers, D.P., 1989: The Marine Boundary Layer in the Vicinity of an Ocean Front. *J. Atmos. Sci.*, **46**, 2044-2062.

N91-25480

Title: Airborne Coherent Continuous Wave CO_2 Doppler Lidars for Aerosol Backscatter Measurement

Authors: Jeffry Rothermel, NASA/Marshall Space Flight Center
William D. Jones, NASA/Marshall Space Flight Center
Diana Hampton, Sverdrup Technology, Inc.
Vandana Srivastava, University Space Research Association
Maurice Jarzembski, NASA/Marshall Space Flight Center

Discipline: Atmosphere

Two focused coherent, continuous wave (CW) lidars have been developed by the Marshall Space Flight Center (MSFC) for airborne and ground-based measurement of aerosol backscatter coefficients. The first of these instruments uses a mixture of CO_2 and other gases, and measures backscatter at 10.6 m. The second lidar uses an isotope of carbon dioxide, which enables lasing at 9.1 m. The 10.6 m backscatter measurement serves as a reference to allow variations in backscatter due to aerosol concentration to be distinguished from variations due to spectral variability. The 10.6 m lidar has been used in airborne field programs since 1981. Development of the 9.1 m lidar was completed in early 1989. Recently, both lidars were flown on the NASA/Ames Research Center DC-8 research aircraft in the remote Pacific Basin as part of the NASA GLObal Backscatter Experiment (GLOBE) survey missions (GLOBE I, November 1989; GLOBE II, May-June 1990). The GLOBE program, of which the survey missions are the centerpieces, supports design and simulation studies for NASA's prospective Laser Atmospheric Wind Sounder (LAWS). LAWS is under development by the Marshall Space Flight Center (MSFC) as a facility instrument for the Earth Observing System (EOS), NASA's earth system science initiative. The 9.1 m lidar operates on the wavelength proposed for LAWS. Results from the GLOBE program are also applicable to other satellite-borne, lidar-based sensors that rely upon aerosols as scattering targets.

During airborne operation, the lidars are directed through separate germanium optical ports in the side of the aircraft. The transmit/receive axis is oriented a few degrees off normal to produce a Doppler shifted return signal that is distinct from the strong, non-shifted reference signal from the laser. The focal distance for both lidars can be varied. During GLOBE I, focal distances of approximately 10 m were used. For GLOBE II, focal distances of approximately 50 m were employed for improved sensitivity. The output signal from each lidar detector is processed by a Surface Acoustic Wave (SAW) spectrum analyzer/spectrum integrator. This processor provides the full spectrum of the lidar output signal, allowing the signal-to-noise ratio (SNR) of the Doppler-shifted signal to be estimated. During real-time and post-flight data analysis, a multi-stage signal processing algorithm is used (Rothermel *et al.*, 1990ab), which is based on the theoretical formulation by Vaughan *et al.* (1989). Calibration of signal processing is accomplished using a rotating diffuse target in the laboratory. Additionally, direct measurement of SNR is made from a manually-tuned spectrum analyzer to give backscatter estimates for checking instrument performance during missions.

For the second and most recent GLOBE survey mission, a developmental signal processing/data recording system was implemented. This system consists of a 6.5 MHz anti-aliasing low-pass filter, a 13.3 MHz sample rate analog-to-digital converter (ADC) and a digital signal processing (DSP) integrated circuit board. These system components are installed in a 80386-class, industry standard architecture personal computer. In operation, a time segment of the lidar detector output (containing the lidar return signal) is digitized by the ADC board, then transferred to the DSP board, where the lidar signal spectrum is calculated using discrete Fourier transform (DFT) algorithms. The resulting spectrum is integrated with previous spectra, in a fashion analogous to the SAW processor. After a number of spectra have been integrated, the data are transferred to the personal computer for display and real-time estimation of the SNR and backscatter using an identical signal processing algorithm. The "raw" spectra are recorded on write-once, read-many (WORM) optical disc for post-flight analysis, as well. In addition, the recorded data include universal time, aircraft and meteorological parameters, and operator comments. Several different types of displays of the data are used to assess instrument performance and atmospheric backscatter in real time.

During the GLOBE survey missions, transit flights were made from various waypoints between California and Tokyo, Japan and between the Arctic and Antarctic Circles. Standard flight altitude was typically 8-9 km; deviations for cloud avoidance were typically below 13 km altitude. The aerosol backscatter was found to vary with altitude, geographic location, and aerosol size and chemical composition (as determined by accompanying instrumentation). Backscatter values from optically clear air were found to vary over as much as five orders of magnitude. Examples of horizontal and vertical profile measurements will be shown.

References

Rothermel, J., D.A. Bowdle, A.A. Woodfield, J.M. Vaughan, and D.W. Brown, 1990a: Calculation of aerosol backscatter from airborne CW focused CO_2 Doppler lidar measurements, 1, Algorithm description. *J. Geophys. Res.*, in press.

Rothermel, J., D.A. Bowdle, and J.M. Vaughan, 1990b: Calculation of aerosol backscatter from airborne CW focused CO_2 Doppler lidar measurements, 2, Algorithm performance. *J. Geophys. Res.*, in press.

Vaughan, J.M., R. Callan, D.A. Bowdle, and J. Rothermel, 1989: Spectral analysis, digital integration, and measurement of low backscatter in coherent laser radar. *Applied Optics*, **28**, 3008-3014.

Title: Observations of High Altitude Tropical (HAT) Cirrus and Their Implications

omit TO
p. 241

Authors: Dan J. Rusk, Aeromet, Inc.
Ray Harris-Hobbs, Aeromet, Inc.
Mark Bradford, Aeromet, Inc.

Discipline: Atmosphere

Widespread, persistent cirrus cloud decks in the tropics can have important effects on the atmospheric column. Many investigators have shown that latitudinal variations in radiative heating can be attributed to tropical mid- and upper-tropospheric cloud sheets. However, the cirrus clouds studied were, or were assumed to be, thunderstorm-generated. There is another, less well-known, type of cirrus in the tropics that exists at higher altitudes. Called High Altitude Tropical (HAT) cirrus, it lies at altitudes of 50,000 ft and higher, and can exist over areas of several thousand square kilometers. Also, HAT cirrus overcasts can persist over a location for periods of weeks. Although usually thin, HAT cirrus must be taken into account when considering the various effects of tropical cirrus clouds.

HAT cirrus over the Republic of the Marshall Islands (RMI) has been extensively observed. The obvious distinction between HAT cirrus and other, lower-level varieties is chiefly in the very high altitudes (bases are at ~ 15 km, where temperatures are ~ -80°C) at which it exists. HAT cirrus is often very tenuous, and can be invisible to ground-based observers, often only becoming visible as it is approached in an aircraft, or when the sun is low and shining across the bottom of the layer. Not only is it virtually invisible from the ground, conventional satellite pictures do not show HAT cirrus.

Heymsfield (1986) reported on the composition of a HAT cirrus layer sampled over the RMI. The layer, only about .5 km thick, was encountered at altitudes just above 16 km. Ice crystal habits were about half trigonal plates and half columns, with ice water contents estimated to be ~ 10^{-4} g m^{-3}. Booker and Stickel (1982) also reported penetrating a HAT cirrus layer over the RMI at altitudes between 14 and 15 km; maximum particle sizes were measured to be 140 microns, in a concentration of 1 m^{-3}, with an equivalent ice water content of less than 10^{-4} g m^{-3}.

HAT cirrus is also very persistent, and apparently very widespread. An inspection of five years of sunrise and sunset surface observations taken by Aeromet meteorologists on Kwajalein, RMI, shows that, on average, less than 4 days per

month can be counted upon to be reasonable clear of upper-level cirrus. These figures can be seen in Table 1. Uthe and Russell (1976) used a lidar to show a very high frequency of occurrence of high altitude subvisible cirrus in all seasons near the Kwajalein Atoll.

The mechanisms that form and dissipate HAT cirrus are not known. The occurrence of HAT cirrus is apparently not directly linked to either local convection, or to convection on the intertropical convergence zone (ITCZ). HAT cirrus has often been observed thousands of feet above local shower anvils, with a clear gap between. HAT cirrus has also been observed when winds at cloud level were 180° opposed to the direction of the ITCZ. Wave structures near the tropopause have been found that apparently are not linked to surface features, as can be seen in Figure 1. It is possible that such waves are in some measure responsible for HAT cirrus.

Since HAT cirrus can impact many different types of missions, from radiation studies to reentry vehicle performance, it is important that it be studied. For instance, we have made attempts to locate HAT cirrus layers via their effects on a rawinsonde sounding due to radiative effects. Several soundings were found where layers of HAT cirrus might have been detected if the radiative effects were correctly hypothesized. Aeromet, in the near future, plans to conduct investigations with further aircraft data analysis, airborne lidar studies and numerical modeling.

References

Booker, D.R. and P.G. Stickel, 1982: High Altitude Tropical Cirrus Cloud Observations. Preprints, Conference on Cloud Physics, Nov. 15-18, Chicago, IL, 215-217.

Heymsfield, A.J., 1986: Ice Particles Observed in a Cirriform Cloud at -83°C and Implications for Polar Stratospheric Clouds. J. Atmos. Sci., 43, 851-855.

Uthe, E.E. and P.B. Russell, 1976: Lidar Observations of Tropical High Altitude Cirrus Clouds. Preprints, IAMAP Symposium on Radiation in the Atmosphere. Garmisch-Partenkirchen, Germany, August 19-28, 5 pp.

	Average Duration	Maximum Duration;Year	Maximum # Clear Days;Year	Minimum # Clear Days;Year
January	1.76	6.0; 1986	10.0; 1985,1986	2.5; 1987
February	1.45	3.5; 1985	8.0; 1985	.5; 1987
March	1.24	2.5; 1985,1989	7.5; 1985	2.0; 1986
April	1.02	3.0; 1985	11.5; 1985	0.0; 1986
May	.96	3.0; 1985	12.0; 1985	2.0; 1985,1989
June	1.08	2.5; 1985	8.0; 1985	1.0; 1986,1987,1988
July	.86	2.5; 1987	7.5; 1985	1.0; 1988
August	1.0	3.5; 1988	8.0; 1985	.5; 1986,1989
September	1.03	1.5; 1985,86,88,89	7.0; 1985	.5; 1987
October	1.12	3.0; 1986	10.0; 1985	1.0; 1988
November	.55	1.5; 1988	4.0; 1985	0.0; 1986
December	.55	1.5; 1988	2.5; 1985	0.0; 1987

Table 1 Average duration of periods free of upper-level cloudiness, in days, the recorded maximum, in days, and the maximum and minimum number of days relatively free of upper-level cloudiness per month. Data from Kwajalein, RMI, and surface observations.

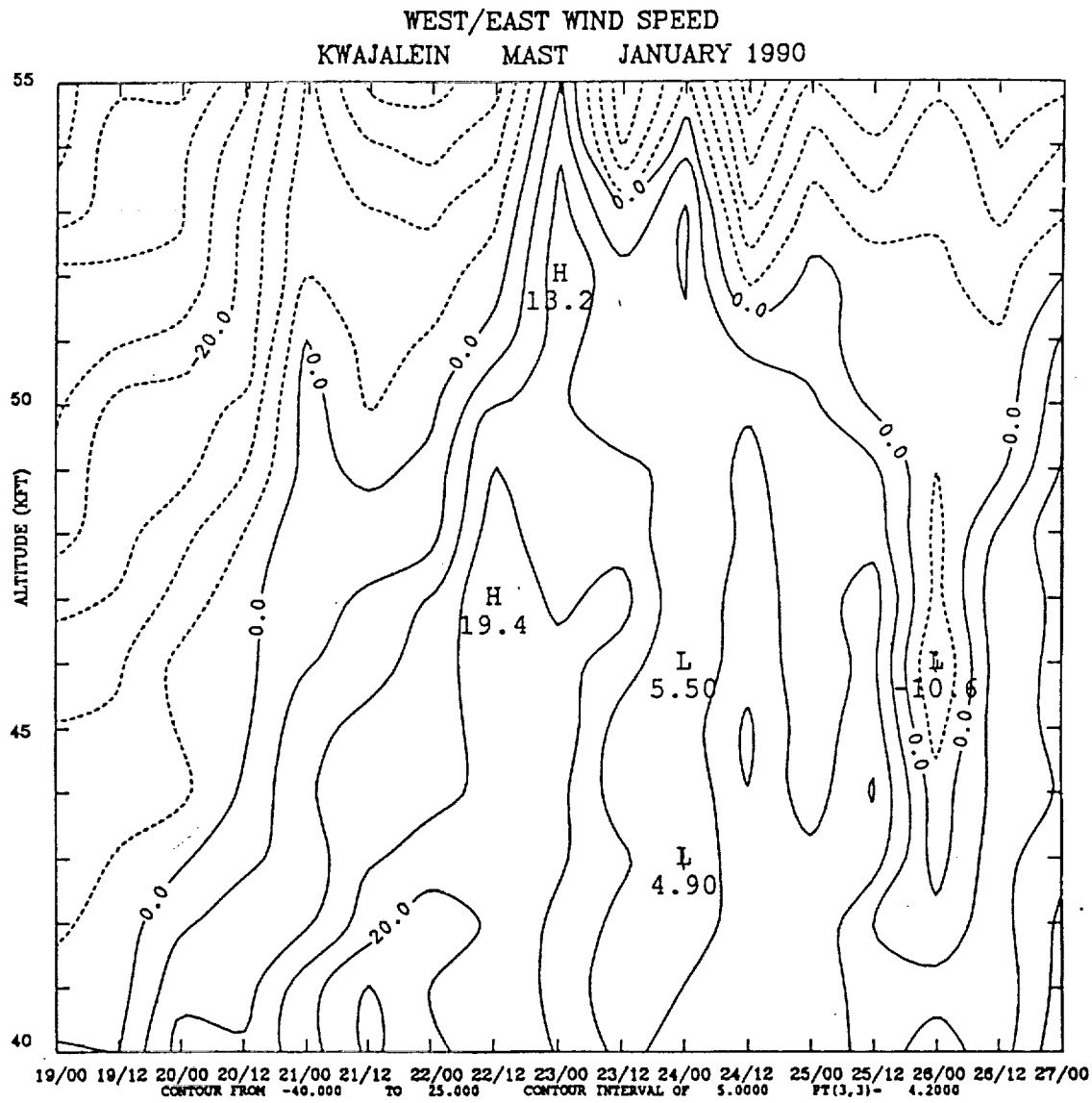

Figure 1 East-west wind speed (kts) profiles at Kwajalein from 19 to 27 January 1990. Altitude range is between 40,000 and 50,000 ft. The tropopause was always above 55,000 ft.

N91-25481

Title: Science Requirements and Feasibility/Design Studies of a Very-High-Altitude Aircraft for Atmospheric Research

Authors: Philip B. Russell, NASA/Ames Research Center
David P. Lux, Dryden Flight Research Facility
R. Dale Reed, PRC Systems Services
Max Loewenstein, NASA/Ames Research Center
Steven Wegener, NASA/Ames Research Center

Discipline: Atmosphere

1. Introduction

Recent successes of the NASA ER-2 aircraft in missions to study polar ozone and stratosphere-troposphere exchange have highlighted the strengths of aircraft measurements as a complement to other atmospheric research platforms (e.g. spacecraft, balloons, and rockets). Specifically, aircraft provide a fine spatial resolution and range of measured constituents and meteorological variables (as required for process studies, for example) that cannot be achieved solely by remote measurements from space. And they provide a controllability, launch frequency, choice of launch sites, and probability of payload recovery that cannot be matched by large-payload balloons.

In spite of these strengths, the recent missions have also pointed out shortcomings of aircraft currently available for atmospheric research. Specifically, the ER-2 ceiling of 21 km (70,000 ft), allowed range of 3,200 nautical miles, and restrictions on flight over oceans and into the polar night have prevented flights with existing and planned payloads that could answer important questions now facing atmospheric science.

The advantages and shortcomings of currently available aircraft pose the question of whether to develop advanced aircraft for atmospheric research. To answer this question, NASA conducted (1) a workshop to determine science needs and (2) feasibility/design studies to assess whether and how those needs could be met.

2. Science Requirements Workshop and Report

The Workshop on Requirements for a Very-High-Altitude Aircraft for Atmospheric Research was held in Truckee, California, July 15-16, 1989. Participants included experts in stratospheric theory and measurements (by spacecraft, balloons, and aircraft), aircraft operations, and aircraft design and development. The focus of the workshop was on stratospheric science and measurement needs, with secondary attention to broader atmospheric science needs, such as climate change by radiatively active gases ("greenhouse gases").

The Workshop participants defined key questions now blocking progress in atmospheric science and related policy decisions. They then defined aircraft missions needed to address those

questions, and deduced the aircraft characteristics needed to conduct those scientific missions. Examples of key questions include:

- What causes ozone loss above the dehydration region in Antarctica?
- To what extent are dehydration, denitrification, and ozone loss transmitted to midlatitudes?
- What maintains the geographical distribution of polar stratospheric clouds, and how do they transform the chemical balance as a function of temperature and pressure?
- What is the chlorine content, and what are its chemical forms, in the tropical middle stratosphere?
- How do volcanic injections, especially in their first few months, affect the chemistry of trace gases (including ozone) and radiation and temperature fields? How do particle chemistry and physics evolve during this period?
- What do stratospheric profiles of radiative fluxes and radiatively active constituents, in conjunction with tropospheric profiles, reveal about the onset and predicted evolution of the greenhouse effect?

The aircraft missions required to answer these questions pointed to a need for an aircraft with the following characteristics: cruise altitude of 30 km (100,000 ft), subsonic cruising speed, range of 6,000 n mi with vertical profiling capability down to 10 km (33,000 ft) and back at remote points, and a payload capacity of 3,000 lb. A capability to "pop up" to 35 or 40 km altitude (115,000-130,000 ft), even with a considerably reduced payload, is highly desirable. Required operating characteristics imply a need for both manned and unmanned operations.

3. Feasibility/Design Studies

Designing an aircraft to meet the above requirements presents a unique challenge to aeronautical engineering. The regime of low Reynolds numbers combined with Mach numbers near 0.7 is not well explored. Fundamental to the problem is the extremely low air density at 100,000 ft and above. This implies challenges in aerodynamics, structures, propulsion, and propeller design. To address these challenges and establish a level of confidence that a vehicle could be built to meet the Workshop specifications, NASA Ames has managed several inhouse and contractor design studies. These studies have addressed questions of the optimum aspect ratio, wing and propeller airfoil designs, turbocharged and supercharged reciprocating engines vs. turbojets, low-wing-loading aerodynamics, heat rejection, cooling drag, and a phased development of ground-test, flight-demonstrator, and mission vehicles. A technology risk assessment based on these studies assigned a rating of "Low Risk" to the task of designing a vehicle to cruise subsonically at 100,000 ft, but a rating of "High Risk" to cruising or "popping up" to 120,000 ft.

The poster will show the conceptual designs and other considerations on which these risk assessments are based.

Current efforts are directed toward expanding the assessment of science needs to cover all of Earth science (i.e., land, ocean, cryosphere, weather and climate--not just stratospheric science). The broad range of aircraft approaches to meeting those needs will then be explored. The goal is to define the most cost-effective way of meeting the advanced aircraft needs of the combined Earth science community.

N91-25482

20150

p.2

NC473657

Title: C-130 Automated Digital Data System (CADDS)

Authors: C.P. Scofield, NASA/Ames Research Center
Chien Nguyen, NASA/Ames Research Center

Discipline: Aircraft Data Management

Real-time airborne data acquisition, archival and distribution on the NASA/Ames Research Center (ARC) C-130 has been improved over the past three years due to the implementation of the C-130 Automated Digital Data System (CADDS). CADDS is a real-time, multitasking, multiprocessing ROM-based system. The system was developed on an Intel Multibus I with an 80286 microprocessor, an 80287 math coprocessor, and five 8085 microprocessors. Application software specific to the CADDS requirements is "buried" with the iRMX86 operating system on EPROM.

CADDS acquires data from both avionics and environmental sensors inflight for all C-130 data lines. Environmental parameters include Total Air Temperature, pressure altitude, radar altitude, wind speed and direction, dew-frost point, and infrared surface temperature. Housekeeping information is distributed, in serial format and at various baud rates, to RS-232 ports at the experimenter stations. The system also displays the data on video monitors available throughout the aircraft. Raw and processed data, which includes a universal time stamp, are archived to a PC-compatible Small Computer System Interface (SCSI) format tape. At any time, the CADDS operator can create a hardcopy of displayed data, enter flight information, or add comments concerning data and/or flight conditions.

CADDS is designed to be flexible and expandable in order to meet the needs of the scientific community on the Ames C-130 platform aircraft. CADDS replaces the NERDAS system.

CADDS C-130 Automated Digital Data System
Data Flow Diagram

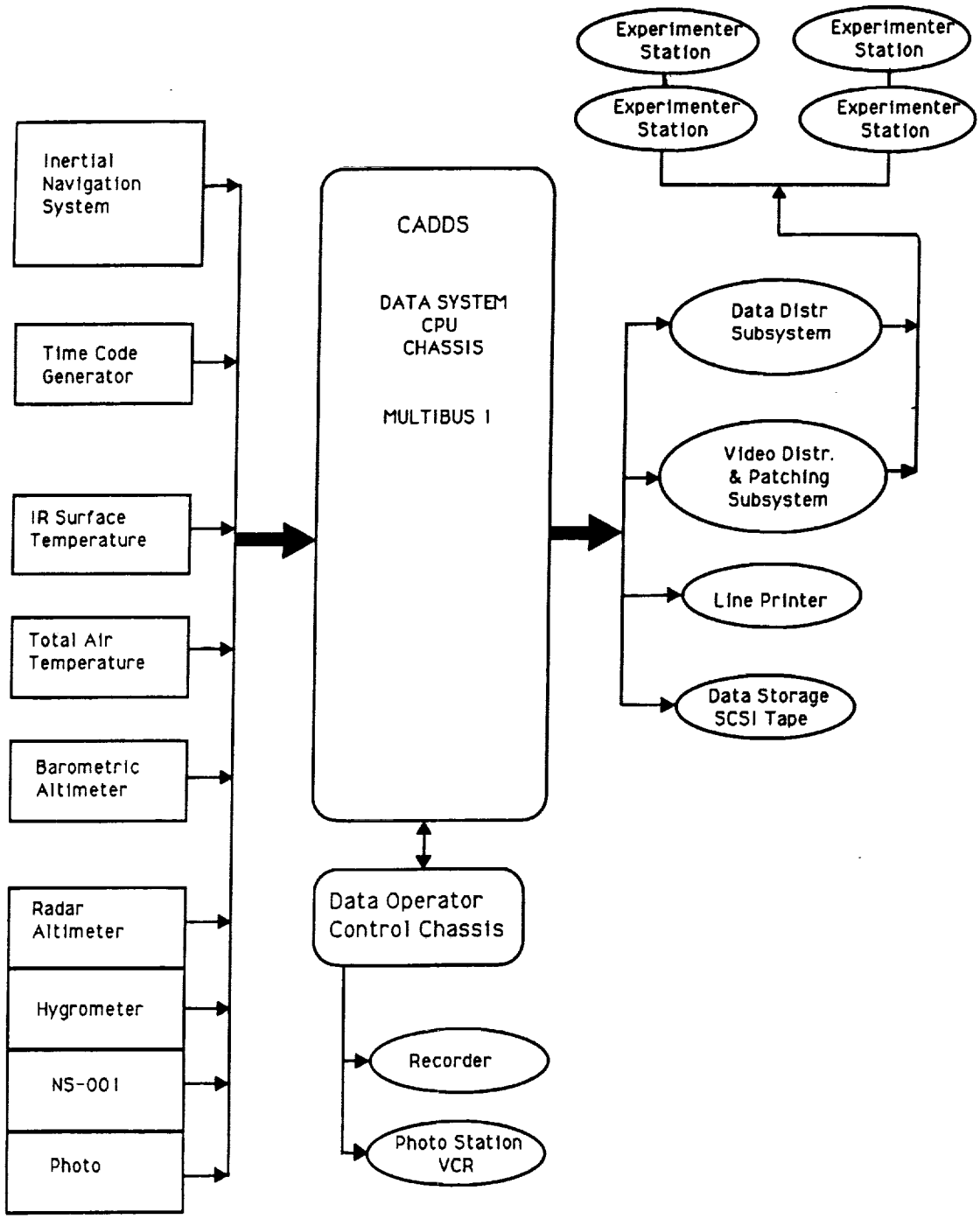

N91-25483 S38-43 20151 ABS ONLY

P1

Title: **The High Altitude Aircraft Program of NASA/Ames Research Center**

Authors: Gary Shelton, NASA/Ames Research Center
Bruce Coffland, NASA/Ames Research Center

NC473657

Discipline: **Multidisciplinary**

The High Altitude Missions Branch at NASA/Ames Research Center operates three high altitude ER-2 aircraft employed for Earth science research in support of NASA's Airborne Science and Applications Program. The ER-2s are used as readily deployable high altitude sensor platforms to collect remote sensing and *in situ* data on Earth resources, celestial phenomena, atmospheric dynamics, and oceanic processes. Additionally, these aircraft are used for electronic sensor research and development and satellite investigative support. The High Altitude Aircraft Program also supports scientific research sponsored by Federal agencies such as the U.S. Forest Service, the Environmental Protection Agency, the U.S. Fish and Wildlife Service, the Corps of Engineers, and the Geological Survey. State agencies, university researchers, and private industry investigators also are supported by the program. The aircraft support these scientific endeavors from deployment sites in Kansas, Texas, Virginia, Florida, and Alaska. Also, ER-2s have been used in cooperative international projects flown from deployment sites in Great Britain, Australia, Chile, and Norway.

omit

Title: SAR Imaging of Slicks in SAXON:CLT

Authors: Omar Shemdin, Ocean Research and Engineering
Dayalan Kasilingam, Ocean Research and Engineering

Discipline: Oceans

During the SAXON:CLT experiment in September, 1988, L-,C- and X-band SAR imaging systems aboard the NADC P-3 aircraft were used for imaging surface waves, internal waves, ship wakes and slicks. The objective of this experiment was to test the validity of the SAR imaging models at the different radar frequencies. Concurrent X-band RAR images were also obtained to compare the imaging processes. In this study, X-band SAR images are used to study the imaging of slicks. Images of the slicks are compared with their backscatter models. The backscatter models predict that the radar signatures of a slick for VV and HH polarizations may be utilized to estimate the thickness of the slick. The model shows that the images of slicks obtained in SAXON:CLT are consistent with their radar signatures. The polarimetric information shows that most of the slicks were very thin ($< 100\mu m$). However, examples of thicker slicks are also observed. Models are used to estimates the thickness of these slicks. Suggestions for the use of high frequency, SAR imaging systems for the detection and measurement of oil slicks are also given.

N91-25484
539-43
20152
p.2
NC999967
46651278

Title: The Remotely Piloted Vehicle as an Earth Science Research Aircraft

Authors: Dean S. Smith, University Research Foundation
Jack L. Bufton, NASA/Goddard Space Flight Center

Discipline: Multidisciplinary

Within the next two years NASA could be flying small scientific experiment payloads on remotely piloted vehicles (RPV) that are now becoming available through various military and industry development programs. A brief study was conducted at the Goddard Space Flight Center (GSFC) during winter 89/90 to identify existing RPV capabilities and to determine if the use of an RPV was advantageous and practical for Earth science investigations.

We conducted only an informal survey that was limited to the Earth Sciences Directorate at the GSFC due to time and budget constraints. The results of the survey were much larger and more enthusiastic that anticipated. A total of 17 instrument systems were identified that involved the following specific investigations or measurements:

(1) atmospheric studies - chemical sampling, boundary layer measurements, drop buoys, vertical profiles of temperature, pressure, moisture, and wind;
(2) crustal dynamics - laser ranging to retroreflectors
(3) ice studies - topographic profiles of Greenland and Antarctic ice sheets, and sea ice structure;
(4) ocean color monitoring;
(5) physical oceanography - wind and wave structure and dynamics;
(6) sensor calibration - visible and near-infrared spectrometer observations; and
(7) vegetation studies - polarization properties and bidirectional reflectance.

In assembling this list we found that RPVs were considered especially valuable for the dangerous missions, e.g. (1) flights through volcano plumes and hurricanes; (2) long duration profiles over inaccessible regions such as the Antarctic; and (3) very low altitude (≤ 50 m) ocean profiling missions.

Instruments for the proposed science missions were grouped by their needs for aircraft altitude, payload weight, and electrical power. There were 9 instruments proposed that weighed between 2 and 111 kg and were targeted for low-to-medium altitude (50 m to 6 km) missions; 4 instruments were very heavy (175 kg to 900 kg); and the remaining 4 instruments

required very high altitude (~ 10 km or above) and weighed between 4 kg and 22 kg. As expected, the power requirements were an increasing function of payload weight. There were 8 instruments that required less than 100 watts; 4 between 100 & 500 watts; and 4 over 1000 watts.

We also found that most payload concept sponsors required what amounted to approximately 1000 watts and 90 kg of basic flight hardware infrastructure to support their science mission. This infrastructure was selected from a list that included: autopilot with inertial reference; central flight guidance computer; digital avionics monitoring and control system; mission logic control unit; Global Positioning System receiver, aircraft nose camera television; satellite transceiver; video data recorder; atmospheric environment monitoring system; and the RPV command, control, tracking, and telemetry system.

Six separate RPV systems were investigated as practical carriers for our array of Earth science payloads. This list included one tethered aerostat and the following five aircraft: (1) the Developmental Sciences Corp. SKYEYE R4E-50; (2) the Litton Applied Technology Division Optionally Piloted Vehicle; (3) the Teledyne Ryan Aeronautical Model 324 SCARAB; (4) the Teledyne Ryan Aeronautical BQM-34A/S FIREBEE; and (5) the Boeing Corp. CONDOR. Detailed capabilities and performance specifications for these systems will be presented. From cost estimates provided by the respective manufacturers, it also became apparent that the initial investment will be on the order of at least $1 M for each RPV and a ground station cost of $1.25 M to $ 5 M for the launcher, tracking, control, and retrieval subsystems. The individual RPVs are, of course, reusable, but the mean time between failures and loss of the RPV is typically 50 missions. Thus, at present, the RPV technology does not appear to compete effectively with manned research aircraft on a dollar per flight hour basis. We believe, however, that the RPV may be a solution for extending the envelope of possible remote sensing missions and could become a valuable adjunct to the NASA Earth science aircraft program as costs come down with mass production and RPV reliability improves.

Omit TO P257

Title: Measurements of Electric Field using the Armored T-28 Aircraft

Authors: Paul L. Smith, South Dakota School of Mines and Technology
Andrew G. Detwiler, South Dakota School of Mines and Technology

Discipline: Atmosphere

The T-28 has been used for more than 20 years to penetrate mature convective storms. The primary purpose of these penetrations has generally been to make in situ measurements of microphysical and kinematic characteristics of storm interiors. Since 1986, steady progress has been made with measurements of static electric fields in and around electrified clouds.

Small, rotating-vane electric field mills can be embedded in the fuselage and wing tips. Each mill responds to a field component normal to its face. The most complete suite of instrumentation employed on the T-28 to date has been a set of four mills mounted as shown in Fig. 1. The symmetry of the arrangement shown allows unambiguous determination of the vertical and transverse field components, and also charge on the aircraft.

Reduction of the data from the four mills to obtain estimates of the ambient field is complicated by the fact that the aircraft distorts the ambient field. Several types of distortions typically arise. First, the conducting aircraft is polarized in any ambient field, and all field lines must be everywhere normal to its surface. This results in an apparent enhancement of the field. Further, the aircraft may become charged due to collisions with particles or may discharge clouds of ions from sharp edges or through the engine exhaust. These charges further distort the field near the aircraft.

Symmetric placement of the mills, as shown in Fig. 1, allows one to subtract the field components due to charge on the aircraft in a relatively straightforward manner, leaving a first estimate of the ambient static field. Charge on the aircraft can be estimated independently from the vertical and the wing-tip pairs. Placement of mills at the wing tips allows one estimate to be based on measurements taken well away from the engine exhaust plume, which may carry charge. Details are available in Dye et al. (1988) and in Jones (1990).

The enhancing effects of the airframe on the apparent field can be evaluated by placing the aircraft in a known field and comparing apparent to actual fields. This has been done with the T-28 by flying close formation flights under electrified clouds with another aircraft carrying

a well-calibrated field measuring system. The vertical field component enhancement factor determined from these intercomparisons is approximately 2.5 times the field sensed by the bottom mill. For the horizontal components sensed by the wing tip mills, the enhancement factor is approximately 20 times. The enhancement factor for the wing tip mills is higher because they are placed in surfaces of much greater curvature than the fuselage mills.

The T-28 has penetrated more than three dozen electrified clouds while carrying electric field mills. A variety of electrical and microphysical environments has been encountered. The effects of charge in the engine exhaust plume, and also of plumes of charge from corona discharge, on the measured field are still being evaluated using these data. These charge plumes affect mainly the apparent charge on the aircraft. They seem to have only a weak effect on the estimated ambient field, which is usually the primary information of interest.

An example of electric field measurements during successive penetrations of a growing electrified cloud is shown in Fig. 2. These penetrations were through a growing feeder cell near a thunderstorm over the western North Dakota plains and were made at ~ 5.5 km MSL where the temperature was about -12°C. There is an apparent correlation between the exponentially increasing concentration of ice particles and the linearly increasing magnitude of the vertical electric field at the penetration altitude.

The T-28 facility hopes to add soon the capability to carry a fifth field mill facing aft, allowing an estimate of the longitudinal field component, in addition to the vertical and transverse field components. This will greatly improve our ability to determine three-dimensional fields and the inferred charge distribution in electrified clouds. Such measurements are critical for understanding the interrelationships among cloud microphysical, dynamical and electrical evolution.

Acknowledgments. We thank Hugh Christian (NASA Marshall), Bill Winn and Dan Jones (New Mexico Institute of Mining and Technology), and John Helsdon (SDSM&T) for assistance in developing these measurement and data reduction techniques. In addition we thank Hugh Christian, Bill Winn and the NCAR Research Aviation Facility for generous loans of electric field mills. The T-28 facility is operated under Cooperative Agreement No. ATM-8620145 with the National Science Foundation.

References

Dye, J. E., J. J. Jones, A. J. Weinheimer and W. P. Winn, 1988: Observations within two regions of charge during initial thunderstorm electrification. Quart. J. Roy. Meteor. Soc., 114, 1271-1290.

Jones, J. J., 1990: Electric charge acquired by airplanes penetrating thunderstorms. J. Atmos. Ocean. Tech. [In press]

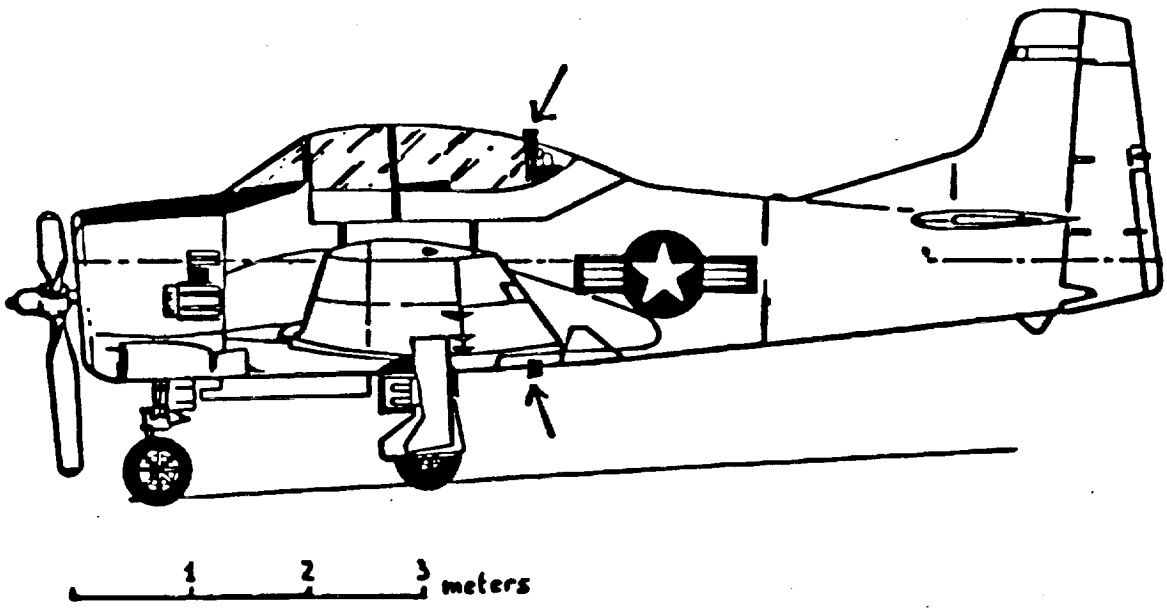

Fig. 1: The T-28 carries rotating-vane field mills mounted in its canopy and baggage bay door (arrows) and facing out from each wing tip.

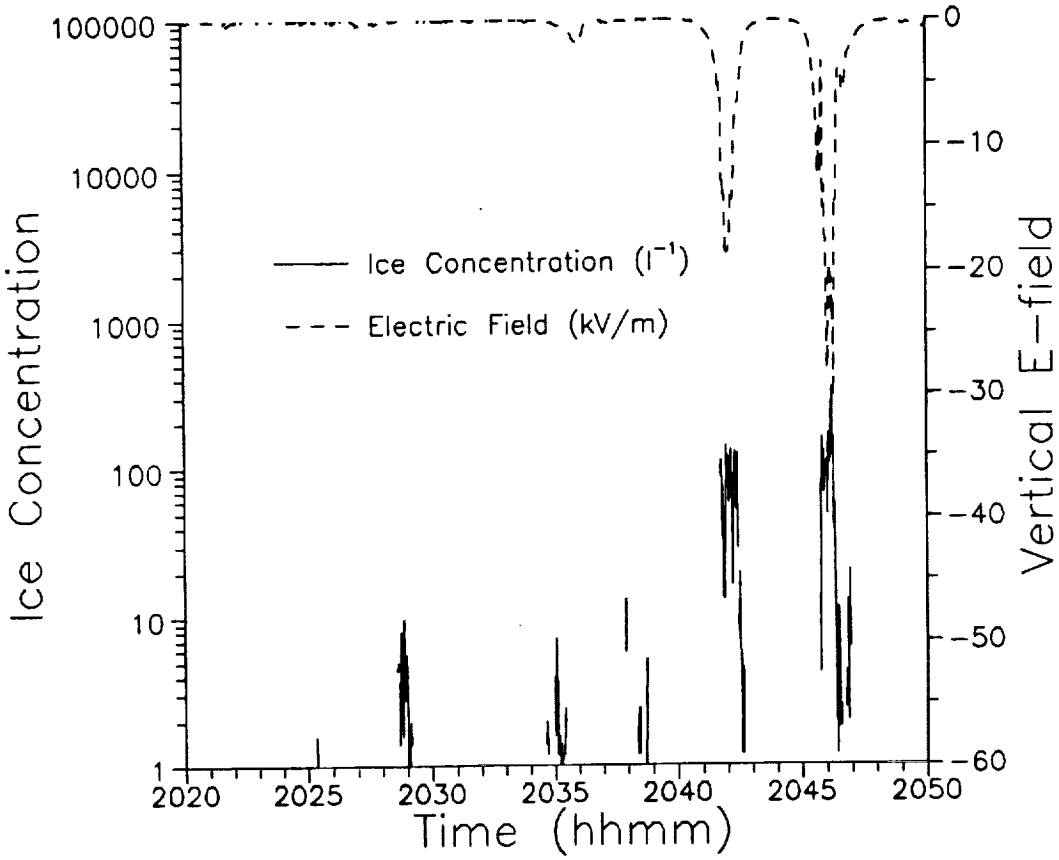

Fig. 2: Ice concentration and vertical electric field component are shown for six successive cloud penetrations. The ice concentration is increasing exponentially and the field linearly beginning around 20:35.

Title: Cloud and Trace Gas Remote Sensing with the High-Resolution Interferometer Sounder (HIS)

Authors: William L. Smith, University of Wisconsin, Madison
Steven A. Ackerman, University of Wisconsin, Madison
Hugh B. Howell, University of Wisconsin, Madison
Allen H.-L. Huang, University of Wisconsin, Madison
Robert O. Knuteson, University of Wisconsin, Madison
Henry E. Revercomb, University of Wisconsin, Madison
Harold M. Woolf, University of Wisconsin, Madison

Discipline: Atmosphere

Observations of the 0.27 cm^{-1} resolution High-resolution Interferometer Sounder (HIS) have been used to infer microphysical properties of cirrus and liquid water clouds. The HIS measurements have also been used to obtain trace gas profiles for the greenhouse gases ozone (O_3), methane (CH_4), and carbon monoxide (CO). These retrieved properties are in addition to the simultaneous retrieval of temperature and water vapor profiles in the atmosphere.

The poster contains four sections summarizing the HIS program at UW-Madison. These sections cover 1) a HIS instrument description and summary of past and future aircraft flights, 2) current geostationary satellite designs based on HIS aircraft experience, 3) analysis of HIS data with regard to retrieval of cloud properties and to extending temperature and water vapor sounding through semi-transparent clouds, and 4) the use of HIS data in source/sink case studies for trace gas retrieval.

The HIS instrument is a nadir viewing Michelson interferometer designed for operation within an aircraft pod under the NASA U2/ER2 high altitude research platform. The HIS has also been flown on the NOAA P3 Orion aircraft. The HIS measures a wide portion of the infrared spectrum, 3.7 to 16.6 μm, with a resolution of 0.275 - 0.5 cm^{-1} (unapodized) with high absolute accuracy (< 1°C). At this resolution, the significant line structure in the lower troposphere is adequately resolved revealing atmospheric absorption due to carbon dioxide, water vapor, and greenhouse gases as well as clear window channels for investigation of cloud emissivity and surface properties. Over forty aircraft flights were made in 1985-1986 over the east central U.S., Wisconsin, and Southern California.

The HIS has acted as a proof-of-concept of the interferometeric technique to facilitate the design of space-based sensors which will provide a dramatic improvement in the measurement of meteorological parameters over the current filter wheel radiometers. The current designs include a geostationary sounder for the NOAA operational satellite GOES as well as an enhanced research instrument design, including improved tropospheric trace gas sensing capabilities, for the NASA Earth Science Geostationary Platform (ESGP).

HIS data from the 1986 FIRE I cirrus cloud experiment has been used to obtain detailed spectroscopic information that reveal information on cloud height, emissivity, transmittance, and reflectance. Using models of cloud particle distributions, classification schemes have been developed that allow HIS data to be used to identify likely cloud microphysical properties, such as particle size and shape. Examples of coincident airborne lidar measurements will be shown along with a comparison of observed ice particle and liquid water droplet emissivities. Advances in the ability to extend infrared sounding capability of temperature and water vapor into and below semi-transparent ice and water clouds will also be demonstrated.

Trace gas profile information is contained in the HIS spectrum which contains infrared absorption features of ozone, methane, and carbon monoxide as well as the more long-lived nitrous oxide and CFC/CCl_4. The retrieval of these gas vertical concentrations in the troposphere and lower stratosphere has been the focus of ongoing activity at CIMSS. The results of the retrieval analyses will be presented using actual HIS data taken from the NASA high altitude platform in 1986. The poster will show the correlation of retrieved gas parameters with underlying possible sources and sinks using land use and land cover information obtained from the U.S. Geological Survey.

N91-25485

Title: Remote Sensing of the Seasonal Variation of Coniferous Forest Structure and Function

Authors: Michael Spanner, NASA/Ames Research Center
Richard Waring, Oregon State University

Discipline: Land

One of the objectives of the Oregon Transect Ecosystem Research (OTTER) project is the remotely sensed determination of the seasonal variation of leaf area index (LAI) and absorbed photosynthetically active radiation (APAR). These measurements are required for input to a forest ecosystem model which predicts net primary production, evapotranspiration and photosynthesis of coniferous forests. The OTTER study area includes six coniferous forest stands along an east-west trending temperature and moisture gradient across western Oregon. Remotely sensed determinations of LAI and APAR will be made from Thematic Mapper Simulator (TMS) data acquired from a Daedalus scanner onboard a NASA ER-2 high altitude aircraft collected during a Multi-sensor Aircraft Campaign in support of the OTTER project.

The TMS data were acquired for the OTTER project during four time periods in 1990. The time periods were in March (pre-budbreak conditions), June (maximum LAI and understory), August (maximum LAI, understory senescence) and October (reduced LAI). Field measurements of leaf area index and absorbed photosynthetically active radiation were made at each of the six sites during the four time periods. Measurements of LAI were made using allometric equations relating diameter at breast height and sapwood basal area to leaf area index for each of the forest stands. The seasonal variation of LAI, and the APAR for each stand was calculated using ceptometer measurements of the amount of incoming photosynthetically active radiation and absorbed radiation under the forest canopy during the four time periods.

Field spectral measurements were made of the understory at some of the sites using a Spectron 590 spectroradiometer and a Barnes Modular Multiband Radiometer. A low altitude ultralight aircraft obtained Spectron and Barnes measurements of the coniferous forest canopy during the four time periods at most of the sites. These measurements will be used to help interpret the soil and vegetation background contribution to the TMS data. Measurements of atmospheric optical properties were made at the study sites concurrent with the four TMS data acquisitions. These measurements were made with two ground based Sunphotometers, allowing a determination of the aerosol optical depths. Atmospheric correction of the TMS data will be performed using a radiative

transfer model from measurements obtained by the Sunphotometers at each of the OTTER study sites.

Relationships will be determined between single channels of TMS data and LAI and APAR, as well as relationships between TMS near infrared/red radiance and LAI and APAR. Previous relationships developed between near infrared/red radiance and LAI will be used to estimate LAI for the OTTER study sites. Seasonal variability of LAI and APAR will be analyzed with respect to the seasonally acquired TMS data. The Sail canopy model will be used to help understand the relationships between LAI, APAR and TMS data. Preliminary analysis indicates that the TMS data are of high quality. The TMS was calibrated just before or just after each flight. Analysis of the Sunphotometer data indicates that there was considerable variability in aerosol optical depths both between time periods and between sites during the data acquisition periods (Figure 1). The August data had very high optical depths, resulting from field burning near some of the sites. Sunphotometer data acquired during March and June show very clear atmospheric conditions. These early results highlight the necessity for measurement of atmospheric optical properties concurrent with remotely sensed data acquisition, particularly when analyzing remotely sensed data acquired from different locations at different times.

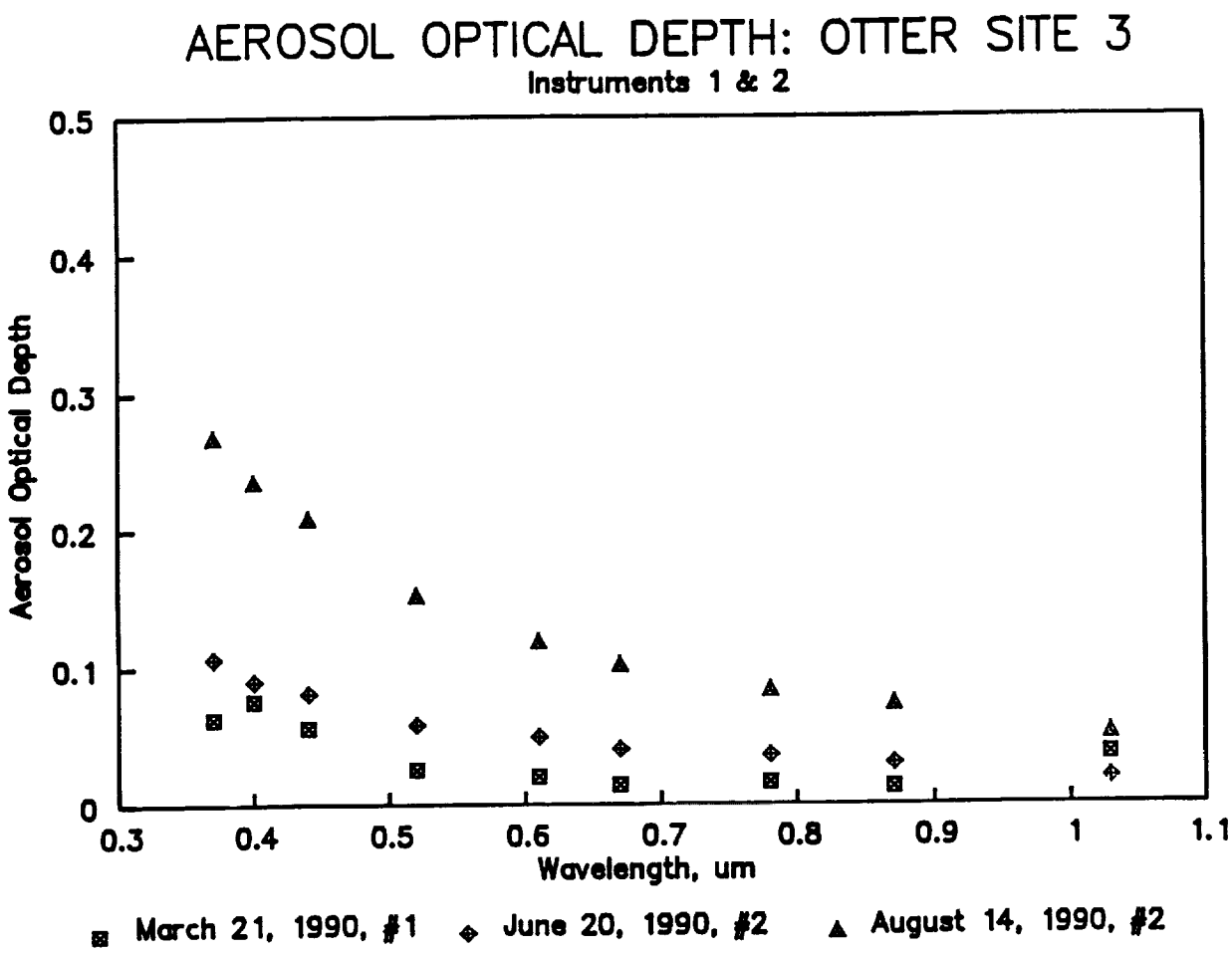

Figure 1. Aerosol optical depths measured at OTTER site 3 in the Cascades Mountain Range in March, June and August concurrent with the ER-2 overflight.

N91-25486

Title: **Visible and Near Infrared Observation on the Global Aerosol Backscatter Experiment (GLOBE)**

Authors: James D. Spinhirne, NASA/Goddard Space Flight Center
John F. Cavanaugh, NASA/Goddard Space Flight Center
S. Chudamani, Science Applications International Corporation
Jack L. Bufton, NASA/Goddard Space Flight Center
Robert J. Sullivan, NASA/Goddard Space Flight Center

Discipline: **Atmosphere**

The Global Aerosol Backscatter Experiment (GLOBE) was intended to provide data on prevailing values of atmospheric backscatter cross-section. The primary intent was predicting the performance of spaceborne lidar systems, most notably the Laser Atmospheric Wind Sounder (LAWS) for EOS. A second and related goal was to understand the source and characteristics of atmospheric aerosol particles. For remote ocean locations, and the Southern hemisphere in general, a significant lack of knowledge exists. The major components of the experiment were flight surveys throughout the Pacific region by the NASA DC-8 aircraft. A Goddard Space Flight Center lidar system was operated on the missions to obtain aerosol backscatter cross-section at the fundamental and doubled Nd:YAG laser wavelengths of 1.064 and 0.532 μm and, in addition, at a wavelength of 1.54 μm which was generated by Raman shifted down conversion of the 1.064 μm radiation. The system was the first operational lidar at the one-and-a-half micron wavelength region. Advantages of one-and-a-half micron lidar is eye safe operation and increased sensitivity to aerosol characteristics. An important factor of the visible/near infrared backscatter measurements is accurate calibration. A new scattering cross-section calibration technique based on hard target laser measurements was developed for the experiment. In this paper, we will present details of the instrument design and aircraft operations and also discuss initial results.

The lidar instrument was integrated on the NASA DC-8 to operate through nadir and zenith windows. A 50 Hz PRF Nd:YAG laser was the basic transmitter. The 1.54 μm transmitted pulse was generated by Raman shifted down conversion of the 1.064 μm radiation by transmitting the 1.064 μm pulse through a Raman cell containing 300 psi of methane gas. The cell converted approximately 15% of a 200 mJ pulse to 1.54 μm energy. The longer wavelengths were combined with the 0.532 μm pulse, and all three wavelengths were transmitted co-axial to the receiver telescope. In order to obtain the calibrated backscatter cross-section measurement, a critical component of the system was an accurate pulse energy monitor. In the design that was used, a polarization insensitive flat directed a small fraction of the transmitted pulse energies into an integrating sphere, and fiber optics carried signals to filters and pulse integrators. In order to maintain stability, the energy monitor filters and detectors were temperature-controlled. The receiver filters and detectors

were also temperature-controlled. All detectors were solid state. The receiver telescope was designed to be rotated in order that observations could be acquired in either the nadir or zenith direction. Signals were digitized by a CAMAC data system and recorded on optical disks.

The GLOBE flights were carried out in November 1989 and May-June 1990. The region of the central and eastern Pacific was traversed by the NASA DC-8 at an altitude range of roughly 8 to 10 km. Latitudes from approximately 70°N to 70°S were covered. In addition to point-to-point traverse flights, there were local missions where flight lines at different altitudes were flown at a single location. On the local flights, lidar measurements from different heights could be intercompared. Also, the lidar backscatter measurements could be intercompared to the complement of *in situ* particle probe measurements that were included on the DC-8 mission. A number of intercomparisons to ground-based lidar and measurements by other aerosol sampling aircraft were also carried out during the missions.

The overall analysis of results from the GLOBE missions is not yet completed, but initial results can be discussed. In general, there were three vertical regions observed: the mixed boundary layer, a cloud-pumped layer, and the free troposphere. Aerosol scattering varies by over four orders of magnitude, and cross-sections in the mixed and cloud-pumped layer are typically several orders of magnitude above that for the free troposphere. The upper troposphere is generally very free of aerosol scattering. However, areas of increased aerosol concentration are found. It may be generally stated that the upper troposphere aerosol scattering cross-section was low in the Southern hemisphere for the May-June flights and low for the Northern hemisphere for the November flights. The initial results indicate that the instrumentation and calibration techniques applied for the near IR lidar measurements were successful.

From the GLOBE flights, extensive data have been obtained on the structure of clouds and the marine planetary boundary layer. A notable result for all observations is the consistency of the large increases in aerosol scattering ratio for the marine boundary layer. Large increases in scattering ratio at the boundary layer, as mentioned above, were found in most all cases. Another interesting aspect of the lidar cloud observations over the Pacific, at least for the November data, was the frequency of low cloud density. For a large fraction of the cloud observations, lidar return signals were obtained through extended layers. Large areas of clouds with observed vertical structure from 4 to 8 km thick were under and over flown. The potential for extended signal returns through clouds is a possibly significant factor for laser wind measurements.

Title: A Four Aircraft Intercomparison of Air Chemistry Measurements

Authors: J.W. Strapp, Atmospheric Environment Service (Canada)
W.R. Leaitch, Atmospheric Environment Service (Canada)
H.A. Wiebe, Atmospheric Environment Service (Canada)
K.G. Anlauf, Atmospheric Environment Service (Canada)
J.W. Bottenheim, Atmospheric Environment Service (Canada)
K. Puckett, Atmospheric Environment Service (Canada)
G.A. Isaac, Atmospheric Environment Service (Canada)
C.W. Spicer, Battelle Memorial Institute
T. Kelly, Battelle Memorial Institute
J. Hubbe, Battelle Memorial Institute
N. Laulainen, Battelle Memorial Institute
F. Slemr, Fraunhofer-Institute
J. Werhahn, Fraunhofer-Institute
H. Giehl, Fraunhofer-Institute

omit TO
p285

Discipline: Atmosphere

During the summer of 1988, the Atmospheric Environment Service (AES) of Environment Canada organized and conducted an extensive field program to make air and cloud chemistry measurements to support the evaluation of the Canadian Acidic Deposition and Oxidant Model (ADOM). A Twin Otter (TO) aircraft owned and operated by the National Aeronautical Establishment, and a DC-3 (DC3) owned and operated by the Innotech Aviation were instrumented for this project. A second independent project overlapped the Canadian experiment, collecting a similar data set in the US to evaluate the Regional Acidic Deposition Model (RADM). A Gulfstream G-1 (G1) aircraft owned and operated by Battelle, a Hawker Siddeley jet (HS) operated by the Fraunhofer Institute, and a Beechcraft King Air (KA) owned and operated by NOAA, were instrumented for this project. Planning and strategy were shared between the two experiments, but each group utilized its own traditional instrumentation and analysis procedures.

In order to ensure that the sophisticated and costly data sets being collected by each group were consistent, an intercomparison of 4 aircraft was conducted on 27 August in the Canadian project area (the KA was unfortunately unavailable). The purpose of this paper is to examine the comparability of air composition and related measurements from these 4 aircraft which possess highly variable speed ranges, different instrumentation, and are calibrated and analyzed by different groups using different procedures. The problems of comparisons in an evolving airmass are detailed.

The aircraft (see Table 1) were flown at their normal operating speeds, to ensure that comparisons were relevant to the typical use of the aircraft. Consequently, only the TO and the DC3 were flown in wing to wing formation. The pattern chosen was a compromise between air traffic and safety considerations, and the desire to obtain comparable measurements. A racetrack pattern around two surface monitoring stations ~ 120 km apart was lapped once by each aircraft at 0.6 km MSL and once at 1.1 km MSL (the TO due to short endurance performed only the 0.6 km leg). A filter was exposed by each aircraft at each altitude . In addition, each aircraft descended from 3 km in a spiral over the intensive surface monitoring site at one end of the racetrack (Egbert) , enabling some comparisons with surface measurements. The HS departed first, followed 15 minutes later by the slower DC3 and TO in formation, followed 30 minutes later by the G1. In retrospect, it would have been preferable to have the G1 and HS in formation for at least part of the flight, since there are no direct comparisons with the HS. The comparisons were made on a sunny day with low to moderate pollution levels. The boundary layer was reasonably well mixed to about 2.7 km MSL, although separate NO_y and SO_2 plumes reappeared at opposite ends of each leg. Due to the transient nature of these plumes, the leg average values quoted below and contained in Table 4 exclude most of the plume portions of the each leg.

Comparisons:

The results of the filter exposures along the racetrack patterns at 2 altitudes are given in Table 2. All particulate $SO_4^=$ and NH_4^+ values are within ~30% between the DC3, TO, and the HS, indicating fairly well mixed boundary layer and good comparability between the 3 aircraft. The small difference between the TO and the DC3 in close formation is within the < 7% difference in the DC3 duplicates. The higher HS $SO_4^=$ values at both altitudes may be due to a temporal variation in the airmass, or may indicate a laboratory or flow rate bias. The most striking difference in the aerosol is observed in the G1 data, which are consistently lower in $SO_4^=$ and higher in NO_3 than the other aircraft by up to a factor of 6, and whose duplicate samples vary by more than a factor of 3 at the lower altitude. This difference has since been attributed to an extraction problem, and there are some hopes that re-extraction will result in an improved G1 data set. HNO_3 comparisons display a different pattern. The G1 and HS values agree favourably, but are lower than the TO and DC3 values by up to a factor of 2 at the lower altitude. Precision on both the DC3 and G1 duplicate samples is high. These factors may indicate a laboratory bias, or that measurement is sensitive to the slightly different sampling systems on the different aircraft.

Results of hydrocarbon analysis for the four aircraft by three different labs and three different sampling techniques are given in Table 3. An unexpectedly high level of agreement is observed between aircraft for most compounds, although there is some indication of toluene contamination in the TO data. The Canadian data are consistently higher than the G1 and HS data, perhaps indicative of a laboratory induced difference. Also notable is that although the TO, DC3 and HS are grab samples over the end points of the legs, the G1 data are continuous collections; the degree of agreement would imply that hydrocarbons are quite evenly distributed at this altitude.

The aircraft had a varying array of instruments to measure a subset of NO_y, NO_x, and NO, and all measured NO_2. HS instruments were modified to operate at a constant pressure of 60 KPa. The NO_2 time trace of leg 2 (Fig. 1b) is typical of the four legs. The HS values are consistently higher than the other aircraft by almost a factor of 2. The TO, DC3 and G1 agree within 20% for legs 2, 3 and 4. The only NO_x comparisons between the TO and DC3 are reasonable, with the DC3 higher on legs 1 and 2 by 28% and 34% respectively. There are no NO comparisons. Using leg 2 as an example, the sum of NO and NO_2 is not too far off the NO_x values. The HNO_3 (filter) + PAN + NO_x values (plumes included) exceed the G1 NO_y values by a small amount, and probably indicate a small error in measurement of NO_y or one of its component species.

PAN comparisons are made only between the G1 and the DC3. The HS instrument did not provide data, and the analysis from the TO's Luminol instrument has not yet been completed. Both aircraft show values decreasing from ~1 ppb at Egbert to ~0.6 ppb at Dorset (see fig 1c), and on legs 3 and 4, which are the closest in time for the two aircraft, the leg average values are within 13% and 24% respectively (Table 4).

O_3 comparisons were surprisingly poor. The time trace of Fig 1d is typical, with average G1 and TO values agreeing very well (<1% or ~0.5 ppb), the DC3 values ~ 11% or 7 ppb lower, and the HS 26% or 15 ppb lower than the G1/TO (Table 4). Comparisons of vertical profiles of the 4 aircraft, O_3 sonde, and surface O_3 data over Egbert (not shown) indicate that the DC3 O_3 monitor needs to be pressure corrected, although this effect could not explain the entire difference with G1/TO values. They also imply a sonde/G1/TO/DC3 (corrected) agreement to within ~10%. The HS discrepancy, evident on other early HS/G1/KA intercomparisons, was rectified shortly after this intercomparison, and very good HS/G1/KA agreement was subsequently observed.

SO_2 comparisons of the TO and DC3 in formation using the same type of instrument are excellent (figure 1e), as are the G1 comparisons outside the plume. Run average values outside the plume (Table 4) are within 35% for all legs, and are within 10% for the legs (2 and 3) most close in time. On leg 3, the DC3/G1 time traces are nearly identical, even in the plume peak of ~ 9 ppb. The HS SO_2 instrument did not provide data.

H_2O_2 comparisons for the three identical H_2O_2 gas phase monitors are somewhat sparce. The TO and DC3 formation legs 1 and 2 exhibit good agreement (leg averages within 13%, see figs 1f and Table 4), although each leg has incomplete data due to in-flight calibrations. The HS monitor was inoperative. Direct G1 comparison is possible only with the DC3/leg 4, which indicates a somewhat different time trace but a run average agreement within 11%.

In conclusion, many large projects supplying data to the research community have not had the benefits of such intercomparisons. This study demonstrates the large differences that can be present in aircraft chemistry data sets, and the resulting difficulty for example in analysis of regional differences between different data sets. The study also demonstrates the usefulness of intercomparisons in refining and correcting data bases.

Figures 1a-1f. Time histories of trace gas concentrations during the second leg of racetrack pattern between Egbert and Dorset, Ontario, at 0.6 km MSL.

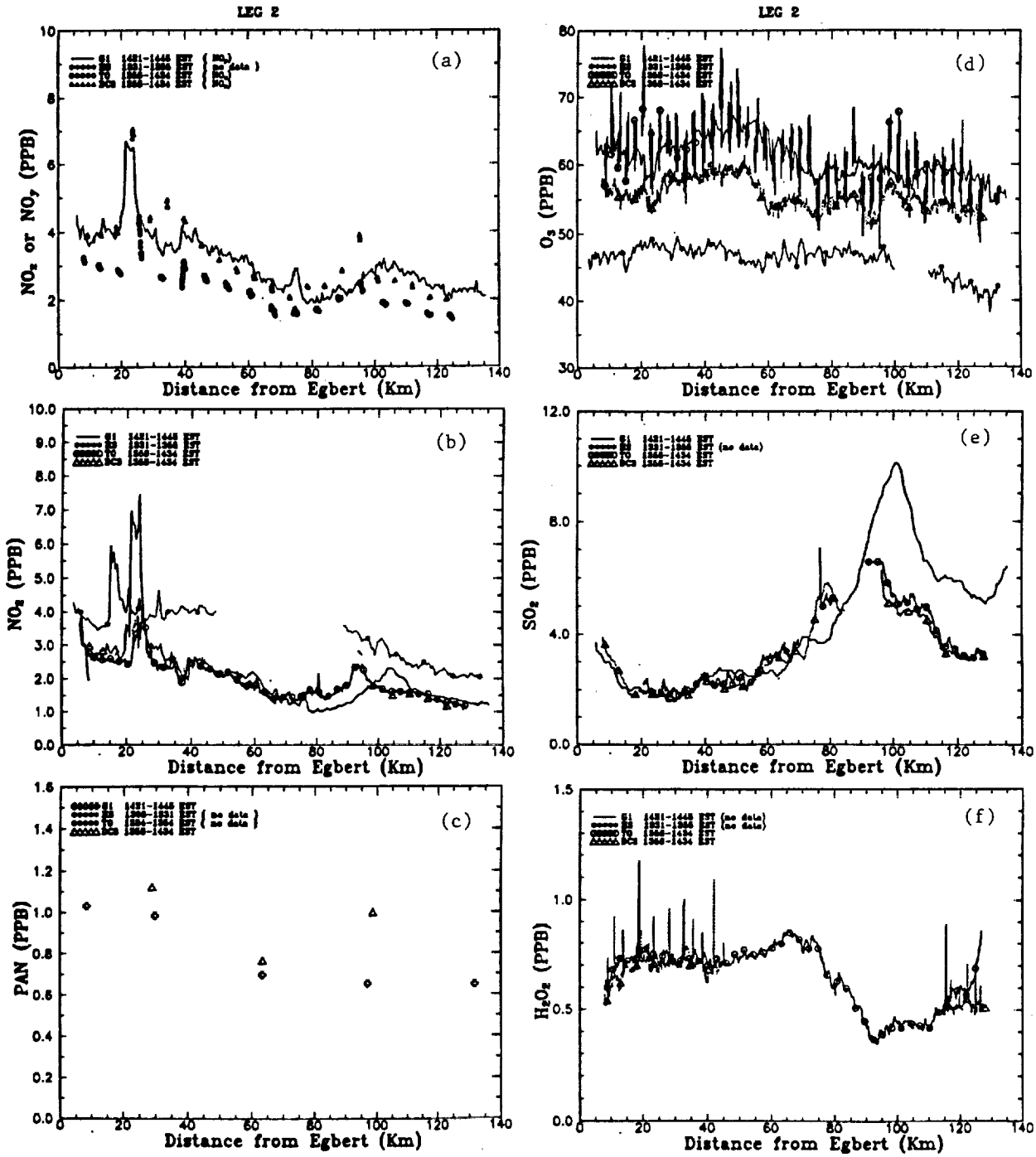

Table 1. List of instruments operated on the 4 aircraft.

Measurement	G1	HS	TO	DC3
$SO_4^=$, NO_3^-, NH_4^+	1st stage of filter pack, teflon	same as G1	1st stage of filter pack, Whatman 41	same as TO
HNO_3	2nd stage of filter pack, nylon	2nd stage of filter pack, NaF impregnated	2nd stage of filter pack, nylon	same as TO
NH_3	3rd stage of filter pack, phosphoric acid impregnated	3rd stage of filter pack, H_3PO_4 impregnated	3rd stage of filter pack, citric acid impregnated	same as TO
NO_y	Battelle analyzer, chemiluminescence with molybdenum converter	n/a	n/a	n/a
NO_x	n/a	n/a	Luminol LMA-3, with CrO_3 converter	same as TO
NO_2	Luminol LMA-3	same as G1	same as G1	same as G1
PAN	GC, electron capture	n/a	Luminol LMA-3 and gas column, data not available yet	GC (same as G1)
O_3	TECO 49	Dasibi 1008 PC	Luminol LMA-3 modified, using EOSIN-Y dye	Monitor Labs 8410
SO_2	TECO 43S	same as G1	same as G1	same as G1
H_2O_2	flourometric- enzyme	n/a	same as G1	same as G1

Table 2. Comparison of filter pack data at two altitudes from the 4 aircraft. Duplicate samples for the G1 and DC3 appear in parentheses.

Aircraft	Alt. (Km)	Time (EST)	$SO_4^=$ µg/m³	NO_3^- µg/m³	NH_4^+ µg/m³	NH_3 µg/m³	HNO_3 PPB
G1	0.6	1359-1445	2.18	2.39	0.90	n/a	1.32
			(0.66)	(0.97)	(0.13)	n/a	(1.24)
HS	0.6	1307-1354	4.22	< 0.73	1.56	< 0.79	1.24
TO	0.6	1323-1433	3.82	0.55	1.40	0.25	2.78
DC	0.6	1323-1433	3.74	< 0.10	1.50	< 0.10	2.03
						(< 0.10)	(2.04)
G1	1.1	1451-1536	1.26	2.39	0.23	n/a	1.65
			(0.93)	(1.07)	(0.34)	n/a	(1.39)
HS	1.1	1358-1443	4.84	< 0.76	1.82	< 0.82	1.53
DC	1.1	1438-1549	3.84	< 0.10	1.51	< 0.10	1.68
			(3.58)	(< 0.10)	(1.43)	(< 0.10)	(1.87)

Table 3. Comparison of VOC data from the 4 aircraft at 0.6 Km MSL. HS/DC3/TO are averages of grab samples at opposite ends of legs. G1 is composite sample over legs 1 and 2.

Compound	G1 (ppt)	HS (ppt)	TO (ppt)	DC3 (ppt)	Δ %
C_2H_4	1709	1700	2222	2230	28
C_2H_2	602	685	727	783	26
C_2H_6	669	773	829	864	25
iC_4H_{10}	221	255	293	307	33
nC_4H_{10}	540	592	663	685	24
nC_5H_{12}	177	164	234	229	35
isoprene	30	40	55	64	72
nC_6H_{14}	63	-	91	122	64
benzene	153	233	-	309	67
toluene	217	237	1512	379	54[1]

[1] excluding TO data

Table 4. Leg average concentrations for the 4 aircraft, excluding data from plumes at ends of each leg.

Leg	AC	Time (EST)	Alt (Km)	Temp (C)	T_d (C)	NO_x (PPB)	NO_y (PPB)	NO_2 (PPB)	NO (PPB)	PAN (PPB)	O_3 (PPB)	SO_2 (PPB)	H_2O_2 (PPB)
1	G1	1401-1408	0.6	19.4	11.6			1.63		0.87	60.8	2.08	
1	HS	1310-1317		18.1	11.4			3.77	0.70		42.9		
1	TO	1327-1337		17.6			2.97	2.20 (2.13)			56.9	2.77	0.72
1	DC3	1327-1337		16.8	10.1		3.80	2.42		0.69	54.5	2.56	0.64
2	G1	1432-1441	0.6	19.8	11.8	3.33		2.17		0.84	63.3	2.57	
2	HS	1341-1351		18.3	11.8			4.01	0.66		47.2		
2	TO	1413-1428		18.0	8.9		2.49	2.03 (1.72)			63.8	2.53	0.76
2	DC3	1413-1428		17.5	10.2		3.34	2.16		0.94	56.9	2.47	0.71
3	G1	1451-1504	1.1	15.7	9.9	3.16		1.49		0.79	60.3	2.45	0.68
3	HS	1400-1414		14.0	9.8			2.51	0.43		45.8		
3	DC3	1443-1504		12.9	8.2		2.22	1.25		0.89	51.1	2.28	0.82
4	G1	1515-1527	1.1	15.8	10.2	3.03		1.46		0.76	62.2	2.15	0.57
4	HS	1425-1436		14.2	9.85			2.77	0.52		49.7		
4	DC3	1521-1540		13.1	8.4		2.09	1.25		0.94	53.1	2.08	0.63

Title: Airship Support Services for Airborne Geoscience Applications

Author: John A. Taylor, Lighter Than Air Technologies

Discipline: Air Vehicles

A number of geoscientists are currently making use of airships as airborne data collection platforms. The airship offers advantages over both fixed-wing aircraft and helicopters in a number of geoscience applications. Principally, it is able to operate at a much lower speed than fixed-wing aircraft; it does not disturb the water surface or generate noise pollution as does a helicopter; on station, it is extremely stable in position and attitude; it offers very low airframe vibration levels for sensors, and a comfortable, non-fatiguing working environment for long missions; it readily accepts non-aerodynamic protruberances and all manner of external attachments including winches; it is ideal for the deployment and recovery of free-floating sensors and swimmers; and it generally offers considerably lower hourly operating costs than conventional aircraft or helicopters.

The airship comprises a helium-filled envelope, a car or "gondola", a flying control system and a propulsion system. Unlike a fixed-wing aircraft or helicopter which depends ultimately on propulsive power to generate lift, an airship derives the bulk of its lift from the buoyancy of its helium. For a number of reasons, an airship is normally flown slightly "heavy", where the vehicle gross weight slightly exceeds the buoyancy, the difference being made up by flying the ship as an aerodynamic lifting body at a small angle of incidence. The propulsion system provides the forward flight capability, and in certain models of airship, a thrust vectoring capability.

Vectored thrust airships can sustain a hover in zero wind using thrust vectoring, but at the expense of fuel consumption, water surface disturbance if operating at low level, and considerably increased airship structural weight and cost. Conventional (non-vectored thrust) airships have to maintain some small airspeed when operated "heavy", but can still maintain static position in a wind of 10kt or so. It is quite normal to operate airships as low as 100 ft above the sea surface for a period of hours. The airship also has the option to dump water ballast, achieve "equilibrium", cut propulsive power and fly in a neutral buoyancy state known as "free ballooning", in which the ship drifts with the wind. This condition uniquely enables an airship to travel, again for a period of hours, within a defined packet of air in a completely non-polluting mode. At the completion of the experiment, the pilot may then pick up sea water ballast for the flight home. An airship may typically cruise to and between its mission stations at 30-50 kt, and be able to loiter or maintain station for up to 8-12 hours.

Lighter Than Air Technologies has teamed with US-LTA Incorporated to offer the US-LTA 138S airship to the scientific community. The 138S is a conventional (non-vectoring thrust) airship offering a mission payload (including onboard scientists but exclusive of flight crew and fuel) of 1,500 to 2,500 lb depending on mission. Available endurance for a station-keeping

exercise is 12-16 hours, reducing to 5 hours endurance at max cruise speed. Missions can be undertaken up to 100 miles or so off-shore. The ship utilizes single flight crew operation, and offers up to five seats or the capability to install any configuration of seating, consoles or personal computers, electronics racking, air or marine sample storage, etc., based on the standard aircraft seat-track mounting system. The bulk of an airship's operating cost is related to fixed costs, the direct hourly cost being quite low. Costs for the 138S fall within the range of $1,500 per flight hour, down to $7,000 per day for unlimited flight hours on a multi-day program.

The 138S car is based on a tubular steel structure. This provides the opportunity to offer customized external sensor mountings on one or both sides of the car, which can in general be based on an in-house universal mounting truss, thus offering minimum cost and time for system integration and removal. The universal mount will be able to accept cameras, infrared/TV sensors, etc., with the ability to extend the sensors below the car during operation and retract them vertically alongside the car for take-off and landing, or for in-flight servicing such as lens cleaning or film changing, with accessibility via sliding windows in the car. The 138S is also equipped with a ground handling rail which runs around the the sides and front of the base of the car. Small cameras or instruments which do not in-flight access can simply be clamped to the rail.

A number of winch options will be available, again as standard in-house units which can be installed as required. The three primary forms of winch will be a sample-collecting and sensor-deploying winch accessible through the car window, a door winch for the deployment and recovery of surface sensors or larger samples, and a man-rated door winch for the deployment and recovery of swimmers.

The airship hull form offers ideal locations for antennas and small sensors, which can be strapped or patched to, or suspended from or positioned within the envelope. Examples would include UHF/VHF blades or whips, horizontally or vertically polarized dipoles, trailed HF, satellite communications dishes, microwave and GPS. The helium envelope is 158 ft long and 42 ft in diameter; the size offers ample opportunity to separate electromagnetically sensitive items. Once any internal cabling is installed, the antennas can be readily installed or removed whenever a project is flown. In many cases, because of the low speed characteristics of the airship, cables can be easily slung or attached on the exterior of the envelope. Small antennas, such as microwave for surface-air data transfer, can be clamped on the ground handling rail.

To assist the rapid installation and removal of project equipment, standard plug-in electrical power outlets will be available in the car, including 28V DC, 115V 60Hz single phase and 115V 400Hz 3-phase. The 115V 60Hz supply will be compatible with domestic/commercial personal computer requirements.

Figure 1 shows the US-LTA 138S airship. The opportunities for external antenna and small instrument mounting will be apparent from the photograph. Figure 2 shows an elevation of the car, and figure 3 the basic floor plan. Seating shown in figure 3 can be removed and replaced with any seat-track mountable equipment or storage configurations.

Figure 1

US-LTA 138S Airship

Antennas and small instruments may be attached anywhere on the envelope

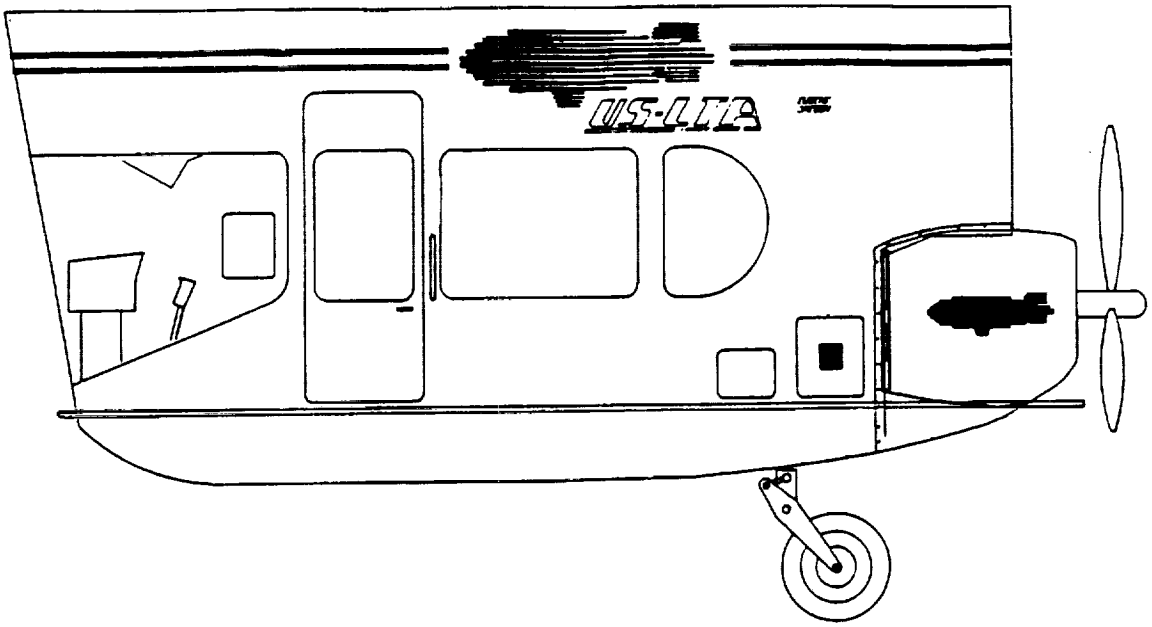

Figure 2

Airship Car Elevation

Equipment mounts and winches may be attached to the car exterior

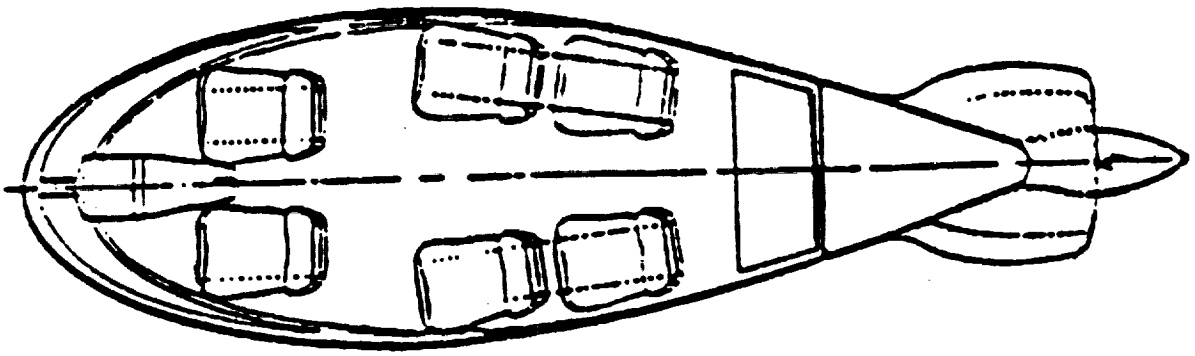

Figure 3

Basic Floor Plan

Seats may be replaced with any configuration of seat-track mountable equipment

Title: Airborne Observations of the Inhomogeneous Marine Boundary Layer in a Coastal Region

Author: Michael Tjernström, Uppsala University

Discipline: Atmosphere

The study of planetary boundary layer (PBL) properties in coastal areas is motivated by several factors. In Sweden, many major cities are situated along the coast and along with the population comes numerous industries that release pollutants whose dispersion in the PBL is strongly dependent on the local PBL conditions. It has also been suggested that wind energy station should be based off shore in some such areas both to increase the available power through the higher wind speed and to increase their lifetime due to the expected lower turbulence levels that is expected over a smoother surface. From a modelling point of view, water surfaces are often regarded as a simplification. The surface temperature is measured at one or a few points and the lower boundary values in the model is prescribed to be constant in time and often in space. There are also numerous field experiments to study internal boundary layer where towers are erected at the shoreline to sample the "undisturbed homogeneous upstream conditions". It is thus well motivated determine how homogeneous and undisturbed the coastal marine PBL actually is.

The department of Meteorology, Uppsala University, thus carried out a field experiment with this purpose in the south-east of Sweden during the end of May and beginning of June, 1989. The land area here is relatively rough, forested with coniferous forests. The coastline is located in an approximately east-.west direction for a substantial distance and turns almost 90° north at the far east end (see Fig. 1). Most of the measurements were carried out in the are where the coastline changes direction abruptly. Parts of the coastline also consists of a small archipelago. During this time of the year, land surfaces are often heated during daytime while the Baltic sea is still relatively cold (typically 12-15°C) and temperature contrasts of 5-15 °C (surface temperature) often forms. The experimental equipment consisted of a ground station and an aircraft equipped for PBL measurements. The ground station was located at a small island facing the Baltic sea in a wide sector and equipped with a 30m tower instrumented with profile and turbulence sensors. Radiosoundings were also carried out here. The aircraft is a Sabreliner 40A equipped with a so called "radome-system" for wind measurements. Also measured is air temperature, humidity, cloud water, surface temperature and radiation. The system has been carefully calibrated and tested against independent tower based turbulence instruments and is described in detail in Tjernström and Friehe (1990).

A total of 13 missions was carried out with this aircraft flying in different patterns, of which two will be described in this paper and a few more in the poster. The data is not yet completely analysed, but it shows clearly that the coastal PBL in this area is very far from homogeneous, some of the inhomogeneities arising from the presence of the land surface nearby, some probably from the geometry of the shoreline and some both from the temperature contrast between land and water but also from inhomogeneities in the sea surface temperature distribution.

The flight pattern for the first case, flown at the hight of 100m, is shown in Fig. 1 and the vertical profiles of wind speed and direction, potential temperature and specific humidity taken during an ascent well up-stream of the measured area is shown in Fig. 2.The low level wind was from the south-west and quite strong. The south-east part of the flight pattern is in an area where the air has not crossed over land and should ideally be homogeneous and undisturbed, near neutral judging from the profiles in Fig. 2, while the north-west corner of the flight pattern should sea the remnants of the unstable PBL generated over land. The wind speed filed shown in Fig. 3 clearly reveals the latter as a much reduced wind speed close to the shore line but fails to show any homogeneous PBL. Instead there is a week maxima in the wind speed starting in the south-west corner that divides up to two parts, one parallel to the coastline and the other heading for the southern tip of the island of Öland. The same feature is seen in the temperature field where the inland air is clearly visible out to Öland over 30km from land along the mean wind direction. The transition from inland PBL to marine PBL is indicated in the variances of the wind components (shown in Fig. 4 for the w-component) as a minima closely associated with the eastern maxima in wind speed. This is however not the case for the momentum flux which also shows a pronounced minima which seems to be more aligned with the western maxima along the coast. Several factors probably interact to form this complex situation. There is the formation of an internal boundary layer above which the turbulence generated over land is slowly decaying interacting with the flow pattern set up due to the change in direction of the coast line. Also contributing may be the distribution of sea surface temperature shown in Fig. 5 with a marked minima in temperature aligned with the coast and also with the eastern wind speed maxima. For the second case, a north-south cross section over the coast directly south of Ronneby (see Fig. 1) was flown. The wind direction was from north, and the purpose for this flight was actually to study the stable internal PBL formed over the colder sea. As can be seen in Fig. 6, such a layer exists but is extremely shallow - ~30m deep at a distance of 50km from the coast - capped by an inversion of several degrees. The cross section of the v-component of the wind (perpendicular to the coast) is shown in Fig. 7 and reveals the onset of a very weak sea-breeze with a vertical extension of some 500m. The sea-breeze front is most clearly sean in the wind and seams to have a double nature, the gradient being strongest right at the coast line at 60-80m and some distance inland at 200m. The temperature shows three areas with sharp gradients two of which coincides with the front in wind speed and one along the surface. It suggests that the marine stable internal PBL formed during the night does not participate in the sea-breeze circulation at this time and that this circulation is more or less sliding on top of the stable layer close to the surface. This is supported by the turbulence analysis showing the vertical flux of momentum to be practically zero in the whole region south of the coast. This air does not seam to interact with the surface at all.

Tjernström, M., och Friehe, C.A., 1990.: Analysis of a radome air-motion system on a twin-jet aircraft for boundary-layer research., Accepted for publication in Journal of Atmospheric and Oceanic Technology.

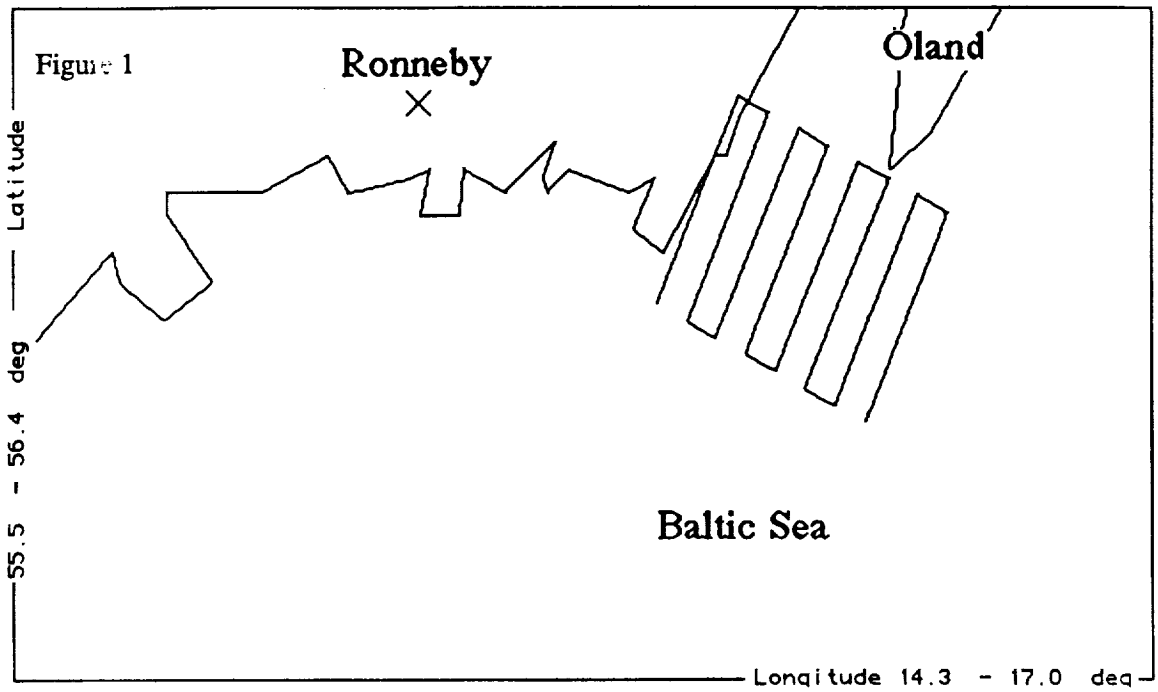
Figure 1
Ronneby
Öland
Baltic Sea
Latitude
55.5 - 56.4 deg
Longitude 14.3 - 17.0 deg

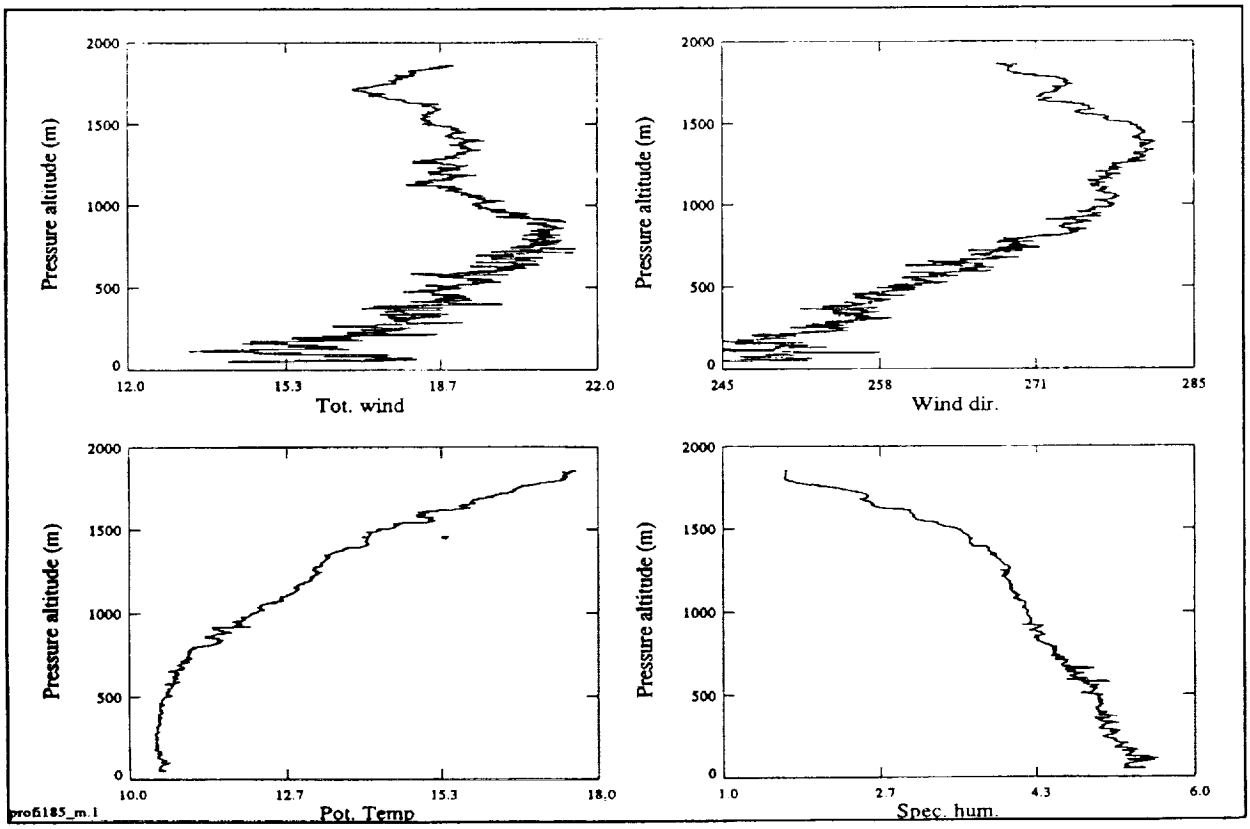
Pressure altitude (m)
Tot. wind
Wind dir.
Pot. Temp
Spec. hum.
profi185_m.1

Figure 2

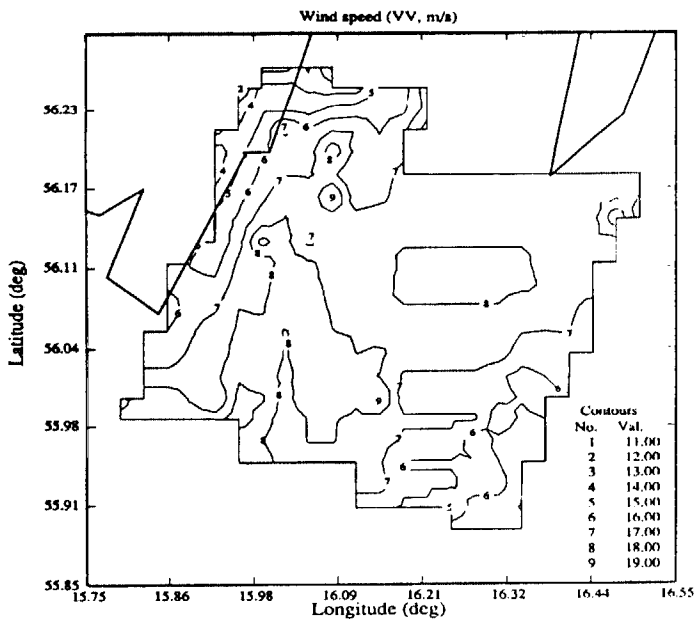

Figure 3

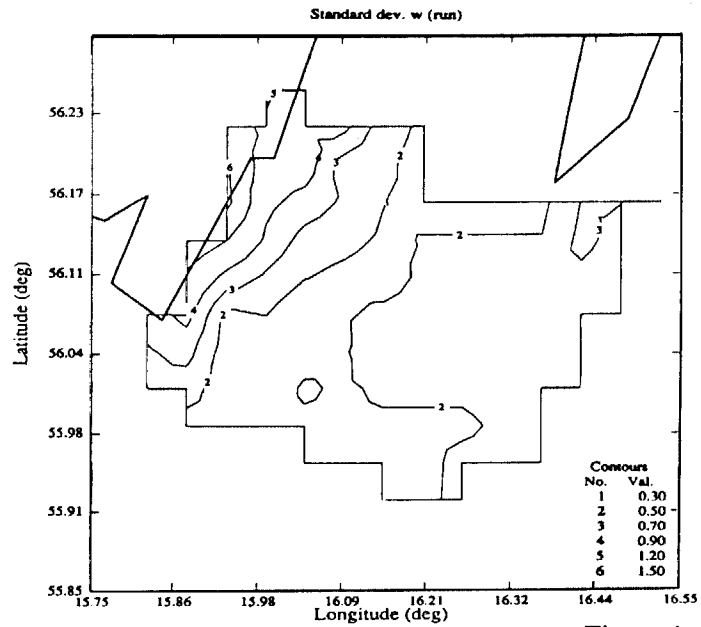

Figure 4

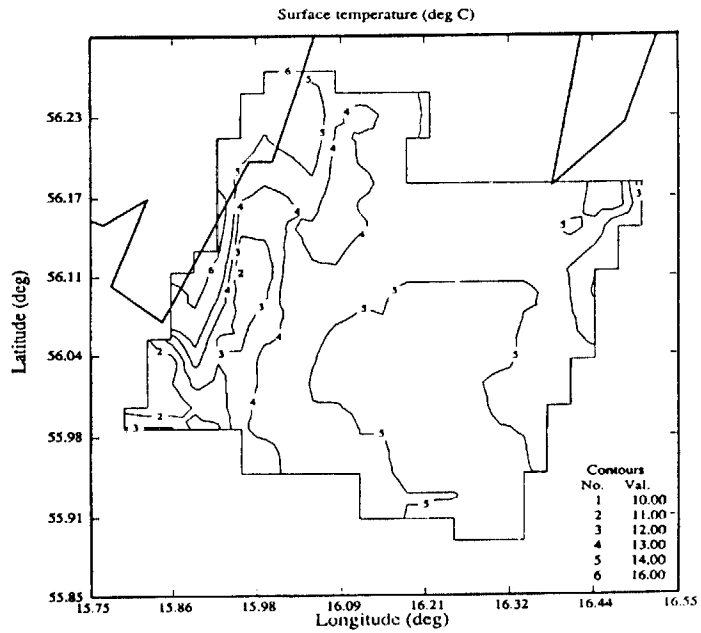

Figure 5

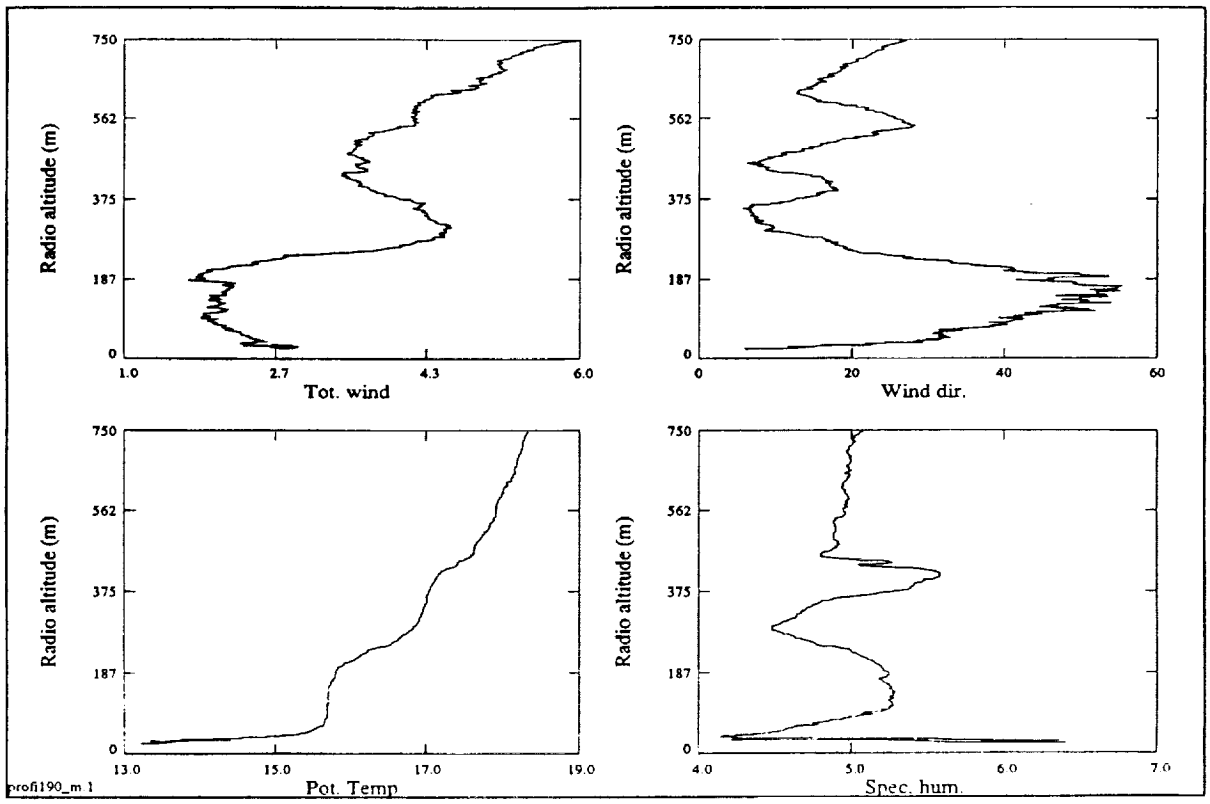

Figure 6

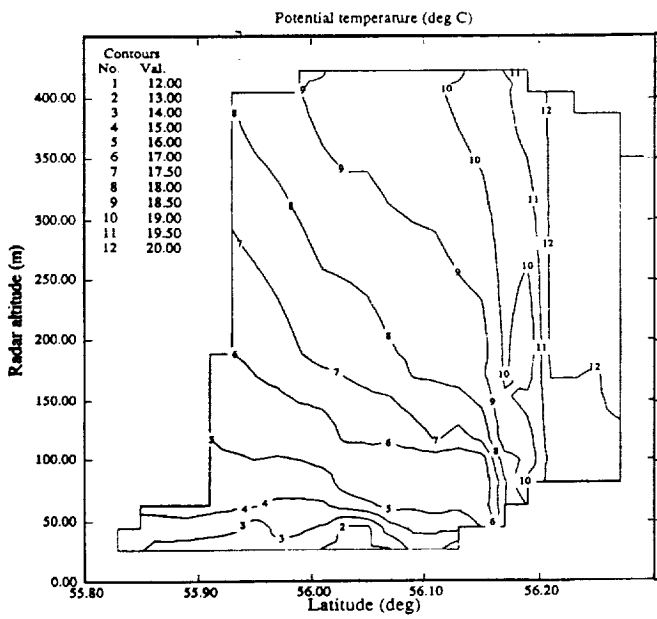

Figure 8

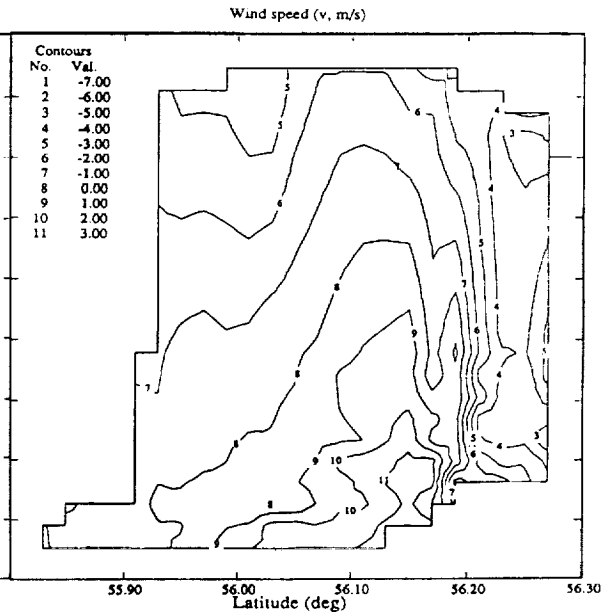

Figure 7

Title: Gulfstream IV—The Productive Research Aircraft

Author: Mike Vance, Gulfstream Aerospace Corporation

Discipline: Aircraft Applications

ORIGINAL PAGE
BLACK AND WHITE PHOTOGRAPH

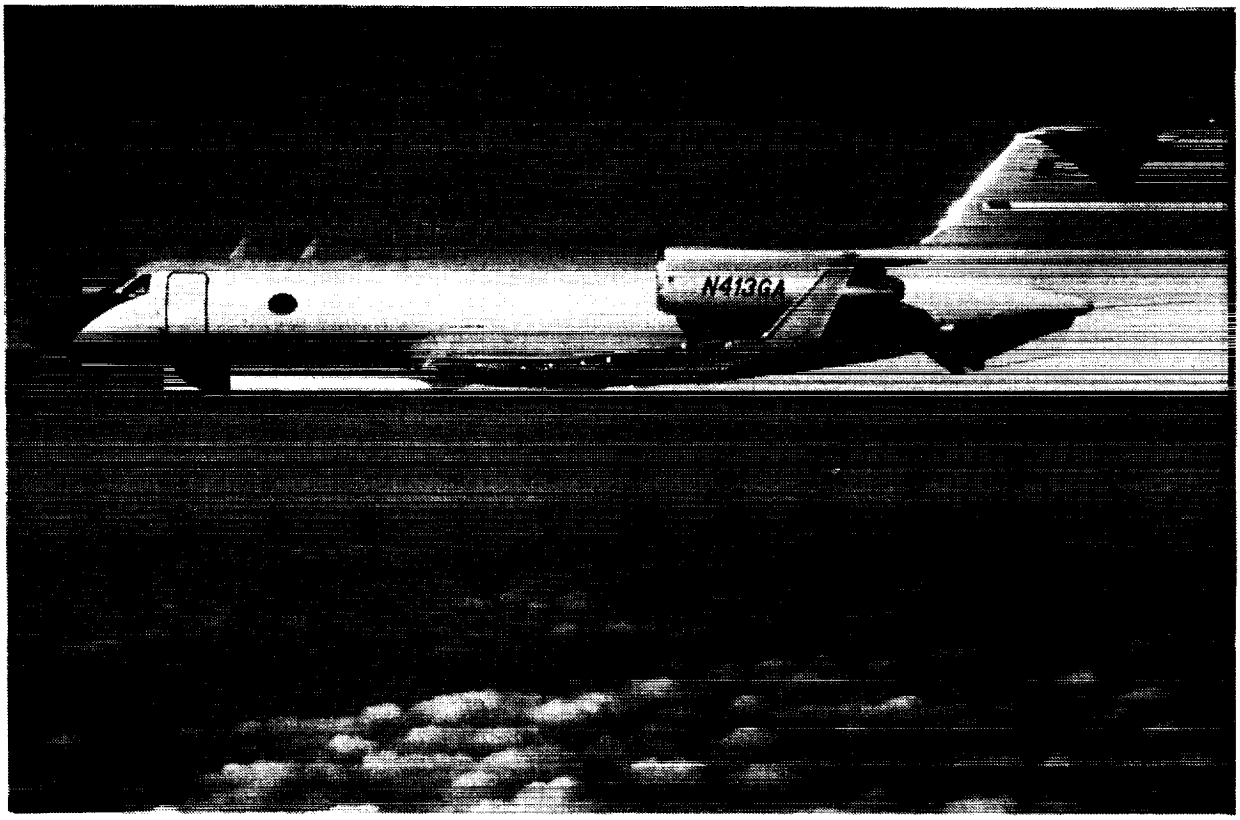

Gulfstream IV/SRA-4

The Gulfstream IV, world renown as a business jet, has attributes which make it a capable and productive platform for science, research, and reconnaissance applications. Flights requiring high altitude performance at and above **51,000** feet, range in excess of **4000** nautical miles, and heavy.loads can be handled by this rugged aircraft. Electrical systems capable of **180 KVA** of power are available providing for all system needs. The G-IV provides a stable platform from which to conduct research in all phases of airborne geoscience.

The aircraft is powered by two Rolls-Royce Tay engines capable of 13,850 lbs of thrust each. The engines have sufficient margin to allow operation off of short runways, under high temperature and high altitude conditions. The G-IV is certified to operate as high as 15,000 for take-off and landing. This allows flight operations from La Paz, Bolivia, the highest airport in the world located at 13,320 ft.

Rolls-Royce Tay Mk 611-8

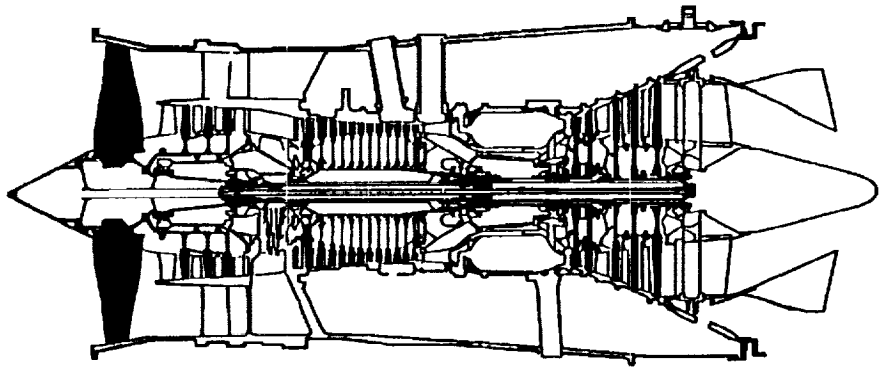

The fuselage of the Gulfstream consists of a 45 foot long tube with over 6 feet of headroom throughout its length. With the width, 250 square feet of floor space is available for placing consoles, racks, and equipment. The aircraft is available with cargo door measuring 5'3"x6'11", making it easy to remove and replace any systems that have been installed. A cabin volume of over 1300 cubic feet and the capacity to carry a 10,000 payload affords excellent working space.

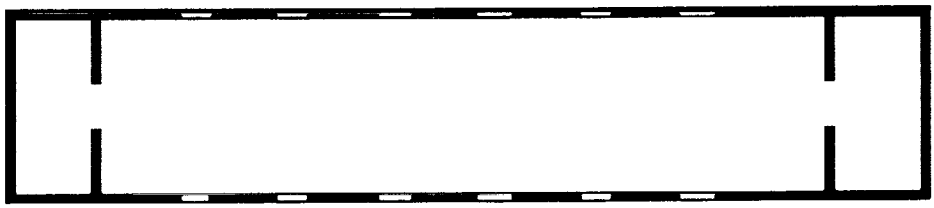

The wing area equals 950.39 square feet with a span of 77.83 feet. The design of the wing, while having no leading edge, or other complex high lift devices, provides a wide margin for operation at very high altitudes, and yet remains efficient for various flight regimes. The Buffet Boundry chart shows a 60,000 lb aircraft (mid-weight) at 41,000 ft with .35 M between low speed buffet (stall) and high speed buffet. This amounts to 180 kts TAS. Additionally, the classic "coffin corner" is located at 56,000 feet, above the G-IV's altitude capability.

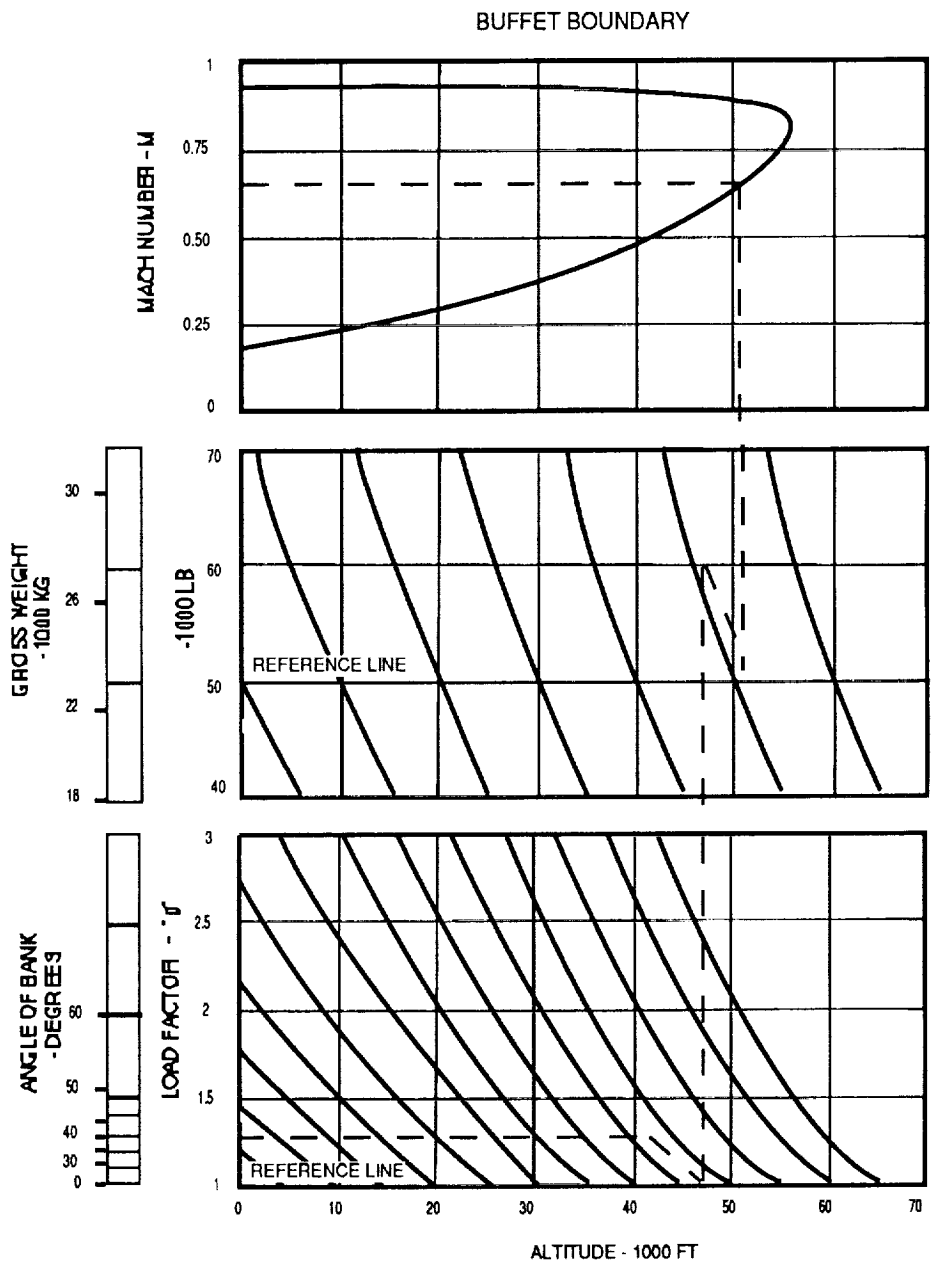

Title: METEOPOD—An Airborne Module for Atmospheric Turbulence Measurements

Author: Peter Wachs, Aerodata Flugmeßtechnik GmbH
P. Vörsmann, Aerodata Flugmeßtechnik GmbH

Discipline: Atmosphere

For many years aircraft have been equipped for research in wind and turbulence measurements. Very often the system installation consisted of sensors and recording hardware, which was spread all over the aircraft. Conventional systems often use a nose boom in order to measure the undisturbed airflow ahead of the aircraft. For those booms stiffness is a very important design criteria. Low eigen-frequencies of elastic booms often show up as peaks in the turbulence spectra.

In the last years there seems to be a trend to change from a nose boom to airflow sensing in the nose of the aircraft. This can be achieved by installing a 5-hole-probe directly in the nose. Certainly the airflow around the nose is more disturbed than at the tip of a nose boom, but it seems to be possible to calibrate the flow and correct for nonlinear effects. Even though all airflow and temperature sensors as well as an IRU (Inertial Reference System) can be concentrated close to the nose, which is a prerequisite for turbulence measurements, there is a need for further integration and quick-change systems.

The Meteopod was developed by Aerodata for the Alfred Wegener Institut for Polar and Marine Research and was operated during three German meteorological experiments. It is a new solution to combine all sensing units necessary for airborne wind and turbulence measurements in one external compartment. The sensor configuration allows the registration of the long term values as well as the turbulent fluctuations of wind, temperature and humidity.

The pod itself is of fiber glass construction, 4 meter in length and about 40 centimeters in diameter. The total weight depends on the actual system configuration and is about 100 kg excluding the aircraft pylon. The power requirement for sensors, control units, and data acquisition/preprocessor-system is about 500 Watts. For operation in arctic regions it is equipped with a temperature controlled heating system of about 2000 Watt. Primary power supply is 115V/400Hz from the cabin. Converters then generate all required voltages.

Figure 1 gives a schematic presentation of the hardware location of sensors, control units, and data acquisition in the pod.

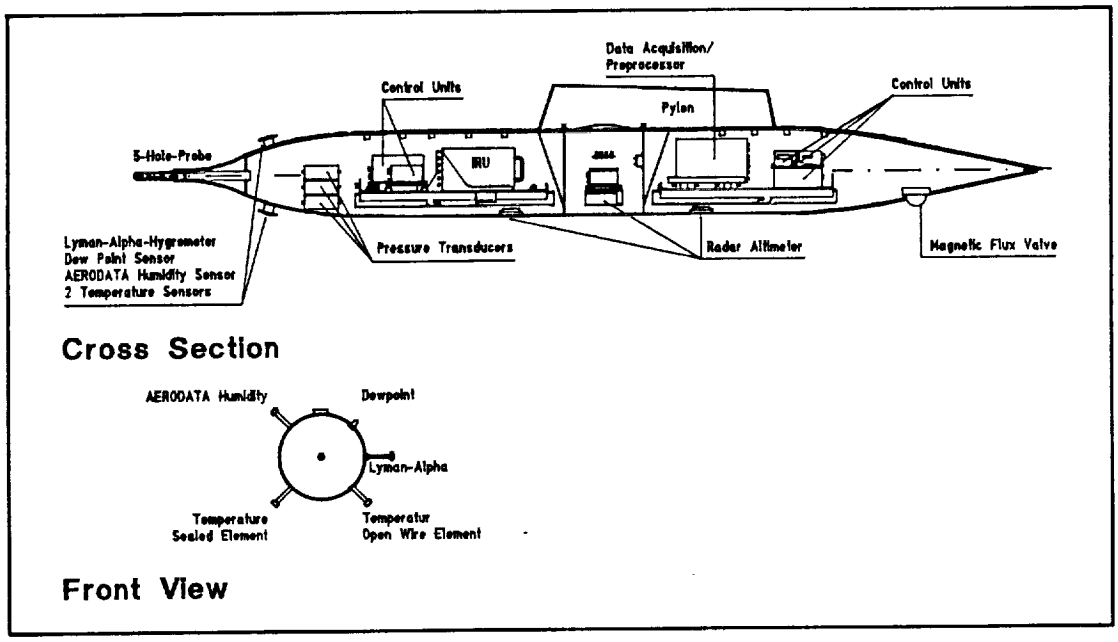

Fig. 1: Cross section of the Meteopod with Location of Sensors, Control Units and Data Acquisition.

The main advantages of the Meteopod compared to conventional systems are manifold:

- short distance between flow sensing head and IRU
- short distance between flow sensing head, temperature and humidity probes
- short tubings between 5-hole-probe and pressure tranducer
- analog data acquisition/preprocessing-system close to sensors
- variability concerning operation on aircraft or helicopters

Turbulence spectra from nose boom systems often show peaks in the frequency range of boom oscillation (5 to 20 Hz). Sensors themselves may also cause resonances. The dynamic behavior of Flight-Logs and tubings between pressure ports and pressure transducers (organ-pipe effect) are typical examples for this problem.

Both problems do not occur in the Meteopod. The fiber glass construction is very stiff and tubings are very short. Thus no peaks are to be expected in turbulence spectra due to these effects. It is of interest that the IRU sensor package registers the movement of the wing-pylon-pod structure. As an example for the dynamic behavior of this system Figure 2 shows the energy spectra of 50 Hz data of an 8 minutes' horizontal flight. Rollangle, Body Lateral-, and Body Normal-Acceleration with their associated peaks are pictured.

However, in contrast to boom oscillations, these

oscillations are precisely sensed by the IRU and accordingly considered in the calculation of the wind components. Thus the spectra of the wind components show the classic -5/3 slope without any knowable peak, see Figure 3.

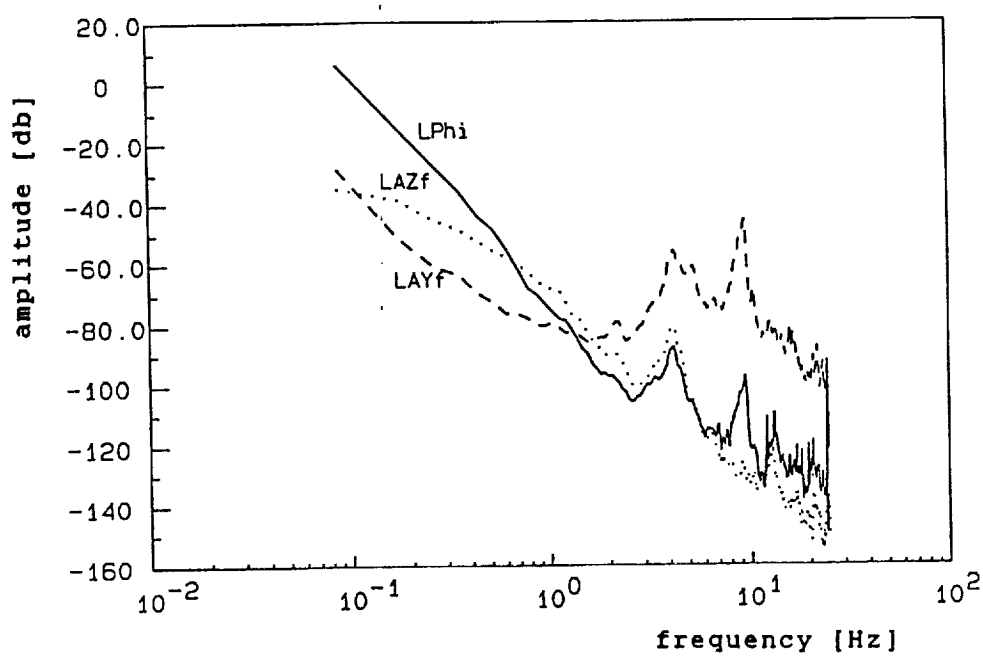

Fig. 2: Energy Spectra of IRU-Parameters LPhi (Rollangle), LAYf (Body Lateral Acc.), LAZf (Body Normal Acc.).

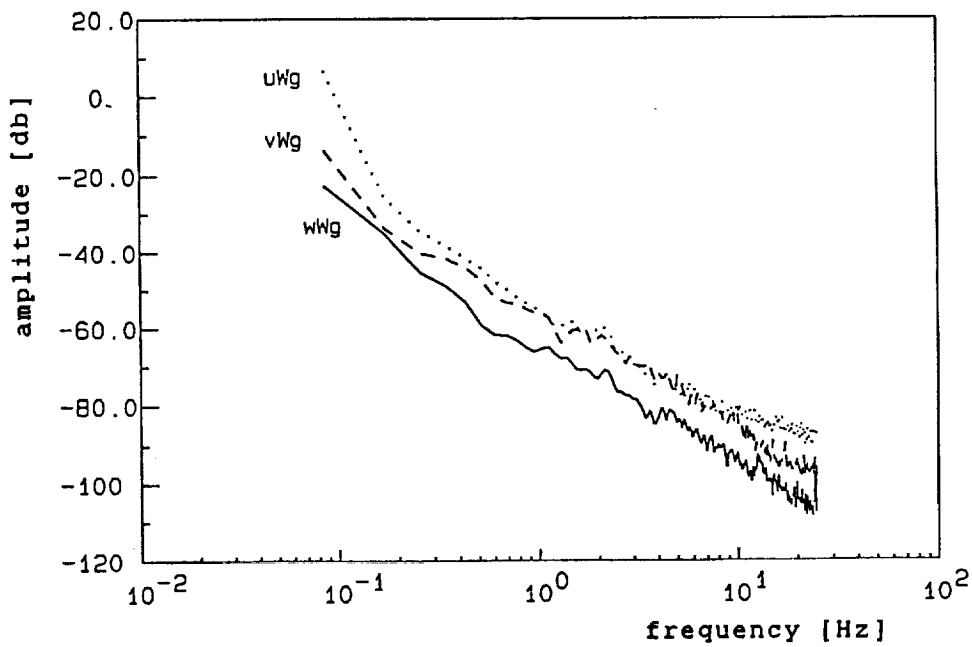

Fig. 3: Energy Spectra of Wind Components.

Typical absolute accuracies in horizontal flight conditions, which are currently achieved with the Meteopod system, are in the order of 0,7 m/s for the horizontal components and 0,3 m/s for the vertical component of the wind vector.

Title: Profiles of $\partial^{13}C$ and ∂D in Methane from the Lower Stratosphere

Authors: Martin Wahlen, Wadsworth Center for Laboratories and Research
Nori Tanaka, Yale University
Robert Henry, New York State Dept. of Environmental Conservation
Harley Weyer, NASA/Johnson Space Center

Discipline: Atmospheric Chemistry

Methane is an important green house gas of biogenic and anthropogenic origin for which global budgets are being constructed from a variety of data. One approach to a global methane budget is the use of the stable isotopes ^{13}C and D, and the radionuclide ^{14}C as tracers (1). We measured the isotopic composition of methane from various sources and in tropospheric air for a number of locations. Here we report on the isotopic composition of methane collected from the lower stratosphere. As in the troposphere, the main sink for methane in the lower stratosphere is the oxidation by OH radical; higher up oxidation by O^1D and Cl become increasingly important. Measurements of the isotopic methane composition in the stratosphere can yield estimates for the kinetic isotope effects in the methane destruction reactions. These effects have to be known for quantitative isotopic methane budgets.

Large air samples were collected from the lower stratosphere (tropopause to about 19 km altitude, in mid and low latitudes of the northern hemisphere) aboard the NASA WB-F57 airplane with a compressor system similar to those we use to collect samples from sources and tropospheric air. Compatibility of the airborne collection system for CH_4 and N_2O concentrations and isotopic methane composition measurements was established by ground tests using both sampling systems simultaneously. The samples were processed and measured identical to the procedures described in (1). The radionuclide ^{85}Kr was also measured in these samples.

The observed CH_4 and N_2O concentrations decrease with altitude, and the profiles for different latitudes look similar to those obtained by others. The profiles become most coherent when concentrations are plotted against altitude above the local tropopause heights, which were obtained by interpolating sounding data from weather stations along the flight path. The concentrations of CH_4 and N_2O linearly correlate with a slope characteristic for the lower stratosphere. As N_2O concentrations drop faster relative to CH_4 concentrations higher up in the stratosphere, complications by subsiding air can be excluded in our data set.

The methane $\delta^{13}C$ and δD values become significantly and successively enriched with increasing altitude and decreasing CH_4 concentration when compared to the tropospheric values. This behavior is attributed to the effect of isotopic fractionation occuring in the destruction reactions. The kinetic isotope effect α is the ratio of the reaction rate constants for two isotopically different molecules, and $(\alpha - 1) \times 1000$ is the enrichment factor ϵ for a reaction. In a

simple steady state 1-box approach the factor is also $\epsilon = \Delta\delta / \ln(CH_{4\,local}/CH_{4\,troposphere})$, i. e. the ratio of the change in isotopic composition to the natural logarithm of the fraction of CH_4 surviving the destruction, and thus given by the slope in the profiles shown below.

More detailed chemical models will be presented and discussed to deduce estimates for the enrichment factors of ^{13}C and D of CH_4 in the OH destruction reaction. The model considers transport by using the measured ^{85}Kr concentrations which indicate the age of the air as function of altitude (time since it left the troposphere). The obtained results will be compared to existing ones from laboratory experiments (for ^{13}C), and the implications for methane budget calculations will discussed.

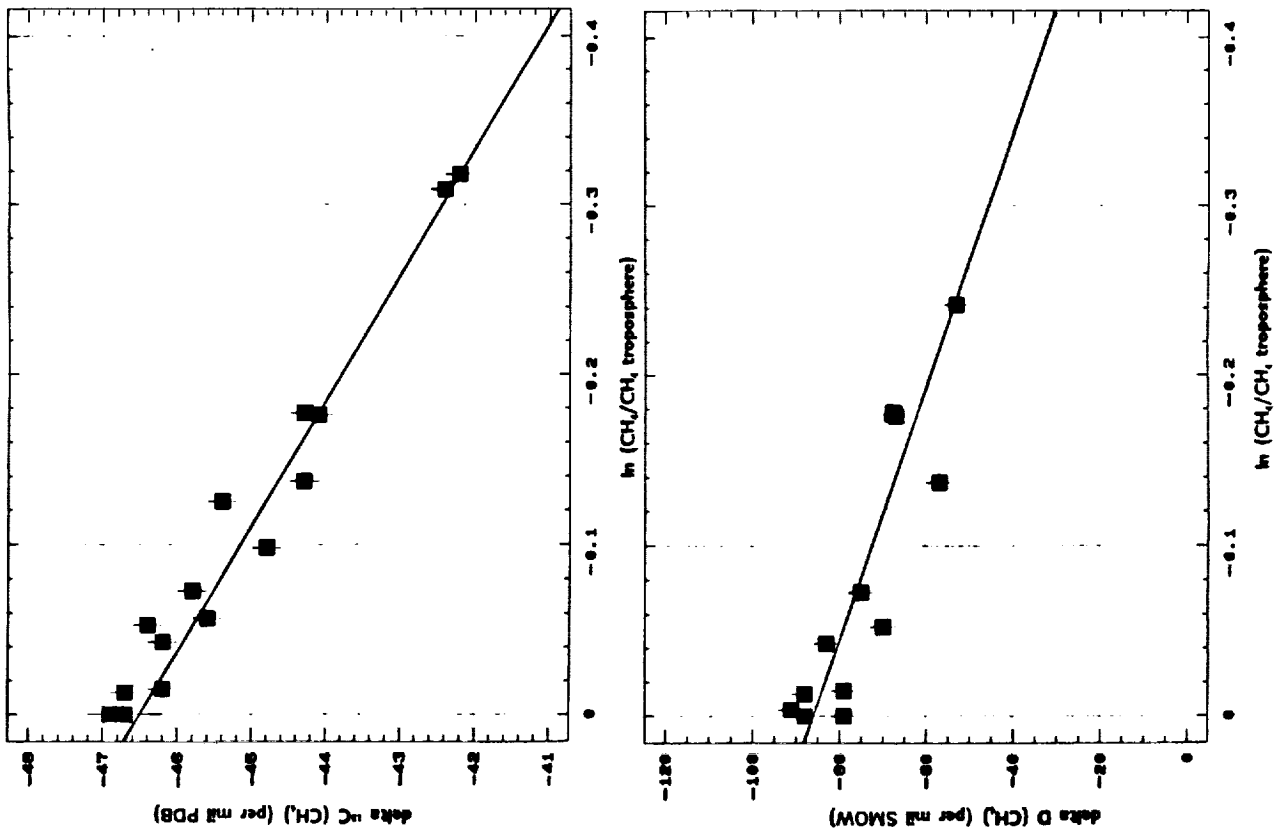

Ref.: (1) M. Wahlen et al., Science 245 (1989) 286.

S43-43
N91-25488
p2

Title: Advanced Solid-State Array Spectrometer (ASAS) Data Sets from the 1990 Field Season: A Unique Look at Two Forested Ecosystems

Authors: Charles Walthall, University of Maryland
James Irons, NASA/Goddard Space Flight Center
Phillip Dabney, NASA/Goddard Space Flight Center
David Peterson, NASA/Ames Research Center
Darrel Williams, NASA/Goddard Space Flight Center
Lee Johnson, TGS Technology, Inc.
Jon Ranson, NASA/Goddard Space Flight Center

M1 915766
NC499967
NC473657
TV 743199

Discipline: Land

Calibrated data sets, especially in digital image format, of forested canopies exploiting both the spectral and bidirectional domains of remotely sensed information are limited. The difficulties of getting instrumentation above the canopy necessitate the use of airborne scanners to provide this type of data. For these reasons the Advanced Solid-state Array Spectrometer (ASAS) was flown aboard the NASA C-130 during the 1990 summer field season as part of the Oregon Terrestrial Transect Ecosystem Research (OTTER), and Forest Ecosystems Dynamics (FED) Multi-sensor Aircraft Campaigns (MAC's). ASAS was used as the priority imaging device aboard the C-130 for both OTTER, which was conducted along a forested transect in West Central Oregon, and FED, which was conducted at the International Paper Northern Experimental Forest near Howland, Maine. Both OTTER and FED utilized several concentrated study sites within the larger study areas. ASAS was used to provide bidirectional multispectral image data of these sites at a variety of solar angles coincident with ground-based and other airborne measurements.

ASAS is a pointable imaging spectrometer which uses a solid-state array to acquire imagery of terrestrial targets in 29 spectral bands from .4 to .8 um. ASAS is unique in that it can be pointed at off-nadir angles up to 45 degrees fore and aft along the track of the aircraft. As the aircraft flies over a target, the instrument is moved to seven preset angles along the ground track. Data is usually collected along and perpendicular to the solar principal plane. Calibration is performed using a laboratory setting prior to and following the data collection season. In-flight calibration checks are possible with a built in shutter for dark current checks, and in-field checks are possible using a

portable calibrated lamp when the platform aircraft is not flying.

The ASAS data sets obtained during the 1990 MACs provide a unique look at forest canopies from two different northern forest regions of the North American continent under varying temporal, spectral, and bidirectional conditions. These data sets will be used to study such parameters as the albedo of forest canopies, and the dynamics of scene radiation due to factors such as canopy architecture, moisture stress, leaf chemistry, topography, and understory composition. Additionally, these data sets will provide inputs to models dealing with the physics of the interaction of light with forest canopies, and ecosystem changes. Insights from the results of these analyses will provide new tools for inventory and monitoring of global forest ecosystems using data sets from sensors like the proposed EOS HIRIS and MODIS systems. New calibration and correction procedures will be developed which will allow further interpretation of existing image data sets, thus moving closer to the creation of long term data sets for monitoring global changes.

The developement and partial implementation of a dedicated ASAS data processing system have allowed a shorter turn-around of ASAS data to investigators. A number of the ASAS image data sets from the 1990 MACs have been processed and distributed to the investigators involved in OTTER and FED. Several example data sets are presented from both the OTTER and FED missions.

Title: Monitoring Forest Freeze-Thaw Cycles with Airborne SAR

Authors: JoBea Way, Jet Propulsion Laboratory
Ron Kwok, Jet Propulsion Laboratory
John Holt, Jet Propulsion Laboratory
M. Craig Dobson, University of Michigan
Kyle McDonald, University of Michigan
F.T. Ulaby, University of Michigan

CONT TO P.293

Discipline: Land

One goal in utilizing remote sensing systems for forest ecosystem analysis is to infer characteristic biophysical parameters from the remotely sensed data. With the proposed launchings of a variety of space-based imaging radar systems throughout the 1990's, there has been an increasing interest in the utility of radar data for forest ecosystem analysis. The first of these spaceborne synthetic aperture radars (SARs) will be on the European Space Agency's (ESA's) Earth Resources Satellite (ERS-1) to be launched in late 1990. During its two year lifetime, data may be acquired over a region every one to three weeks, depending on latitude, allowing frequent acquisition of selected forest sites over a variety of seasons.

In order to understand the kinds of biophysical properties that may be detected with spaceborne SAR systems such as ERS-1, a series of multi-season aircraft missions over selected forest sites is in progress. The first of these occurred in March, 1988 over the Bonanza Creek Experimental Forest (BCEF) near Fairbanks, Alaska. The purpose of the Alaskan SAR Forest Experiment was: (1) to determine whether changes in plant fluid status associated with thawing and freezing resulted in changes in radar backscatter which could be detected on SAR imagery; and (2) based on measurements of tree geometry and biomass levels, and dielectric measurements of the surface (snow) and trees, could the changes in radar backscatter be predicted by theoretical models.

Over the two-week period during which airborne multipolarization, multifrequency SAR data were acquired, temperatures ranged from unseasonably warm (1 to 8°C) to well below freezing (-8 to -15°C), and the moisture content of the snow and trees changed from a liquid to a frozen state. The difference in image intensity between these two environmental conditions is significant and indicates that changing environmental state is indeed detected by SAR systems.

The purpose of this airborne SAR research is twofold: (1) to demonstrate that changes in canopy moisture state result in changes in radar backscatter that can be observed on SAR imagery and predicted by theoretical models; and (2) to discuss the opportunity presented by the ERS-1 SAR in developing long-term studies of changes in radar backscatter from forest ecosystems caused by temporally-varying moisture changes.

Title: **High Altitude Observatory (HALO) Aircraft Capabilities**

Authors: Paul Weckler, Aeromet, Inc.
Charles Pruszynski, Aeromet, Inc.

Discipline: **Multidisciplinary**

Airborne observatories offer significant advantages over ground-based and space-based platforms. Airborne observations can be deployed worldwide, so they provide a level of consistency and experimental control not available from ground-based sensors. Aircraft, unlike other assets, can normally choose any test support position within safety limits, with optimized aspect angles and slant range. Flying at 50,000 feet, an aircraft is above 88% of the atmosphere, and nearly always above obscuring clouds. Compared to space-based observations, aircraft observations are far less costly.

The **H**igh **AL**titude **O**bservatory **(HALO)** is an instrumented high-performance Gulfstream II-B aircraft that is optimized for airborne optical measurements. HALO is operated by Aeromet Inc., Tulsa, Oklahoma under contract to the U.S. Army Strategic Defense Command. See Figure 1. Although the U.S. Government maintains numerous airborne optical aircraft, the HALO is unique because it is operated and maintained under civilian regulations. The advantages of civilian operation are very significant, and include the following: aircraft availability, flexible sensor accommodation, high reliability, and low cost.

The HALO aircraft can deploy a wide variety of optical sensors. They include calibrated radiometric imagers, high-speed film and video cameras (1000 frames per second), UV-visible-IR spectral imagers (305 nanometer to 12 micrometer wavelengths), ultra-high dynamic range CCD cameras (10^7 to 1 $^S/_N$), intensified CCD and SIT cameras, and spectroscopic sensors. Currently, the HALO aircraft is configured with three optical platforms. Each optical platform is equipped with a gyro-stabilized pointing mirror and specialized optics. Aeromet has developed the Airborne Pointing System **(APS)** to continuously compute the optimal steering strategies for the gimbaled pointing mirrors. The APS uses aircraft INS, GPS, radar position data and nominal target tracks for these computations. Up to four targets can be tracked simultaneously by the APS. The optical platforms are light-tight and purged with dry nitrogen to prevent optical window fogging.

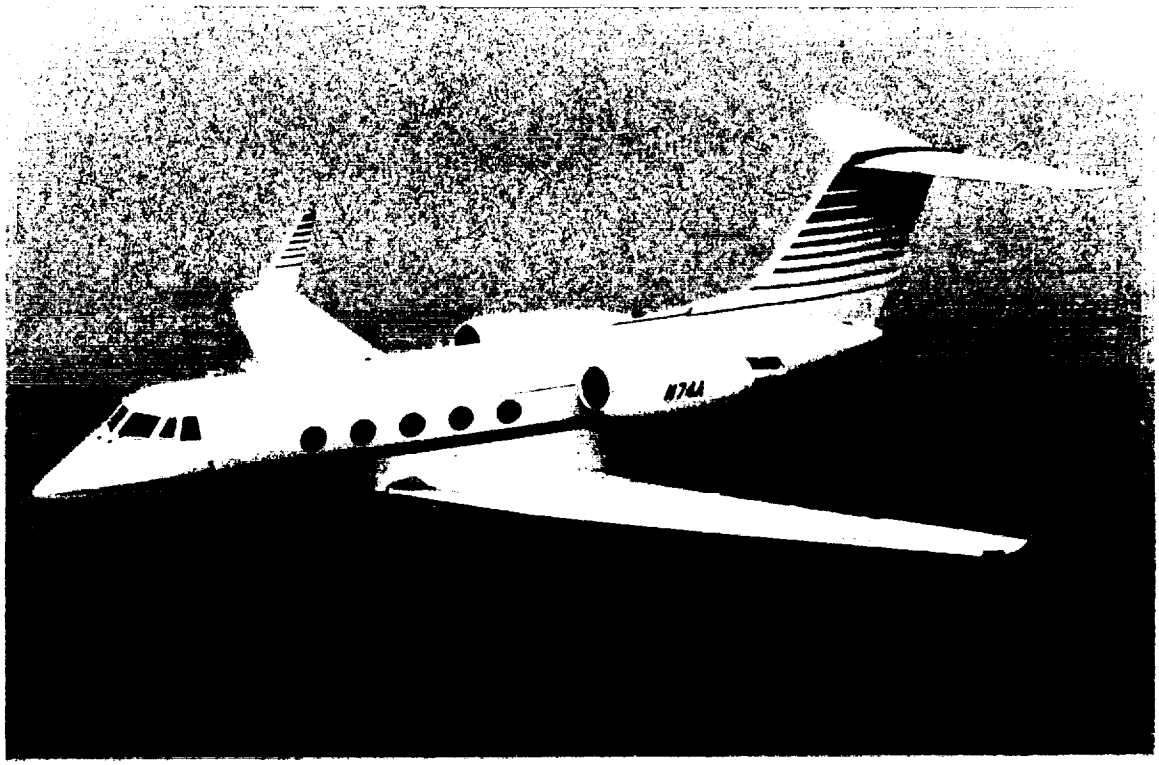

Figure 1.

Past missions have documented Space Shuttle launches, measured missile and rocket plume signatures, and collected data on re-entry vehicles, NASA chemical release experiments, and exoatmospheric objects. Mission data can include high-resolution high-speed photodocumentation, calibrated radiometric imagery, relative or absolute target metrics and spectroscopy data. This poster is intended to describe the baseline capabilities of the HALO aircraft and its instrumentation, and present selected data summaries from past missions.

Title: High Altitude Aircraft Direction using Real-Time Scientific Analysis of Telemetered Data

Authors: Steven Wegener, NASA/Ames Research Center
K. Roland Chan, NASA/Ames Research Center
Leonhard Pfister, NASA/Ames Research Center
John Arvesen, NASA/Ames Research Center

Discipline: Atmosphere

1. Introduction

Microscale and some mesoscale scientific targets (waves, turbulence bursts, cloud edges, tropospheric folds, jets, vortices) are often small and fast moving in a dynamic atmosphere. In this environment, the ER-2 may spend only a small time sampling the phenomena of interest. The ER-2 scientists currently rely on post-flight analysis to determine the success of the mission and to provide input for planning the next flight. Real-time analysis, combined with realistic modeling, can provide important clues to significantly enhance the probability of success in the investigation of specific scientific targets.

2. Telescience Demonstrations

In August 1989, a NASA ER-2 equipped with the Ames Meteorological Measurement System (MMS) flew in support of the launch of the Space Shuttle Columbia. This demonstration provided analysis products (wind and shear profiles to 60,000 feet) in real time to the Johnson Space Center.

In the fall of 1990, an ER-2 flight is planned over the northern Sierras to delineate meteorological, aerosol, and trace gas structures in the stratosphere. The data will be distributed for remote, near real-time analysis and data products will be linked to a Project Control Center. Data products including aircraft position, meteorological state variables, temperature profile, ozone concentration and particle size and density will be displayed along with forecasted potential vorticity fields and satellite

imagery. These will be used to direct the aircraft to specific targets.

Use of a two-way aircraft satellite communication link is being investigated. We have initiated the development of requirement documents for the use of NASA Tracking and Data Relay Satellite (TDRS) to support ER-2 flights world wide. Data rates range from 50 kilobits per second to 10.7 megabits per second.

The poster will show progress in the efforts described above.

N91-25490

Title: The 1990 Forest Ecosystem Dynamics Multisensor Aircraft Campaign

Authors: Darrel L. Williams, NASA/Goddard Space Flight Center
K. Jon Ranson, NASA/Goddard Space Flight Center

NC999967

Discipline: Land

A Multisensor Aircraft Campaign (MAC) was conducted in mid-July and early September, 1990 at International Papers' Northern Experimental Forest (NEF), located approximately 56 km north of Bangor, Maine. The MAC was initiated to support the Forest Ecosystem Dynamics (FED) project, a major research activity within the Biospheric Sciences Branch at NASA's Goddard Space Flight Center. Numerous investigators from Goddard, other U.S. government agencies and universities participated in this MAC.

The 1990 FED MAC experiment design called for a suite of airborne instrument observations and supporting ground observations at several preselected locations within the NEF. Because of aircraft scheduling conflicts in 1990, the FED MAC experiments were conducted as two campaigns, each emphasizing measurements in different portions of the electromagnetic spectrum. A series of active and passive microwave measurements were emphasized in mid-July, while optical-reflective measurements were acquired in September.

During the mid-July measurements campaign, the NASA/Ames Research Center (ARC) DC-8 equipped with the Jet Propulsion Laboratory's (JPL) 3-band, quad-polarized Synthetic Aperture Radar (SAR) overflew the NEF on July 15th and 17th (i.e., before and after an ½" rainstorm event on July 16th). Also, on July 15th, the NASA/Wallops Flight Facility (WFF) P-3 aircraft carrying the Push-broom Microwave Radiometer (PBMR) and Electronically Steered Thinned Array Radiometer (ESTAR) sensors, which are used for assessing soil moisture conditions, flew several flightlines over the NEF a few hours before the DC-8 overflight. An extensive set of soil moisture measurements were made on July 15th concurrent with the P-3 and SAR overflights. Also during the mid-July field campaign, the NASA Wallops UH-1B helicopter, equipped with a pointable (2-axis) set of bore-sighted instruments including a Barnes Modular Multiband Radiometer (MMR), a Spectron Engineering SE-590 spectroradiometer, an Everest infrared temperature sensor, and a Sony CCD video camera, was utilized to collect bidirectional reflectance data over a variety of targets.

On September 8, 1990, multiple and/or concurrent overflights of the FED MAC NEF study area were completed under extremely clear atmospheric conditions by: (a) NASA ARC's ER-2 carrying JPL's Airborne Visible/Infrared Imaging Spectrometer (AVIRIS) instrument [overflight at 11:30 - 11:45 eastern daylight savings time (EDST)]; (b) NASA's

C-130 equipped with Goddard's Advanced Solid-state Array Spectroradiometer (ASAS) and the NS-001 Thematic Mapper simulator [overflights from 09:10 - 14:30 EDST]; and (c) the NASA Wallops UH-1B helicopter equipped as summarized above [flights from 09:00 - 15:00 EDST]. Goddard's Airborne Laser Polarimeter System (ALPS) was also mounted on the helicopter, and was utilized to acquire data over numerous targets on other days when sky conditions were not ideal for making optical-reflective measurements.

FED Objectives and Long Range Goals

The overall objective of the FED research activity is to develop a better understanding of the dynamics of forest ecosystem evolution over a variety of temporal and spatial scales. Primary emphasis is being placed on assessing the ecosystem dynamics associated with the transition zone between northern hardwood forests in eastern North America and the predominantly coniferous forests of the more northerly boreal biome. The approach is to combine ground-based, airborne, and satellite observations with an integrated forest pattern and process model which is being developed to link together existing models of forest growth and development, soil processes, and radiative transfer.

Airborne measurement campaigns such as the 1990 FED MAC conducted in mid-July and early September at the NEF, are undertaken to acquire data which are needed either to improve our understanding of these processes so that the models can be updated/modified, or to compare modeled results with actual field observations.

Eventually, the results anticipated from this type of research will enable development and validation of an integrated model to usefully characterize the ecosystem dynamics of the boreal forest under a variety of conditions. A number of questions pertinent to the combined experiment may then be considered. For example, how do climatic gradients determine the spatial distribution of species within the boreal forest? What are the possible effects of global climate change on the boreal forest? Is the boreal forest a net source or sink of carbon and methane and will the present state change if climate changes? Also relevant to the issue of global change are the magnitudes of the feedbacks between climate and vegetation. The model, as formulated, can provide insights into the effects of climate change on ecosystem dynamics, but does not consider the effects of ecosystem changes on climate directly. However, the model can provide, as outputs, factors that impact climate such as albedo, evapotranspiration, and trace gas fluxes (i.e., CO_2, CH_4 and N_2). These questions are also relevant to the BOREAS (SIFE/TE/ABLE) experiment planned for the 1993/1994 time frame.

N91-25491

Title: A Pointable, Helicopter-Based Remote Sensing Data Acquisition System for Collecting Bidirectional Reflectance Data

Authors: Darrel L. Williams, NASA/Goddard Space Flight Center
Charles L. Walthall, University of Maryland
Douglas Young, NASA/Wallops Flight Facility

Discipline: Land

Since 1983, researchers at the Goddard Space Flight Center and the University of Maryland have worked with engineers at the Wallops Flight Facility (WFF) to develop and refine a helicopter-based remote sensing data acquisition system. During this period of time, our evolving helicopter-borne remote sensing system has been utilized extensively to support field measurements programs such as studies of forest decline damage associated with atmospheric deposition, FIFE'87 & '89, and Goddard's current Forest Ecosystems Dynamics project. However, the level of refinement in this system reached a new plateau in 1990 as the result of significant improvements in the way the instrument package is mounted on the helicopter and in the way the data from the instruments are captured and stored.

In the new configuration, the sensor payload is mounted externally on a hinged pallet located on the starboard side of the WFF Bell Iroquois UH-1B (HUEY) helicopter[1] (see schematic, Fig. 1). This pallet is attached to the aircraft by utilizing existing ordinance mounting lugs which are located strategically near the center-of-gravity of the aircraft. Attached to this pallet is a two degree-of-freedom gimbal device which permits the sensor payload to be rotated 360° and pointed up to 60° off-nadir. The hinge in the pallet permits the sensor payload to be tilted up (using an actuator) for take-off and landing, and leveled again once in flight. This was necessitated by the need to lower the sensor payload below the helicopters' landing skids to insure that the FOV of the instruments would not be obstructed by the skids when the gimbal was positioned 60° off-nadir while pointing underneath the helicopter.

The sensor payload includes a set of bore-sighted instruments consisting of a Barnes Modular Multiband Radiometer (MMR) (1° field-of-view, FOV), a Spectron Engineering

[1] NOTE: An identical pallet can be (and has been) mounted on the port side of the aircraft to provide counterbalance and/or accommodate additional sensors.

(SE) 590 spectroradiometer (1° FOV), an Everest infrared temperature sensor (2° FOV), and a Sony CCD video camera with 10x zoom lens. Controller units for this equipment, as well as for the pallet and gimbal, are mounted within a three-bay instrumentation rack located inside the cabin of the helicopter. The centerpiece of the support instrumentation is a 20 MHz 80386 personal computer (PC) equipped with a 100 MB hard disk and a 16 bit, 16 channel differential input A/D converter board. This PC configuration permits simultaneous, high speed acquisition and storage of digital data from all of the instruments in the sensor payload. Thus, we are able to acquire more measurements in much less hover time over each target, and we avoid a significant amount of flight down-time which was required in the past to dump the MMR dataloggers.

This new payload and PC-based controller arrangement were thoroughly tested during a Multisensor Aircraft Campaign (MAC) which was conducted in mid-July and early September, 1990 at International Papers' Northern Experimental Forest (NEF), located approximately 56 km north of Bangor, Maine. The MAC was initiated to support the Forest Ecosystem Dynamics (FED) project, a major research activity within the Biospheric Sciences Branch at NASA's Goddard Space Flight Center (see abstract and poster re: 1990 Forest Ecosystem Dynamics Multisensor Aircraft Campaign).

Although there are some minor adjustments which remain to be made in this pointable, helicopter-based data acquisition system, excellent data were collected in 1990. Figure 2 illustrates the collection of bidirectional reflectance data with the pointable instrument mount, while Figure 3 illustrates the significant differences in target reflectance that one can expect as a function of sensor view angle. The capability to acquire bidirectional reflectance data permits us to closely simulate the type of radiance data acquired currently by GSFC's Advanced Solid-state Array Spectroradiometer (ASAS), as well as that which is to be acquired by several Earth Observing System (EOS) instruments. Thus, with this latest configuration, we feel that we have developed a truly unique, reliable capability to acquire multi look-angle data sets of specific targets. Furthermore, we feel that this type of data will be extremely useful to the remote sensing science community in validating the bidirectional reflectance distribution functions (BRDF) for numerous earth surface features.

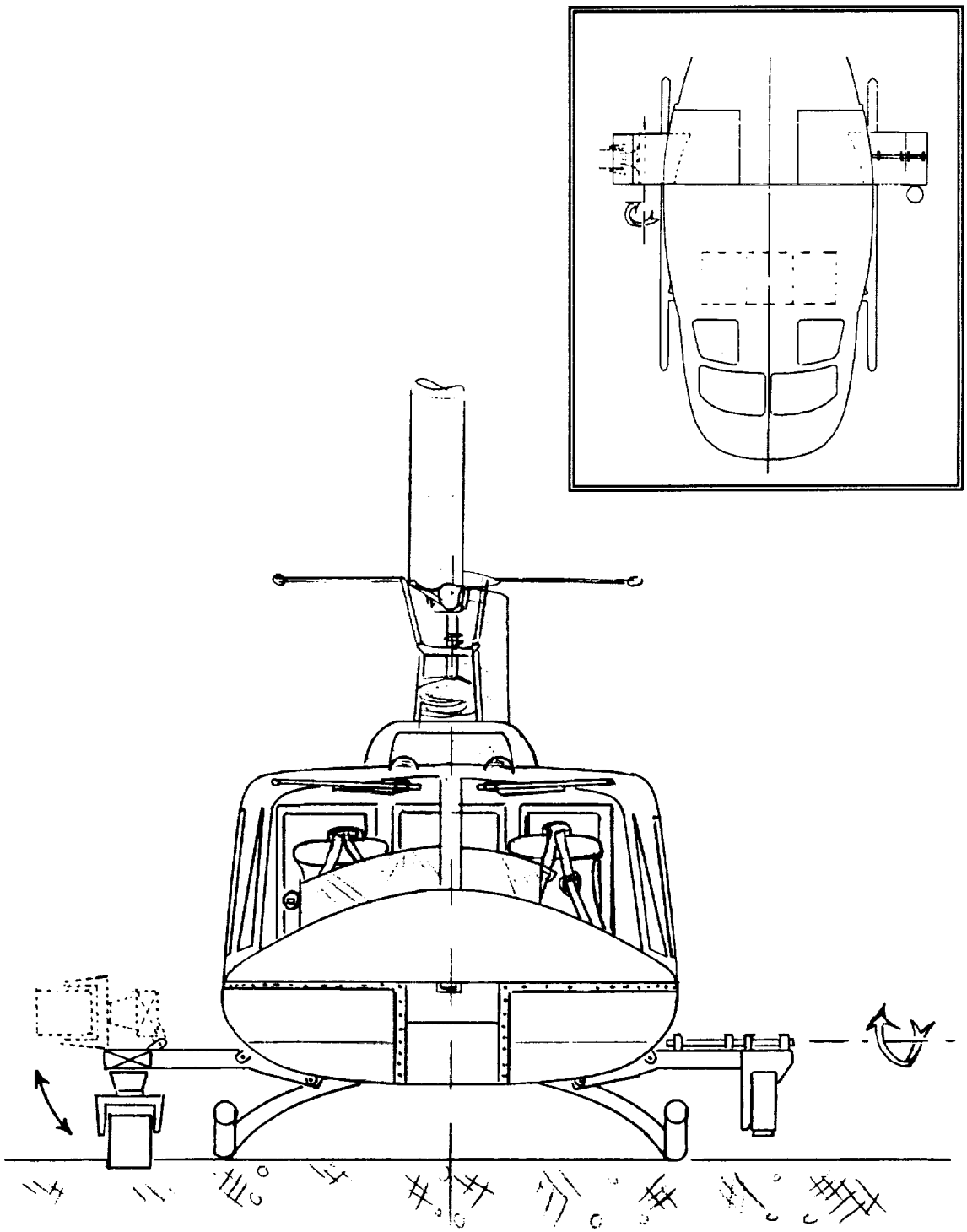

Figure 1. Frontal view schematic of a UH-1B helicopter showing the location of instrument pallets on the starboard and port sides of the aircraft. The insert (top, right) illustrates the location of the pallets on the fuselage near the center-of-gravity of the aircraft.

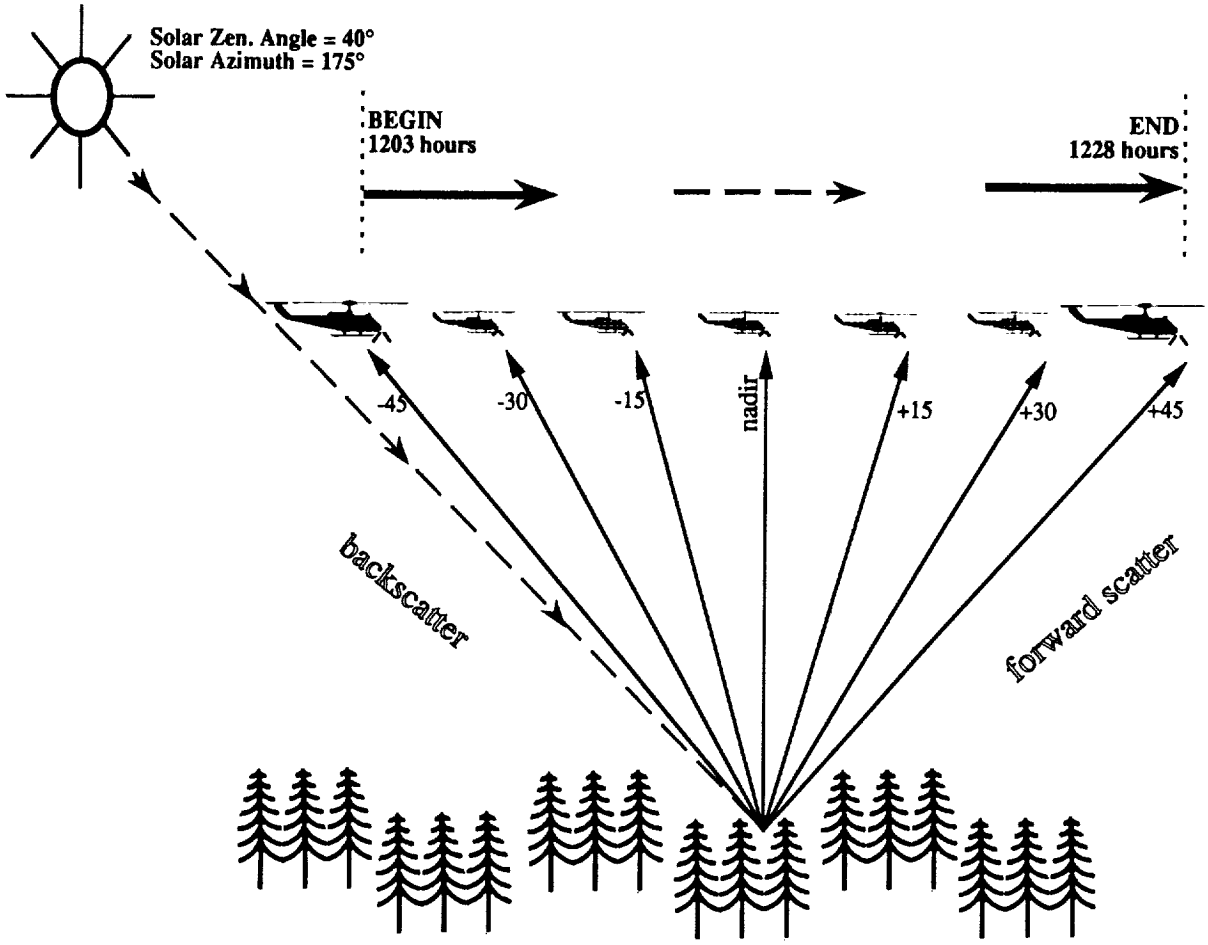

Figure 2. Cartoon drawing illustrating the collection of bidirectional reflectance data made possible with the pointable instrument mount. It should be noted that the azimuth orientation of the sensor payload can be adjusted independent of the helicopter azimuthal orientation, which is typically into the prevailing wind.

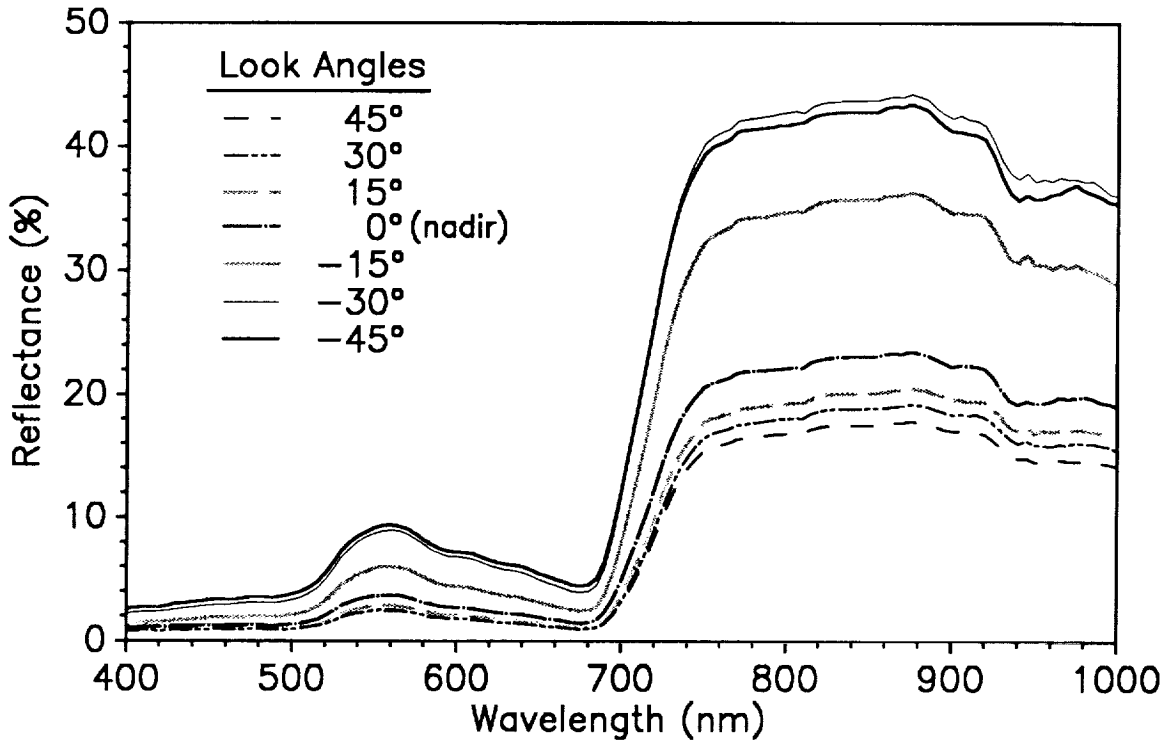

Figure 3. Graph illustrating the significant changes in the magnitude of reflectance for a hemlock/mixed hardwood forest stand as a function of sensor look angle. In this case, data were taken parallel to the principal plane of solar illumination. The magnitude of reflectance is much greater in the backscatter direction (i.e., -45° to -15°), than at nadir (0°) or in the forward scatter direction. Each curve represents the mean of ~ 50 scans at that particular look angle; data were acquired with an SE-590 spectroradiometer.

N91-25492

Title: Polarimetric Radar for Assessing Subsurface Characteristics

Author: Shih-Tseng Wu, NASA/Stennis Space Center

Discipline: Land

This paper describes the potential of using the NASA airborne polarimetric radar system to assess the subsurface characteristics of the Rogers lakebed and the Atchadafaya Basin study sites.

An airborne radar data set was acquired over the Atchadafaya Basin, Louisiana study site with the NASA Jet Propulsion Laboratory polarimetric radar system flown in the Ames Research Center DC-8 research aircraft on February 27, 1988. It was flown with a northwest to southeast flight pass with the radar antenna looking to the northeast (the antenna was mounted at the left side of the aircraft).

The raw data were preprocessed and stored in a compressed digital format. The received compressed data tapes contained ten channels of digital data from which the four polarization (HH, HV, VV and VH) were produced. Jet Propulsion Laboratory provided the reformatting computer program, which was used to decompress the data, together with the compressed data tapes.

The subsurface features in the Atchadafaya Basin are sediments, sediment distribution, and the formation of new isles and banks. Preliminary analysis of acquired data indicated VV polarization is capable of muddy-water penetration and the radar system could be used to assess underwater sediment distribution. Statistical analysis of the data will provide insight on the depth of muddy-water penetration and the results of analysis will be reported.

A second radar data set was acquired over the Rogers lake bed study site using the same radar system on June 29, 1990. According to Dr. Mike Kobrick of JPL all flight lines appeared to get good radar data. The data set will be used to assess the subsurface characteristics of the lake bed area to monitor its suitability for Shuttle landing. Preliminary analysis of the acquired data will be performed after the receival of the data set from JPL and the results of the analysis will be presented while available.

Title: Aircraft Remote Sensing of Phytoplankton Spatial Patterns during the 1989 Joint Global Ocean Flux Study (JGOFS) North Atlantic Bloom Experiment

Authors: James A. Yoder, University of Rhode Island
Frank E. Hoge, NASA/Goddard Space Flight Center

Discipline: Oceans

The NASA P-3 aircraft and the Airborne Oceanographic Lidar (AOL) system provided remote sensing support for the North Atlantic Bloom Experiment-the first JGOFS field program. The principal instrument of the AOL system is a blue-green laser that stimulates fluorescence from phytoplankton chlorophyll, the principal photosynthetic pigment. Other instruments on the P-3 include up- and down-looking spectrometers (256 spectral bands), PRT-5 for infrared measurements to determine sea surface temperature and a system to deploy and record AXBTs to measure subsurface temperature structure.

The purpose of this report is to discuss mesoscale phytoplankton chlorophyll variability near the JGOFS study sites along the 20 W meridian at 34 N, 47 N and 59 N. Shipboard results during the same study showed that the spatial distributions of chlorophyll and the partial pressure of dissolved carbon dioxide (PCO2) in the surface mixed layer were inversely correlated, as would be expected if phytoplankton productivity was the dominant process removing carbon dioxide from surface ocean waters.

Structure functions (semi-variograms) showed that chlorophyll spatial distributions were characterized by dominant length scales averaging ca. 50 km (wavelengths). Chlorophyll length scales were highly correlated with length scales associated with surface temperature distributions. Power spectra of the spatial series for results collected along some of the longer transects showed spectral power law exponents near -2 for both chlorophyll fluorescence and temperature for wavelengths ranging from 6 to 80 km. These results indicate that physical mixing processes, such as ocean eddies, were the dominant process affecting the near-surface distribution of surface chlorophyll. The results are useful for developing numerical models linking ocean productivity to air/sea exchange of carbon dioxide.

Fourth Airborne Geoscience Workshop
National Aeronautics and Space Administration
Embassy Suites Hotel
La Jolla, California
January 29 - February 1, 1991

Registrants

Peter Abel
PO Box 57380
Washington, DC 20037

Bruce A. Albrecht
Pennsylvania State University
Department of Meteorology
505 Walker Building
University Park, PA 16802

George M. Alger
Ames Research Center
Mail Stop 211-12
National Aeronautics and
Space Administration
Moffett Field, CA 94035

Robert Arnone
Naval Ocean Research &
Development Agency
Advanced Instrumentation Branch
Mail Code 352
Stennis Space Center, MS 39529-5000

John Arveson
Ames Research Center
High Altitude Missions Branch
Mail Stop 240-6
National Aeronautics and
Space Administration
Moffett Field, CA 94035

Gary Athey
Stennis Space Center
U.S. Naval Oceanographic Office
Code OPAS
Stennis Space Center, MS 39522-5001

John M. Bane
University of North Carolina
Marine Sciences Program
Campus Box #3300, Venable Hall
Chapel Hill, NC 27599-3300

Darrel Baumgardner
National Center for
Atmospheric Research
PO Box 3000
Boulder, CO 80307

Alex Becker
University of California, Berkeley
Dept. of Material Science
and Mineral Engineering
336 Hearst Mining Building
Berkeley, CA 94720

Michael Bellmore
Aeromet, Inc.
PO Box 701767
Jones Airport
Tulsa, OK 74170

Robert Billings
Ames Research Center
Code 211-4A
National Aeronautics and
Space Administration
Moffett Field, CA 94035-1000

Ted Blanc
Naval Research Laboratory
Atmospheric Physics
Code 4223
4555 Overlook Avenue, SW
Washington, DC 20375-5000

Aerlene Booker
Aeromet, Inc.
P.O. Box 701767
Jones Airport, OK 74170-1767

Ray Booker
Aeromet, Inc.
P.O. Box 701767
Jones Airport, OK 74170-1767

David A. Bowdle
University of Alabama, Huntsville
Johnson Research Center
PO Box 212
Huntsville, AL 35899

Stuart Bowen
Ames Research Center
Mail Stop 245-5
National Aeronautics and
Space Administration
Moffett Field, CA 94035

Janice D. Boyd
U.S. Navy
NOARL
Code 331
Stennis Space Center, MS 39529-5004

Leon Bronstein
Canada Centre for Remote Sensing
Data Acquisition Division
Ottawa, Ontario K1A 0Y7
CANADA

Edward V. Browell
Langley Research Center
Mail Stop 401A
National Aeronautics and
Space Administration
Hampton, VA 23665-5225

Jack L. Bufton
Goddard Space Flight Center
Code 920
National Aeronautics and
Space Administration
Greenbelt, MD 20771

Robert Burpee
NOAA/AOML
Hurricane Research Division
Code R/E/AO1
4301 Rickenbacker Causeway
Miami, FL 33149

Carolyn F. Butler
ST Systems Corporation
28 Research Drive
Hampton, VA 23666

Andy Cameron
Earth Science Support Office
600 Maryland Avenue, SW
Suite 440
Washington, DC 20024

William Campbell
U.S. Geological Survey
Ice and Climate Project
University of Puget Sound
Tacoma, WA 98416

Richard E. Carbone
National Center for
Atmospheric Research
PO Box 3000
Boulder, CO 80307-3000

Dawn Cardascia
Earth Science Support Office
600 Maryland Avenue, SW
Suite 440
Washington, DC 20024

J. P. Chalon
C.N.R.M.
42, Av. Coriolis
Toulouse, Cedex 31057
FRANCE

K. Roland Chan
Ames Research Center
Mail Stop 245-5
National Aeronautics and
Space Administration
Moffett Field, CA 94035

Susan Cherniss
Ames Research Center
Mail Stop 248-1
National Aeronautics and
Space Administration
Moffett Field, CA 94035

Dave Clem
Code 672, Hangar D-1
Wallops Flight Facility
National Aeronautics and
Space Administration
Wallops Island, VA 23337

William A. Cooper
National Center for
Atmospheric Research
Research Aviation Facility
PO Box 3000
Boulder, CO 80307

Debby Critchfield
Earth Science Support Office
600 Maryland Avenue, SW
Suite 440
Washington, DC 20024

Robert Curran
Earth Science Support Office
600 Maryland Avenue, SW
Suite 440
Washington, DC 20024

Kenneson Dean
University of Alaska, Fairbanks
Geophysical Institute
Fairbanks, AK 99775-0800

Bruce Deck
New York State Dept. of Public Health
Woodsworth Center
PO Box 509
Albany, NY 12201

Leo H. Degreef
Ames Research Center
MS 211-12, Code OMM
National Aeronautics and
Space Adminstration
Moffett Field, CA 94035

Richard A. Dirks
National Center for Atmospheric
Research
PO Box 3000
Boulder, CO 80307

Louis Dod
Goddard Space Flight Center
Code 975
National Aeronautics and
Space Administration
Greenbelt, MD 20771

Ed Doherty
Pacific Missile Test Center
Code 4032
Point Mugu, CA 93042

David Dokken
Earth Science Support Office
600 Maryland Avenue, SW
Suite 440
Washington, DC 20024

Jeff Dozier
University of California,
Santa Barbara
Computer Systems Laboratory
Center for Remote Sensing and
Environmental Optics
Santa Barbara, CA 93106
or
Goddard Space Flight Center
Code 900
National Aeronautics and
Space Administration
Greenbelt, MD 20771

Reuben Erickson
Ames Research Center
MS 211-12
National Aeronautics and
Space Administration
Moffett Field, CA 94035

Diane L. Evans
Jet Propulsion Laboratory
Mail Stop 300-233
4800 Oak Grove Drive
Pasadena, CA 91109

Marta A. Fenn
ST Systems Corporation
28 Research Drive
Hampton, VA 23666

Pierre H. Flamant
CNRS
Ecole Polytechnique
Lab. of Meteorologie Dynamique
Palaiseau, Cedex F-91128
FRANCE

William S. Flothmeier
Pacific Missile Test Center
Department of the Navy
Electromagnetic System Div.
Laser/Optical Br., Code 4032
Point Mugu, CA 93042-5000

Betty Foster
Ames Research Center
Mail Stop 240-6
National Aeronautics and
Space Administration
Moffett Field, CA 94035

Cathy Freeland
Earth Science Support Office
600 Maryland Avenue, SW
Suite 440
Washington, DC 20024

Carl A. Friehe
University of California, Irvine
Department Mechanical
Engineering
Irvine, CA 92717

James B. Garvin
Goddard Space Flight Center
Code 622
National Aeronautics and
Space Administration
Greenbelt, MD 20771

Albin J. Gasiewski
Georgia Institute of Technology
School of Electrical Engineering
777 Atlantic Drive
Atlanta, GA 30332-0250

Catherine Gautier
University of California,
Santa Barbara
Geography Department
Santa Barbara, CA 93106

Tom Gerish
National Oceanographic and
Atmospheric Administration
Office of Aircraft Operations
PO Box 020197
Miami, FL 33122-0917

Alexander F. H. Goetz
University of Colorado
CSES/CIRES
Campus Box 449
Boulder, CO 80309-0449

Alan Goldstein
National Oceanographic and
Atmospheric Administration
Office of Aircraft Operations
PO Box 070197
Miami, FL 33102-0197

Gerald L. Gregory
Langley Research Center
Mail Stop 483
National Aeronautics and
Space Administration
Hampton, VA 23665-5225

Andrew Griffis
University of Massachusetts
ECE Department
Marcus Hall, Room 10
Amherst, MA 01003

Robert L. Grossman
University of Colorado
CIRES
Campus Box 449
Boulder, CO 80309-0449

Jorg M. Hacker
Flinders University
FIAMS
GPO Box 2100
Adelaide, South Australia 5000
AUSTRALIA

James Hain
Associated Scientists at Woods Hole
PO Box 721
Woods Hole, MA 02543

G. Warren Hall
Ames Research Center
Mail Stop OM/240-2
National Aeronautics and
Space Administration
Moffett Field, CA 94035-4000

J. Michael Hall
Interagency Airborne
Geoscience Steering Group
Office of Global Programs
1335 East-West Highway
Silver Spring, MD 20910

Philip D. Hammer
Ames Research Center
Mail Stop 245-4
National Aeronautics and
Space Administration
Moffett Field, CA 94035

Earl Hansen
Jet Propulsion Laboratory
Mail Stop 168-427
4800 Oak Grove Drive
Pasadena, CA 91109

Ray Harris-Hobbs
Aeromet, Inc.
PO Box 701767
Jones Airport
Tulsa, OK 74170-1767

Frank L. Herr
Office of Naval Research
Code 1122/RS
800 North Quincy Street
Arlington, VA 22217-5000

Scott Higdon
Langley Research Center
Mail Stop 401A
National Aeronautics and
Space Administration
Hampton, VA 23665-5225

James Hochstetler
Pacific Missile Test Center
Code 4032
Department of the Navy
Point Mugu, CA 93042-5000

Ron Hochstetler
Airship Operation & Service
324-2C Selwgn Drive
Frederick, MD 21701

Axel Hoff
Aerodata
Rebenring 33
Braunschweig, D-3300
Federal Republic of Germany

LaMont Holmes
Pacific Missile Test Center
Code 4032
Point Mugu, CA 93042

Robbie Hood
Marshall Space Flight Center
Code ES43
National Aeronautics and
Space Administration
Huntsville, AL 35812

William Hooke
NOAA/CSD
Herbert Hoover Bldg., Room 5809
14th & Constitution Ave., NW
Washington, DC 20230

James Horvat
Ames Research Center
Code 211-4A
National Aeronautics and
Space Administration
Moffett Field, CA 94035-1000

Janice Hostetter
Birch & Davis Associates, Inc.
8905 Fairview Road
Suite 200
Silver Spring, MD 20910

James Huning
NASA Headquarters
Code SE
600 Independence Ave, SW
Washington, DC 20546

Syed Ismail
Langley Research Center
Mail Stop 401A
National Aeronautics and
Space Administration
Hampton, VA 23665

_____ Jaggie
Stennis Space Center
8201 Lockheed
Stennis Space Center, MS 39529

L. J. Jahnsen
JTD Environment Systems, Inc.
PO Box 91503
Pasadena, CA 91109

Dean Jaynes
Ames Research Center
National Aeronautics and
Space Administration
Mail Stop 211-12
Moffett Field, CA 94035

Gary J. Jedlovec
Marshall Space Flight Center
Earth Science & Appl., ES43
National Aeronautics and
Space Administration
Huntsville, AL 35812

Anne M. Jochum
Institute fur Physik der
Atmosphaere, DLR
Oberpfaffenhofen, D-8031
Federal Republic of Germany

Doug Johnson
Met. Research Flight
Y46 Building
Royal Aerospace Establishment
Farnsborough Hants GU14 6TD
United Kingdom

Lee Johnson
Ames Research Center
Mail Stop 242-4
National Aeronautics and
Space Administration
Moffett Field, CA 94035

Warren Johnson
National Center for
Atmospheric Research
10800 West 120th Avenue
Jefferson County Airport
Broomfield, CO 80020

David P. Jorgensen
National Oceanic and
Atmospheric Administration
National Severe Storms Laboratory
Mail Code R/E/NS1
325 Broadway
Boulder, CO 80303

Anne B. Kahle
Jet Propulsion Laboratory
Mail Stop 183-501
4800 Oak Grove Drive
Pasadena, CA 91109

Dayalan Kasilingam
Ocean Research & Engineering
255 South Marengo Avenue
Pasadena, CA 91101

Patrick Kelly
Stennis Space Center
Science and Technology Laboratory
National Aeronautics and
Space Administration
Stennis Space Center, MS 39529

Robert Kelly
Lockheed Engineering &
Sciences Company
2625 Bay Area Boulevard
Suite 700-A16
Houston, TX 77058

Susan A. Kooi
ST Systems Corporation
28 Research Drive
Hampton, VA 23666

Mark Koozer
Ames Research Center
Mail Stop 211-13
National Aeronautics and
Space Administration
Moffett Field, CA 94035

Allan N. Kover
U.S. Geological Survey
927 National Center
Reston, VA 22092

William Krabill
Goddard Space Flight Center
Mail Code 672
National Aeronautics and
Space Administration
Wallops Island, VA 23337

Joachim Kuettner
National Center for
Atmospheric Research
PO Box 3000
Boulder, CO 80307

Paul E. LaViolette
Mississippi State University
Research Center
Stennis Space Center
Stennis Space Center, MS 39529

John S. Langford
Aurora Flight Sciences Corporation
PO Box 11998
Alexandria, VA 22312

James G. Lawless
Ames Research Center
Mail Stop 239-20
National Aeronautics and
Space Administration
Moffett Field, CA 94035

David M. LeVine
Goddard Space Flight Center
Code 975
National Aeronautics and
Space Administration
Greenbelt, MD 20771

Robert Leifer
Department of Energy
Environment Measurement
Laboratory
376 Hudson Street
New York, NY 10014

Donald H. Lenschow
National Center for
Atmospheric Research
PO Box 3000
1850 Table Mesa Drive
Boulder, CO 80307

Marlon R. Lewis
Dalhousie University
Department of Oceanography
Halifax, Novia Scotia B3H 4J1
CANADA

John O. Lilly, Jr.
E-Systems
CBN-077
Box 6056
Greenville, TX 75601

Joseph Lindinger
U.S. Naval Air Development Center
Code 3031
Wyminster, PA 18974

Charles Luther
Office of Naval Research
800 North Quincy Street
Arlington, VA 22217

Jeffrey Luvall
Stennis Space Center
Science and Technology
Laboratory
National Aeronautics and
Space Administration
Stennis Space Center, MS 39529

Paul MacCready
AeroVironment, Inc.
222 East Huntington Drive
Monrovia, CA 91016

J. Ian MacPherson
National Research Council
Flight Research Laboratory
Montreal Road
Ottawa, Ontario K1A 0R6
CANADA

Lisa J. Mann
Ames Research Center
Mail Stop 242-4
National Aeronautics and
Space Administration
Moffett Field, CA 94035

James J. Margitan
Jet Propulsion Laboratory
Mail Stop 183-301
Atmospheric &
Oceanographic Sciences
4800 Oak Grove Drive
Pasadena, CA 91109

Brian L. Markham
Goddard Space Flight Center
Code 923
National Aeronautics and
Space Administration
Greenbelt, MD 20771

Chreston F. Martin
EG&G
Washington Analytical Services
5211 Auth Road
Suite 204
Suitland, MD 20746-4324

Patrick Mascart
CNRM
42 Av. Coriolis
Toulouse, 310057
FRANCE

Allen S. Mason
Los Alamos National Laboratory
Mail Stop J541
PO Box 1663
National Aeronautics and
Space Administration
Los Alamos, NM 87545

Richard McCreight
Oregon State University
Forest Science Department
Peavy Hall 154
Corvallis, OR 97331

Robert E. McIntosh
University of Massachusetts
Microwave Remote Sensing Lab
Department of Electrical and
Computer Engineering
Amherst, MA 01003

Jack A. McKay
Physical Sciences, Inc.
635 Slaters Lane
Alexandria, VA 22314

Robert J. McNeal
NASA Headquarters
Code SEU
600 Independence Avenue, SW
Washington, DC 20546

S. Harvey Melfi
Goddard Space Flight Center
Code 917
National Aeronautics and
Space Administration
Greenbelt, MD 20771

Robert T. Menzies
Jet Propulsion Laboratory
Mail Stop 169-214
4800 Oak Grove Drive
Pasadena, CA 91109

Michael Miller
USAF Wright-Patterson
Air Force Base
4950th Test Wing
Wright-Patterson AFB, OH 45433-6518

Edward C. Mitz
NSI Technology Services Corporation
Building 211, Room 312
Ames Research Center
National Aeronautics and
Space Administration
Moffett Field, CA 94035

Erik Mollo-Christensen
Goddard Space Flight Center
Code 670
National Aeronautics and
Space Administration
Greenbelt, MD 20771

Francis D. Moran
National Oceanic and
Atmospheric Administration
Office of Aircraft Operations
PO Box 020197
Miami, FL 33102-0197

Robert D. Morris
Ames Research Center
OMM, Mail Stop 211-12
National Aeronautics and
Space Administration
Moffett Field, CA 94035

W. Muller
Niedersachsisches Lqandesamt f.
Immissionsschutz

Robert E. Murphy
NASA Headquarters
Code SEL
600 Independence Avenue, SW
Washington, DC 20546

Jeff Myers
Ames Research Center
Mail Stop 240-6
National Aeronautics and
Space Administraction
Moffett Field, CA 94035

Roger L. Navarro
Wallops Flight Facility
Operations Division
National Aeronautics and
Space Administration
Wallops Island, VA 23337

Chien Nguyen
Ames Research Center
Code 244-10
National Aeronautics and
Space Administration
Moffett Field, CA 94035-1000

Bernard Nolan
Earth Science Support Office
600 Maryland Avenue, SW
Suite 440
Washington, DC 20024

William C. Patzert
NASA Headquarters
Code SET
600 Independence Avenue, SW
Washington, DC 20546

Ramona E. Pelletier-Travis
Stennis Space Center
Mail Code HA-10
National Aeronautics and
Space Administration
Stennis Space Center, MS 39529

Earl V. Petersen
Ames Research Center
Mail Stop 240-2
National Aeronautics and
Space Administration
Moffett Field, CA 94035

David L. Peterson
Ames Research Center
Mail Stop 242-4
National Aeronautics and
Space Administration
Moffett Field, CA 94035

Paul Pikell
USAF Wright-Patterson
Air Force Base
4950th Test Wing
Wright-Patterson AFB, OH 45433-6518

Michael Poellot
University of North Dakota
Dept. of Atmospheric Sciences
PO Box 8216, University Station
Grand Forks, ND 58202-8216

Frederick Portigal
University of Nevada System
Desert Research Institute
Reno, NV 89506

Chuck Pruszynski
Aeromet, Inc.
PO Box 701767
Jones Airport
Tulsa, OK 74170

Lawrence F. Radke
University of Washington
Atmospheric Sciences Dept., AK40
Seattle, WA 98195

John Reller
Ames Research Center
Mail Stop 211-12
National Aeronautics and
Space Administration
Moffett Field, CA 94035

Henry E. Revercomb
University of Wisconsin
Space Science and
Engineering Center
1225 West Dayton Street
Madison, WI 53706

Randolph S. Reynolds
Ames Research Center
Mail Stop 240-2
National Aeronautics and
Space Administration
Moffett Field, CA 94035

David P. Rogers
Scripps Institution of Oceanography
Mail Stop A-021
La Jolla, CA 92093

R. Lynn Rose
Aeromet, Inc.
PO Box 701767
Jones Airport
Tulsa, OK 74170

J. Rothermel
Marshall Space Flight Center
USRA, Code ED43
National Aeronautics and
Space Administration
Huntsville, AL 35812

Philip B. Russell
Ames Research Center
Mail Stop 245-5
National Aeronautics and
Space Administration
Moffett Field, CA 94035

Russ Schnell
University of Colorado
NOAA/ERL
Campus Box 449
325 Broadway
Boulder, CO 80309

Christine P. Scofield
Ames Research Center
Code 248-1
National Aeronautics and
Space Administration
Moffett Field, CA 94035-1000

Robert Serafin
National Center for
Atmospheric Research
PO Box 3000
Boulder, CO 80307

Julian A. Shedlovsky
National Science Foundation
Div. of Atmospheric Sciences
Centers & Fac. Section, Rm. 644
1800 G Street, NW
Washington, DC 20550

Gary A. Shelton
Ames Research Center
Mail Stop 240-6
National Aeronautics and
Space Administration
Moffett Field, CA 94035

Omar H. Shemdin
Ocean Research & Engineering
255 South Marengo Avenue
Pasadena, CA 91101

Richard Siquig
Naval Oceanographic and
Atmospheric Research
Code 442
Monterey, CA 93943-5006

Joseph W. Skiles
Ames Research Center
Mail Stop 242-4
National Aeronautics and
Space Administration
Moffett Field, CA 94035

Paul L. Smith
South Dakota School of Mines &
Technology
Institute of Atmospheric Science
501 East Joseph Street
Rapid City, SD 57701-3995

Ronald B. Smith
Yale University
Department of Geology
& Geophysics
PO Box 6666
New Haven, CT 06511

Michael A. Spanner
Ames Research Center
Mail Stop 242-4
National Aeronautics and
Space Administration
Moffett Field, CA 94035

James D. Spinhirne
Goddard Space Flight Center
Code 917
National Aeronautics and
Space Administration
Greenbelt, MD 20771

J. W. Strapp
Atmospheric Environment Service
4905 Dufferin Street
Downsview, Ontario M3H 5T4
CANADA

Richard Studarus
Pacific Missile Test Center
Code 4032
Point Muga, CA 93042

Carl Sweetland
Aeromet, Inc.
555 Sparkman Drive, NW, #1600
Huntsville, AL 35816

Calvin T. Swift
University of Massachusetts
Electrical & Computer
Engineering Department
Marcus Hall
Amherst, MA 01003

Robert N. Swift
EG&G
5211 Auth Road
Suite 204
Suitland, MD 20746

James V. Taranik
University of Nevada System
Desert Research Institute
7010 Dandini Boulevard
PO Box 60220
Reno, NV 89506

John A. Taylor
Lighter Than Air Technologies
Route 3, PO Box 3
Breton Woods Court
Leonardtown, MD 20650

Michael Tjernstrom
University of Uppsala
Department of Meteorology
PO Box 516
Kyrkogardsgatau 6
Uppsala, S-75120
SWEDEN

David M. Tratt
Jet Propulsion Laboratory
Mail Stop 169-214
4800 Oak Grove Drive
Pasadena, CA 91109

Adrian F. Tuck
NOAA/ERL
Aeronomy Laboratory
Code R/E/AL6
325 S. Broadway
Boulder, CO 80303

Jacob van Zyl
Jet Propulsion Laboratory
Mail Stop 300-233
4800 Oak Grove Drive
Pasadena, CA 91109

Mike Vance
Gulfstream Aerospace
1000 Wilson Boulevard
Suite 2701
Arlington, VA 22209

Deborah Vane
Jet Propulsion Laboratory
Mail Stop 11-116
4800 Oak Grove Drive
Pasadena, CA 91109

Gregg Vane
Jet Propulsion Laboratory
Mail Stop 180-703
4800 Oak Grove Drive
Pasadena, CA 91109

Peter Wachs
Aerodata
Rebenring 33
Braunschweig, D-3300
FRG

Martin Wahlen
New York State Department
of Public Health
WCLR
PO Box 509
Albany, NY 12201
Charles L. Walthall
University of Maryland
Department of Geography
College Park, MD 20742

Robert Watson
NASA Headquarters
Code SEP
600 Independence Avenue, SW
Washington, DC 20546

JoBea Way
Jet Propulsion Laboratory
Mail Stop 300-233
4800 Oak Grove Drive
Pasadena, CA 91109

Christopher Webster
Jet Propulsion Laboratory
Mail Stop 183-301
4800 Oak Grove Drive
Pasadena, CA 91109

Paul Weckler
Aeromet, Inc.
PO Box 701767
Jones Airport
Tulsa, OK 74170

Steven Wegener
Ames Research Center
Mail Stop 245-5
National Aeronautics and
Space Administration
Moffett Field, CA 94035

Ming Ying Wei
NASA Headquarters
Code SET
600 Independence Avenue, SW
Washington, DC 20546

Charles L. Weinert
201 Appaloosa Drive
Willew Park, TX 76087

Alan Weinstein
Office of Naval Research
800 North Quincy Street
Room 1122
Arlington, VA 22217

Carol A. Wessman
University of Colorado
CSES/CIRES
1540 30th Street
Room 201
Boulder, CO 80309-0449

Diane Wickland
NASA Headquarters
Code SEL
600 Independence Avenue, SW
Washington, DC 20546

Darrel L. Williams
Goddard Space Flight Center
Code 923
National Aeronautics and
Space Administration
Greenbelt, MD 20771

Gregory S. Wilson
NASA Headquarters
Code SE
600 Independence Avenue, SW
Washington, DC 20546

Frank H. Wright
Jet Propulsion Laboratory
Mail Stop 183-335
4800 Oak Grove Drive
Pasadena, CA 91109

Shih-Tseng Wu
NASA Science Technology Laboratory
Stennis Space Center
Code HA20, Building 1100
Stennis Space Center, MS 39529

James A. Yoder
University of Rhode Island
Graduate School of Oceanography
Narragansett Bay Campus
South Ferry Road
Narragansett, RI 02882

Fourth Interagency Airborne Geoscience Workshop
Embassy Suites Hotel
La Jolla, California

Alphabetical Listing of Speakers and Poster Presenters

Alphabetical Listing of Speakers and Poster Presenters (Continued)

Alphabetical Listing of Speakers and Poster Presenters (Continued)

Alphabetical Listing of Speakers and Poster Presenters (Continued)

Alphabetical Listing of Speakers and Poster Presenters (Continued)

Alphabetical Listing of Speakers and Poster Presenters (Continued)

Alphabetical Listing of Speakers and Poster Presenters (Continued)

Alphabetical Listing of Speakers and Poster Presenters (Continued)

Alphabetical Listing of Speakers and Poster Presenters (Continued)

Alphabetical Listing of Speakers and Poster Presenters (Continued)

Alphabetical Listing of Speakers and Poster Presenters (Continued)

Alphabetical Listing of Speakers and Poster Presenters (Continued)

Alphabetical Listing of Speakers and Poster Presenters (Continued)

Alphabetical Listing of Speakers and Poster Presenters (Continued)

	Program Book Page Number
Yoder, James A., University of Rhode Island; and Frank E. Hoge, NASA/Goddard Space Flight Center Aircraft Remote Sensing of Phytoplankton Spatial Patterns during the 1989 Joint Global Ocean Flux Study (JGOFS) North Atlantic Bloom Experiment	305